Biomarker development to assess bone health

A thesis presented in partial fulfilment of the requirements for the degree of

Doctor of Philosophy

in

Nutritional Science

at Massey University, Palmerston North, New Zealand.

Diana Leticia Cabrera Amaro

2019

Abstract

Postmenopausal women experience an accelerated bone loss with increased fracture risk caused by oestrogen deficiency. Biomarkers of bone turnover assess the changes of bone metabolism in postmenopausal women; however, prediction of bone loss with these common biomarkers cannot be achieved because bone biomarkers might not reflect the bone microenvironment status. Thus, there is a need for discovering new bone biomarkers that can efficiently predict bone loss in postmenopausal women. Previous studies suggest that the ovariectomised sheep in combination with injected glucocorticoids may be a reliable model to evaluate the biological response to oestrogen withdrawal as well as the bone remodelling process.

The purpose of this research programme was to test the following hypotheses: 1) ovariectomising sheep in combination with monthly injections of glucocorticoids would result in decreased bone mineral density (BMD) and increased plasma bone remodelling marker concentration over a shorter period of time; 2) the plasma metabolome and lipidome of ovariectomised sheep would be different, and the biochemical changes in plasma and bone remodelling would be associated with bone loss; 3) and finally, there would also be a difference in the plasma metabolome and lipidome of Singaporean–Chinese postmenopausal women according to their bone mineral density status. The hypotheses were evaluated using the OVX sheep in combination with glucocorticoids as a large animal model for postmenopausal osteoporosis, as well as comprehensive LC–MS-based metabolomics as a diagnostic approach to identify lipids and metabolites associated with bone loss in postmenopausal women.

The OVX sheep model was successfully validated over five months of this study period, and bone mineral density was decreased and bone biomarkers increased after five months. Then, plasma samples from this animal model were analysed to measure the metabolome and lipidome of the OVX sheep. In the OVX sheep, metabolite and lipid alterations associated with bone loss included methionine, glutaric acid, tryptophan, 5-methoxytryptophan, CL and CerP, and these correlated with OC, CTx-1, femoral BMD and lumbar spine BMDThese studies revealed dynamic changes of the metabolite and lipid profiles from affected sheep, such as perturbation in multiple amino acids, metabolites, and fatty acid *β*-oxidation. Additionally, the results from the Singaporean–Chinese postmenopausal women showed alterations in proline, threonine, methionine, 4-aminobutyric acid, aminopropionitrile, phosphatidic acid, diacylglycerol, CerP and phosphatidylinositol correlated with low femoral neck BMD. Methionine and CerP were the common compounds altered in OVX sheep and SC women with low BMD when compared with healthy groups. Those compounds, which are known to be involved in bone remodelling, have the potential for studying early bone loss in postmenopausal women, where identifying new bone-specific biomarkers may aid in clarifying novel molecular mechanisms of bone loss.

Acknowledgements

This PhD would have not been possible without the collaboration, dedication, and friendship of many people that contributed in some way towards this project. I would like to thank my Massey University supervisors, Marlena Kruger and Fran Wolber, and my Agresearch supervisors, Karl Fraser and Nicole Roy, for their guidance and being so generous with their time and sharing their knowledge and expertise. I am lucky to have got an opportunity to work with them. I particularly appreciated their always kept me motivated, supported my ideas and made me question my knowledge. During all these years their kept maintaining their doors open and smiling regardless of how many interruptions were.

I would also like to thank the Ministry of Business, Innovation and Employment, New Zealand; Singapore-New Zealand Foods for Health Grant (MAUX1309) and The Mexican National Council for Science and Technology (Scholarship No. 383233) for financially supporting my project and my PhD scholarship.

My time living in New Zealand has been one of the greatest experience in my life and I would also like to thank to all the people that made me feel at home. In these years I have crossed paths with wonderful friends with who I shared many laughs and received their support, thank you for expanding my world view.

I would like also to thank to all family and friends back home. I would specially like to thank to my father Armando, my mother Leticia and my brother Armando for all the love and support they have given me, and for encouraging me to pursuit all my dreams.

Table of Contents

List of figures

List of tables

Structure of the thesis

This thesis is written according to the Graduate Research School regulations for PhD thesis by publications. The list below presents the publication status of each chapter.

Chapter 1

Thesis introduction

This chapter was written by Diana Cabrera as an introductory section of this thesis and is not intended for publication.

Chapter 2

Literature review

Basic concepts in bone biology, the pathogenesis of osteoporosis, a review of metabolomics approaches and recent findings on the plasma metabolome in models of osteoporosis are discussed. This literature review was written by Diana Cabrera and is not intended for publication.

Chapter 3

Glucocorticoids affect bone mineral density and bone remodelling in ovariectomised sheep: a pilot study

Cabrera, D., Wolber, F., Dittmer, K., Rogers, C., Ridler, A., Aberdein, A., Parkinson, T., Chambers, P., Fraser, K., Roy, N., Kruger, M. 2018. Glucocorticoids affect bone mineral density and bone remodelling in OVX sheep: A pilot *Bone Reports*, *9*, 173-180.

Chapter 4

Bone changes in response to glucocorticoids in ovariectomised sheep: a peripheral quantitative computed tomography (pQCT) study**.** (Manuscript under preparation)

Chapter 5

Application of MS-based metabolomics approach in ovariectomised sheep as a model of osteoporosis (Manuscript under preparation)

Chapter 6

MS-based lipidomics approach reveals changes in lipid profiles of ovariectomised sheep (Manuscript under preparation)

Chapter 7

Association of plasma lipids and polar metabolites with low bone mineral density in Singaporean-Chinese Menopausal women: a pilot study

Cabrera, D., Kruger, M., Wolber, F. M., Roy, N. C., Totman, J. J., Henry, C. J., Cameron, David and Fraser, K. (2018). Association of plasma lipids and polar metabolites with low bone mineral density in Singaporean-Chinese Menopausal women: a pilot study. *Intl J Environ Res Public health*. *5*(5), 1045.

Chapter 8

Thesis discussion

This chapter was written by Diana Cabrera as a discussion section of this thesis and is not intended for publication.

Abbreviations

ACN	acetonitrile
BMD	bone mineral density
BMU	basic multicellular unit
BMC	bone mineral content
CL	cardiolipin
CTx-1	c-terminal telopeptide of type 1 collagen
CerP	ceramide-1-phosphate
DG	diacylglycerol
DXA	dual x-ray absorptiometry
EDTA	ethylenediamine tetraacetic acid
HILIC-MS	hydrophilic-interaction liquid chromatography–mass spectrometry
IL-1	interleukin-1
IL-6	interleukin-6
lysoPE	lysophosphatidylethanolamines
M-CSF	macrophage colony-stimulating factor
MSCs	mesenchymal stem cells
MS	mass spectrometry
NMR	nuclear magnetic resonance
OC	osteocalcin
OPLS	orthogonal partial least squares
OVX	ovariectomy
OVXG	ovariectomised plus five doses of glucocorticoids
OVXG2	ovariectomised plus two doses of glucocorticoids
OPG	osteoprotegerin
PA	phosphatidic acid
PI	phosphatidylinositol
PG	phosphatidyglycerol
PCA	principal component analysis
Plasmenyl-PE	plasmenylphosphatidylethanolamine
PPARy	peroxisome proliferator-activated receptor
PS	phosphatidylserine
PTH	parathyroid hormone
pQCT	peripheral quantitative computed tomography
RANK	receptor activator of nuclear factor-κB
RANKL	receptor activator of nuclear factor-κB ligand
ROS	reactive oxygen species
UPLC-MS	ultra-performance liquid chromatography−mass spectrometry
S1P	sphingosine-1-phosphate
SC	Singaporean–Chinese
SD	standard deviation
SEM	standard error of mean
TCA	tricarboxylic acid cycle
TNF-α	tumor necrosis factor-α
TG	triacylglycerol

Tb vBMD	trabecular volumetric bone mineral density
Tb BMC	trabecular bone mineral content
QC	quality control
WHO	World Health Organization
PC	principal component
vBMD	volumetric bone mineral density

Chapter 1

Thesis Introduction

1.1 Thesis background

Osteoporosis is a degenerative bone disease and a major health concern worldwide. Globally, 200 million people are affected, placing a considerable burden on financial healthcare systems (Reginster and Burlet, 2006). In women, oestrogen loss affects mainly the bone remodelling process, where overexpression of osteoclasts (bone resorbing cells) leads to bone loss (Riggs, 2000). Deregulation of the bone remodelling process is often associated with bone diseases such as osteoporosis in women (Charatcharoenwitthaya et al., 2007). Elucidation of the metabolic signals that regulate bone remodelling and mineralisation may allow the identification of new bone biomarkers to predict bone loss, as well as the development of new therapies to prevent bone loss in women. Specific metabolic pathways such as glycolysis, the tricarboxylic acid cycle (TCA), glutamine metabolism and fatty acid metabolism are regulated by oestrogen (Chen et al., 2009). Therefore, understanding the complex interactions of these metabolic pathways will not only improve the understanding of bone remodelling, but also could lead to the discovery of the relevant signalling pathways leading to bone metabolic alterations and osteoporosis in women.

There has been an interest in developing accurate biomarkers that can predict bone loss, as well as interest in characterising cellular and extracellular components of the bone metabolism that are produced in health or disease states. Most of these biochemical biomarkers are used to monitor bone loss and measure the level of response to treatment for osteoporosis (Eastell and Hannon, 2008). Bone biomarkers are released during bone remodelling and can be classified into two categories. Bone resorption markers reveal osteoclast activity, such as degradation of products of type 1 collagen. Bone formation markers

reflect osteoblast activity with products of collagen synthesis (Kuo and Chen, 2017). There are many limitations involving these biomarkers, such as biological, exogenous and technical reasons, as well as both intra- and inter-laboratory variability. These current bone biomarkers can also not be used for early diagnosis of bone loss. The main function of these biomarkers is to aid in monitoring the response of treatments (drugs and diets), as an increase in the biochemical marker levels has been shown to be related to greater fracture risk (Hlaing and Compston, 2014).

New biomarkers for improving the understanding of physiological interactions and metabolic responses to oestrogen loss need to be investigated. Novel technologies and bioinformatics tools offer the potential to investigate these complex interactions. Metabolomics aims to obtain the most relevant biochemical information from any health condition, as well as tracking the effects of drug or diet interventions (McNiven et al., 2011); however, metabolomics has not been used extensively to understand the association between the plasma metabolome and bone loss in postmenopausal women. Outcomes from metabolomics analyses would be expected to facilitate the discovery of new biomarkers associated with bone loss that aid an understanding how oestrogen loss influences the metabolic regulation of bone remodelling during menopause.

1.2 Initial research questions

This PhD project was part of a collaboration between Massey University, three institutes from Singapore's Agency for Science, Technology and Research, the University of Auckland and AgResearch. The project was funded via the bilateral agreement between the New Zealand Ministry of Business, Innovation and

Employment, and A*Star in Singapore. The aims of the overarching project were to identify and validate biomarkers using imaging and metabolic methods for clarifying the underlying mechanism of the diabetes risk in Singaporean–Chinese (SC) women. The project focused on the Chinese phenotype as it represents 70% of the Singapore demographic. The project addressed two research questions in three objectives. 1) Can novel imaging and metabolic markers be identified and validated to improve the detection of SC women at increased diabetes risk? 2) Can appropriate dietary strategies improve metabolic health in SC women at increased diabetes risk?

- Objective 1: improved body composition assessment of SC women for detection of early diabetes risk.
- Objective 2: new metabolic markers in SC women for identification of early diabetes risk.
- Objective 3: improved analyses of alterations in metabolic control in response to acute dietary interventions in SC women.

During menopause, there are several changes associated with a variety of pathologies such as diabetes and bone loss, and postmenopausal women are also at increased osteoporosis risk, which increases with age (Karimifar et al., 2012). The study cohort included a group of 97 postmenopausal women aged between 55 and 70 years. Thus, this PhD thesis was part of this project and was part of objective 2, where the aim was to provide rationale for gaining knowledge of the specific altered mechanisms and interactions between bone cells and bone remodelling in postmenopausal osteoporosis. The OVX sheep as a large animal model for postmenopausal osteoporosis was used to prove and explore how

these perturbed mechanisms and their interactions result in bone loss. The OVX sheep model has a faster rate of bone healing than in humans, but is still considered a suitable model for human bone turnover and remodelling activity (Pearce et al., 2007). There is, however, a lack of knowledge on the association between the metabolome and bone loss.

The objectives of my project were to:

1) optimise and characterise a sheep model for postmenopausal osteoporosis;
2) identify novel biomarkers to improve our understanding of bone loss in women;
3) acquire knowledge on how oestrogen loss influences the metabolic regulation of bone remodelling during menopause;
4) determine the interaction between the plasma metabolome and lipidome of sheep and bone remodelling; and
5) describe the association between the plasma metabolome and lipidome of postmenopausal SC women and bone loss.

1.3 Thesis introduction

Chapter 2 defines the scope of the thesis and presents the current knowledge about postmenopausal osteoporosis and the recent findings on the plasma metabolome and bone health. Chapter 3 describes a sheep model for bone loss over a short period of time. Chapter 4 presents variations within skeletal sites and discusses bone loss at different anatomical areas in OVX sheep. Chapter 5 employs the sheep model developed in Chapter 3 and presents for the first time results of a MS-based metabolomics approach, and discusses the association of the plasma metabolome with bone loss in the sheep model. Chapter 6 presents the results of altered plasma lipidome in the OVX sheep and discusses the relationship between the plasma lipid profiles and the bone remodelling process. Chapter 7 presents the findings in a human cohort of SC postmenopausal women using the same MS-based metabolomics approach, and discusses the association of the serum metabolome and lipidome with bone loss in women. Chapter 8 presents general discussions and then conclusions on all the findings obtained during this project. Future work and perspectives are also suggested.

Chapter 2

Literature review

This chapter reviews the current knowledge about the biology of bone tissue. In addition, the pathogenesis of osteoporosis and its current assessments are discussed. Next, a review of metabolomics approaches and recent findings on the plasma metabolome in models of osteoporosis are discussed. Finally, knowledge gaps are defined, where the aim was to evaluate whether LC–MS-based untargeted metabolomics was suitable to identify lipids and metabolites associated with bone loss in postmenopausal women.

2.1 Bone

2.1.1 Bone structure

Bone is an active tissue undergoing a continuous remodelling process to preserve skeletal strength. Bone is a component of the skeletal system with several functions in the body; one of them is its structural function, which gives support and protection to vital organs such as the heart and lungs, and it also provides strength and rigidity. Further, bone stores minerals such as calcium and phosphates, and regulates these to maintain the levels in blood (Barrère et al., 2006; Cohen Jr, 2006; Hadjidakis and Androulakis, 2006).

The adult skeleton is formed out of more than 206 bones, including long bones (humerus, femur and tibia), short bones (wrist and ankle), flat bones (sternum and skull) and irregular bones (pelvis and lumbar spine). Bones can be classified into two categories depending on their structure, and the long bones can be used to describe the macrostructure of bone. A long bone has two cylindrical ends (epiphyses), which are formed out of trabecular bone and a central shaft (diaphysis) formed with cortical bone. The diaphysis and epiphysis are connected by a narrowed shape named metaphysis. Moreover, bone structure can be arranged either in a cortical (compact) or cancellous (trabecular) manner. Approximately 80% of the skeleton is formed by cortical bone, while cancellous bone is found in the interior of the end of long bones as well as within flat and irregular bones such as the sternum, skull, pelvis and lumbar spine, whose cavities are composed of blood vessels, marrow and adipose tissue (Barrère et al., 2006; Stevens, 2008; Brandi, 2009).

Bone consists of two types of structures: a mineral phase formed by crystals of hydroxyapatite [$Ca_{10}(PO_4)_6(OH)_2$] with carbonate, magnesium and acid phosphate (70–90% mineral/dry weight) and ions such as Na^+, Mg^{2+}, HPO_4^{2-}, Cl^-, F^- and CO_3^{2+}; and an organic part consisting of collagen fibres (90% type 1 collagen) and noncollagenous proteins (Flynn, 2003; Clarke, 2008). Collagen plays a key role in the structure and function of bone tissue, where collagen type 1 is the most abundant (Young, 2003). This has a repetitive amino acid sequence of glycine–X–Y, where X is proline and Y is hydroxyproline. Along this repetitive structure, three polypeptide chains are formed: two 1α chains and one 2α chain. This confers to the type 1 collagen a singular triple-helical structure, which is responsible for the crosslinking chemistry and structure given to the organic phase characterised by some properties such as strength and viscoelasticity (Fratzl et al., 2004) .

Bones are adapted to changes in the mechanical loadings and physical activities of life without breaking (Liebschner, 2004). This adaptation is mainly due to bone materials and their relative amount, arrangement and molecular structure. These comprise minerals and proteins (type 1 collagen) both having different mechanical properties; the mineral confers strength and stiffness to the bone and the collagen is tough providing flexibility. Thus, the combination of these properties and the proportion of those in space provide the ability to disperse energy under mechanical deformation, stiffness and resistance to avoid fractures (Currey, 2003; Fratzl et al., 2004; Turner, 2006).

2.1.2 Bone cells

Bone is a mineralised connective tissue containing three types of bone cells: osteoblasts, osteocytes and osteoclasts (Figure 2.1).

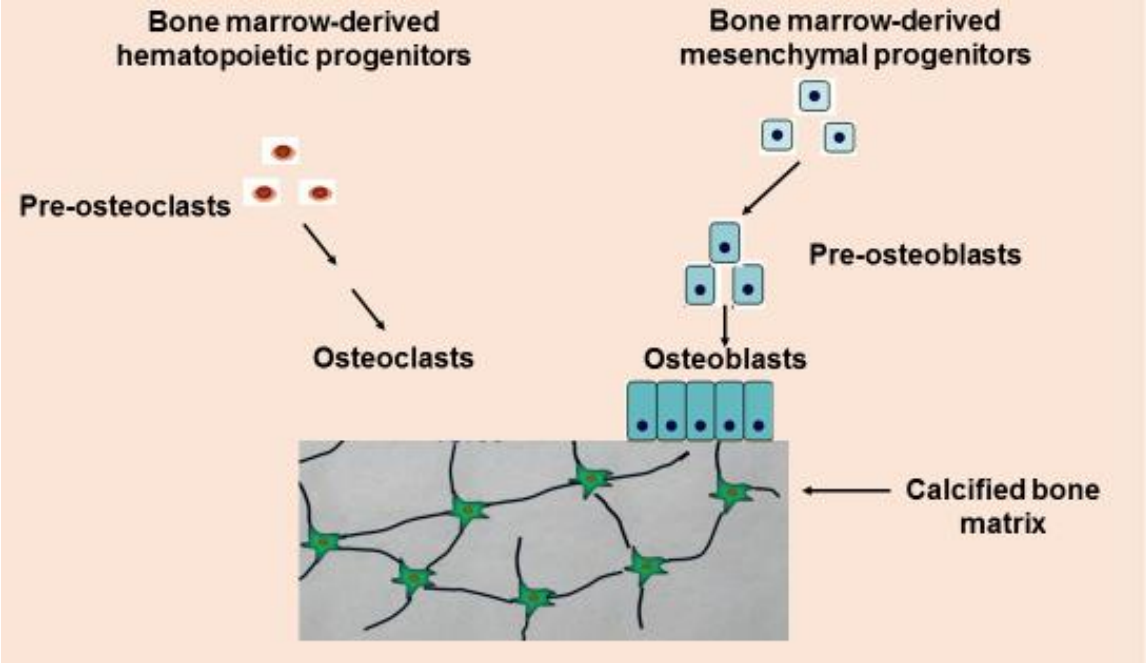

Figure 2.1: Schematic of the bone remodelling process and the basic multicellular unit (BMU). The bone remodelling compartment consists of the cells compromising osteoblasts, osteocytes and osteoclasts. Osteoblasts and osteoclasts are derived from mesenchymal and hematopoietic precursors, respectively. Diagram is modified from (Kapinas and Delany, 2011).

Bone is a dynamic organ that is continually formed by osteoblasts and reabsorbed by osteoclasts. The balance between bone formation and bone resorption cells, which are highly coupled to ensure that the bone mass is preserved, depends on the actions of local and systemic factors, including hormones, cytokines and biochemical stimulation, that regulates bone cell differentiation and functions (Crockett et al., 2011).

2.1.2.1 Osteoblasts

Osteoblasts are bone cells responsible for the formation of new bone. Osteoblasts are mononucleated cells, and their roles are in the formation of the organic matrix called osteoid, in calcification and in the synthesis of proteins. Osteoblasts develop from mesenchymal stem cells (MSCs); MSCs require the factor Sry HMG box protein 9-positive ($SOX9^+$) to derive osteoblasts and chondrocytes, and the synthesis of bone morphogenetic proteins (BMPs) and members of Wingles (Wnt) (Calvi et al., 2001). Then, runt-related transcription factor 2 ($RunX2^+$) is expressed and MSCs differentiate to osteoprogenitors. Simultaneously, the differentiation depends on some transcriptional factors such as $SOX9^+$ to differentiate to chondrocytes; whilst osteoblasts develop when osterix (OSX^+), $RunX2^+$ and β-catenin are elevated (Gaur et al., 2005; Hill et al., 2005). Wnts and Wnt pathway components affect early bone development stages. Wnts are cysteine-rich glycoproteins involved in cell differentiation, cell-fate specification and cell survival. The Wnt/β-catenin pathway promotes $RunX2^+$ expression to induce osteoblast differentiation (Bain et al., 2003; Gaur et al., 2005). Then, the osteoblasts become activated and are located alongside the bone surface, where they form the bone matrix (osteoid) during bone formation. Mature osteoblasts may undergo apoptosis, differentiate into osteocytes or become lining cells. Osteoblasts produce type 1 collagen and noncollagenous proteins including osteocalcin and alkaline phosphatase. Total alkaline phosphatase activity is an indicator of osteoblast differentiation. Osteoblasts regulate osteoclast differentiation by expressing two cytokines, macrophage colony-stimulating factor (M-CSF) and receptor activator of nuclear factor-κB ligand (RANKL) (Capulli et al., 2014). Osteoblasts also inhibit osteoclastogenesis

by blocking the RANKL–RANK interaction via osteoprotegerin (OPG), a tumor necrosis factor (TNF) receptor expressed in osteoblasts (Proff and Römer, 2009; Yamashita et al., 2012).

2.1.2.2 Osteocytes

Mature osteoblasts that have finalised their role in the bone matrix become osteocytes. Among the bone cells, osteocytes are the most abundant (around 95%). It is hypothesised that they detect alterations in skeletal bone such as microfractures, and maintain bone structure. The osteocytes are connected with osteoblasts from the surface and adjacent osteocytes in the bone matrix, and form long dendritic processes. These form a mechano-sensing network of signalling that evaluates the mechanical loading of bone. When a microfracture is present, a signal is generated which travels throughout this matrix until it reaches the bone surface, where it provokes the start of bone remodelling, although this has not been fully validated (Prentice, 2001; Young, 2003; Bonewald, 2007; Matsuo and Irie, 2008). Then, osteocytes appear to use the Wnt/β-catenin signalling pathway to send signals of mechanical loading to bone cells (osteoblasts) on the surface (Bonewald and Johnson, 2008). Osteocytes also secrete sclerostin to downregulate bone response to a mechanical loading. Hence, sclerostin inhibits bone formation through Wnt/β-catenin signalling in osteoblast differentiation by binding to the low-density lipoprotein-related protein 5/6 (LRP5 and LRP6) and inhibiting canonical Wnt/β-catenin signalling (Li et al., 2005). This is supported by Wijenayaka et al. (2011), who found that sclerostin upregulates osteoclastogenesis. Further, osteocytes promote bone resorption due to expressing RANKL. Nakashima et al. (2011) reported that mice lacking

this factor in osteocyte cells showed an osteopetrotic phenotype, which is characterised by an altered bone resorption and increased bone density.

2.1.2.3 Osteoclasts

Osteoclasts resorb bone through secretion of acid and proteases at a small compact and cortical bone area named a basic multicellular unit (BMU; Figure 1) (Proff and Römer, 2009). Osteoclasts have several morphological and phenotypic characteristics such as multinuclearity and expression of tartrate-resistant acid and the calcitonin receptor (Teitelbaum and Ross, 2003). These cells develop from hematopoietic stem cells (Robling et al., 2006). Osteoclasts are multinucleated cells with apical and basolateral sides, each having different structures and functions (Clarke, 2008). Osteoclast differentiation is controlled by proteins, cytokines and growth factors that affect maturation of the monocyte–macrophage lineage (Väänänen et al., 1998). The proteins involved are M-CSF and RANK, which are regulated by the cytokine TNF-α. The pre-monocyte produces M-CSF which allows the differentiation of the osteoclast precursor, and during this stage, the cells express RANK. Thus, it is possible to activate osteoclasts through RANK and colony stimulating factor 1 (CSF-1), which are cytokines needed for osteoclast differentiation and survival (Raggatt and Partridge, 2010). Additionally, some chemoattractants have been reported as being responsible for migration and targeting of the osteoclasts on the BMU, such as stromal cell-derived factor-1 (SDF-1). There are also other matrix metalloproteinases (MMPs), required by osteoclasts, such as MMP14, to move through the bone surface (Bar-Shavit, 2007). Active osteoclasts are highly polarised with specific membrane domains; one of them, the sealing zone, is

responsible for sealing the resorption area. In addition, adhesion molecules such as the integrin αvβ3 mediate the attachment of the osteoclast to the bone matrix (Ross and Teitelbaum, 2005).

The activation of osteoclasts is regulated by osteoblastic lineage cells, as mentioned above. These cells of osteoblastic lineage express the factors receptor activator of nuclear factor-kappa ligand (RANKL), M-CSF and osteoprotegerin (OPG); while the pre-osteoclasts express RANK and c-Fms. RANKL on the osteoblastic lineage cells activates osteoclastogenesis by binding to and activating RANK on the osteoclast precursor. This activation by RANKL is controlled by three cytokines: interleukin-1 and -6 (IL-1 and IL-6) and TNF-α; as well as by vitamin D (1,25-dihydroxyvitamin D_3). On the other hand, transforming growth factor β (TGF-β) and oestrogens may cause inhibition of osteoclastogenesis and bone resorption. M-CSF plays an important role in bone resorption due to being an important factor in the initiation of differentiation of the pre-osteoclasts. Finally, OPG is another key factor in this process because it has the ability to maintain a balance between bone resorption and formation, thereby blocking the effects of RANKL on osteoclasts. OPG expression is regulated by most of the factors that induce RANKL expression (Boyce and Xing, 2006). Further, oestrogen increases the levels of OPG (Riggs, 2000). In addition, Wnts/β-catenin controls osteoclastogenesis by enhancing the OPG-to-RANKL ratio in osteoblasts (Glass et al., 2005). The Wnt5 produced by osteoblasts promotes RANK expression in osteoclast precursors (Maeda et al., 2012). Thus, factors and hormones act in harmony, inducing the osteoclast formation directly and/or blocking activation via OPG to control and maintain the homeostasis of

bone remodelling (Christenson, 1997; Khosla, 2001; Robling et al., 2006; Proff and Römer, 2009; Kular et al., 2012; Rosenberg et al., 2012).

2.1.3 Bone remodelling

Bone is an active tissue with metabolic activity and the ability to grow and synthesise new bone through the activity of several types of bone cells. Bone remodelling is a complex process and depends on the synchronisation of bone resorption and subsequent bone formation, where osteoclasts are active early in this phase (Christenson, 1997). Bone remodelling is initiated in response to changing mechanical environments and to repair microcracks in the bone matrix. Bone remodelling occurs at the BMU, and multiple active BMUs are present in the skeleton at any one time. These processes are dependent on bone cells, mechanical demands, growth factors, enzymes and hormones (Flynn, 2003; Turner, 2006; Peacock, 2010). The bone cells play a key role in this metabolic process. Osteoclasts act on resorption and the osteoblasts on formation of bone and mineralisation, but only the osteocytes take part during all the processes (Marks and Popoff, 1988; Kular et al., 2012).

The remodelling of the bone comprises resorption, reversal, formation and resting phases (Figure 2.2).

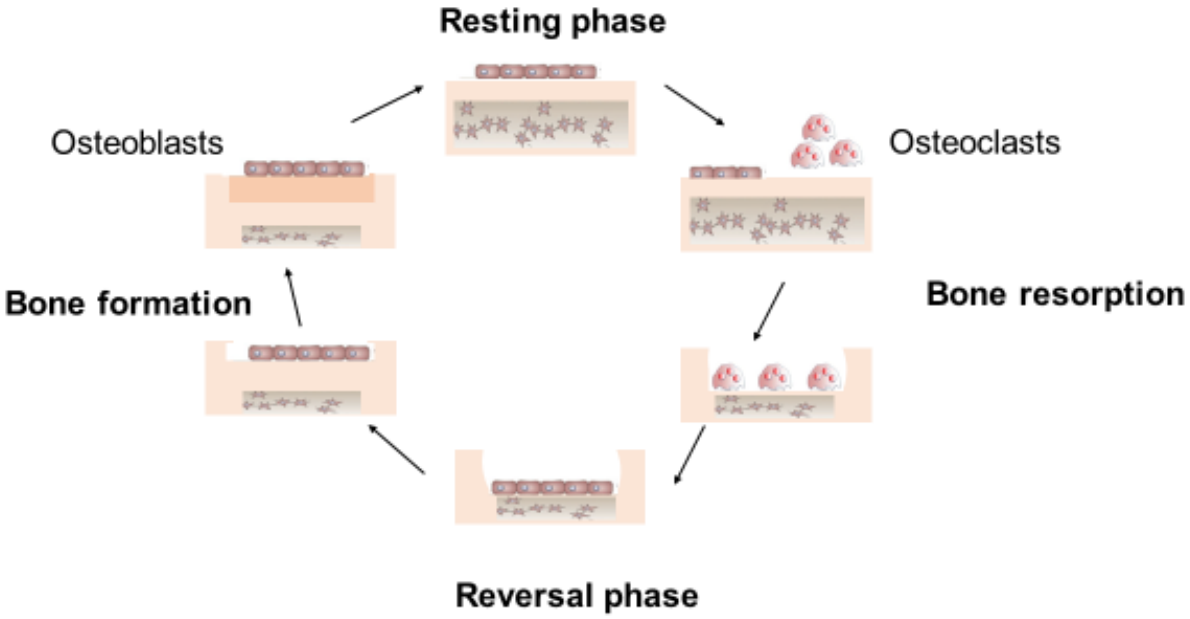

Figure 2.2: Bone remodelling stages**.** Simplified scheme of bone remodelling stages, where osteoclasts reabsorb old bone and stimulate osteoblasts to make new bone. Modified from (Bonjour et al., 2014).

The production and differentiation of osteoclast precursors from the hematopoietic stem cells is known as the initiation phase, followed by a differentiation phase which turns them into mature osteoclasts, which then initiate erosion of bone. This phase is named resorption, and osteoclasts normally reduce the bone and form lacunae approximately 100 µm in diameter and 50 µm deep. During the first stage of resorption, calcium phosphate crystals are digested through their link to collagen by the osteoclasts in the bone matrix. Then, the collagen residues are digested by enzymes (collagenases) and these residual molecules are internalised or transported across the cells from the apical to the basolateral side. The apical side facing the bone secretes proteolytic enzymes such as acidic hydrolases, including cathepsin K, and MMPs, such as the MMP-9 important for the degradation of the organic component of bone. While the basolateral side facing the vascular stream has receptors for hormones and other substances important for ion transport and response to signals (Christenson,

1997). During the reversal phase, osteoclasts are detached from the bone surface, and macrophage-like cells are thought to contribute to stimulating osteoblasts and removing old bone from the resorption phase. Once the eroded area has been cleaned, bone resorption changes to bone formation by osteoblast precursors. Then, new bone is formed by osteoblasts during the formation phase, where the osteoblasts lay down the osteoid matrix (mainly type 1 collagen). After this, when the BMU is filled with osteoid, the mineralisation phase takes place, and this matrix is mineralised with hydroxyapatite. Bone remodelling is a regulated process and therefore an imbalance may result in bone mass reduction with a subsequent bone loss. Factors such as parathyroid hormone and gonadal steroids control bone remodelling, but cytokines and growth factors are also crucial to regulate bone cells (Christenson, 1997; Teitelbaum, 2000; Martin and Sims, 2005; Henriksen et al., 2009; Proff and Römer, 2009; Kular et al., 2012).

2.1.3.1 Systemic regulation of bone metabolism

Bone metabolism is regulated mainly by several circulating hormones and growth factors, including PTH, vitamin D and oestrogen (Figure 2.3).

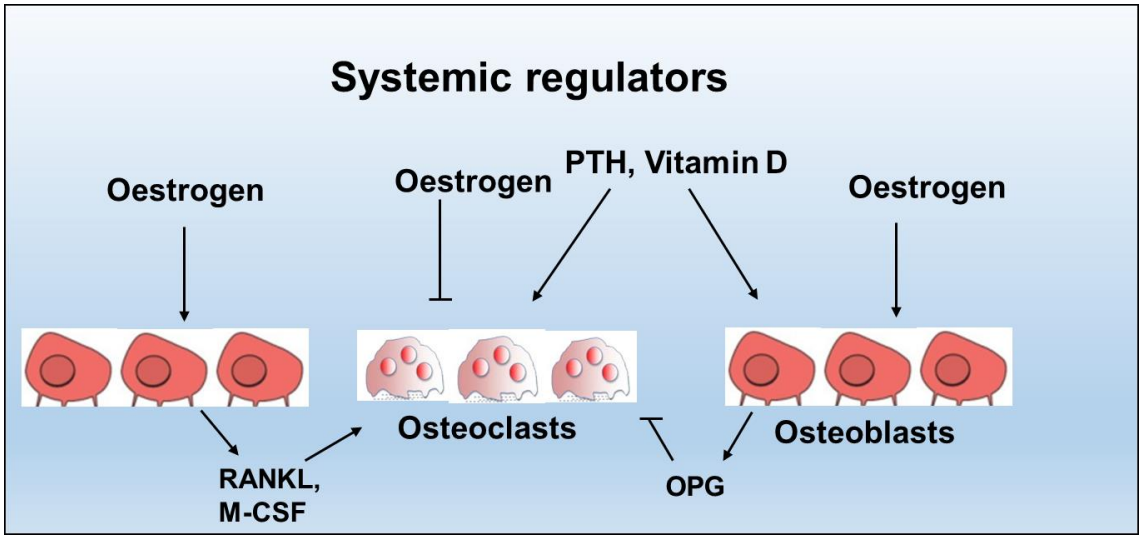

Figure 2.3: Systemic regulation of bone remodelling. In osteoclasts, oestrogen prevents bone resorption by directly inducing apoptosis of osteoclasts. Oestrogen blocks RANKL/M-CSF, thus suppressing RANKL-induced osteoclast differentiation. In osteoblasts, oestrogen inhibits osteoblast apoptosis. Oestrogen controls the expression of RANKL, OPG and M-CSF. PTH induces differentiation of osteoblast precursors. PTH activates bone resorption through producing RANKL and M-CSF. Vitamin D enhances osteoblastogenesis through differentiation by mesenchymal stem cells (MSCs) to osteoblasts. Arrows and T-bars indicate activating and inhibiting functions, respectively. Modified from (Tsartsalis et al., 2012)**.**

2.1.3.1.1 Parathyroid hormone (PTH)

PTH regulates the commitment of mesenchymal stem cells to the osteoblast lineage, and has both anabolic and catabolic effects on bone metabolism (Silva and Bilezikian, 2015). PTH increases the number and activity of osteoclasts, and promotes both recovery of Ca^{2+} at the level of the kidney and production by the kidney of calcitriol, the active form of vitamin D. PTH is the main regulator of plasma calcium and plays a vital role in bone remodelling (Wein and Kronenberg, 2018). Thus, calcium homeostasis is maintained as a result of the release of PTH when there is a reduction of plasma calcium. Upon release, PTH

activates bone resorption, resulting in an enhancement of osteoclastogenesis through promoting MCP-1 and RANKL in osteoblasts (Poole and Reeve, 2005; Raggatt and Partridge, 2010); when PTH is administered constantly, it promotes bone resorption. As a result, high doses of PTH stimulate RANKL production by osteoblasts and suppress OPG levels, causing an increase in bone resorption (Ma et al., 2001; Hofbauer et al., 2004; Qin et al., 2004). PTH also controls osteoblastogenesis, osteoblast/osteocyte apoptosis and bone mineralisation (Isogai et al., 1996; Goltzman, 1999). Conversely, low PTH as a result of high plasma calcium enhances osteoblast formation and differentiation by activating $RunX2^{+}$, promoting osterix expression and the β-catenin pathway, and the ultimate deposition of calcium in bone. Thus, bone formation is enhanced when PTH is administered intermittently or in low doses (Selvamurugan et al., 2000; Kim et al., 2003; Boumah et al., 2009). PTH blocks sclerostin expression in osteocytes and increases bone formation rate. Mechanical stimulation and the PTH signal via PTH receptors on osteocytes enhances the Wnt signalling pathway, allowing bone formation to occur and improving bone mineral density (Bellido et al., 2013).

2.1.3.1.2 Vitamin D (1,25-dihydroxyvitamin D_3)

Vitamin D impacts on bone metabolism, and the most active form of vitamin D promotes removal of calcium from the bone to control calcium metabolism. Vitamin D is changed to 25-hydroxyvitamin D in the liver, and is subsequently converted to 1,25-dihydroxyvitamin D_3 (the active metabolite of vitamin D) in the kidneys. The synthesis of osteocalcin by osteoblasts is dependent on 1,25-dihydroxyvitamin D_3 (Beresford et al., 1984). 1,25-Dihydroxyvitamin D_3 binds to a vitamin D receptor and osteoblasts to control the

calcium-specific nuclear hormone receptor, and thus there is an increase in intestinal calcium absorption and regulation of bone turnover (Holick, 2004). However, calcium absorption is regulated by a cytosolic calcium-binding protein, calbindin-D9k, and its synthesis is dependent on 1,25-dihydroxyvitamin D_3. Thus, the diffusion of Ca^{2+} is facilitated by calbindin-D9k across the intestinal cell, where a Ca-ATPase at the basolateral membrane mediates the active extrusion of Ca^{2+} and takes place against an electrochemical gradient (Bouillon et al., 2003; Cashman, 2007). It has been reported that 1,25-dihydroxyvitamin D_3 enhances calbindin-D28k synthesis as well as osteocalcin and alkaline phosphatase activity. In *in vitro* studies, calbindin-D28k has been reported to have a role in mineralised matrix formation in bone marrow stromal cells. Hence, 1,25-dihydroxyvitamin D_3 is crucial for the intestinal absorption of calcium and is therefore essential for maintaining calcium homeostasis and mineralisation (Heaney, 2002).

2.1.3.1.3 Glucocorticoids and oestrogen

Glucocorticoids are steroid hormones of the corticosteroid class, and are often used clinically to reduce inflammation. They can cause secondary osteoporosis, as a result of suppression of osteoblast function and bone formation, through increasing apoptosis of the osteoblasts (Rodan and Martin, 2000; Canalis, 2003). Glucocorticoids increase the expression of RANKL and M-CSF and OPG is suppressed, resulting in impaired bone remodelling (Hofbauer et al., 1999; Canalis, 2003). Growth factors are also affected by glucocorticoids. Principally insulin-like growth factors (IGFs) increase the formation of type 1 collagen and mineral apposition rates, and reduce bone collagen degradation; however, glucocorticoids may have an effect on IGF I synthesis of mature

osteoblasts, where glucocorticoids may exert control by downregulation of osteoblastic IGF I expression, and this may lead to an uncoupling of bone remodelling (Delany et al., 2001). Glucocorticoids inhibit calcium absorption from the intestine by opposing vitamin D actions (Canalis et al., 2007).

Oestrogen, the primary female sex hormone, plays a key role in the bone resorption on the BMUs by inhibiting osteoclast differentiation and promoting apoptosis of osteoclasts (Khosla et al., 2012). Oestrogen also increases bone formation activity of osteoblasts, and is directly involved in bone remodelling to reduce bone turnover rate and maintain the balance between osteoclast activity and osteoblasts (Harada and Rodan, 2003). Osteoclast formation is controlled by oestrogen due to the inhibition of cytokines, and RANKL is suppressed by this hormone while OPG secretion is stimulated (Rodan and Martin, 2000; Saika et al., 2001). Additionally, oestrogen promotes osteoclast apoptosis by promoting the Fas ligand (FasL) in osteoblasts, where oestrogen receptor-alpha (ERα) is its target gene (Nakamura et al., 2007; Krum et al., 2008). Oestrogen deficiency enhances TNF-α production by T cells. TNF-α increases osteoclastogenesis by increasing RANKL and M-CSF.

The complex process of bone remodelling is controlled by oestrogen, PTH, vitamin D and cytokines (RANKL, OPG and M-CSF). The interaction between osteoblasts, osteoclasts and systemic regulators plays a significant role in regulation of physiological bone remodelling. Overall, an imbalance in the systemic regulators, as reflected by bone cells, involves several factors and their interactions. Currently the antiresorptive drugs for treatment of osteoporosis are well known to alter osteoclast functions, where those agents have shown a reduction in bone resorption but the effects of these in bone formation are still

under discussion. Better understanding of the mechanisms of bone remodelling will lead to the development of better treatments to target growth factors in osteoporosis or other bone pathologies.

2.2 Pathogenesis of osteoporosis

Bone is maintained by the dynamic balance of bone formation and bone resorption, and imbalances in these bone processes are responsible for bone diseases. Osteoporosis is characterised by low bone mass and deterioration of bone tissue with the consequent increase in fracture risk. Osteoporosis represents a huge public health problem in the elderly population and results in high care costs for health systems (Holroyd et al., 2008). The most frequent fractures are in the proximal femur, lumbar spine and distal forearm, but before the fractures occur, osteoporosis can be diagnosed with noninvasive methods to measure bone mineral density (BMD) (Cosman et al., 2014).

Osteoporosis is the most common metabolic bone disease and one of the most prevalent conditions associated with ageing. Osteoporosis can be classified as primary or secondary osteoporosis (Orimo et al., 2001). Primary osteoporosis can be classified into two different types. Type 1 affects postmenopausal women from the ages of 50–75 years, where higher trabecular bone loss occurs as a result of menopause (Riggs et al., 1998). This is mainly attributed to oestrogen deficiency, where the bone turnover cycle is impaired, and the amount of bone reabsorbed exceeds the amount of new bone deposited. Further, PTH overstimulates osteoclasts, and a reduced bone mass is the result (Raisz, 2005). Type 2 osteoporosis is age related and affects both men and women after the age of 70. Type 2 osteoporosis affects osteoblast function, where bone mass

decreases with microarchitectural alterations in bone as a result of a poor calcium absorption, an increase in PTH levels as well as a decreased intestinal 1,25-dihydroxyvitamin D_3 response (Riggs et al., 1998). Secondary osteoporosis bone loss occurs from diseases of the endocrine system, diseases of bone marrow, gastrointestinal diseases or treatment with corticoids, leading to fragility fractures and bone loss (Fitzpatrick, 2002).

2.2.1 Current assessments of osteoporosis

Postmenopausal women will exhibit bone loss and changes in their bone remodelling rate. Currently, several assessment methods are used to diagnose osteoporosis and it is frequently done through bone density measurements. These aid in the estimation of percentages of bone loss, prediction of the risk of fracture, and evaluation of the efficacy of treatments to prevent fractures (Bonnick and Shulman, 2006).

2.2.1.1 Dual-energy x-ray absorptiometry (DXA)

Dual-energy x-ray absorptiometry (DXA) is the gold standard for diagnosing osteoporosis. It measures bone mineral content and density, as well as fat mass and lean mass by using X-rays at two different energy levels, 40 and 70 keV (Rothney et al., 2009). This technique is a recognised method for measuring bone mineral density (BMD), determining a treatment and observing its effects. Further, this equipment permits noninvasive and reproducible assessments of bone density with a low radiation exposure.

The World Health Organisation (WHO) established criteria for diagnosis of osteoporosis. These criteria are used for assessments at the lumbar spine, hip

and forearm, which are the most common fracture sites in postmenopausal women. The bone mineral density measurements are reported in standard deviation (SD) values referred to as T-scores. Therefore, a T-score < –2.5 has been classified as osteoporosis, a T-score between –2.5 and –1.0 as osteopenia, and a T-score T ≥ –1.0 as normal BMD (Table 2.1) (World Health Organization, 1994). The hip, posterior and anterior spine (L1–L4) measurements are performed in order to diagnose osteoporosis (Damilakis et al., 2007). Although DXA is the gold standard method for screening, monitoring and assessing the risk of bone fractures, it cannot predict bone loss. DXA scans can only identify bone loss in a patient when serial BMD assessment have been done over a period of years. Therefore, other methods that offer the opportunity of measuring the metabolic alterations in biofluids for fracture prediction should be investigated.

Table 2.1: T-score scale. The WHO defines a T-score on the scale shown below. A BMD test compares the subject bone density to a "young normal" adult bone density. Results are given as a T-score.

DXA BMD values	Classification
T score > –1.0 SD	Normal BMD
T score between –1.0 and –2.5 SD	Osteopenia
T score between –2.5 and –3.0 SD	Osteoporosis
T score < –3.0 SD with 1 or more fragility fractures	Severe osteoporosis

(WHO working group definition of osteoporosis.)

2.2.1.2 Peripheral quantitative computed tomography (pQCT)

Quantitative computed tomography is another method for the assessment of bone mass and densitometry. The method is based on computed tomography, provides a cross-sectional image slice and assesses volumetric BMD (vBMD) in the peripheral skeleton. Peripheral quantitative computed tomography (pQCT) can differentiate cortical and trabecular bone, and assesses geometric properties of bone tissue. This technique has the advantage of measuring accurately the

density, dimension and distribution of bone. Trabecular bone can easily be differentiated from cortical bone, and bone strength can also be predicted by this technique. The disadvantage is that it underestimates vBMD when the cortical bone thickness is low (Rüegsegger et al., 1976; Blake and Fogelman, 2001; Szabo et al., 2011). Thus, advanced imaging techniques are important to identify individuals at risk for fractures to predict bone loss, evaluate bone fragility and monitor response to treatments.

2.2.2 Biochemical markers of bone turnover

Biochemical markers can be used for aiding in osteoporosis diagnosis. The importance of bone remodelling is well established, and as bone is continually changing, specific biomolecules (markers) are released into circulation as a result of bone remodelling. Biochemical markers of bone turnover are normally classified according to a bone process. High-turnover bone biomarkers offer the clinical potential to assess changes in bone remodelling over short periods of time, to monitor treatment efficacy and to provide complementary information to BMD (Swaminathan, 2001).

2.2.2.1 Bone formation markers

Markers of bone formation are by-products of active osteoblasts that are released during different phases of osteoblast development (Table 2.2).

Table 2.2: Bone formation markers for bone remodelling.

Marker	Origin	Advantages	Disadvantages
BAP	Enzyme present on the outer cell surface of osteoblasts	Indicator of osteoblast activity	High cross-reactivity with liver alkaline phosphatase
OC	Osteoblasts synthesise this noncollagenous Gla protein	Specific for bone formation	Rapid degradation
P1CP	Cleavage of the carboxy terminal (N-terminal propeptide of type 1 collagen (P1CP))	Measure new deposition of type 1 collagen	Single protein; rapid degradation; regulated by thyroid and IGF-1
P1NP	Cleavage of the amino terminal (N-terminal propeptide of type 1 collagen (P1NP))	Measure new deposition of type 1 collagen	Affected by small circadian rhythm

BPA = bone alkaline phosphatase, OC = osteocalcin, P1CP = procollagen type 1 carboxy-terminal propeptide, P1NP = procollagen type 1 amino-terminal propeptide.

The most used bone formation markers are bone-specific alkaline phosphatase (BAP), carboxy- and amino-terminal procollagen type 1 propeptide and osteocalcin. BAP is a membrane isoenzyme with multiple isoforms including placental, intestinal, germ cell and tissue-nonspecific. The tissue-nonspecific enzyme is expressed in the liver, kidney and bone, and has been used as a marker of osteoblast activity (Langlois et al., 1994). Osteocalcin (OC) or bone GLA-protein (γ-carboxyglutamic acid (Gla) residues) is a noncollagenous protein and regulates calcium and bone formation. This noncollagenous protein accounts for up to 10% of total noncollagenous proteins. It is produced by osteoblasts, and vitamin 1,25-dihydroxyvitamin D_3 regulates its expression (Risteli and Risteli, 1993; Christenson, 1997; Allen, 2003). This small protein is vitamin K dependent,

as this vitamin is a cofactor necessary for the formation of γ-carboxyglutamic acid (Gla) residues, which support the calcium binding characteristics of the protein (Risteli and Risteli, 1993). OC is released from bone cells during formation and from bone matrix during resorption (Swaminathan, 2001).

Type 1 collagen is the most abundant form of collagen in the organic phase of the bone. Up to 90% is synthesised by osteoblasts as procollagen precursor molecules. The procollagen molecule has amino- and carboxy-terminal extension peptides. These peptides, named procollagen type 1 amino-terminal propeptide (P1NP) and procollagen type 1 carboxy-terminal propeptide (P1CP), are used as clinically relevant bone formation markers. P1NP has two major components with fragment sizes of 100 and 30 kDa. P1NP has been proposed to indicate bone turnover in postmenopausal women (Vasikaran et al., 2011b). P1CP is a protein with a molecular weight of 115 kDa, and contains mannose receptor chains of the hepatic cells (Melkko et al., 1990).

2.2.2.2 Bone resorption markers

During bone resorption, osteoclasts release collagen breakdown products such as collagen crosslinks, telopeptides and enzymes (Risteli and Risteli, 1993; Swaminathan, 2001; Seibel, 2005). These collagen breakdown products can be used as markers to measure the bone response to therapies (Table 2.3).

Table 2.3: Bone resorption markers for bone remodelling.

Marker	Origin	Advantages	Disadvantages
TRAP5b	Enzyme synthesised by osteoclasts	Secreted by osteoclasts during bone resorption	Enzyme is unstable to pH; current analytical methods lack specificity and sensitivity
Cathepsin K	Enzyme synthesised by osteoclasts	Secreted by osteoclasts during bone resorption	
CTx-1	Telepeptides of type 1 collagen released during bone resorption by cathepsin-K	Sensitive marker of bone resorption	Affected by food intake and circadian rhythm
NTx-1	Telepeptides of type 1 collagen released during bone resorption by cathepsin-K	Sensitive marker of bone resorption	Not affected by food intake
DPD	Released when type 1 collagen breaks down	Measures degradation of mature collagen	Nonspecific 24-h collection, needs to be corrected for creatinine
PYD	Released when type 1 collagen breaks down	Measures degradation of mature collagen	Nonspecific 24-h collection, needs to be corrected for creatinine

TRAP5b = tartrate-resistant acid phosphatase–isoform 5b, CTx-1= carboxy-terminal cross-linked telopeptides of type 1 collagen, NTx-1 = amino-terminal cross-linked telopeptides of type 1 collagen, DPD = Deoxypyridinoline, PYD = Pyridinoline.

Tartrate-resistant acid phosphatase–isoform 5b (TRAP5b) is a bone enzyme synthesised by osteoclasts and released into the circulation by leakage during resorption (Halleen et al., 2001). Similarly, cathepsin K is an enzyme synthesised by osteoclasts which is present in the outer membrane of these cells. During bone resorption, cathepsin-K is released by osteoclasts and its key role is the degradation of bone matrix composed of hydroxyapatite and proteins, especially type 1 collagen (Garnero et al., 2003).

Crosslinks of collagens, such as pyridinoline (PYD) and deoxypyridinoline (DPD), are released during bone resorption when mature type 1 collagen is broken down by osteoclasts (Seibel, 2005). The concentrations of these crosslinks in the peripheral blood reflect the degradation rate of mature collagen.

PYD is found in cartilage, bone ligaments and vessels, whereas DPD is only found in bone and dentin (Eastell et al., 1993).

Other degradation products of bone collagen are telopeptides of type 1 collagen (NTx). Amino-terminal crosslinked NTx is released into circulation from the amino terminus of the mature type 1 collagen (NTx-1). NTx-1 is reported to be a sensitive marker of bone resorption (Christenson, 1997).

Carboxy-terminal extension peptides of mature type 1 collagen (CTx-1) are also released during bone collagen resorption. The CTx-1 marker has a linear eight amino acid sequence (Garnero et al., 2003) and has been shown to be highly bone specific. Higher blood plasma levels of CTx-1 are correlated with risk of osteoporotic fracture (Garnero et al., 2000; Rosen et al., 2000). During early menopause there is an increase in bone resorption (Seifert-Klauss et al., 2002), and CTx-1 levels continue to increase during late menopause (Garnero et al., 1996). Reginster et al. (2001) reported that CTx-1 can be used to establish a powerful discriminator in postmenopausal women with normal versus low BMD.

Biochemical markers of bone turnover serve as indicators of bone remodelling activity. Biochemical marker analyses are relatively noninvasive methods to assess bone remodelling status, as blood or urine samples can be easily collected. Further, these bone turnover markers increase during menopause and the proportion of bone loss is dependent on the active bone metabolism (Garnero et al., 1996; Chen et al., 2005). It has been proposed that assessment of procollagen type 1 amino-terminal propeptide (P1NP) and crosslaps (CTx-1) levels are appropriate for approximating the rate of bone turnover in postmenopausal women (Łukaszkiewicz et al., 2008). However,

current analytical methods have limitations in the detection of for whom treatment is suitable, or in the establishment of prognosis.

The clinical parameters used in the diagnosis of bone loss in postmenopausal women, including bone densitometry by DXA and bone turnover markers, are often considered too insensitive to provide diagnostic information on disease onset, prognosis and fracture risk. Further research is needed to better understand the changes in biomarkers of bone turnover, monitor treatment efficacy and provide better treatment for diseases of bone metabolism and osteoporosis (Szulc, 2012). Therefore, the search for novel markers that indicate what is occurring in bone will aid our understanding and will lead to the development of novel dietary and physical interventions to improve quality of life by reducing the osteoporotic risk in postmenopausal women.

2.2.3 Animal models of bone health

In clinical research, the use of animal models is important due to the well-known limitations associated with the use of humans as volunteers, including ethical challenges, specifically when the studies involve a novel therapy being tested in humans for the first time. Thus, to study osteoporosis, several animal models have been developed and tested in clinical research with the gold standard approach for osteoporosis being surgical ovariectomy (OVX) (Miller et al., 1995); however, comparing animal models to the human condition remains challenging. Clinical research in postmenopausal osteoporosis has been performed in mice, rats, rabbits, dogs, goats and sheep (Reichert et al., 2009). Rats are the animal model used most frequently due to their size and lower cost compared to large animals (Gomes and Fernandes, 2011). The rat model

has been used more frequently in experimental procedures for induction of bone loss such as hormonal interventions, immobilisation and dietary manipulations (Lelovas et al., 2008). Bone metabolic disorders related to postmenopausal women require animal models that have similar phenotypes as humans in order to compare the findings from animal models to humans (Egermann et al., 2005). Further, the FDA has recommended the use of non-rodent models (large animal models) for osteoporosis and emphasised the study period, which should be long enough to obtain significant changes in the skeletal system of the animal model (Thompson et al., 1995).

Sheep may provide a better animal model than rats in postmenopausal osteoporosis research, as sheep have more similarities to humans than the rodent models. Sheep are often used in biomedical research as their bone anatomy and metabolism are similar to those of humans (Newman et al., 1995; Reichert et al., 2009). The ovariectomised sheep has been explored more recently to examine the response of bone to OVX (Newton et al., 2004b). Several studies have been conducted using an OVX sheep model for osteoporosis with differences in bone mass and bone turnover (Lill et al., 2002c; Augat et al., 2003; Schorlemmer et al., 2005; Sigrist et al., 2007; Ding et al., 2010; Holland et al., 2011). Lill et al. (2002c) reported that glucocorticoids changed the bones of OVX sheep; however, the results did not reach statistical significance because of the small numbers per group. The sheep model therefore can be used to generate bone samples of a size approximating human bones for bone composition assessment by established or experimental methods, as well as to provide serial blood samples in sufficient volumes for measurement of known or novel bone markers. Finally, the sheep model is of interest for further exploration as recent

data suggest that sheep may be able to reverse osteoporotic bone loss (Ding et al., 2010).

2.3 The application of metabolomics to the study of postmenopausal osteoporosis

In normal bone remodelling, bone homeostasis is maintained between bone formation and bone resorption, with this process being highly regulated. Studies are required to better describe the sequence of events that result in bone loss in postmenopausal women, and in particular to identify the specific alterations in molecular signalling, gene expression and bone cell physiology that occur due to oestrogen withdrawal and the subsequent changes in bone remodelling and bone loss.

2.3.1 Metabolomics

Metabolomics is a recent “omics” technique, which comprises the analyses of metabolites and their chemical reactions produced by the metabolic pathways (Wood et al., 2014). The term omics refers to a field of study in biological sciences that aims to characterise and measure biological molecules (e.g., genes, proteins and metabolites translate to genomics, proteomics and metabolomics) of an organism. Omics-based technologies have been used to unravel mechanisms involved in disease pathogenesis. According to the central dogma of molecular biology and the ‘omic’ cascade, where genomics and proteomics (which are the most established omics platforms) focus on regulatory processes and post-translational modifications, metabolomics provides information on downstream biochemical end-products that correlate with the

cellular phenotype and important biochemical alterations (Whitfield et al., 2004; Patti et al., 2012).

Metabolomics studies the overall metabolome and the biochemical changes in biological samples (Mishur and Rea, 2012). Oliver et al. (1998) referred to the metabolome as “the characterisation and measurement of all small molecules (within a mass range of 50 – 1000 daltons) existent and detectable in a particular cellular condition or biological systems such as enzymes, cofactors, products and intermediates”. Metabolites can be divided into many classes based on their chemical properties, and are commonly separated and described based on their affinity for water as hydrophilic compounds (e.g., nucleotides, amino acids and carbohydrates) or hydrophobic compounds (e.g., mostly lipids).

In any biological system, both intrinsic and extrinsic factors are responsible for chemical changes occurring in metabolism, and therefore the use of analytical methodologies is required to allow their full identification (Oliver et al., 1998). The use of mass spectrometry (MS) and nuclear magnetic resonance (NMR) is common in metabolomics analysis (Cubbon et al., 2010), with both aiming to profile hundreds of metabolites and obtain complex and comprehensive data sets. When these data are associated with other information, such as clinical measurements or those from other ‘’omics’’ techniques, for example, transcriptomics or proteomics, it becomes possible to obtain a better picture of the way in which metabolites are affected by factors such as phenotype or genotype in an organism (Dixon et al., 2006).

Metabolomics is increasingly used to better understand the mechanisms of action, diagnosis and monitoring of disease (German et al., 2005). Additionally, metabolomics has the potential to develop non-invasive tests to quickly diagnose

diseases, and could influence progression from health research to clinical practice. Currently, diagnosis of pathologies such as osteoporosis is an important area of research, where the aim is to evaluate altered metabolic pathways and address early detection to prevent bone loss and osteoporosis-related fractures. Several metabolites are involved in bone metabolism; thus, the use of analytical technologies that allow the identification of those metabolites is required to detect and characterise novel bone biomarkers. The analytical methods can be applied for discovering early prognostic biomarkers to achieve the prediction of diagnosis and enhance treatment therapy for osteoporosis diseases. Currently, metabolomics is used to evaluate altered metabolic pathways of several diseases such as diabetes, cancer and cardiovascular diseases (Lindon et al., 2004; Zhang et al., 2012).

2.3.1.2 Experimental approaches

The metabolomics approach depends on the scope of the study, with both targeted analysis and metabolomics profiling (untargeted analysis) approaches being used.

Targeted analysis detects and quantifies a particular number of known metabolites from a selected pathway or pathways. This approach only focuses on a small portion of the metabolome and all the other mechanisms are disregarded. The targeted metabolomics workflow is applied on studies where a hypothesis is tested and the metabolites to be analysed are usually isolated from the sample matrix with extensive sample preparation (Dunn et al., 2011a; Mishur and Rea, 2012). In contrast, metabolite profiling identifies and quantifies a large variety of metabolites under defined conditions. This approach is used to

generate an analytical database of a broad set of metabolites from a biological system or matrix component, which allows the identification of alterations in the metabolism induced by disease state or interventions (Theodoridis et al., 2008; Dunn et al., 2011a; Vuckovic, 2012).

2.3.2 The workflow for untargeted metabolomics analysis

The analytical aspects involved in typical untargeted metabolomics experiments are experimental design, sample collection and preparation, separation technique, analytical experiments, data analysis, and interpretation (Figure 2.4) (Büscher et al., 2009; Álvarez-Sánchez et al., 2010a).

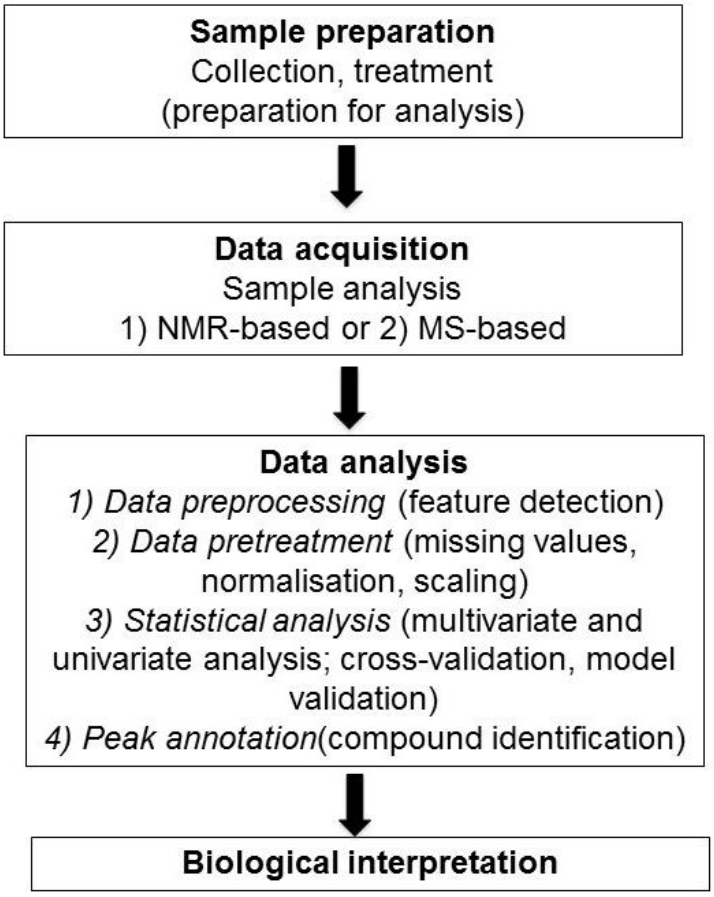

Figure 2.4: Scheme of a general metabolomics profiling workflow**.**

2.3.2.1 Sample preparation

Sample preparation is a crucial step in the analytical process, as it impacts on the metabolites extracted. Biological samples collected for metabolomics analysis require careful sample handing to ensure a reproducible extraction is performed. The steps in the sample preparation begin with experimental design, where designing the study, deciding on the number of samples, and collecting and temporarily storing samples all require definition, and strict standard operating procedures should be implemented to ensure reduction of unwanted variation in the dataset. In addition, for nontargeted metabolomics, sample preparation is optimised to avoid metabolite loss during the extraction and analytical procedure, ensuring a wide overview of the metabolome will be analysed (Álvarez-Sánchez et al., 2010b; Gika and Theodoridis, 2011).

After blood collection, in order to obtain a representative sample of the extracellular and intracellular reactions of the physiological state of interest, metabolism of the cells needs to be deactivated. Therefore, for sample collection factors such as the brand of vacutainer for blood collection, anticoagulant, temperature, velocity and duration of the centrifugation should be strictly monitored and controlled. Protocols for the extraction of metabolites will vary depending on the objective of the study. The most common methods for metabolite extraction include liquid-liquid extraction, solid-liquid extraction and solid phase extraction (Zhou et al., 2012). In general, metabolite extraction should be fast and with minimal handing to minimise metabolite degradation during preparation (Yin et al., 2013; Yin et al., 2015). The simultaneous extraction of the metabolome and lipidome can be achieved with a combination of solvents such

as aqueous methanol and chloroform for partitioning the polar and non-polar metabolites respectively. This allows the extraction of intracellular metabolites due to there is a disruption of the cell structure, while releasing the metabolites from the interior of the cell to the exterior (Bruce et al., 2009; Dunn et al., 2011b; Chen et al., 2013). In addition, to increase the permeability of the cells, freeze and low temperature cycles are included in the extraction process. Following extraction, freeze drying (lyophilisation) or evaporation using either vacuum or nitrogen blow-down are the most common methods for sample concentration. Freeze-drying samples is suitable for aqueous samples and with reduces the possibility of metabolite degradation as the solvent is evaporated without using heat. However, this approach is time consuming and it not suitable for organic solvents. Vacuum and nitrogen evaporation is more suitable for organic solvents than aqueous solvents, although the evaporation of the aqueous solvent takes longer and usually involves heating which is not suitable for thermally metabolites (Zou et al., 2013; Anton et al., 2015).

2.3.2.2 Data acquisition

The separation and description of all detectable metabolites in a sample is the aim of metabolomics. However, there is no single analytical method to cover the whole metabolome due to the wide range of molecular diversity within the metabolome, such as molecular weights, concentrations and polarities. NMR on the whole extract or MS coupled with a separation technique (usually liquid chromatography (LC) or gas chromatography (GC) on a small amount of the extract are the common analytical technologies used.

NMR has been one of the main approaches used in metabolomics and involves magnetic resonance fields and radio-frequency pulses in the nuclei of the atoms. When the atoms change from a low- to high-energy state, the radiation emitted when they return to low energy is measured. Little sample preparation is required for NMR and this technique provides highly reproducible results. However, NMR is relatively insensitive to metabolites present at low concentrations (Larive et al., 2015; Wolfender et al., 2015).

In contrast, the principle of MS is to generate ions from organic or inorganic compounds and separate these ions by their mass-to-charge ratio (*m/z*). Hence, both the qualitative and quantitative detection of these ions is possible by measuring their *m/z* and abundance (Dunn et al., 2011a). MS allows one to characterise the molecular weight of molecules and obtain their chemical information(Zhang et al., 2012). Generation of the ions prior to detection by MS has been a rapidly developing area over the past 20–30 years, and there are now many ion sources available to ionise metabolites. The most commonly used for metabolomics with LC–MS is electrospray ionisation (ESI), which ionises the components eluting from the liquid chromatographic separation of molecules (Theodoridis et al., 2012). Moreover, ESI–MS systems utilising LC are the method of choice for the analysis of complex samples due to their ability to measure a wide range of compounds (e.g., from amino acids to triglycerides), often without the need to chemically alter/derivatise prior to analysis, as is often required for GC–MS. In ESI-MS the mobile phase solvent containing the separated analytes is evaporated during the ionisation step. ESI is performed by applying a high electric charge to the evaporating solvent droplet containing the analyte, enabling the ion formation of the analyte followed by the charged ion

entering to the mass analyser by an electric potential and pressure difference. The formation of the positive or negative ions depend on the polarity of the electrical field applied to the ESI probe needle. In general, in positive mode molecules will be protonated with a non-covalent addition, while in negative mode deprotonated molecules or loss of chemical species are generally detected (Allwood and Goodacre, 2010). After a sample has been ionised, the ions need to be separated according to their *m/z,* thus the type MS analyser must be considered depending again on the goal of the experiment. There are many types of mass analysers, and the most common are: 1) time of flight (TOF), in which the time of flight of the ion from the source to the detector is correlated to the *m/z* of the ion. In this way, the ions are separated according to their differential speed; 2) the quadrupole (Q) uses the stability of the ions from the source to the detector to separate them per their *m/z* ratios by oscillating electric fields; and 3) the ion trap (IT), which uses an electrostatic field to trap ions and produce MS data (Dunn et al., 2011a). Quadruple-based MS analysers are recommended for quantitative profiling of metabolite concentrations and for the analyses of low concentration metabolites. For identification of metabolites, a mass analyser with MS/MS or high-quality tandem mass spectra (MS^2) capabilities for structural fragmentation data is needed, such as an ion-trap or Q-TOF system. Advances in mass spectrometry have led to the manufacture of the Orbitrap mass analyser, which is an ion-trap instrument capable of collecting very high-resolution mass spectral data. The Orbitrap mass analyser is now widely used for identification, analyte characterisation (i.e. classification if ambiguous identification is not possible) and quantification of molecules in biological systems. An Orbitrap can maintain high mass accuracy, does not require the constant use of calibration standards in

every sample or scan. The Orbitrap mass analyser can be coupled to a linear ion trap, quadrupole mass filter or simply used directly to provide high resolution data. Orbitrap mass spectrometers are commonly used in proteomics and metabolomics studies (Lu et al., 2010; Xiao et al., 2012; Zhou et al., 2012; Zubarev and Makarov, 2013).

MS systems can rapidly and accurately provide measurement of a diverse range of molecular ions and concentration ranges, then contribute data towards the identification of the molecules via the generation of MS fragments to obtain chemical composition in a comprehensive, selective and sensitive way. MS can be applied with GC or LC separation before detection. GC allows the separation of complex samples with different stationary phases. GC-MS is performed to metabolites of low boiling points, and as many of the endogenous metabolites do not have sufficient volatility for GC analysis a chemical derivatisation is needed to detect those metabolites that can be made volatile enough to be resolved by GC (Begley et al., 2009). LC allows the separation as result of metabolite equilibration between a liquid mobile phase and a solid stationary phase. The reversed phase LC separation is compatible with the analysis of aqueous samples for metabolome characterisation and analysis. This reversed phase separation uses a solvent system with a high water content and a gradient elution increases the organic solvent such as methanol or acetonitrile. This reversed phase is ideal in the analysis of non-polar metabolite species such as lipids. Conversely, hydrophilic interaction chromatography (HILIC) uses gradient elution from high organic to high aqueous, which allows the analysis and separation of polar metabolites including amino acids, organic acids, sugar and carbohydrates (Cubbon et al., 2010). Given the complex nature of the untargeted metabolite

profiling, both the highest resolution methods for the separation and identification of the complex array of metabolites in plasma is required. In addition, when the reversed phase is used with HILIC the coverage of the metabolome can be improved (Gika et al., 2014). Therefore, the use of this analytical technique is the best choice for detecting early prognostic biomarkers for bone health. For untargeted profiling, the preferred platform is LC–MS using electrospray ionisation (LC–ESI–MS), as this platform can resolve a wide range of chemical compounds into discreet individual peaks (Smith et al., 2006).

2.3.2.3 Data analysis

The main goals of data preprocessing are: 1) extraction of features from the LC-MS spectral data to determine identity and estimate relative abundance of possible metabolites; 2) alignment of multiple samples to correct retention time shifts within runs so that known and unknown metabolites can be compared correctly across the sample set; and 3) production of a table with the possible metabolites with their quantitative information for subsequent statistical analysis (Halket et al., 2005; Sugimoto et al., 2012).

The feature extraction procedure aims to group several signals (detected *m/z*) into features. There are many algorithms on how to extract features but XCMS and CAMERA are the most commonly used packages for metabolomics data preprocessing (Smith et al., 2006; Kuhl et al., 2011). The first step in data processing is converting the LC-MS raw data in a numerical format that can be used for statistical analysis. For LC-MS data processing, peaks from each chromatogram are detected, aligned and grouped across samples. Each group of peaks has a unique *m/z* and retention time and are subsequently called a

feature. The XCMS package provides tools for peak detection, non-linear retention time alignment, visualisation and relative quantification. First, XCMS requires the LC-MS raw data to be converted into mzXML format. Then the data can be imported and processed in R. XCMS uses a series of different algorithms/functions to sequentially process the LC-MS data. The first step is to detect and filter ion peaks using a function ‘xcmsSet’ and a ‘minfrac’ command calculation which determines the minimum percentage of features present in a single sample group. The CentWave algorithm is used for performing peak detection of high resolution MS data, and it utilises two parameters, ppm and peakwidth. Ppm indicates the mass spectrometer accuracy across the experimental dataset while peakwidth indicates the range of the chromatographic peak width in the experiment. Thus, the xcmsSet method slices the data into predefined mass widths and then detects peaks in the chromatogram fitting within the peak width thresholds. The minfrac value determines if features are representative across a portion of the samples (usually a pooled quality control samples made using a small portion of each experimental sample) and are then thus classed as valid features within this experiment to be incorporated into the data matrix. The next step after filtration and peak detection is matching the same peak from each sample across the whole experimental sample set. Peaks with similar retention times across multiple samples must be placed into groups and use the similar peaks for the time alignment function group. The function ‘retcorr’ uses a single sample to identify (usually the sample with the most features detected in it) and realign the samples by correcting the retention time drifting to the single reference sample. Finally, the ‘fillpeak’ function re-examines the raw mzXML data files and fills the intensity values of each of the missing peaks. The

final data matrix output is a list of features with peak areas for each feature across the complete sample set, with the features identified with a mass (*m/z*) and retention time (Smith et al., 2006). In addition, CAMERA is another package developed in R that aids to extract compound spectra, annotate isotopes and adducts (originating from the same metabolite) while providing a reduction in data complexity (Kuhl et al., 2011; Perez de Souza et al., 2017).

During data acquisition, quality control measurements are used to monitor the performance of metabolomics data collected, and these samples also provide a critical part of the data analysis workflow to detect problems such as injection problems, instrumentation failures, loss of sensitivity, noise and instrument chromatographic or mass drift. These quality control measurements include the use of internal standards of known metabolites, blanks samples and pooled samples. Internal standards for known metabolites are employed to review in real time the retention time and peak intensity during the analysis of large numbers of samples. The use of blanks aims to the identify system contaminants and batch-batch accumulation of unwanted biological contaminants within the analytical system. Pooled quality control (QC) samples are regular and repeated measurements of a representative sample. Pooled QC samples are aliquots of a sample pooled from multiple subjects in an equal amount mixed homogeneously. Thus, during data processing, pooled QC samples are used to standardise data across datasets. In addition, pooled QC samples aid to evaluate the coefficients of variation for every feature detected and filter those ones with many missing values or features above a coefficient of variation threshold. Thus, periodic analysis of pooled QC samples evaluate the measurement of reproducibility for

all signals and standardise the data between batches (Dunn et al., 2012; Broadhurst et al., 2018).

Then, data normalisation is used to reduce error in the data, such as decreasing sensitivity drift across the analytical batch of samples being analysed as the instrument becomes dirty/contaminated. There are two common normalisation methods used: 1) fitting an algorithm across all the samples based on the trends in the pooled QC samples within the experiment to subsequently adjust the peak areas of the samples (e.g., linear normalisation, locally weighted regression scatterplot smoothing (lowess) methods), or 2) using multiple internal standard compounds injected into the sample to correct the target compounds based on the internal standard response of the most similar internal standard in chemical structure/class (Katajamaa and Orešič, 2005; Sysi-Aho et al., 2007).

After processing, the data matrix can be exported into an Excel file or similar and explored with other software such as SIMCA, Minitab and R or online databases such as Metaboanalyst, which have the ability to perform statistical analysis and process multivariate data (Smith et al., 2006; Xia et al., 2015).

After loading the data matrix in MetaboAnalyst 4.0, two steps are followed to achieve consistency within the dataset prior to conducting the statistical analysis. Firstly, the quality control step, where the aims are to check the integrity and number of peaks, confirm the number of samples and treatment groups, and deal with missing values (Chong et al., 2018).

Missing values are features that are below the limit of detection and can be replaced using imputation methods for handling missing values such as half minimum (HM), mean, median, random forest (RF) and k-nearest neighbour (kNN) (Xia and Wishart, 2002; Liland, 2011). Secondly, data is normalised to

remove variation between analytical conditions unrelated to the biological difference so that the mass intensities can be comparable. The normalisation can be done by sample or feature normalisation. Feature normalisation methods are auto-scaling (mean-centred and divided by standard deviation of each variable), range scaling and Pareto scaling. After normalisation peak intensities should follow a normal distribution, then univariate and multivariate analysis can be conducted (van den Berg et al., 2006).

Multivariate analysis is used to find meaning in the whole dataset from the metabolome with the aim to identify changes of a metabolite between groups and find the correlation of the individual molecules. Principal component analysis (PCA), partial least squares (PLS) and orthogonal projections to latent structures discriminant analysis (OPLS-DA) are generally the most common multivariate analysis techniques applied in metabolomics (Liland, 2011).

PCA plots create lower-dimensional data based on variation from original high-multidimensional data (Ringnér, 2008). PLS is a supervised multivariate linear regression method aiming to find the association between two variables (X and Y) by maximising their covariance. The objective of this is to understand which variables (features) of X are more correlated to a response Y to make predictions of new biomarkers (Zernicke et al., 2006; Indahl et al., 2007). OPLS-DA is a multivariate linear model for classification and discrimination. The classification refers to the classification of new objects into one of two or more possible classes, and the discrimination is used for the two-class case, in which the objective is to maximise the separation between the two classes and highlight the key features contributing the most to the separation. The use of OPLS-DA

has been increasing for discrimination and biomarker development (Trygg and Wold, 2002).

Univariate analysis measures metabolites that discriminate the treatments under comparison. Common univariate approaches such as those in MetaboAnalyst include fold-change (FC) analysis, *t*-tests, and the volcano plot, which is a combination of FC analysis and *t*-tests for comparison of metabolites from two treatment groups (Xia et al., 2015).

There are two types of metabolite identification: putative identification and definitive identification. After performing statistical analysis the identification of the chemical composition of significant metabolic features identified by univariate methods and *t*-tests is based on: 1) a comparison of exact masses and retention times with those of compounds in internal libraries of chemical standards; 2) comparison with human metabolome database (HMDB) or MassBank; and 3) identification of peaks of the respective parent and potential fragment ions (Styczynski et al., 2007). The exact mass (*m/z*) of the selected peaks along with possible fragment mass data is used to identify compounds in databases. Databases such as HMDB contain metabolites with ESI and MS/MS spectra, where the identification of precursor ions is allowed followed by matching experimental MS/MS data against that one from the database. There are four levels for metabolite identification according to the metabolomics standard initiative. Level 1 requires at least two molecular properties of the putative metabolite to be corroborated with a pure standard analysed under identical analytical conditions. Identification of metabolites comparing against literature and database data is acceptable for level two and three of the metabolite identification. Finally, level four is for unknown metabolites (Vinaixa et al., 2016).

These levels of identification help standardise the annotation confidence of metabolomic data and assist in comparisons within the literature.

2.3.3 Metabolomics approaches in bone health

Osteoporosis is a common disease in the elderly. Treatment is focused on antiresorptive drugs, which generally shorten osteoclast formation and function, where the most common being selective oestrogen receptor modulator, bisphosphonates and calcitonin (Feng and McDonald, 2011). Despite the advancement in pharmacological treatments for the management of osteoporosis there is still a need to improve the existing therapies and find more effective therapeutic options for prevention of bone loss in postmenopausal women. During bone loss, there are changes in bone mass and these are associated with disturbed bone remodelling. Understanding signalling pathways in bone remodelling, specific to bone cells and systemic regulators, will aid in the development of new therapeutic options for osteoporosis.

2.3.3.1 Altered metabolic pathways in bone cells post-menopause

2.3.3.1.1 Bone cells and lipid metabolism

Whilst osteoblastogenesis is reduced in menopause as a result of oestrogen deficiency, adipogenesis and osteoclastogenesis are increased, and as a result, bone loss occurs; this has been associated with higher lipid levels in bone marrow stromal cells (Rosen and Bouxsein, 2006). Adipocytes and osteoblasts are derived from a common bone marrow stromal cell. The balance between adipocyte and osteoblast differentiation is regulated by a signalling communication pathway that requires extracellular stimuli (Muruganandan and

Sinal, 2014). Cell membranes are complex bilayers formed of lipids and proteins that limit the interior from the exterior environment (Ingólfsson et al., 2014). Thus, lipid metabolism disorders may affect osteoblastogenesis by interfering with key signalling pathways. Lipid metabolism plays a key role in bone mineralisation and has been linked to pathological conditions including obesity, metabolic syndrome, cardiovascular diseases and bone loss (Cui et al., 2005). Lipids such as acidic phospholipids and phosphatidylserine may form matrix vesicles containing calcium ions that can be utilised in the initial mineral nucleation stages (Reid et al., 2012). During menopause, with oestrogen deficiency, cholesterol levels are associated with low BMD in postmenopausal osteoporosis (Tankó et al., 2003). This is related to the cholesterol biosynthetic pathway, which has a key role for osteoblastic differentiation of MSCs and determines cholesterol levels and bone resorption cell activity (Parhami et al., 2002; Ikonen, 2008). Sphingosine 1-phosphate (S1P) levels are associated with lower femoral BMD and bone resorption markers in postmenopausal women. Here, S1P may stimulate bone resorption with a subsequent bone loss due to S1P interacting with the S1Pr in osteoblasts and T cells, and this interaction increases RANKL expression and osteoclastogenesis (Lee et al., 2012).

In addition, changes in mitochondria are progressive with ageing and oestrogen deficiency, where a decrease in oxidation resistance could lead to bone loss in women. Mitochondrial dysfunction leads to the generation of reactive oxygen species (ROS); studies indicate ROS act as mediators for osteoclast differentiation (Lee et al., 2005; Weitzmann and Pacifici, 2006). *In vitro* and animal models have shown that ROS have an impact on osteoclast differentiation and function as well as on osteoblast function. During ageing, ROS

lead to oxidative damage of macromolecules and mitochondrial DNA (mtDNA). Mutations of mtDNA decrease GH and IGF-1 concentrations (Garrett et al., 1990; Varanasi et al., 1999; Bai et al., 2004; Lean et al., 2005). This mtDNA dysfunction may impair IGF-1 action and lead to reduced BMD (Chan, 2006). Lipid oxidation products enhance intracellular oxidative stress in osteoblasts. Bioactive lipids and their intracellular molecular intermediates, and the associated increase of ROS production in ageing postmenopausal bone loss, remain to be fully elucidated (Tintut and Demer, 2014).

2.3.3.1.2 Bone cells and amino acid metabolism

Amino acids are involved in bone formation and they can improve BMD and bone strength; however, during menopause, changes in amino acids associated with oestrogen deficiency and ageing may affect bone mass. Amino acid pathways such as threonine, glutamine, arginine and proline metabolism have been reported to be altered in postmenopausal bone loss. Arginine increases GH and IFG-1 levels, reflecting an increased osteoblastic bone formation; arginine also releases nitric oxide, which is an inhibitor of bone resorption. The glutamine metabolism pathway regulates cellular differentiation and proliferation in osteoblasts and produces proline and amino acids present in the collagen structure. Taurine has been shown to have a stimulatory effect in the bone anabolic phase (Hanaa and Hamza, 2009).

During bone resorption, collagen is released into the circulation. Collagen is formed by three polypeptide chains, which gives it the triple-helical structure. Glycine (Gly) is needed to be present as every third residue in order for the chains

to form that triple helix; the sequence of collagen is a repeated Gly–X–Y, where X and Y are usually proline and hydroxyproline (Brodsky and Persikov, 2005).

Glycan metabolism may also mediate bone mass during oestrogen deficiency. Proteoglycan and glycosaminoglycan are extracellular components which regulate the osteolytic process. Proteoglycans and glycosaminoglycans also contribute to stimulate bone remodelling and matrix mineralisation, and to control hydroxyapatite crystal formation in trabecular bone as a function of metabolic activity and tissue age (Gamsjaeger et al., 2013). A study showed that glycan regulates the bone turnover process as a response to oestrogen deficiency, where glycan increased trabecular bone turnover and bone loss in OVX mice (Allen, 2003).

Further, histamine metabolism may be involved in trabecular bone loss in long bones of OVX rats, where histamine may be a first-line mediator of bone resorption. Oestrogen depletion releases histamine, IL-6 and TNF-α from MCs and precursors in the osteoclastic pathway (Lesclous et al., 2006).

Overall, lipids and amino acids are involved in crucial mechanisms by communicating among bone cells, and lately, there has been a growing interest in understanding their role in bone diseases. Therefore, the mechanistic links between adipogenesis, bone cell differentiation and amino acid metabolism may be the key findings to understand the mechanism of bone disease, and be useful as targets for the prediction of bone metabolism diseases.

2.3.3.2 Metabolomics analyses in animal models for osteoporosis

Several studies in rodent models have used serum metabolomics to identify non-invasive biomarkers of postmenopausal osteoporosis. The OVX rat

as an animal model of osteoporosis has shown an altered plasma metabolome after oestrogen depletion. A study analysed the OVX rat model for osteoporosis, where the relation between the metabolome and low BMD was the target analysed (Ma et al., 2013a). This study reported increased levels of arachidonic acid (AA, 20:4n-6), which stimulates RANK-L expression and blocks OPG secretion in osteoblasts (Coetzee et al., 2007), as well as reporting increased levels of cholesterol due to estrogen insufficiency, which blocks the activity of osteoblasts (Parhami et al., 2002), and increased levels of homocysteine, which promotes osteoclast formation. Another study reported that sphingolipid, ether lipid, glycerophospholipid and glycerolipid metabolisms were identified in OVX rats as novel biomarkers for oestrogen-deficient conditions induced by OVX (Vinayavekhin et al., 2016). Serum levels of AA, eicosapentaenoic acid (EPA), ergocalciferol and cholecalciferol in OVX rats were changed when compared to sham control by ultra-performance liquid chromatography–quadrupole time-of-flight mass spectrometry (Zhu et al., 2010). Changes in pathways of lipids, energy and amino acid metabolism, some of which involved the oxidative system, were identified in OVX rats by using NMR (Xue et al., 2011). Another study reported the effects of menopause on lipid peroxidation, glycolysis, the TCA cycle, choline and amino acid metabolisms in OVX rats using NMR and GC–FID/MS methods (Zhang et al., 2014a). In OVX mice, the TCA cycle intermediates aspartate, taurine, glycine, glucose and 3-hydroxybutyrate were lower than in sham groups using NMR spectroscopy (Chen et al., 2014). Similarly, another study in OVX mice reported lower concentrations of amino acids, energy metabolites and intestinal microbial compounds in OVX mice compared with the sham group also using NMR (Chen et al., 2015). A recent study reported data from and integrative

bone metabolomics and lipidomics using UPLC-Q-TOF-MS, to generate a bone metabolism profile in a postmenopausal osteoporosis mouse model. Several metabolites were down-regulated including amino acids, purine and pyrimidine and lipids were up-regulated including glycerophospholipids, triacylglycerols, sphingolipids and sterol lipids once osteoporosis was established (Zhao et al., 2018a).

In summary, the existent literature suggests that perturbations in specific metabolic pathways such as the TCA cycle, glutamine metabolism, amino acid metabolism and fatty acid metabolism due to oestrogen deficiency might impact on bone remodelling in OVX rats and mice. All those findings may be used as biomarkers in diagnosis for postmenopausal osteoporosis. However, the clinical symptoms in these rodent models are poorly representative of the naturally occurring postmenopausal condition in humans (Chavassieux et al., 1997a). Bones and bone remodelling from rats differ from that of humans.

Sheep are more similar to humans in their anatomical dimensions, and they possess metabolic and bone remodelling rates similar to those of humans (den Boer et al., 1999; McGovern et al., 2018). The sheep model therefore is a more optimal animal model to generate bone and blood samples for metabolomics analyses in the search of novel markers for bone health.

2.3.3.3 Metabolomics analyses in postmenopausal women for osteoporosis

Metabolomics has proven to be successful in measuring metabolite profiles in postmenopausal women using both NMR and LC–MS technologies. Two studies have reported metabolic alterations related to postmenopausal changes in Caucasian women. Auro et al. (2014) reported associations between

menopause and the plasma metabolome in Finnish and Estonian women. Using a NMR-based metabolomics technique, they found relationships between menopause status and glutamine, tyrosine, isoleucine and glycine, along with serum cholesterol measures and atherogenic lipoproteins, and total, monounsaturated and omega-7 and -9 fatty acids in the serum of Finns and plasma from Estonians.

A recent study published findings from a metabolic characterisation of menopause in plasma samples of UK midlife women using an NMR-based metabolomics approach. Circulating lipids and metabolites from both cross-sectional and longitudinal studies were associated with a variety of changes of metabolic markers in menopause. The altered metabolites were low-density lipoproteins (LDLs), intermediate-density lipoproteins, LDL remnants, LDL cholesterol and LDL particle size, glutamine and albumin (Wang et al., 2018). Sousa et al. (2018) reported the association between the plasma fatty acid profile and inflammatory metabolic markers among Portuguese Caucasian postmenopausal obese and overweight women using a GC–flame ionisation (FID) detector. Anti-inflammatory pathways were correlated with omega-3 and omega-6 fatty acids, unsaturated cis and polyunsaturated cis fatty acids, and short-chain fatty acids. Pro-inflammatory pathways were associated with omega-9 fatty acids, polyunsaturated trans fatty acids, monounsaturated cis fatty acids, and saturated fatty acids.

Another study reported the circulating changes of potential markers of menopause in plasma samples of Chinese women, including acylcarnitines, fatty acids, and lysophosphatidylcholines using an ultra-performance liquid chromatography–mass spectrometry (UPLC–MS) approach (Ke et al., 2015).

Yamatani et al. (2014) reported the metabolite profiling of adipose tissue between premenopausal and postmenopausal women using capillary electrophoresis (CE) ESI TOF–MS. Intermediate products of the pentose pathway increased in premenopausal women, while intermediate products of glycolysis and fatty acid metabolites increased after menopause. These changes in fatty acid metabolites where alterations of glycolysis and pentose phosphate pathways were also observed could be related to the metabolic syndrome (abdominal adiposity, insulin resistance, and dyslipidaemia) that emerges with oestrogen deficiency. Overall, the results from these studies show how menopause promotes substantial changes in diverse metabolites and these disturbances may have an impact on bone health by loss of oestrogen in women.

Studies are limited in examining the associations between bone turnover markers and bone metabolism in postmenopausal women. You et al. (2014) reported a metabolomics study using NMR in plasma samples, where low BMD was related to elevated glutamine levels of Taiwanese postmenopausal women; simultaneously, metabolites that protected against low bone mineral density were lactate and acetone (You et al., 2014). Further, Qi et al. (2016), using GC–MS, reported that in the plasma of Chinese postmenopausal women, the levels of linoleic acid increased by 60% and 190% in the osteopenia and osteoporosis groups, respectively, and changes in the levels of tryptophan, 3-hydroxy-L-proline and fumaric acid were also noted.

In another study using CE–TOF–MS, lower levels of the dipeptide Gly–Gly and of cysteine, and higher levels of hydroxyproline, were found in Japanese postmenopausal women with low versus normal BMD (Miyamoto et al., 2017). In a recent study Miyamoto et al. (2018) reported serum metabolomics profiles using

CE–TOF–MS in pre- and post-menopausal women Gly–Gly and of cysteine levels were lower in the post-menopausal women, confirming their previous findings. Levels of citrate and cis-aconitate, two metabolic intermediates seen early in the TCA cycle increased in the postmenopausal women. Hydroxyproline and branched chain amino acids (BCAAs), including valine, isoleucine and leucine concentrations significantly increased in post-menopausal women. The limitation of this study is that only focused in analysing polar metabolites and to have a full coverage of the metabolome, lipid species should be also investigated.

Zhu et al. (2016) reported the study of the necrotic trabecular femoral head in humans based on UPLC–MS/MS. This study identified 67 differential metabolites and biomarkers, where lipid metabolism was associated with the necrotic period and disturbed protein metabolism may occur during all the disease stages.

From the literature review, only one study has investigated the metabolomic profiles of young women with low and normal BMD. There were differential changes in the metabolism of amino acids (GABA, threonine, cysteine, taurine, and glutamic acid), bile acids (cholic acid, ursodeoxycholic acid, and tauroursodeoxycholic acid) and organic acids (succinate and N-acetylneuraminic acid) in serum samples of young (pre-menopausal) Caucasian women with low and high BMD, suggesting those metabolites as candidates for developing biomarkers for early bone loss detection (Zhao et al., 2018b).

Clearly, environmental, genetic and dietary differences between Western and Chinese populations may have produced conflicting results. There is limited information on this subject in the Chinese population. Therefore, metabolomics offers the potential to identify compounds for the prediction of osteoporosis, some

of which may even be specific to racial populations. Thus, metabolites and lipids might serve as candidate biomarkers to improve bone health in postmenopausal women.

Even though metabolomics has been utilised to identify novel biomarkers, only a few studies have been reported using metabolomics in human studies for osteoporosis. Furthermore, no study has investigated whether the OVX sheep model is able to increase the knowledge of the mechanisms driving postmenopausal bone loss. Therefore, the present study will evaluate the relation between the metabolome and BMD in the OVX sheep model as well as in middle-aged women using a comprehensive untargeted LC–MS metabolomics approach.

2.4 Problem statement

Most of the studies reported to date have focused only in the analysis of the metabolite or lipid profiles in postmenopausal studies; however, both metabolite and lipid profiles should be analysed to have a better metabolome coverage for better understanding of the dynamic and complex interactions in bone remodelling. Little evidence exists to define the combined effect of OVX and glucocorticoid treatment on bone health and the association with the metabolome in sheep as a model of postmenopausal osteoporosis. There are also limited data available on the association of the plasma metabolome and BMD of postmenopausal women. In this research samples were utilised from Singaporean–Chinese women with varying bone densities as part of the overarching larger project.

2.5 Research questions

1) Is there any association between the effect of loss of oestrogen and exposure to glucocorticoids and BMD and the plasma metabolome in OVX sheep?
2) Is there any association between menopausal status, plasma metabolome and BMD in Singaporean–Chinese women?

2.6 Research hypothesis

The study hypotheses of this thesis are that the plasma metabolome and lipidome will differ between animals with induced osteoporosis and normal animals, and that the metabolome and lipidome will differ between Singaporean–Chinese postmenopausal women with healthy bones and those with bone loss.

The aims of this study were to:

1) optimise and characterise a large animal model of postmenopausal osteoporosis;
2) determine the interaction between the plasma metabolome and bone remodelling in sheep;
3) describe the association between the plasma metabolome and bone remodelling in postmenopausal Singaporean–Chinese women; and
4) compare between sheep and humans the metabolomic markers correlated with bone loss.

Chapter 3

Glucocorticoids affect bone mineral density and bone remodelling in ovariectomised sheep: a pilot study

This chapter employs the sheep to optimise and characterise a large animal model for postmenopausal osteoporosis. This chapter also evaluates the impact of short-term and long-term ovariectomy (OVX) and glucocorticoid hormonal interventions in the OVX sheep, and the relationship between bone mineral density measurements and bone turnover markers.

This chapter is based on paper 1

Diana Cabrera[2], Frances M Wolber[3], Keren Dittmer[1], Chris Rogers[1], Anne Ridler[1], Danielle Aberdein[1], Tim Parkinson[1], Paul Chambers[1], Karl Fraser[4,5,6], Nicole C Roy[4,5,6], Marlena Kruger[2,4] (2018). Glucocorticoids affect bone mineral density and bone remodelling in OVX sheep: A pilot *Bone Reports*, *9*, 173-180

[1]*Institute of Veterinary, Animal and Biomedical Sciences,* [2]*School of Food and Nutrition,* [3]*Centre for Metabolic Health Research,* [4]Riddet Institute*, Massey University,* [5] Food Nutrition & Health Team, Food & Bio-Based Products Group, AgResearch Grasslands, *Tennent Drive, Palmerston North 4442,* [6]High-Value Nutrition National Science Challenge, Auckland 1142, *New Zealand*

Author contribution

Diana Cabrera contributed to collection data and drafting the article. Frances Wolber participated in design of the study. Keren Dittmer participated in the OVX surgery, routine care, health surveillance and corticosteroid treatment of the animals. Chris Rogers participated in doing the CT scans. Anne Riddler and Danielle Aberdein participated in the routine care, health surveillance and corticosteroid treatment of the animals. Tim Parkinson participated in the OVX surgery. Paul Chambers participated in the OVX surgery anaesthesia. Karl Fraser, Nicole Roy and Marlena Kruger participated in the conception design of the study. All the authors contributed to review the article for intellectual concept and the final approval of the version submitted.

The format has been adjusted to the general format of the thesis. Tables and figures were kept as in publication.

Abstract

The aim of this study was to validate the combination of ovariectomy and glucocorticoid treatment in sheep as a large animal model for osteoporosis by measuring the concentration of specific biomarkers in the blood of the sheep and measuring bone loss over five months. Aged Merino ewes were randomly allocated into four groups: control, ovariectomy (OVX), and two OVX groups receiving glucocorticoids—one group once-monthly for five months (OVXG), and the other for two months followed by no treatment for three months (OVXG2). Parameters measured were biochemical markers of bone turnover, areal bone mineral density, volumetric bone mineral density, and total and trabecular bone parameters. Ovariectomy increased the concentrations of bone resorption marker C-terminal telopeptides of type 1 collagen (CTx-1) and bone turnover marker serum osteocalcin (OC) concentrations in the OVX group compared to control sheep. The combination of ovariectomy and glucocorticoid treatment increased the concentrations of CTx-1 and decreased serum OC concentrations in the OVXG group compared to OVXG2. Femur and lumbar spine bone density were lower in experimentally treated groups when compared with the control group. Total and trabecular volumetric bone mineral density ($_{v}$BMD) in the proximal tibia were significantly lower in the treatment groups when compared with the control group. A significant negative correlation between femoral bone density and CTx-1 was found. The results of this study suggest that the combination of OVX and glucocorticoids induces bone loss in a short period of time in sheep.

3.1 Introduction

Because of the increased aging population and the rise in the number of bone fractures in elderly people, osteoporosis is considered a major public health issue (Harvey et al., 2010). In women, low levels of oestrogen have effects on bone remodelling, causing loss of bone mass and bone strength due to increased bone resorption and decreased bone deposition (Snyman, 2014). Dual energy x-ray absorptiometry (DXA) and peripheral quantitative computed tomography (pQCT) are useful to measure bone mineral density (BMD) in order to diagnose osteoporosis but cannot predict bone loss (Engelke et al., 2008). To reduce this disease worldwide, assist with understanding the mechanisms involved, and help with early diagnosis, more research must be conducted.

Large animal models are approved by the US Food and Drug Administration for mimicking human osteoporosis in orthopaedic research (Reinwald and Burr, 2008). A well-known method used to induce osteoporosis is ovariectomy (OVX). This method has a direct effect on bone mass due to the induction of oestrogen deficiency. Oestrogen deficiency affects the bone remodelling process, and induces bone loss due to a direct effect on osteoblasts and osteoclasts (Klein-Nulend et al., 2015). Bone formation is inhibited while bone resorption is stimulated, resulting in bone loss (Khosla et al., 2011; Drake et al., 2015). In addition, treatment with glucocorticoids is known to cause secondary osteoporosis, due to increased bone resorption leading to a rapid initial bone loss, and decreased bone formation through suppression of osteoblasts and osteocytes (Compston, 2010; Andreasen et al., 2015).

The OVX sheep is an established large animal model of osteoporosis. Sheep have the advantage that their bone structure and bone metabolism is

similar to humans (Newman et al., 1995; Wilke et al., 1997). The model has been used in several studies, and has shown that OVX will induce osteoporosis over six months (Hornby et al., 1995; Turner et al., 1995; Lill et al., 2002a; Wu et al., 2008; Zhang et al., 2014b; Dias et al., 2018). These studies have reported increased bone turnover in OVX sheep, and all proposed that long periods of time were required for establishing osteoporosis in the sheep (Chavassieux et al., 1993; Chavassieux et al., 1997b; MacLeay et al., 2004; Sigrist et al., 2007; Ding et al., 2010). Studies have indicated that when OVX is combined with glucocorticoids, further bone loss is induced (Lill et al., 2002a; Schorlemmer et al., 2005; Ding et al., 2010; Veigel et al., 2011). Therefore, a combination of OVX with glucocorticoids will increase bone loss in sheep; using both OVX and glucocorticoids could reduce the time needed to develop osteoporosis, and the trial time could be reduced. However, weekly treatment with glucocorticoids after long-term treatment has been shown to negatively impact the animals' health with severe side effects such as infections and hair loss (Lill et al., 2002a; Schorlemmer et al., 2003). More importantly, how glucocorticoid withdrawal effects the rebound of bone is not yet fully understood in OVX sheep. Thus, strategies to reduce future complications of long-term glucocorticoid treatment in OVX sheep need to be considered.

It was hypothesised that ovariectomising sheep in combination with monthly injections of glucocorticoids would result in decreased BMD and increased plasma bone remodelling marker concentration over a shorter period of time than previously reported, while eliminating the negative side effects. The aims of this study were to: 1) validate the OVX sheep model by measuring the concentration of serum biomarkers and bone loss over a five-month period; and 2) investigate

the effects of short- and long-term glucocorticoid administration on BMD in the lumbar spine, femur and tibia, as well as bone biomarkers, in the OVX sheep.

3.2 Materials and methods

3.2.1 Experimental animals

Aged Merino ewes (7–9 years old, *n* = 28) were obtained from a commercial farm in the Whanganui region, New Zealand. The animals were housed in a barn and adapted to indoor pens with rubber mat flooring. Sheep had free access to water and were fed the control diet described below for 20 days. After adaptation, sheep were randomly allocated into groups: control group (*n* = 10), the OVX group (*n* = 12), and two OVX groups receiving glucocorticoids, one group once a month for five months (OVXG) (*n* = 3) and the other group once a month for two months followed by no treatment for three months (OVXG2) (*n* = 3) (Figure 3.1).

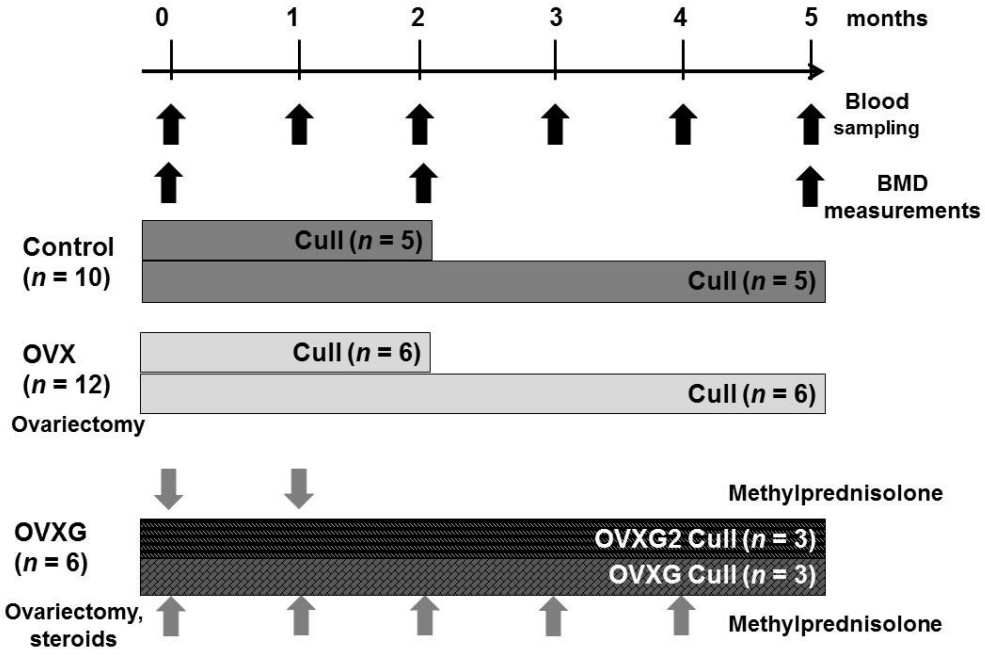

Figure 3.1: Flow diagram of the experimental study. Merino ewes were randomly divided into groups, 10 underwent no treatment (control group), 12 ewes underwent ovariectomy (OVX), and the remaining 6 ewes underwent OVX and received an injectable suspension of 400 mg methylprednisolone (OVXG group). Half of the ewes in the OVXG group received the methylprednisolone treatment for five months, while the other half received this treatment for only two months (OVXG2 group). Blood samples were collected monthly. BMD measurements were done at baseline (month zero) by pQCT, and at post-cull (month two or month five) by pQCT and DXA. Half of the sheep in the control group and OVX group were euthanised after two months, and the remaining sheep for each group were euthanised after five months. All the sheep in the OVXG group and OVXG2 were euthanised after five months.

Control and low-calcium sheep pellet concentrate diets were formulated from soya, brollard and wheat to contain 11% protein, 34% starch, and 29% nondigestible fibre, as well as >2000 IU/kg vitamin D3/cholecalciferol and <200 IU/kg vitamin D2 (ergocalciferol), which are required for calcium absorption. While 2–4 g/kg calcium is sufficient for sheep under normal circumstances, the animals in the current study were housed indoors and had limited exposure to sunlight and no exposure to sun-cured forage. Under these circumstances, calcium absorption was likely to be impaired. It was considered undesirable to risk vitamin D toxicity by increasing the vitamin D levels to aid calcium absorption in the gut,

so the dietary calcium levels were increased to compensate. Ewes were fed at approximately 200 g/sheep/day. Wheat straw and water were available to all sheep *ad libitum* throughout the study.

Sheep were anaesthetised using 0.5 mg/kg diazepam (Ilium, Troy Laboratories Pty Ltd., Glendenning, Australia) and 10 mg/kg ketamine (Phoenix Pharm Distributors Ltd., Auckland, New Zealand) intravenously, followed by endotracheal intubation and maintenance of anaesthesia with halothane. The distal tibia from each sheep was pQCT-scanned under general anaesthesia. The sheep, except for the control group, underwent bilateral OVX. The OVX was performed via a ventral abdominal incision. The linea alba and subcutaneous tissues were closed using 1 USP polydioxanone (PDS II, Ethicon Inc., USA) and the skin with 1 USP nylon suture (Kruuse A/S, Langeskov, Denmark), and the sutures were removed 14 d after the surgeries. Prior to extubation, each sheep was given 20 mg/kg meloxicam (Metacam, Boehringer Ingelheim GmbH, Ingelheim am Rhein, Germany) for pain. At the same time, the 10 sheep in the control group were anaesthetised but no surgery was performed. Post-surgery, until suture removal, sheep were examined twice daily. After suture removal, sheep were checked twice daily and food, water, activity and hair condition monitored.

On day two after OVX, six OVX sheep were administered an injectable suspension of 400 mg methylprednisolone (Vetacortyl®, Vetoquinol SA, Lure Cedex, France) subcutaneously in the neck. Methylprednisolone treatment started before the sutures were removed. Three of the sheep were given four further treatments at the same dose once a month (OVXG). The remaining three sheep received the initial treatment and then an additional treatment was given

one month later, after which the treatment was discontinued in order to observe the effect on bone after glucocorticoid withdrawal (OVXG2).

All experimental procedures were approved by the Massey University Animal Ethics committee (approval number 14/103) and performed according to the Code of Ethical Conduct for the use of live animals for research at Massey University, Palmerston North, New Zealand.

3.2.2 Blood sampling

Blood sample from each sheep was collected via jugular venepuncture into three different plain (serum), heparin and EDTA tubes (BD Vacutainer, Franklin Lakes, New Jersey, USA). Heparin and EDTA tubes for plasma samples were put on ice for 40 minutes and then centrifuged at 2000 *g* for 10 min, and plasma removed and stored at –80 °C for later analysis. The tubes designed for serum samples were left at room temperature for 45 minutes to clot prior to being processed as above. Blood samples were collected on the day of surgery (month 0) and then monthly for the duration of the study until the animals were euthanised. Blood samples were taken between 08:00 and 10:00 hours to limit any circadian effect.

3.2.3 Euthanasia and dissection

Half of the ewes from the control group (*n* = 5) and half from the OVX group (*n* = 6) were euthanised using a captive bolt followed by exsanguination at two months. At the end of the study (five months), the remaining ewes from the control group (*n* = 5) and the OVX group (*n* = 6), and all of the ewes from the OVXG (*n* = 3) and the OVXG2 (*n* = 3) groups, were similarly euthanised. After

euthanasia, the femurs, lumbar spines (LSs) and tibias were collected and stored at 4 °C. Samples of ileum, liver, kidney, heart and lung were collected and stored in 10% neutral buffered formalin until processing for histology. Microscopic examination of 3 µm paraffin-embedded haematoxylin- and eosin-stained sections confirmed the absence of unrelated disease.

3.2.4 Analysis of biochemical markers of bone

Osteocalcin (OC) was measured in serum using an immunoassay kit (MicroVue Osteocalcin, San Diego, CA, USA) according to manufactures instructions. This The MicroVue immunoassay kit uses a monoclonal mouse antibody that recognises only intact (*de novo*) OC in serum. The MicroVue immunoassay used has cross-reactivity with sheep species (Dias et al., 2008).

Serum C-terminal cross-linked telopeptides of type I collagen (CTx-1) was measured in heparinised plasma using CrossLaps ELISA kit (IDS, London, UK), which uses two highly specific monoclonal antibodies. The IDS immunoassay has been used for sheep (Wilkens et al., 2014).

The quantification of OC serum CTx-1 were tested in duplicate according manufactures' instructions. For the OC analysis the optical density was measured at 405 nm and for the CTx-1 at 450 nm using a EL_x 808 ultra microplate reader (Bio-tek Instruments Inc., USA). A 4 parameter curve fitting was used to analyse the results and the sample absolute concentrations were extrapolated from the standard curves of each biochemical bone marker. OC and CTx-1 were measured in the sheep at baseline (month zero), two months and five months of the trial.

3.2.5 Analysis of bone parameters

3.2.5.1 DXA

Lumbar spine and femur were thawed at room temperature. *Ex vivo* measurements of bone mineral component (BMC) and areal BMD (aBMD) for the lumbar spine and femur were determined using the Hologic Discovery A Bone Densitometer (Hologic Discovery **QDR 4500A** densitometer, Hologic Inc., Bedford, Massachusetts, USA).

3.2.5.2 pQCT

Three-dimensional analyses of the left tibial bone were performed using pQCT. The first initial baseline scan was obtained after the sheep were anaesthetised for surgery. *In vivo* measurements were made of total volumetric BMD ($_{v}$BMD), bone area, bone mineral content (BMC), cortical/subcortical and trabecular $_{v}$BMD, cortical/subcortical and trabecular bone area, cortical/subcortical and trabecular BMC, and geometric variables of the mid-metaphysis 10 mm from the distal surface of bone and at the mid-diaphysis 70 mm from the distal end.

Left tibias were thawed at room temperature. *Ex vivo* measurements were made of total *v*BMD, bone area, BMC, cortical/subcortical and trabecular $_{v}$BMD, cortical/subcortical and trabecular bone area, cortical/subcortical and trabecular BMC and geometric variables of the proximal tibia, the mid-metaphysis and at the mid-diaphysis using the XCT2000 peripheral quantitative computed tomography (pQCT) scanner (Stratec Medizintechnik GmbH, Pforzheim, Germany). The measurement site was located at the proximal metaphysis 15 mm from the

proximal surface of bone. The pQCT scan for the *in vivo* and *ex vivo* measurements had a voxel size of 0.3 mm.

Norland/Stratec XCT 5.50 software was used for scan imaging analysis. The trabecular compartment was obtained at the central 45% of bone at the trabecular sites. The manufacturer's contour threshold was set at 280 mg/cm^3 to separate soft tissue from the outer edge of bone. For cortical bone, the threshold was set at 710 mg/cm^3.

3.2.6 Statistical analyses

Data for bone marker concentrations were analysed to report the effects of treatments at specified time points. For analysis of percentage of change from baseline, baseline results were included as covariate and the analysis was based on the results from month two and month five. Data for lumbar spine, femoral and tibial parameters were analysed to test the effect of the OVX plus glucocorticoid treatments after sacrifice at month two and month five. Data are expressed as mean and standard deviation (SD). Statistical analyses were performed with the nonparametric Kruskal–Wallis test to assess whether the treatment means were significantly different. The nonparametric Kruskal–Wallis test was followed by post-hoc comparisons of treatment means using Dunn's post-hoc test. Statistical analyses on data were conducted using R (R 3.1.1, R Foundation for Statistical Computing, Vienna, Austria). Spearman rank-order correlation were performed to assess the association between BMDs of the lumbar spine, femur and tibia with bone biomarker concentrations. This test was done using Minitab 17.2.1 (Minitab Inc., Pennsylvania, USA). In all statistical analyses, p-values < 0.05 were considered statistically significant.

3.3 Results

3.3.1 Effect of OVX alone or combined with glucocorticoid on biochemical markers of bone in the sheep model

During bone loss in osteoporosis, measurable metabolites are released in the blood, including OC and CTx-1. OC is a noncollagenous bone protein, which is released from osteoblasts during bone formation and from bone matrix during bone resorption. CTx-1 is a collagen breakdown product, which is released during bone resorption (Swaminathan, 2001; Allen, 2003; Garnero et al., 2003).

Figure 3.2 and Table 3.1 show the changes in OC and CTx-1 markers over five months of treatment in OVX sheep. The percentage change from baseline of individual sheep is shown for each parameter (Figure 3.2). Sheep exhibited serum OC concentration mean values between 12 and 15 ng/mL at baseline (Table 3.1). Serum OC concentration in the control sheep increased by 22% at two months, and increased further by 40% at five months (Figure 3.2A). Similarly, serum OC increased by 35% (*p*-value = 0.337) within two months and by 43% (*p*-value = 0.384) at five months compared to baseline in OVX sheep. On the other hand, serum OC concentration decreased by 24% (*p*-value = 0.040) at two months and remained at this decreased level (*p*-value = 0.099) at five months compared to baseline in the OVXG group. However, when the glucocorticoids were discontinued in the OVXG2 group at two months, the serum OC concentrations observed at five months increased by 26% (*p*-value = 0.209), compared to baseline in the OVXG2 group.

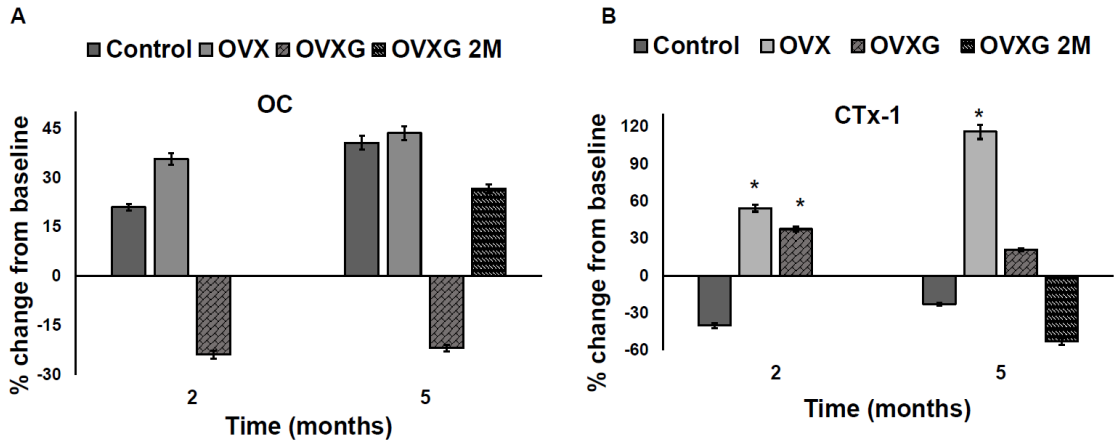

Figure 3.2: The concentrations of OC and CTx-1 in the serum of the OVX sheep. Percentage change in the bone turnover marker serum OC (A) and percentage change in the bone resorption marker CTx-1 (B) compared with the pretreatment baseline from Merino ewes that were either ovariectomised (OVX), ovariectomised and given five doses of glucocorticoid at monthly intervals (OVXG), ovariectomised and given two doses glucocorticoid at monthly intervals (OVXG2), or received no treatments (Control). OC and CTx-1 were measured at two months and five months after initiation of the treatments. The results are presented as serum OC and CTx-1 mean percent change from baseline. * *p*-value < 0.05. Error bars denote standard error of mean.

Table 3.1: Changes of OC and CTx-1 over five months in the OVX sheep.

	OC (ng/ml)				CTx-1 (ng/ml)			
Time (Month)	Control	OVX	OVXG	*p*-value	Control	OVX	OVXG	*p*-value
0	12.19 (4.97)	15.07 (4.86)	15.86 (6.66)	0.107	0.96 (0.78)	0.71 (0.36)	0.74 (0.18)	0.87
2	13.17 (4.17)	19.33 (6.72)	10.78 (7.48)	0.013	0.61 (1.13)	0.93 (0.56)	0.87 (0.36)	0.005
5	16.25 (7.24)	18.38 (8.87)	12.71[a] (4.13) 16.95[b] (4.33)	0.77	0.28 (0.04)	0.95 (0.58)	0.66[a] (0.14) 0.4[b] (0.24)	0.01

[a] Half of the ewes in the OVXG group received the methylprednisolone treatment for five months (OVXG group). [b] Half of the ewes in the OVXG group received the methylprednisolone treatment for only two months (OVXG2 group). Data are presented as serum OC and CTx-1 mean (SD). The resulting *p*-values obtained by Kruskal–Wallis are given. *p*-value < 0.05 was considered as statistically significant.

3.3.2 Effect of OVX alone or combined with glucocorticoid on bone parameters in the sheep model

The results of DXA scans of the lumbar spine and femur are shown in Figure 3.3. After OVX, the lumbar spine and femur parameters did not differ between treatments compared with controls at two months (Figure 3.3). Lumbar spine aBMD was slightly reduced by 6% (*p*-value = 0.36) after OVX, but lumbar spine BMC was not affected two months after OVX. In addition, femoral aBMD did not vary between the control group and OVX group at two months.

Similarly, the lumbar spine and femur did not show any significant differences in bone parameters compared with controls at five months. However, the lumbar spine and femoral aBMD of experimentally treated animals were decreased from controls at five months (Figure 3.3). The highest impact on aBMD was found in the OVXG group. Lumbar spine aBMD was reduced by 7%, 28% and 12% (*p*-value =0.06) in the OVX, OVXG and OVXG2 groups, respectively (Figure 3.3A). Lumbar spine BMC was decreased by 6.7%, 27% and 7% (*p*-value = 0.15) in the OVX, OVXG and OVXG2 groups, respectively (Figure 3B). Femoral aBMD was reduced by 10%, 21% and 6% (*p*-value = 0.06) in the OVX, OVXG and OVXG2 groups, respectively (Figure 3.3C). Femoral BMC was slightly but not significantly reduced after five months of treatment in all treated groups (*p*-value = 0.19) (Figure 3.3D).

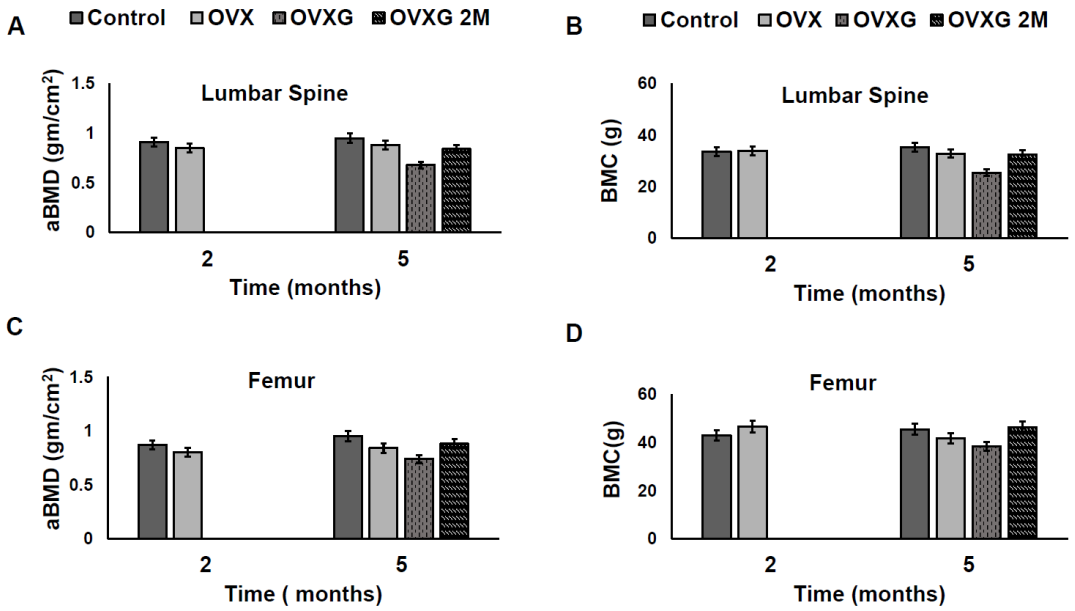

Figure 3.3: Bone parameters of lumbar spine and femur at month two and month five measured by DXA. (A) lumbar spine aBMD, (B) lumbar spine BMC, (C) femoral aBMD and (D) femoral BMC are shown for half of the ewes euthanised at month two in the control group (n = 5) and OVX group (n = 6), and for the remaining ewes at month five for each group. Data is presented as mean and 95% confidence intervals.

The results of pQCT scans of the proximal metaphysis of the tibia post-cull are shown in Figure 3.4. The proximal metaphysis of the tibia at two months (Figure 3.4A, 3.4C, 3.4E) did not show significant differences between control and OVX treatment groups (*p*-value > 0.05). Total vBMD was reduced by 8% after two months of treatment (*p*-value = 0.1). Bone area and BMC did not vary between groups at two months. No difference could be found in trabecular vBMD (*p*-value = 0.72), trabecular area (*p*-value = 0.14) and trabecular BMC (*p*-value = 0.58).

The proximal metaphysis of the tibia at five months (Figure 3.4B, 3.4D, 3.4F) showed a significant treatment effect. Tibial vBMD was decreased by 8% (*p*-value = 0.052), 27% (*p*-value = 0.0009) and 13% (*p*-value = 0.057) in the OVX, OVXG and OVXG2, respectively (Figure 3.4B). BMC was decreased by 14% (*p*-value 0.051), 28% (*p*-value = 0.001) and 1% (*p*-value = 0.293) in the OVX, OVXG and OVXG2, respectively (Figure 3.4F). Trabecular vBMD was reduced by 20% (*p*-value = 0.019) and 30% (*p*-value = 0.003) in the OVX and OVXG, respectively (Figure 3.4B). Trabecular BMC was reduced by 22% (*p*-value = 0.044) and 20% (*p*-value = 0.109) in the OVX and OVXG, respectively (Figure 3.4 F).

The data were pooled from all the treatment groups at two months and five months, and further analyses performed to investigate any possible associations between parameters. Relationships of BMD of femur and tibia with OC and CTx-1 concentrations in sheep at two months were not significant using Spearman's rank-order correlations (Table 3.2). However, a significant correlation was observed between lumbar spine aBMD and OC (r = –0.636; *p*-value = 0.048). The correlations between biochemical markers and BMD of lumbar spine, femur and tibia at five months were positive for OC and negative for CTx-1, but not significant using Spearman's rank-order correlation (Table 3.2). However, a strong and significant negative correlation between femoral aBMD and CTx-1 was found (r = –0.505; *p*-value = 0.039).

Table 3.2: Correlation between biochemical markers and BMD of lumbar spine, femur and tibia in OVX sheep at month two and month five of the study.

	OC Spearman's correlation	*p*-value	CTx-1 Spearman's correlation	*p*-value
Month 2				
Lumbar spine aBMD	–0.636	0.048	–0.345	0.298
Femur aBMD	–0.261	0.466	0.346	0.297
Tibia				
vBMD	–0.418	0.229	–0.336	0.312
Trabecular vBMD	–0.479	0.162	–0.409	0.212
Month 5				
Lumbar spine aBMD	0.262	0.309	–0.212	0.414
Femur aBMD	0.140	0.593	–0.505	0.039
Tibia				
vBMD	0.130	0.619	–0.284	0.269
Trabecular vBMD	0.184	0.480	–0.404	0.107

p-value < 0.05 was considered as statistically significant.

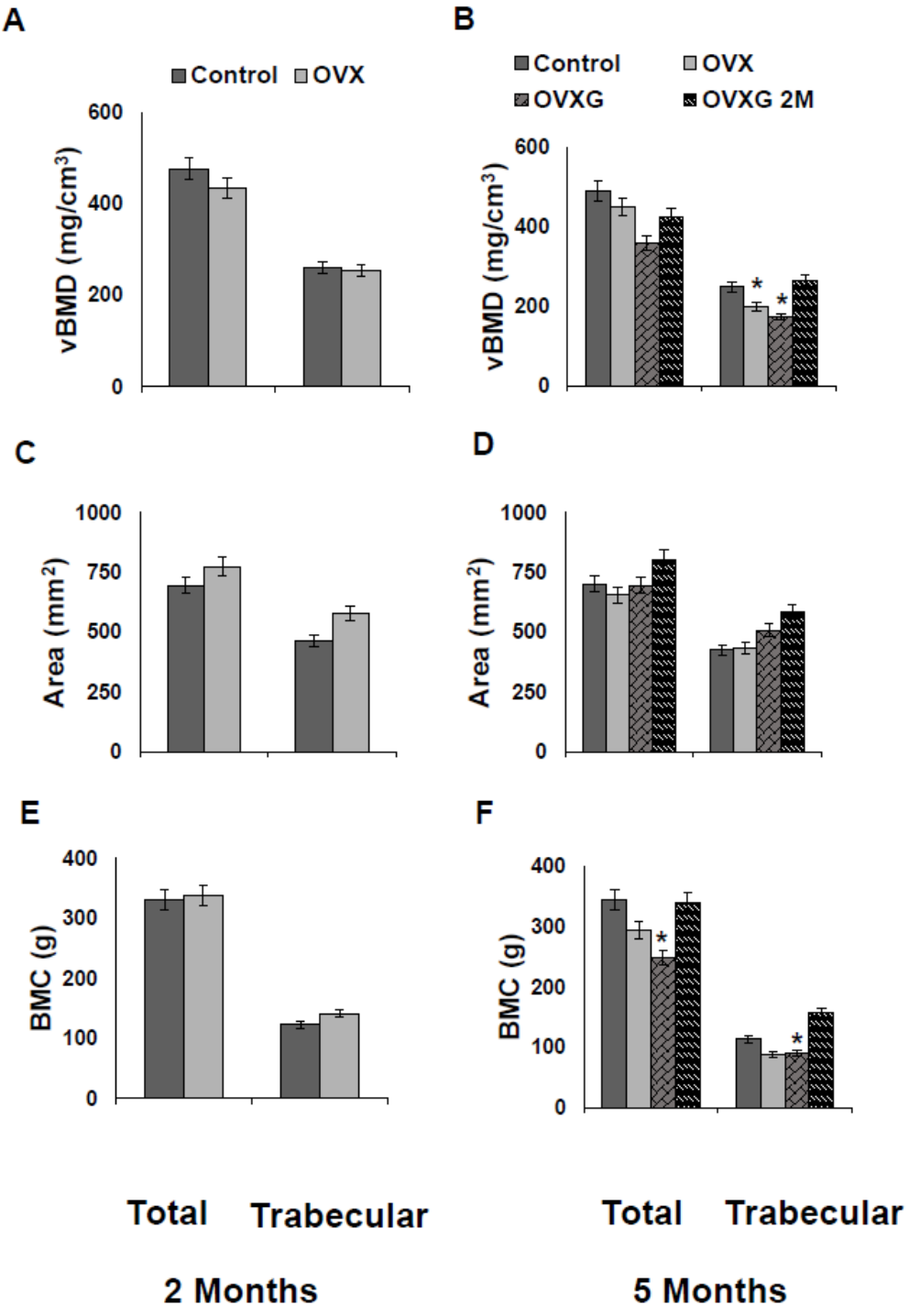

Figure 3.4: Bone variables at the proximal metaphysis of the tibia at month two and month five measured by pQCT. Total and trabecular tibial vBMD, area and BMC (A), (C) and (E), respectively, at month two. Total and trabecular tibial vBMD, area and BMC (B), (D) and (F), respectively, at month five are shown for half of the ewes euthanised at month two in the control group (n = 5) and OVX group (n =6); and the remaining ewes at month five for each group. Data is presented as mean and 95% confidence intervals. *p-value < 0.05 was considered as statistically significant.

3.4 Discussion

In this study, we applied a combination of advanced age, OVX and glucocorticoid treatment to determine bone mass quantity, quality and bone markers using sheep as a large animal model for postmenopausal osteoporosis. A period of five months caused a decreased BMD in the glucocorticoid OVX sheep with a significant reduction of aBMD in the lumbar spine and femur as measured by DXA, and a significant decrease in tibial cortical and trabecular vBMD as measured by pQCT. The decreases in aBMD and vBMD were greater in the glucocorticoid-treated ovariectomised sheep compared with the control groups and those that only underwent OVX. Interestingly, after cessation of glucocorticoid administration, there was a recovery of bone mass in sheep treated with glucocorticoids for only two months. Serum biomarkers were increased in the ovariectomised sheep; however, those same serum markers were reduced in the glucocorticoid-treated OVX sheep.

3.4.1 Effect of OVX on bone biomarkers and bone parameters in sheep

Bone turnover markers can be used as measures of the status of bone remodelling. The bone remodelling depends on the synchronization of bone resorption cells—osteoclasts and subsequent bone formation cells—osteoblasts. During menopause, bone resorption increases as a result of oestrogen deficiency as well as bone formation to fill the bone cavities that have been destroyed (Vasikaran et al., 2011a). In this study, after five months of OVX on a diet providing the minimum required level of calcium, the bone resorption serum biomarker CTx-1 increased at two months in the OVX group and remained increased until the end of the study. Similarly, serum OC increased after OVX

and remained increased during the study. These results are in agreement with Kiełbowicz et al. (2015) that reported increased serum CTx-1 concentrations in OVX sheep. Other authors have reported an increase in urinary CTx-1 three months, and serum pyridinoline concentrations two months, after OVX (Chavassieux et al., 2001; Sigrist et al., 2007). Other studies also support these findings with regards to serum OC concentration; also showing that serum OC concentrations increased after OVX treatment in sheep (Chavassieux et al., 2001; Johnson et al., 2002; Newton et al., 2004a). It was also observed that OC and CTx-1 concentrations were significantly negatively correlated with lumbar spine aBMD and femoral aBMD, respectively. These results suggest a possible association between bone turnover and bone density, where bone turnover is able to predict a reduction of BMD. These increased serum concentrations of OC and CTx-1 reflect increased bone resorption in lumbar spine and femur due to OVX promoting bone loss and increasing bone turnover (Yoon et al., 2012). These findings suggest that a two-month time point may be sufficient for assessing the early effects of OVX on bone resorption and can reliably predict changes in bone structure.

In this study, a reduction of lumbar and femur BMD was found, as assessed by DXA, when compared with the control group that was not ovariectomised and was fed a diet with plentiful calcium. These results are similar to those reported by previous studies; with a decrease of aBMD reported in the spine at six months (Turner et al., 1995) and 12 months after OVX (Hornby et al., 1995; Wu et al., 2008; Zhang et al., 2014b).

In this study, tibia vBMD, trabecular vBMD and cortical/subcortical vBMD as assessed by pQCT showed a decrease in bone mass after five months of

OVX. However, published reports are controversial, as two of the few studies published to date reported no significant differences in trabecular vBMD in the proximal tibia after twelve months of OVX in sheep (Augat et al., 2003). However, Sigrist et al. (2007) observed a significant decrease in trabecular vBMD of the distal radius after four months of OVX. Taken together, these findings suggest that five months or less is a sufficient time period post-ovariectomy to reliably measure physical changes in BMD in the sheep model, where DXA and pQCT are suitable methods of measurement to assess BMD.

3.4.2 Effect of glucocorticoid treatment on bone biomarkers and bone parameters in OVX sheep

The combination of OVX, minimal dietary calcium, and glucocorticoid treatment caused a transient increase in the serum CTx-1 concentrations at two months, after which concentrations were lowered by the end of the study. This result is supported by previous studies, where serum CTx-1 concentrations increased during the first months in OVXG sheep but decreased thereafter (Zarrinkalam et al., 2009a; Ding et al., 2010; Andreasen et al., 2015). The bone resorption marker CTx-1 has been shown to increase during the administration of steroids. The direct effect of glucocorticoids may be in promoting osteoclastogenesis (Takuma et al., 2003) and having an anti-apoptotic effect on osteoclasts (Jia et al., 2006).

In contrast, the serum OC concentration of sheep treated with glucocorticoids for five months decreased until the end of this study. This result is similar to some previous studies, where serum OC concentration rapidly decreased (Chavassieux et al., 1993; Chavassieux et al., 1997b; Ding et al.,

2010) and remained suppressed in sheep (Andreasen et al., 2015) with the combination of OVX and glucocorticoid treatment. However, it is well known that glucocorticoids affect osteoblasts and osteocytes, decreasing their lifespan and bone formation, as reflected by the reduction of serum OC concentrations (Van Staa et al., 2002).

An unexpected outcome of the current study is that the serum OC and CTx-1 concentrations in the group that received only two months of glucocorticoids were closer to the control group after cessation of glucocorticoid administration. This finding is supported by Ding et al. (2010), where serum OC recovered after the glucocorticoid treatment was discontinued at seven months in their study.

In the present study, BMD decreased after five months of the combination of OVX and glucocorticoids in the lumbar spine, femur and tibia, although this reduction varied according to the skeletal site. Previous research reported decreased cortical and trabecular vBMD in the lumbar spine and distal radius with OVX plus glucocorticoids in sheep over a period of six months (Lill et al., 2002a), tibia (Schorlemmer et al., 2005) at 12 months and iliac bone (Andreasen et al., 2015) over a period of seven months. Moreover, other studies reported the reduction of cortical and trabecular vBMD in the lumbar spine, distal radius and proximal tibia with OVX, glucocorticoids and diet in sheep (Lill et al., 2002a; Augat et al., 2003; Veigel et al., 2011). In this study, a significant reduction of trabecular compartment was detected during the administration of glucocorticoids, and this contributed to lower vBMD, which was observed after five months of treatment. Thus, the combination of OVX and glucocorticoids accelerates a profound bone loss in a short time, by inducing bone resorption and suppressing bone formation.

Sheep is recognised as a large animal model for studying human osteoporosis. The OVX sheep model is useful to understand the mechanisms that contribute to bone loss. However, there has been controversy about the optimal period of time for achieving bone loss due to there is no agreement within the literature of the time necessary to establish an osteoporotic (osteopenic) bone in OVX sheep. There have been several hypotheses proposed on the time required to induce measurable bone loss in sheep (Chavassieux et al., 2001; Les et al., 2005; Sigrist et al., 2007), although the duration required remains controversial due to the different breeds used in each study, the small number of animals per sampling, and the different approaches used to evaluate bone quantity and quality (Lill et al., 2002a; Ding et al., 2010; Veigel et al., 2011). However, in this study, it was found that a short-term ovariectomised glucocorticoid-treated model in Merino ewes can be used to induce bone loss without the side effects and complications of using glucocorticoids, such as hair loss, infections, and particularly, ethical concerns around animal welfare for the use of research animals as experimental units (Egermann et al., 2008). These results showed that five months was sufficient to induce bone loss using a combination of OVX and glucocorticoid treatment in Merino ewes, and that once-monthly injections of glucocorticoids resulted in no clinical infections or negative dermatological effects.

The limitations of this study include the small sample size and that bone mineral density was determined as a function of treatment evaluated in OVX sheep. Future studies such as mechanical properties of bone and changes in its extracellular matrix components are required to fully investigate bone quality in OVX sheep. However, the strengths are the induction of bone loss in a short

period of time and the assessment of bone mass during and after the cessation of glucocorticoids combined with OVX. Therefore, this present project should be considered a pilot study, where a combination of OVX and glucocorticoids was used to induce bone loss over a short period of time in sheep. A reduction in time may allow the sheep model to be used more frequently, to test novel therapies for postmenopausal women.

3.5 Conclusions

This pilot study suggested that the interaction of OVX and glucocorticoids plays a significant role and induces bone loss in sheep over five months, and this bone loss is similar to that seen in humans. The combination of OVX and length of glucocorticoid treatment should be carefully considered when designing studies using OVX sheep. Further, the use of experimental animal models for studying bone loss to test new experimental drug therapies and orthopaedic implants offers opportunities to enhance our understanding of bone diseases, particularly postmenopausal osteoporosis.

Chapter 4

Bone changes in response to glucocorticoids in ovariectomised sheep: a peripheral quantitative computed tomography (pQCT) study

Previous work in the ovariectomised (OVX) sheep model has been described in detail (Chapter 3), and these findings demonstrated that glucocorticoid-induced osteoporosis, where bone remodelling and bone loss occurred, was observed in OVX sheep over five months. In this section of my project, the results of pQCT measurements and the three-point bending test in left tibias in the OVX sheep are presented. There were three specific objectives of this study. First, to investigate the direct changes after OVX and glucocorticoid treatment on tibias of sheep. Second, to evaluate correlations between proximal and distal metaphyseal bone parameters of the left tibia. Third, to determine the tibial bone mechanical properties using the three-point bending test.

Abstract

The main objectives of this study were to use pQCT to determine whether glucocorticoid treatment induces changes in the distal metaphysis of the tibia; to assess whether there is a relationship between proximal and distal metaphyseal bone parameters of the tibia; and to compare the effect of ovariectomy (OVX) and glucocorticoid treatments on mechanical properties in the mid-shaft tibial bone in sheep. Twenty-eight aged Merino ewes were selected and randomised into four groups: OVX, OVX plus glucocorticoid treatment for five months, OVX plus glucocorticoid treatment for two months, and untreated control. The left tibias were used for measurement of bone imaging by using pQCT at baseline, at two and five months. The left tibia was also processed for strength evaluation. OVX alone did not affect bone parameters in the proximal and distal tibial metaphyses in OVX sheep at two months. The interaction of OVX plus glucocorticoids had a pronounced effect on volumetric bone mineral density in the group that received five months of this treatment. Conversely, when glucocorticoid treatment was discontinued after two months, a rebound effect was observed. Maximum load, stiffness, and energy to failure decreased over time. This study demonstrated that there are incremental bone changes at both distal and proximal metaphysis sites in OVX and glucocorticoid-induced osteoporosis over five months, some of which may be reversible in Merino ewes.

4.1 Introduction

Bone loss occurs during oestrogen deficiency and is intensified with glucocorticoid treatments in postmenopausal women, which may lead to the development of osteoporosis. Osteoporosis is characterised by a decline in bone quantity and quality, as well as increased fracture risks. Despite the significant progress in diagnosis and treatment of osteoporosis, postmenopausal osteoporosis is still the most frequent cause of fractures in women. Worldwide, it is estimated that 200 million women are affected by osteoporosis, with approximately 1.6 million hip fractures occurring each year (Johnell and Kanis, 2006; Kanis and Group, 2007).

Dual energy x-ray absorptiometry (DXA) is the gold standard method to diagnose osteoporosis by assessing areal bone mineral density (aBMD) in a specific region of interest of clinically important sites of fracture risk. However, DXA only provides a two-dimensional image of apparent density, and this limits its ability to assess fracture risk. DXA also cannot differentiate between cortical or trabecular bone (World Health Organization, 1994). As osteoporosis induces rapid trabecular loss and structural changes, it is important to assess trabecular structure.

pQCT provides a measurement of volumetric bone mineral density (vBMD), and can separate the cortical and trabecular compartments in the peripheral skeleton (Turner, 2002). There are skeletal site differences in bone loss as well as differences between locations within a single bone. In long bones, the trabecular compartment is higher in the metaphysis and epiphysis when compared with the diaphysis, where there is only cortical bone (Clarke, 2008). Thus, trabecular bone mass differs at skeletal sites, and fractures are commonly

observed in the distal radius, lumbar spine and the proximal femur (hip fracture) (Kanis et al., 1997). To date, the response to oestrogen loss of proximal sites has been well documented in postmenopausal women, but it is poorly understood whether there is a high correlation of bone loss between proximal and distal sites (Amstrup et al., 2016).

Animal models have been used to understand osteoporosis and evaluate new treatments for bone loss. Rodent models have been widely used and trabecular bone loss occurs after OVX and glucocorticoid-induced osteoporosis in rats (Lelovas et al., 2008; Komori, 2015). Sheep are another suitable model, as the bone remodelling and response to oestrogen withdrawal approximates human bone biology. Trabecular bone loss has been reported after OVX (Turner et al., 1995; Augat et al., 2003; Newton et al., 2004b; Sigrist et al., 2007; Kennedy et al., 2009; Egermann et al., 2011) or OVX combined with glucocorticoid (Lill et al., 2002b; Goldhahn et al., 2005; Zarrinkalam et al., 2009b; Ding et al., 2010) in sheep models. The subsequent rate and magnitude of the reduction of BMD varies according to the skeletal site examined (Turner et al., 1995). Few studies have reported either the distribution of, or the rate of reduction in, the trabecular and cortical bone in the distal radius in OVX sheep (Lill et al., 2002b; Goldhahn et al., 2005). Further, in sheep, a greater trabecular bone loss in the proximal limbs has been documented, but how OVX affects bone changes in the distal limbs has not been described in detail. These have a greater potential for serial sampling and therefore might be more useful to assess than proximal limbs (Oheim et al., 2016). In addition, there is no agreement within the literature of the time necessary to establish an osteoporotic animal model for bone loss in OVX

sheep. Thus, short-term studies are required to clarify how bone quality responds to oestrogen deficiency in different skeletal sites for evaluating bone status.

A five-month study in OVX sheep was carried out to expand our knowledge of bone quality in postmenopausal osteoporosis. The aims of this study included: 1) to use pQCT to examine whether glucocorticoid treatment induces changes in the distal metaphysis of the tibia; 2) to assess whether there is a correlation between proximal and distal metaphyseal bone parameters of the tibia after measuring these sites separately; and 3) to compare the effect of OVX and glucocorticoid treatments on mechanical properties in the mid-shaft tibial bone in sheep.

4.2 Materials and methods

4.2.1 Animals used and experimental design

The animals used and the experimental design are described in Chapter 3, Section 3.2.1. Briefly, 28 Merino ewes were first fed a basal diet for 10 days (adaptation period), then allocated at random to treatments, followed by OVX procedure. The study treatment groups were: OVX alone, OVX combined with glucocorticoid treatment for five months, OVX combined with glucocorticoids for two months, and untreated control. The study protocol aimed to mimic bone loss in postmenopausal osteoporosis. This study was performed in full compliance with the Massey University Animal Ethics committee (approval number 14/103) and performed according to the Code of Ethical Conduct for the use of live animals for research at Massey University, Palmerston North, New Zealand.

In total, bone samples from 28 ewes were examined: 10 from the control group, 12 from the OVX group, three from the OVX group receiving glucocorticoids once a month for five months (OVXG), and three from another OVX group receiving glucocorticoids once a month for two months (OVXG2).

The initial baseline scan (*in vivo* pQCT, as described below) was obtained after the sheep were anaesthetised for surgery. Control animals were anaesthetised and scanned using the same procedure.

At month two and at the end of the trial (five months), after sacrifice, the left tibias were harvested, stripped of muscle tissues and the bones wrapped in plastic bags, and stored at –20 °C. The tibias were thawed at room temperature before pQCT scans and biomechanical tests were performed (*ex vivo* pQCT, as described below).

4.2.2 pQCT

4.2.2.1 In vivo *and* ex vivo *pQCT*

Three-dimensional analyses of the tibia from the left leg were performed using the XCT2000 scanner (Stratec, Pforzheim, Germany). The measurement protocol was performed in accordance with the manufacturer's instructions. Scout views were acquired to determine the standard measurements for the distal and proximal tibia. The thickness of the scan slice was 2 mm, voxel size 0.3 mm and a scan speed of 10 mm/s. A reference point line was set electronically at the midpoint of the most distal articulating surface of the distal tibia. From this reference line, two scans were performed unilaterally: one at the metaphysis (at 10 mm, relative to the distal end), and one at a metaphyseal site, 15 mm from the proximal end.

4.2.2.2 Imaging analysis

Norland/Stratec XCT 5.50 software was used for scan imaging analysis. For proximal and distal sites, the parameters of trabecular compartment were obtained as the central 45% of bone at trabecular sites. The manufacturer's contour threshold was set at 280 mg/cm^3 to separate soft tissue from the outer edge of bone. In addition, to determine cortical bone, the threshold was set at 710 mg/cm^3 (Neu et al., 2001; Firth, 2006). The following parameters were analysed for both the proximal and distal metaphysis: vBMD, bone area, bone mineral content (BMC), trabecular vBMD (Tb vBMD), trabecular bone area (Tb area), trabecular BMC (Tb BMC), cortical thickness, periosteal circumference, and endosteal circumference.

4.2.3 Bone mechanical properties by three-point bending test of the tibias

Left tibias were thawed and kept at room temperature during the test. Each bone sample was measured using an electronic vernier caliper (resolution 0.02 mm, MitutoyoTM, Japan) and the midpoint of the tibia was marked with a pen. The mechanical properties of the tibia were determined after pQCT scans by a three-point bending test using a mechanical testing machine (Instron 1195 Norwood, MA, USA) (Bozzini et al., 2012). Each tibia was placed on its anterior surface facing upward on two support bars 80 mm apart, centred, and the pressing force was directed vertically to its mid shaft. A compression load was applied at 25 kN load (50 mm/min) until breakage. The force at failure, energy, stress and stiffness were calculated for each sample and derived from the load–deformation curve using the manufacturer's built-in computer software: energy was calculated as the area under the load–deformation curve, stiffness calculated

as the slope of the linear part of the load–deformation curve, and stress was calculated as the area under the load–displacement curve (Gallant et al., 2013).

4.2.4 Statistical analyses

Data for tibial parameters were analysed to test the effect of OVX plus glucocorticoid treatments after sacrifice at two and five months. Data were expressed as mean and standard error of mean (SEM). Statistical analysis was performed with the nonparametric Kruskal–Wallis test followed by Dunn's post-hoc test (p-values < 0.05 were considered statistically significant). Statistical analyses on data were conducted using R (R 3.1.1, R Foundation for Statistical Computing, Vienna, Austria). The data were pooled from all the treatment groups at two and five months, and further analysis conducted to determine any possible correlation between parameters. Linear correlations and Spearman's rank-order correlations were calculated for distal and proximal metaphysis of the tibia at months two and five using Minitab 17.2.1 (Minitab Inc., Pennsylvania, USA).

4.3 Results

4.3.1 Effect of OVX plus glucocorticoid on the distal tibial metaphysis over time

At baseline, there were no significant differences between the control group and the OVX group for vBMD or any of the trabecular parameters (Table 4.1 and Table 4.2). At both two and five months post-surgery, all the treated groups decreased in vBMD. Consistent with the effects in vBMD, bone area and BMC, periosteal and endosteal circumferences were similar at baseline but decreased only slightly over time (Table 4.1 and Table 4.2). However, trabecular vBMD was numerically reduced from baseline at both two and five months in all

groups, although statistical significance was not achieved (p-value > 0.05) (Table 4.1). The trabecular area reduced only slightly; therefore, the decrease in vBMD was due to the decrease observed in BMC. Trabecular BMC was numerically reduced after five months and tended to be lower (p-value = 0.09) in the control group compared with the treated groups (Table 4.1). Similar to vBMD and trabecular vBMD, cortical thickness was lower at both two and five months in the treated groups (p-value = 0.06) (Table 4.2).

Table 4.1: Longitudinal bone measurements of the distal tibial metaphysis in OVX.

		Ovariectomy			Ovariectomy ± glucocorticoid treatment				
		Control (n = 5)	OVX (n = 6)	p-value	Control (n = 5)	OVX (n = 6)	OVXG (n = 3)	OVXG2 (n = 3)	p-value
vBMD[1] (mg/cm^3)	Baseline	611.2 (22.7)	609.9 (19.8)	1	605.6 (24.5)	638.4 (17.6)	621.5 (42.4)	614.5 (29.4)	0.69
	2 Months	592.2 (19.3)	574.6 (18.4)	0.58	-	-	-	-	-
	5 Months	-	-	-	602.8 (28.7)	567 (11.6)	518.7 (31.1)	519.3 (23.9)	0.21
Bone area (mm^2)	Baseline	466.1 (17.8)	477 (41.2)	0.58	483.5 (10.2)	461.7 (17.9)	498.2 (22.3)	512.1 (20.2)	0.56
	2 Months	411.2 (27.6)	440.1 (27.5)	0.47	-	-	-	-	-
	5 Months	-	-	-	430.1 (14.7)	394.9 (12.2)	415.5 (21.2)	448.5 (28.6)	0.43
BMC[2] (g)	Baseline	284.6 (14.2)	293.3 (30.3)	0.36	292.5 (11.4)	295.1 (16.9)	308.1 (18.3)	312.5 (7.1)	0.77
	2 Months	244.3 (20.5)	252.2 (15.3)	0.72	-	-	-	-	-
	5 Months	-	-	-	259.3 (16.1)	223.4 (3.7)	213.5 (7.4)	230.5 (7.9)	0.06
Tb vBMD[3] (mg/cm^3)	Baseline	412.3 (25.1)	373.6 (46.1)	0.86	418.1 (16.2)	365.9 (19.7)	414.9 (15.1)	425.2 (19.9)	0.29
	2 Months	271.4 (54.2)	316.7 (15.4)	0.72	-	-	-	-	-
	5 Months	-	-	-	295.6 (53.5)	189.1 (24.6)	244.8 (16.3)	272.4 (9.1)	0.12
Tb area[4] (mm^2)	Baseline	279.6 (21.1)	281.7 (33.1)	0.72	293.8 (16.9)	239.7 (12.8)	285.8 (38.3)	305.7 (34.2)	0.28
	2 Months	223.4 (26.6)	262.8 (25.7)	0.47	-	-	-	-	-
	5 Months	-	-	-	231.7 (17.9)	214.1 (11.5)	248.7 (22.6)	282.5 (29.2)	0.45
Tb BMC[5] (mg/mm)	Baseline	116.1 (12.1)	111.7 (23.1)	1	122.3 (6.5)	88.1 (7.5)	116.6 (12.7)	129.1 (12.9)	0.10
	2 Months	65.9 (18.9)	84.6 (11.9)	0.36	-	-	-	-	-
	5 Months	-	-	-	70.8 (15.2)	41.4 (6.4)	59.7 (2.8)	76.7 (7.4)	0.09

[1] Volumetric bone mineral density (vBMD).
[2] Bone mineral content (BMC).
[3] Trabecular volumetric bone mineral density (Tb vBMD).
[4] Trabecular area (Tb area).
[5] Trabecular bone mineral content (Tb BMC).
Data expressed as mean (SEM). The resulting p-values obtained by Kruskal–Wallis are given.

Table 4.2: Longitudinal geometric parameters of the distal tibial metaphysis in OVX sheep.

		Ovariectomy			Ovariectomy ± glucocorticoid treatment				
		Control (n = 5)	OVX (n = 6)	p-value	Control (n = 5)	OVX (n = 6)	OVXG (n = 3)	OVXG2 (n = 3)	p-value
Periosteal circumference (mm)	Baseline	76.4 (1.4)	77.1 (3.4)	0.58	77.9 (0.8)	76.1 (1.5)	79.1 (1.7)	80.1 (1.5)	0.56
	2 Months	71.7 (2.4)	74.2 (2.3)	0.47	-	-	-	-	-
	5 Months	-	-	-	73.4 (1.2)	70.4 (1.1)	72.1 (1.8)	74.9 (2.41)	0.43
Endosteal circumference (mm)	Baseline	62.7 (2.1)	62.4 (3.4)	0.86	64.3 (1.7)	58.6 (1.5)	63.3 (3.8)	65.1 (3.4)	0.24
	2 Months	57.2 (2.6)	60.5 (2.6)	0.47	-	-	-	-	-
	5 Months	-	-	-	58.3 (1.5)	55.3 (1.3)	59.5 (2.4)	62.5 (3.1)	0.41
Cortical thickness (mm)	Baseline	2.1 (0.2)	2.3 (0.1)	0.47	2.1 (0.2)	2.7 (0.2)	2.5 (0.4)	2.4 (0.2)	0.36
	2 Months	2.3 (0.1)	2.1 (0.1)	0.47	-	-	-	-	-
	5 Months	-	-	-	2.4 (0.1)	2.4 (0.1)	2 (0.1)	1.9 (0.1)	0.06

Data expressed as mean (SEM). The resulting p-values obtained by Kruskal–Wallis are given.

4.3.2 Effect of OVX plus glucocorticoid on the proximal tibial metaphysis at two and five months following treatments

Table 4.3 shows the effect of glucocorticoid plus OVX on the proximal tibial metaphysis at two and five months. Sheep were euthanised at month two or month five post-surgery, and e*x vivo* measurements of proximal tibial sites were carried out. At month two after OVX, vBMD, trabecular vBMD and cortical thickness decreased by 8.7% (p-value = 0.050), 25% (p-value = 0.357) and 14% (p-value = 0.072), respectively, when compared with the control group. There was no difference in bone area, BMC, trabecular area, trabecular BMC, periosteal circumference and endosteal circumference (p-values > 0.05).

After five months, there were marked differences between the control group and treated groups (Table 4.3). vBMD, bone area and BMC decreased by

8.2% (*p*-value = 0.052), 6.6% (*p*-value = 0.209) and 14% (*p*-value = 0.051), respectively. Trabecular vBMD, trabecular area and trabecular BMC decreased by 14% (*p*-value = 0.019), 20% (*p*-value = 0.435) and 4% (*p*-value = 0.044), respectively. Periosteal and endosteal circumference decreased by 3% (*p*-value = 0.209) and 2% (*p*-value = 0.343), respectively. Cortical thickness decreased by 8% (*p*-value = 0.158). When glucocorticoids were administered for five months, vBMD, BMC and cortical thickness decreased by 20% (*p*-value = 0.034), 4% (*p*-value = 0.056) and 23% (*p*-value = 0.038) when compared with the OVX group, whereas vBMD and cortical thickness decreased by only 5% (*p*-value = 0.407) and 19% (*p*-value = 0.038), respectively, in the OVXG2 group.

Table 4.3: Effect of OVX plus glucocorticoids treatment in the proximal metaphysis of the tibia in OVX sheep at two and five months.

	2 Months			5 Months				
	Control (n = 5)	OVX (n = 6)	p-value	Control (n = 5)	OVX (n = 6)	OVXG (n = 3)	OVXG2 (n = 3)	p-value
vBMD[1] (mg/cm^3)	476.1 (13.7)	434.6 (17.3)	0.10	490.7 (14.2)	450.1 (11.6)	358.7 (14.3)	426.3 (17.1)	0.02
Bone area (mm^2)	695 (30.7)	774.2 (50.2)	0.20	702.2 (31.4)	655.9 (20.8)	695.8 (35.8)	803.3 (71.8)	0.64
BMC[2] (g)	330.3 (12.8)	337 (26.8)	0.86	344.6 (18.8)	294.3 (6.5)	248.1 (9.7)	339.9 (30.5)	0.03
Tb vBMD[3] (mg/cm^3)	260.8 (14.2)	255 (13.3)	0.72	249.4 (6.4)	199.5 (13)	173.7 (7.5)	265.3 (15.5)	0.01
Tb area[4] (mm^2)	464.5 (28.8)	548.2 (41.3)	0.14	452.2 (24.1)	434 (20.4)	509.7 (37.1)	583.7 (62.5)	0.55
Tb BMC[5] (mg/mm)	122.3 (12.2)	141.35 (15.7)	0.58	113.2 (8.3)	87.5 (8.1)	89.5 (9.7)	156.7 (21.52)	0.10
Periosteal circumference (mm)	93.4 (2.1)	98.3 (3.2)	0.20	93.8 (2.1)	90.7 (1.4)	93.4 (2.3)	100.1 (4.6)	0.64
Endosteal circumference (mm)	80.2 (2.5)	86.5 (3.1)	0.14	79.1 (2)	77.1 (1.8)	83.4 (2.9)	89.1 (5.9)	0.52
Cortical thickness (mm)	2.1 (0.1)	1.8 (0.1)	0.14	2.3 (0.1)	2.1 (0.1)	1.6 (0.1)	1.7 (0.1)	0.02

[1] Volumetric bone mineral density (vBMD).
[2] Bone mineral content (BMC).
[3] Trabecular volumetric bone mineral density (Tb vBMD).
[4] Trabecular area (Tb area).
[5] Trabecular bone mineral content (Tb BMC).
Data are shown for half of the ewes euthanized at baseline and month 2 in the control group and OVX group; and the remaining ewes at baseline and month 5 for each group. Data expressed as mean (SEM). The resulting p-values obtained by Kruskal–Wallis are given. p-value < 0.05 was considered as statistically significant.

4.3.3 Relationship between distal and proximal metaphyseal parameters in OVX sheep at two and five months

Table 4.4 shows the association between distal and proximal metaphyseal parameters of the tibia at two and five months. As there are local variations within a bone, these variations need to be assessed for understanding the relationship of bone loss in skeletal sites. The effect of OVX was more pronounced on trabecular bone in proximal sites in this study. However, when metaphyseal sites were examined, bone parameters in both distal and proximal sites correlated well. vBMD (r = 0.73, p-value < 0.01), bone area (r = 0.864, p-value < 0.01) and BMC

(r = 0.791, *p*-value < 0.01) were significantly correlated at both skeletal sites of the tibia. For trabecular vBMD, correlation between distal and proximal metaphyseal sites was significant only at five months (r = 0.528; *p*-value = 0.029). Considering other indices, both skeletal sites correlated well with periosteal and endosteal circumferences at two and five months, respectively.

Table 4.4: Regression and correlation results between distal and proximal tibial metaphysis of the tibia at two and five months.

	2 Months			5 Months		
	R^2	Spearman's rho correlation	*p*-value	R^2	Spearman's rho correlation	*p*-value
vBMD[1] (mg/cm^3)	58.4%	0.730	<0.01	64.4%	0.803	<0.001
Bone area (mm^2)	76.6%	0.864	<0.01	77.4%	0.880	<0.001
BMC[2] (g)	73.6%	0.791	<0.01	44.9%	0.670	<0.01
Tb vBMD[3] (mg/cm^3)	7.3%	0.473	0.142	27.9%	0.528	0.029
Tb area[4] (mm^2)	63.4%	0.709	0.015	79.6%	0.892	<0.001
Tb BMC[5] (mg/mm)	42.8%	0.736	0.010	37%	0.608	0.010
Periosteal perimeter (mm)	75.9%	0.864	<0.01	78.5%	0.886	<0.001
Endosteal perimeter (mm)	65.4%	0.664	0.026	81.4%	0.902	<0.001
Cortical thickness (mm)	45.8%	0.736	0.010	73.8%	0.859	<0.001

[1] Volumetric bone mineral density (vBMD).
[2] Bone mineral content (BMC).
[3] Trabecular volumetric bone mineral density (Tb vBMD).
[4] Trabecular area (Tb area).
[5] Trabecular volumetric bone mineral content (Tb BMC).
p-value < 0.05 was considered as statistically significant.

4.3.3 Effect of OVX plus glucocorticoids on biomechanics in mid-shaft of the tibia at two and five months following treatments

A three-point bending test was used to assess bone strength at the mid-diaphysis of the tibia (Figure 4.1). There were no significant differences in maximum load, stiffness and energy among the four groups determined from the three-point bending test in the mid-diaphysis of the tibia after sacrifice at months two and five (Figure 4.1). However, OVX plus glucocorticoids decreased all the mechanical property parameters of the tibial mid-diaphysis, where maximum load, stiffness and energy decreased after five months of the study in all groups. The decrease in mechanical properties may be affected by the decrease observed in distal and proximal tibial in vBMD.

At two months, maximum load was slightly lower in the OVX group than in the control group (3.85 N vs 4.31 N; *p*-value = 0.228) (Figure 4.1A). Moreover, stiffness was lower in the OVX group than in the control group (1.75 N/mm vs 2.96 N/mm; *p*-value = 0.089). Energy did not differ significantly between the OVX group and the control (2.65 N·mm vs 3.11 N·mm; *p*-value = 0.228).

At five months, maximum load did not differ significantly between the OVX group and the control (4.39 N vs 4.41 N; *p*-value = 0.456). Compared to the OVX group, glucocorticoids decreased the maximum load in the OVXG group (3.57 N vs 4.39 N; *p*-value = 0.012), whereas the OVXG2 group showed an increase in the maximum load (4.64 N vs 4.39 N; *p*-value = 0.389).

Stiffness was slightly higher in the OVX group compared with the control (2.45 N/mm vs 1.94 N/mm; *p*-value = 0.456) (Figure 4.1B). Compared to the OVX group, glucocorticoids decreased the stiffness in the OVXG group (1.6 N/mm vs 2.45 N/mm; *p*-value = 0.115), whereas the OVXG2 group showed an increase in

stiffness (2.57 N/mm vs 2.45 N/mm; *p*-value = 0.389). Energy was lower in the OVX group than in the control group (2.57 N·mm vs 3.23 N·mm; *p*-value = 0.15) (Figure 4.1C). Compared to the OVX group, glucocorticoids showed a decrease in energy in the OVXG group (2.29 N·mm vs 2.57 N·mm; *p*-value = 0.241), whereas energy increased in the OVXG2 group (3.02 N·mm vs 2.57 N·mm; *p*-value = 0.141).

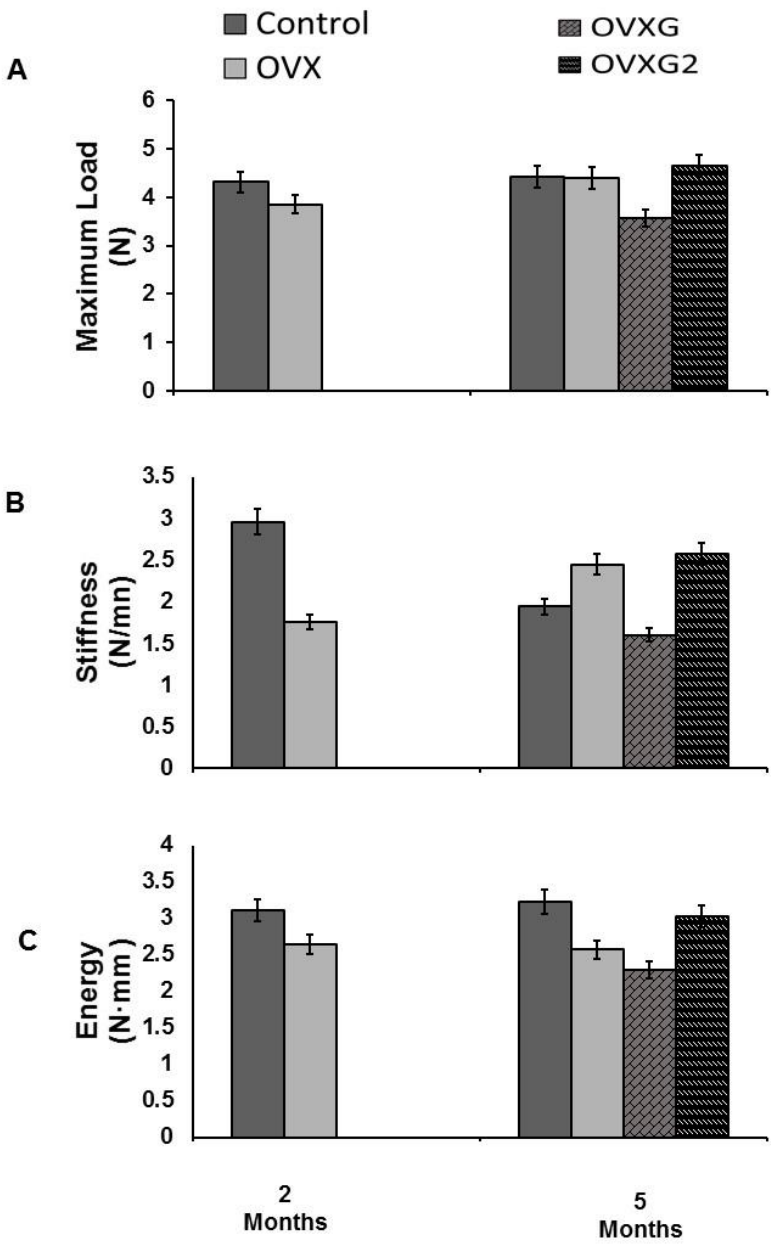

Figure 4.1: Effect of OVX plus glucocorticoids treatment on bone mechanics measured by three bending points in tibia after sacrifice in OVX sheep. Maximum load (A), stiffness (B) and energy (C) at two months and five months in OVX sheep. Data are presented as mean and 95% confidence intervals.

4.4 Discussion

This study demonstrates the effect of OVX plus glucocorticoids on different skeletal sites in sheep. The key findings were that OVX combined with glucocorticoids in sheep resulted in decreased trabecular, cortical and strength parameters of the tibia. Changes in bone mass and strength parameters were consistent with changes in vBMD, but those differences were not significant in the strength parameters analysed using the three bending points. OVX sheep that received five months of glucocorticoid treatment had greater bone changes compared to the control and OVX groups over the five months.

In this study, OVX alone did not affect bone parameters in the proximal and distal tibial metaphyses in OVX sheep at two months post-surgery. No significant differences were seen in any bone parameters between the control and OVX groups as change from baseline after two months. Similar to our findings, studies elsewhere reported that OVX alone did not decrease trabecular vBMD in OVX sheep after six or 12 months of study (Augat et al., 2003; Kennedy et al., 2009). These studies reported that at an early stage of oestrogen deficiency after OVX, oestrogen concentration increased at the tissue level as there were other extra-glandular sources of oestrogen, and this may result in the slow bone loss observed after OVX (Lesclous et al., 2001; Riggs et al., 2002; Oheim et al., 2016). Sigrist et al. (2007) reported a 10% reduction of trabecular vBMD in sheep three months after OVX. Chavassieux et al. (2001) indicated that oestrogen deficiency after OVX increased cortical porosity, but no change was noted in trabecular bone.

In this study, the interaction of OVX plus glucocorticoids had a pronounced effect on vBMD in the group that received five months of this treatment. Similarly,

Eschler et al. (2015) demonstrated the development of severe osteoporosis with OVX, corticosteroid treatment and calcium/phosphorus/vitamin D-deficient diet in sheep after five-and-a-half months of treatment. They reported a decrease in trabecular bone in the distal radius with significantly reduced vBMD in the glucocorticoid treatment group (0.19 g/cm^3) as compared with the control animals (0.27 g/cm^3). Other studies reported severe trabecular loss in the distal radius, lumbar spine and proximal tibia with glucocorticoid treatment alone over seven months (Ding et al., 2010), and with either OVX alone or a combination of OVX and glucocorticoid treatments over six and 12 months in sheep (Augat et al., 2003).

Glucocorticoid-induced osteoporosis has been reported to be reversible after six months of discontinued treatment (Van Staa et al., 2005). In this study, when glucocorticoid treatment was discontinued after two months, a rebound effect was observed, although this was not statistically significant in the OVXG2 groups. A similar effect was reported by Ding et al. (2010), who indicated that three months after cessation of glucocorticoid treatment, the microarchitectural properties of trabecular bone were similar to those in the control group. Glucocorticoids affect bone remodelling directly by decreasing bone formation cells, altering bone remodelling and stimulating osteoclastogenesis (O'brien et al., 2004). Glucocorticoids can suppress expression of cytokines such as interferon-β and induce expression of M-CSF, which are essential molecular factors for osteoclastogenesis (Mazziotti et al., 2006).

Interestingly, sheep in the control group showed a reduction in bone parameters as well over time. This could be attributed to a decline in physical activity which could have affected bone mass in the control group, as the sheep

were on a farm before the study and were kept in a barn during the study period. Studies in animals and humans support that long periods of inactivity will result in a reduction of bone mass and changes in bone structure (Goldhahn et al., 2005; Roghani et al., 2013; Moreira et al., 2014). Bone strength of the long bone shaft predicts fracture risk during osteoporosis, and is associated with the mechanical properties of bone (Beck et al., 2001). Oestrogen modulates mechanical loading responses of bone cells and plays a role in bone homeostasis, but during menopause these responses change and there is an accelerated loss of bone mass and structure (Klein-Nulend et al., 2015).

Bone provides mechanical and protective functions against fracture. In this study, bone maximum load, stiffness, and energy to failure decreased. There were no significant differences between the four groups, but OVX plus glucocorticoid treatment was more effective in deleteriously affecting the biomechanical properties of bone. In other studies, glucocorticoid treatment negatively affected the biomechanical properties of trabecular bone, resulting in reduced bone strength and increased risk of fractures (Lane et al., 2006). Thus, the efficacy of bone materials to protect against fracture is compromised as a result of long-term oestrogen depletion plus glucocorticoid treatment, making the bone vulnerable to mechanical damage. Ding et al. (2012) reported a decrease in cortical microarchitecture of the femoral shaft after seven months of glucocorticoids and malnutrition (low calcium and phosphorus) in sheep, where those changes may increase bone fragility. Lill et al. (2002c) reported a 70% reduction in load-bearing capacity of the lumbar spine, and a 50% reduction in the femoral head, in OVXG sheep. Similarly, results of the present study indicated that after OVX and glucocorticoid treatments, bone structural properties were

reduced, resulting in the observed greater decreased in $_{v}$BMD in the OVXG groups (Lane et al., 2006). The reduction in bone biomechanical properties were consistent with the decrease in total and trabecular $_{v}$BMD. During glucocorticoid-induced osteoporosis reduction of trabecular bone has been reported, where there is decreased in trabecular thickness without reducing trabecular connectivity, affecting bone quality as there are changes in bone composition and strength (Carbonare et al., 2001; Tranquilli Leali et al., 2009).

Trabecular and cortical bone mass can be determined in the total skeleton, but prediction of fracture risk is complicated because bone mass differs between skeletal sites. In this study, vBMD and bone mass measurements between distal and proximal tibial metaphysis were correlated, although bone measurements were greater at proximal sites compared to distal sites. It has been reported that skeletal sites at both red and yellow marrows respond differently to oestrogen deficiency, and trabecular loss occurs mainly in proximal sites at red marrow rather than yellow marrow sites (Ma et al., 1994; Li et al., 1996). Bone loss also occurs as a result of excess production of adipocytes in the marrow, and during menopause, bone loss is associated with lower osteoblastic and greater adipogenic lineage from the mesenchymal stem cells. Thus, after OVX, bone loss in these sites is associated with high bone remodelling in red marrow at proximal sites (Paccou et al., 2015).

4.5 Conclusions

OVX combined with glucocorticoid treatment did influence density and strength parameters of the tibia in OVX sheep over five months. This study showed that there are significant changes at the proximal tibial site, where

trabecular bone loss was observed. vBMD of the distal tibial metaphysis reflects vBMD of the proximal metaphysis, the location of clinically important fractures that occur in women with postmenopausal osteoporosis. This suggests that a relationship between both distal and proximal metaphysis sites does exist and is important for better understanding metaphyseal remodelling, with the potential to enhance the assessment and diagnosis of bone loss in postmenopausal osteoporosis.

Chapter 5

Application of MS-based metabolomics approach in ovariectomised sheep as a model of osteoporosis

This chapter employs the ewe as a large animal model of osteoporosis to investigate the impact of short-term and long-term ovariectomy and glucocorticoid hormonal interventions using a hydrophilic-interaction liquid chromatography–mass spectrometry (HILIC–MS)-based metabolomics approach. This is the first report to describe the effects of dynamic changes of osteoporosis progression on circulating metabolites in a longitudinal study. This chapter also evaluates the relationship between bone mineral density measurements, bone turnover markers and metabolite profiles in order to determine whether those significant features are linked to bone loss.

Abstract

Understanding the early metabolic changes that accompany bone loss in postmenopausal osteoporosis will facilitate better targeting for developing new drugs or nutritional strategies for treatment of bone loss in postmenopausal women. Here, it was hypothesised that the metabolite profiles of ovariectomised sheep would be altered, and that the biochemical changes in plasma and bone remodelling would be correlated with bone loss. 28 skeletally mature ewes were divided randomly into four groups: an ovariectomy group, a group of ovariectomy in combination with five doses of glucocorticoids, a group of ovariectomy with only two doses of glucocorticoids, and a control group. Liquid chromatography–mass spectrometry untargeted metabolomics analysis was applied to serial plasma samples from the sheep model to follow the progression of osteoporosis. To understand the mechanisms behind bone loss in these models, the plasma metabolome, bone turnover markers and bone mineral density of the sheep were evaluated. Separate statistical approaches were used to analyse the first two months (the short-term approach), and the five months (the long-term approach). Eight metabolites showed dynamic changes over time, including 5-methoxytryptophan, valine, methionine, tryptophan, glutaric acid, 2-pyrrolidone-5-carboxylic acid, indole-3-carboxaldehyde, 5-hydroxylysine and malic acid. In the short-term approach, metabolites had significant increases in relative intensities related to the early-onset changes that preceded the interventions. A negative correlation between methionine and osteocalcin was observed, and glutaric acid was negatively associated with femoral and lumbar spine bone mineral density. In the long-term approach, plasma metabolites appeared to be affected one month after initiating the hormonal interventions, where circulating metabolites decreased for a short time, and this decline remained steady

throughout the study. In the long-term study, 5-methoxytrytophan was negatively associated with the C-terminal telopeptide *of type 1 collagen* marker, and 5-methoxytrytophan and methionine were associated with femoral bone mineral density. This study showed that oestrogen deficiency and glucocorticoid interventions generated changes in the metabolite profile of sheep. Further, the study revealed specific metabolites as possible bone formation and resorption markers, suggesting that 5-methoxytrytophan and methionine are potential targets for the prognosis of osteoporosis.

5.1 Introduction

Bone metabolism requires intra- and extracellular factors to maintain balanced bone remodelling. During menopause, oestrogen deficiency induces bone loss. The mechanisms that contribute to bone loss are well understood. Oestrogen withdrawal stimulates bone resorption, resulting in unbalanced bone remodelling in which bone formation is unable to compensate for the amount of bone being resorbed by osteoclasts (bone cells) (Garnero et al., 1996; Manolagas, 2010). Imbalance in bone remodelling results in decreased BMD, micro-architectural deterioration, decreased bone strength and increased fracture risk (Kalervo Väänänen and Härkönen, 1996; Manolagas, 2000). In addition, bone loss is common in glucocorticoid-treated patients. Glucocorticoid-induced osteoporosis is characterised by an increased bone loss and increased fracture risk immediately after beginning the glucocorticoid treatment, leading to fractures in nearly 50% of people treated with long-term systemic glucocorticoids (Canalis et al., 2007; Briot and Roux, 2015).

Currently, the diagnosis of osteoporosis is carried out by measuring BMD (Kanis et al., 1994; Kanis et al., 2008). Specific interest has been in the clinical potential of bone turnover biomarkers as a manner in which to assess fracture risk and to monitor treatment. Biochemical markers of bone metabolism are enzymes, protein fragments, or other molecules released into blood as a result of bone remodelling by osteoblasts and osteoclasts (Delmas et al., 2000). These bone turnover biomarkers represent bone metabolism, and include both bone formation and resorption markers (Vasikaran et al., 2011b; Glendenning et al., 2018). Increased rates of bone turnover have been associated with increased risk of fractures and changes in BMD, but their predictive value is confounded by their

large biological and laboratory variability (Seibel, 2006; Wheater et al., 2013); therefore, more progress is needed towards the search for alternative biomarkers to be used for rapid and reliable early diagnostics of bone loss.

Metabolomics is one of the novel techniques for investigating changes in the metabolome of biological systems. Metabolomics allows the measurement of all the small molecules in fluids or tissues that can be detected, and provides information on the final downstream products of gene expression, the phenotypes, which provides a better understanding of the disease mechanisms. The metabolome is highly dynamic, and changes in its metabolites and metabolic pathways can occur rapidly in response to specific physiological conditions or treatments. Thus, these metabolic alterations may have the potential for detecting early changes of specific metabolic pathways and discovering novel clinical biomarkers that can be associated with human diseases (Goodacre et al., 2004; Assfalg et al., 2008; Scalbert et al., 2009; Beger et al., 2016).

Bone metabolism is a dynamic process, in which oestrogen regulates bone remodelling via osteocytes, osteoblasts, osteoclasts and T-cells. Osteoblasts express pro-inflammatory cytokines that stimulate osteoclastogenesis, including RANKL macrophage-colony stimulating factor, interleukin (IL)-1β, IL-6, IL-1 and leukemia inhibitory factor, both in normal and pathologic conditions. On the other hand, osteoblasts also enhance the production of anti-inflammatory cytokines such as osteoprotegerin, granulocyte–macrophage-colony-stimulating factor, IL-3, IL-12 and IL-18, which inhibit osteoclastogenesis (Martin and Ng, 1994; Teti, 2013). In normal conditions, bone remodelling is coupled and formation and resorption are balanced, and oestrogen inhibits bone resorption by inducing osteoclast apoptosis. Oestrogen also inhibits

the secretion by T-cells of cytokines such as IL-1, IL-6 and RANKL, which at increased concentrations lead to increased osteoclastogenesis (Streicher et al., 2017). Thus, undergoing menopause increases oxidative stress and pro-inflammatory factors (Vaananen et al., 2000; Gerdhem et al., 2009). Therefore, circulating plasma compounds might reflect the biological processes in bone metabolism during menopause. Defining these metabolite perturbations during oestrogen deficiency may be useful to predict the onset of bone loss in postmenopausal women.

Animal models are widely used to understand the processes and mechanisms that contribute to bone loss at different physiological stages. Ovariectomy (OVX), a surgical intervention, is an established method to induce bone loss in mammals for the study of postmenopausal osteoporosis (Lelovas et al., 2008). Sheep are accepted as one of the large animal models for osteoporosis. Most of the preclinical and translational studies have reported effective methods for inducing bone loss in sheep through OVX alone or by the combined treatment of OVX, a calcium- and vitamin D-deficient diet, and glucocorticoid treatments (Dias et al., 2018). Previous studies on sheep have documented the mechanisms underlying bone loss in postmenopausal osteoporosis (Lill et al., 2002c; Egermann et al., 2008; Zarrinkalam et al., 2012), but no research has been conducted to evaluate whether oestrogen deficiency and glucocorticoid interventions affect the plasma metabolite profile of OVX sheep as an animal model of bone loss. Hence, the purpose of this part of the study was to determine the impact of oestrogen deficiency and glucocorticoid hormonal interventions on tissue metabolism in an animal model of osteoporosis using a HILIC–MS untargeted metabolomics approach.

Here, it was hypothesised that OVX alone or combined with glucocorticoids, conditions reflective of osteoporosis, would produce biochemical and molecular changes in the plasma metabolite profile and bone remodelling in sheep that would be unique signatures of bone loss and osteoporosis. The present study employed Merino sheep, a widely used large animal model of osteoporosis. This breed was chosen because it has been proven that the sheep bone remodelling and fracture healing are similar to humans (Augat et al., 2003; Schorlemmer et al., 2005). The study comprised four different groups of animals: a control group, an OVX alone, and two OVX groups combined with glucocorticoids for a short-term or a long-term period. The study protocol aimed to mimic bone loss in postmenopausal osteoporosis, since it is known that oestrogen's key role is to maintain a balanced bone metabolism. This chapter also evaluates the relationship between BMD measurements, bone turnover markers and metabolite profiles at specific time points, at month two and month five, in order to evaluate whether significant features are linked to bone loss in postmenopausal osteoporosis. Furthermore, in this chapter, the metabolic pathways altered by the disease progression were also investigated.

5.2 Materials and methods

5.2.1 Animals used and experimental design

Animals used and experimental design have been described in Chapter 3, Section 3.2.1 (Figure 3.1). Briefly, twenty-eight Merino sheep (ewes) were used in this experiment, aged between 5–9 years, with hormonal interventions resulting from either OVX or OVX combined with glucocorticoids. The study comprised four groups of animals, OVX alone, OVX combined with glucocorticoids (OVXG) for a short-term or a long-term period, and a control group.

5.2.2 Blood collection

Blood samples were collected during the experiment described in Chapter 3, Section 3.1.2. Blood samples were taken from the 28 ewes at the baseline time (pre-surgery), and through the period of this study at one, two, three, four and five months post-surgery. The sheep were given *ad libitum* water and straw, and measure-pelleted twice daily. Blood was collected by venepuncture of the jugular vein and the flow directed into EDTA-treated serum separator vacuum tubes. After centrifugation (2000 *g*, 15 min, 4 °C), the serum was removed and stored (–80 °C) until required.

5.2.3 Bone turnover markers

Bone turnover marker analyses for the experimental work have been described in Chapter 3, Section 3.1.4.

5.2.4 Bone mineral density

Lumbar spine and femoral BMD assessments have been described in Chapter 3, Section 3.1.5.

5.2.5 Metabolomics analysis

5.2.5.1 Standards and reagents

In this study, all standards and reagents used were analytical grade and supplied by Sigma-Aldrich Chemicals Co. (St Louis, MO, USA) unless specified. Ultrapure water was used for preparation of chemicals (Milli-Q-system, Millipore, Bedford, MA, USA). Acetonitrile (ACN), methanol and isopropanol were optima LC–MS grade, chloroform was high-performance liquid chromatography (HPLC) grade, and all were purchased from Thermo Fisher Scientific (Auckland, New Zealand).

5.2.5.2 Sample preparation

Briefly, for the metabolic profiling, samples were collected at baseline, month one, two, three, four and five and stored at –80 °C until experimental analysis. Methods for metabolite extraction were as have been described previously (Xu et al., 2016). The plasma samples were thawed at 4 °C and immediately vortexed for 1 min. Then, a total of 100 μL of plasma was transferred to a microcentrifuge tube and a total of 800 μL of precooled chloroform:methanol (1:1 v/v, containing 0.8 mg ML^{-1} of internal standards, D_4-Citric acid, $^{13}C_6$-D-fructose, D_5-L-tryptophan, D_7-L-alanine, D_{35}-stearic acid, D_5-benzoic acid, D_{10}-leucine, D_2-Tyrosine) at –20 °C was added to each tube. The tubes were mixed

by hand for 1 min and the samples incubated for 30 min at –20 °C. Following incubation, 400 µL of water was added to each sample and they were then vortexed for 30 s. The samples were centrifuged for 15 min at 11,000 rpm at 4 °C. Thereafter, 250 µL aliquots of the supernatants were collected for metabolite analysis and transferred into new microcentrifuge tubes. Each tube was placed under a stream of nitrogen to evaporate the samples to dryness. Thereafter, 300 µL of ACN:water (1:1 v/v) containing formic acid (0.1%) was added to each tube to reconstitute the samples. Then, the samples were vortexed for 1 min, centrifuged for 10 min at 11,000 rpm at 4 °C, and 100 µL was transferred to a vial containing an insert and stored at 4 °C for immediate metabolite analysis. Blank samples were prepared using the same protocol but using 100 µL of water instead of plasma. The pooled quality control (QC) samples were prepared by adding 60 µL of each sample, and were placed in a tube to be pooled and processed in exactly the same manner as the rest of the samples The pooled QC samples were used to compare the analytical performance of the instrument data based on the total number of detected peaks, to detect reproducibility and consistency of detected features through all the analysis.

5.2.5.3 Metabolite analysis

For the LC-MS analysis the order of the sequence runs was blanks, QC samples and individual samples. Pooled QC samples were also injected every ten samples throughout the analytical batch. Data quality was monitored using retention time and signal to intensity ratios during all the analysis.

Metabolites were analysed by hydrophilic-interaction liquid chromatography–mass spectrometry (HILIC–MS) with positive and negative mode electrospray ionisation.

Metabolomics was performed on a Thermo Exactive LC–MS system (Thermo Fisher Scientific, Waltham, MA, USA) that consisted of an Accela 1250 quaternary pump, a Thermo-PAL autosampler fitted with a 15,000 psi injection valve (CTC Analytics AG., Zwingen, Switzerland) and a 2 µL injection loop and an Exactive Orbitrap mass spectrometer.

Metabolites were separated on a ZIC-pHILIC column (100 mm × 2.1 mm, 5 µm; Merck, Darmstadt, Germany) with a gradient elution program at a flow rate of 250 µL/min. The mobile phase was a mixture of ACN:formic acid (99.9:0.1 v/v) (solvent A) and water–ammonium formate (16 mM, pH 6.3) (solvent B). The gradient elution programme was: held at 97% A (0–1 min), 97–70% A (1–12 min), 70–10% A (12–14.5 min), held at 10% A (14.5–17 min), returned to 97% A (17–18.5 min) and allowed to equilibrate for a further 5.5 min prior to the next injection. Samples were run in both positive and negative electrospray ionisation mode separately. Data were collected in profile data acquisition mode over a mass range of *m/z* 55–1100 at a mass resolution setting of 25,000 with a maximum trap fill time of 100 ms using the Xcalibur v2.1 software (Thermo Scientific, Hemel Hemstead, UK) provided by the manufacturer. Positive ion mode parameters were as follows: spray voltage, 2.7 kV; capillary temperature, 275 °C; capillary voltage, 29.1 V; tube lens, 108.8 V. Negative ion mode parameters were as follows: spray voltage, −3.0 kV; capillary temperature, 325 °C; capillary voltage, −90 V, tube lens −100 V.

Each raw datafile consisted of LC–MS spectral features characterised by *m/z*, retention time and ion signal relative intensity. Peak picking, alignment and integration of the LC-MS data set from the plasma metabolites was performed with the open-source software XCMS (Figure 5.1). The metabolomics data preprocessing workflow started by first importing the raw datafiles to MSconvert (ProteoWizard; Software Foundation, San Diego, CA, USA) and converting them to mzXML files using MSconvert file conversion tool. Then, the next step was to extract the features of the spectra, assign them to molecular ions, align peaks across samples and quantify their relative intensity using the open-source program XCMS (Figure 5.1) (Smith et al., 2006). These programming steps consisted of 1) peak detection and filtration using the 'xcmsSet' function 2) Xcms.group to group features together across samples using *m/z* bins to calculate peak distributions in the chromatographic time, 3) retention time correction using 'retcor' function from xcms R package, 4) Annotation of isotope peaks, adducts and fragments with CAMERA.annotate (Kuhl et al., 2011) and finally 5) a 'diffreport' obtained . Table 5.1 summarises the extraction parameters applied for this untargeted LC-MS spectral data.

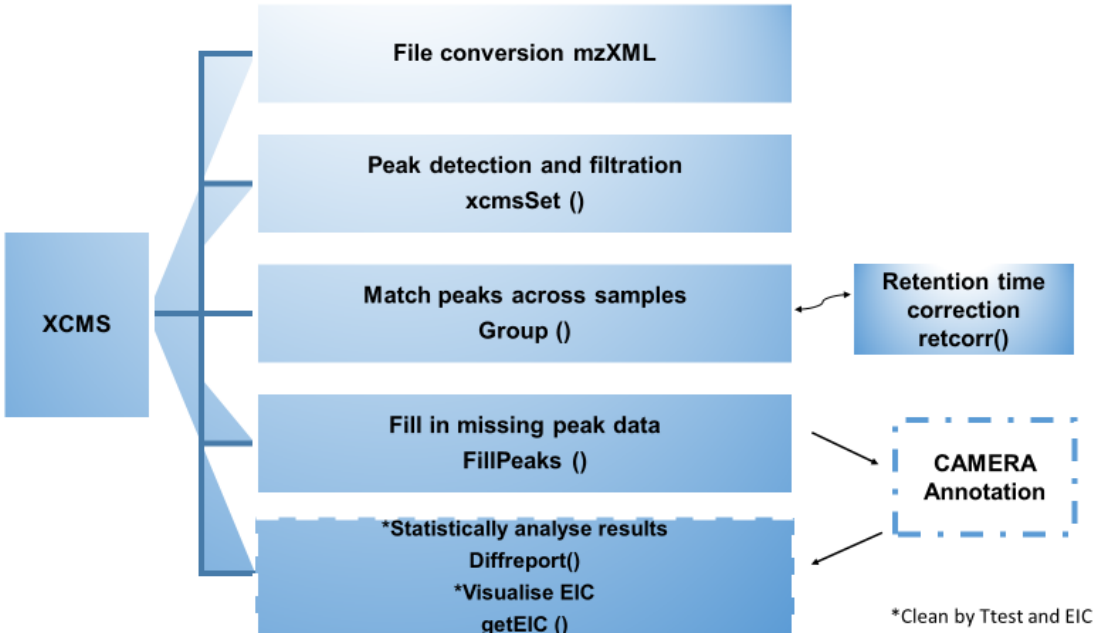

Figure 5.1: Preprocessing workflow in untargeted metabolomics. XCMS functions to preprocess LC-MS data for relative quantification and statistical analysis.

Table 5.1: XCMS main parameters applied for untargeted LC-MS-based metabolomics spectral processing.

Parameters	Related to	Settings
ppm	*m/z*	10
peakwidth	Retention time	20,60
Prefilter	intensity	3, 1000
Snthresh*	intensity	10
noise	intensity	200

*signal to noise threshold

After data extraction, cleaning of the detected feature table using the quality control samples was performed. The data matrix generated with the 'diffreport' function was used to compare QC samples and blank samples and remove all those features with a p-value > 0.05 (i.e. peaks that were not significantly different from the blank to the pooled QC sample were classed as blank features and removed). A QC sample to samples comparison was performed and then each extracted ion chromatogram was visually inspected to verify that peak picking, alignment, and integration was performed adequately

and those failing visual inspection were remove (generally misaligned features and baseline noise).

Thereafter, peak intensities of each sample were corrected for run-order signal correction by using a locally quadratic (loess) regression model to fit the QC values (Giacomoni et al., 2015). Metabolites with a coefficient of variation of their QC values greater than 30% after run-order correction were removed from the peak table. Missing values in the peak tables were replaced using the k-nearest neighbour method.

Putative identification of metabolites was achieved using an in-house library of authentic standards to their respective ionisation mode. Identification were based on *m/z* and experimental precursor mass match and retention time match to the library of authentic standards. METLIN and the Human Metabolome Database were also used for matching against standard metabolite compounds based on accurate mass and MS2 spectra (Smith et al., 2006; Wishart et al., 2013).

5.2.6 Statistical analyses

The metabolite profiles obtained from HILIC–MS positive and negative ionisations were analysed by two main statistical approaches to assess group differences by either multivariate or univariate analysis (Figure 5.2). The separate approaches were analysed to investigate the effects of short-term and long-term glucocorticoid treatment on metabolite profiles in OVX sheep. In the short-term approach, three treatments (n = 28), OVX, OVXG and control groups were analysed at the first two time points. In the long-term approach, four treatment

groups (*n* = 17), OVX, OVXG, OVXG2 and control groups were analysed at all six-time points.

5.2.6.1 Multivariate analysis

PCA is an unsupervised multivariate method and was used to explore and visualise the effect of OVX plus glucocorticoid treatments in ewes. The main objective of PCA is the reduction of the high dimensionality of a dataset, while preserving its variability. PCA reduces a set of possible high-dimensional variables into a lower-dimensional set of uncorrelated variables through a linear transformation that preserves as much of the variance in the original data as possible. In this sense, PCA analyses a smaller set of components called principal components that are organised into decreasing order of relevance, where the first components account for most of the variation in the original data. In this statistical analysis, R2 and Q2 are parameters necessary for evaluating the models. R2 represents the percentage of variation explained by the model (the goodness of fit), Q2 is a parameter to assess the quality of the model, a significant value of 0.5 is generally accepted, and a large discrepancy between R2 and Q2 indicates overfitting of the model (Wheelock and Wheelock, 2013; Triba et al., 2015). In the present study, PCA was performed on plasma samples to explore differences among samples from different time points. The metabolomics data were mean centered, log transformed and autoscaled prior to performing data analysis.

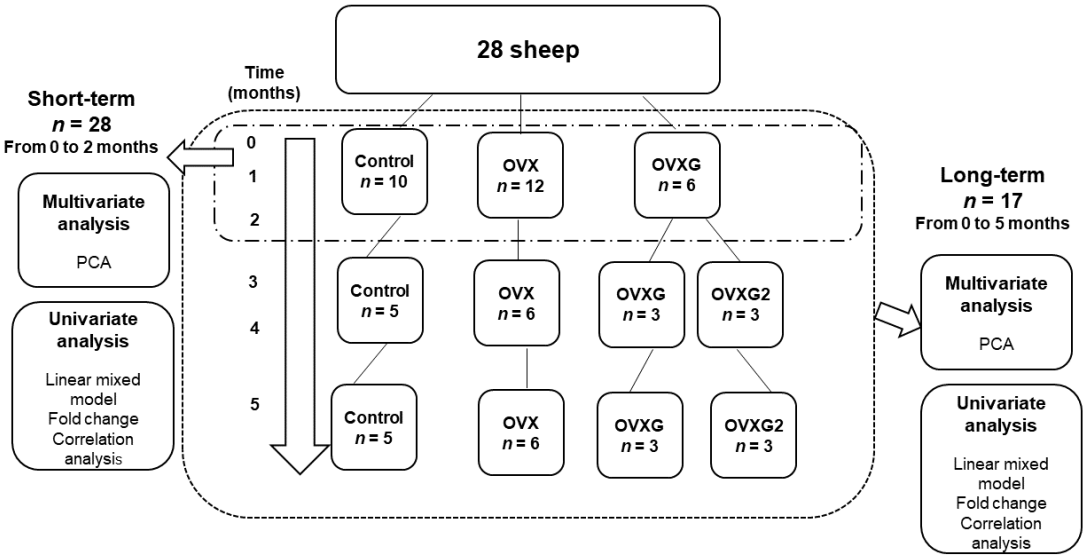

Figure 5.2: Overview of the study design and specific statistical analyses. Short-term study: Plasma metabolite profiles of 28 sheep, control group *n* = 10, OVX group *n* = 12, OVXG *n* = 6, were analysed by multivariate and univariate analyses from baseline to two months. Long-term study: Plasma metabolite profiles of 17 sheep, control group *n* = 5, OVX group *n* = 6, OVXG *n* = 3, OVXG2 *n* = 3, were also analysed by multivariate and univariate analyses from baseline (month zero) to five months.

5.2.6.2 Univariate analysis

A linear mixed model was used to analyse for treatment effects over time in the metabolite profiles in OVX sheep. Homogeneity of group variances was estimated using Levene's test. Changes in the sheep plasma over time were analysed with a linear mixed effect (lme) model for comparison of means, a procedure from R for fitting linear mixed models, using as fixed effects the treatment and time, and animal as random effect (Pinheiro et al., 2015). The differences between the group means of treated sheep were compared using one-way ANOVA, followed by post-hoc Fisher's least significant difference (LSD) test for pair-wise multiple comparison of the group means. Significance was considered at p-value < 0.05, and predicted means from the model with standard error of the means were obtained using the PredictedMeans package of R.

Metabolites that did not show significant differences between the interaction and treatments were not further analysed.

The data were pooled from all the treatment groups at month two and month five, and further analyses performed to investigate any possible associations between bone clinical parameters. Correlations between bone turnover markers (OC and CTx-1), and BMD (lumbar spine and femur) and metabolite profiles were obtained, and values of Pearson's correlation coefficients are presented. *P*-values less than 0.05 were considered statistically significant. Statistical data analysis was performed by SIMCA 14.1 (Umetrics, Umea, Sweden), Minitab 17 statistical software (Minitab Inc., 2008, USA) and the platform R 3.3.3 (R Foundation for Statistical Computing).

5.3 Results

OVX alone or combined with glucocorticoids caused changes of metabolite profiles in plasma samples as revealed by HILIC–MS-based metabolomics. The metabolite profiles of the untreated control group and OVX sheep treated with or without glucocorticoids were obtained at baseline, and one, two, three, four and five months. Overall, 193 features, including positive and negative ions were detected in plasma samples taken over five months of the study period.

Both statistical approaches highlighted changes in detected variations of plasma metabolites related to the time of the study. PCA failed to identify separation between the experimental groups. To analyse the polar metabolites in detail, a linear mixed model approach was then performed. The metabolite profiles revealed significant differences in the plasma metabolome of OVX sheep and OVXG when compared with the control group by univariate analysis. Twenty-six

features were significantly affected by treatment and time in the short-term approach and twenty-four in the long-term approach with *p*-values less than 0.05. Unfortunately, in this study only nine metabolites could be identified. These metabolites included 5-methoxytryptophan, valine, methionine, tryptophan, glutaric acid, 2-pyrrolidone-5-carboxylic acid, indole-3-carboxaldehyde, 5-hydroxylysine and malic acid.

5.3.1 Effect of OVX on the plasma metabolome of sheep: short-term approach

5.3.1.2 PCA: short-term approach

PCA was used to analyse the distribution of polar metabolites among all treatments over two months of the study. PCA was conducted on all the 193 detected features in positive and negative modes. Overall, the PCA models showed no separation, and R2 and Q2 values were lower. Furthermore, in the PCA a few samples could be considered outliers according to the 95% Hotelling's T2 confidence range. However, outliers could be part of a huge variation among samples, so in this study all the outliers were retained for the analyses.

Due to individual variability, it was difficult to directly observe changes in the metabolite profiles among the three groups (see Appendix B, Figure B.1). Thus, all time points for each group were analysed individually to obtain global information regarding the metabolite changes.

The distribution of all the serum samples from the control group at baseline (month zero), and one and two months, is shown in Figure 5.3A. No noticeable differences can be observed in the PCA over the period of time. At baseline, the resulting scatter plot of PC1 and PC2, which explain 28.1% of the variance, showed that over time, samples were clustered in the middle of the plot. Two

outliers were observed in the control group, one at baseline and the other at month one. Moreover, in the OVX group (Figure 5.3B), PC1 and PC2 explained 34.2% of the total variance, showing that plasma samples of OVX at three time points changed; whereas OVX samples at month one exhibited a different pattern with respect to OVX samples from baseline and month two. Two outliers from month one were identified. Similarly, for the OVXG group shown in Figure 3C, PC1 and PC2 explained 30% of the variance, and consistent with the OVX group, the OVXG samples changed over time. Surgical intervention (OVX) combined with glucocorticoid treatment changed the metabolic profiling over time when compared to baseline measurements when samples from all time points were analysed together.

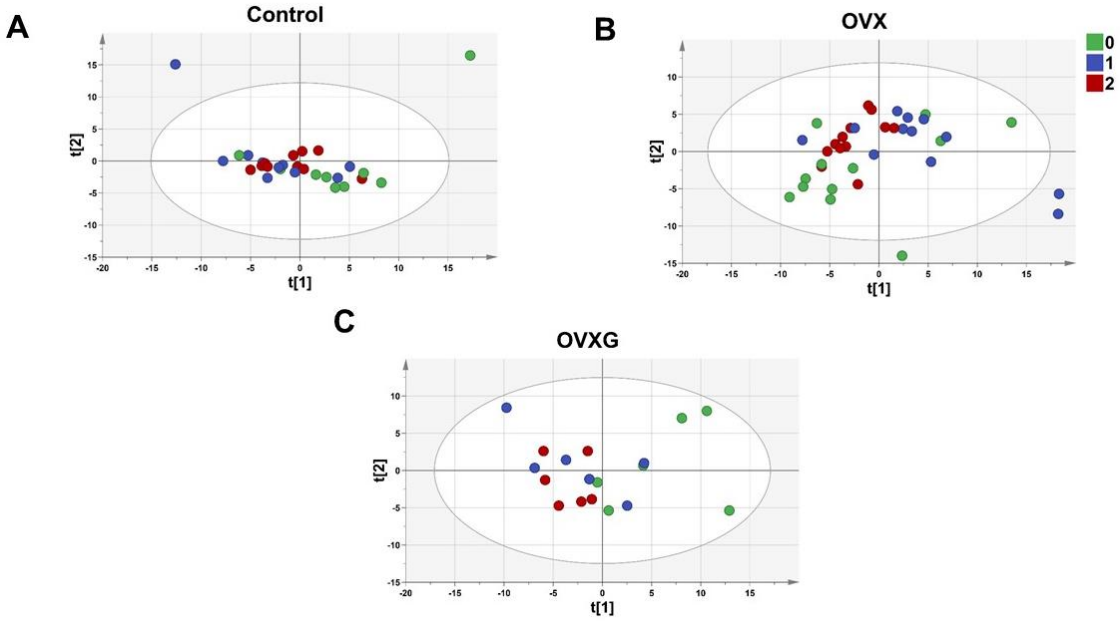

Figure 5.3: Inter-animal variation in the plasma metabolome of sheep over two months of the study period. PCA scatter plots derived from HILIC–MS spectra dataset based on normalised and autoscaled data. Each data point represents the metabolite profile of a single ewe. PCA scoring plot showing the variation of control group (A) (● baseline (month zero), ● month one, ● month two) R2 = 54.2% and Q2 = –5.5%; (B) R2 = 53.8% and Q2 = 16%; and (C) R2 = 30% and Q2 = 1.86%.

5.3.1.2 Linear mixed model: short-term approach

To identify individual dynamic metabolite changes, all features were analysed by using a linear mixed model, and only those features that showed significance based on the interaction of treatment and time were further analysed. Twenty-six features were significant and of these, eight were identified. In this chapter, the eight identified metabolites are described and all the remaining unidentified features are shown in a complementary section of this chapter (see Appendix B, Table B.1).

Changes in the plasma metabolites of the OVX group were observed with a decrease in the relative intensities of all the identified metabolites at month one after OVX, with the exception of 5-methoxytryptophan, methionine and tryptophan (Table 5.2). However, all plasma metabolites increased relative intensities at month two of this study, with the exception of methionine and tryptophan. In contrast, for the OVXG group, a trend for most of the metabolite relative intensities to be higher after OVX plus glucocorticoid treatments was observed. At month one, methionine was the only amino acid with decreased intensity (Table 5.2), while at month two, all metabolite relative intensities decreased, with the exception of valine.

Table 5.2: Effect of OVX and glucocorticoids on the metabolite profile of sheep in the short-term approach. Relative intensities were measured in plasma samples of control group (*n* = 10), OVX group (*n* = 12) and OVXG (*n* = 6). Using a linear mixed model, the relative intensities of the metabolite profiles were found to significantly change over two months.

				Mean						
RT				(Relative intensity, E+05)				*p* -value		
mz	(sec)	Metabolite	Trt	0	1	2	SEM	Trt	Time	Int
233.803	493.615	5-Methoxytryptophan	Control	0.259	0.526	0.433	0.132	<0.0001	<0.0001	<0.0001
			OVX	0.608	1.019	1.279	0.121			
			OVXG	0.249	1.656	1.538	0.171			
148.039	506.035	Methionine	Control	0.373	0.970	0.448	0.136	0.005	<0.0001	0.028
			OVX	0.467	0.875	0.526	0.124			
			OVXG	0.473	1.364	1.411	0.176			
161.903	622.743	5-Hydroxylysine	Control	1.090	1.126	1.094	0.092	0.086	0.275	0.012
			OVX	1.189	0.892	1.214	0.084			
			OVXG	1.132	1.450	1.376	0.119			
144.044	635.951	Indole-3-carboxaldehyde	Control	0.344	0.492	0.394	0.069	0.006	0.386	0.001
			OVX	0.518	0.362	0.452	0.063			
			OVXG	0.484	0.839	0.779	0.089			
116.070	686.643	L-Valine	Control	0.651	0.559	0.558	0.192	0.015	0.096	0.007
			OVX	0.556	0.420	0.589	0.175			
			OVXG	0.576	0.733	0.748	0.248			
128.034	818.824	2-Pyrrolidone-5-carboxylic acid	Control	1.409	1.609	1.530	0.109	0.445	0.4	0.009
			OVX	1.646	1.251	1.574	0.100			
			OVXG	1.512	1.732	1.707	0.141			
131.081	851.654	Glutaric acid	Control	22.371	32.187	25.471	3.222	0.074	0.241	0.008
			OVX	36.051	28.746	29.239	2.942			
			OVXG	30.731	42.420	35.211	4.160			
203.138	926.230	D-Tryptophan	Control	0.772	1.482	1.028	0.153	0.042	<0.0001	0.042
			OVX	0.820	1.077	0.987	0.140			
			OVXG	0.610	1.756	1.179	0.198			

Data presented are predicted means, standard error of the difference (SED) and p-values.
Sec (seconds). Trt (Treatment). Int (Interaction treatment and time)

To identify the individual changes between treatments, the fold change (FC) was calculated. The FC ranks the metabolites in order of greatest change within a dataset. Using plasma samples, a 2-FC cut-off for metabolomics studies has been reported which minimises the effect of biological variation in individuals (Crews et al., 2009; Vinaixa et al., 2012). In this study, the corresponding changes of metabolite profiles are presented in Table 5.3. Overall, the metabolite profile indicated early alterations during oestrogen deficiency, and glucocorticoid treatments were significantly different between treated and control groups in plasma samples. Comparing OVX versus control group, the FC values of only 5-methoxytryptophan were significantly greater than 1 at month one and month two. 2-Pyrrolidone-5-carboxylic acid and tryptophan fold changes were significantly lower than 1 only at month one. However, comparing OVXG vs OVX, the FCs of all the metabolites were significantly greater than 1 at month one, while at month two only the fold changes of indole-3-carboxadehyde and valine were significant. These results suggest that all the metabolites in the OVXG had an immediate response to OVX combined with glucocorticoid interventions.

Table 5.3: FC of the metabolite abundance between the OVX and control groups and between the OVXG and the OVX groups at month one and month two.

Metabolite	OVX vs Control		OVXG vs OVX	
	FC 1 month	FC 2 months	FC 1 month	FC 2 months
5-Methoxytryptophan	**1.938**	**2.955**	**1.625**	1.203
Methionine	0.902	1.172	**1.559**	**2.684**
5-Hydroxylysine	0.792	1.111	**1.626**	1.133
Indole-3-carboxaldehyde	0.736	1.146	**2.317**	**1.725**
L-Valine	0.752	1.055	**1.746**	**1.271**
2-Pyrrolidone-5-carboxylic acid	**0.778**	1.029	**1.384**	1.084
Glutaric acid	0.893	1.148	**1.476**	1.204
D-Tryptophan	**0.727**	0.960	**1.631**	1.195

FC value was calculated by dividing the value of the relative intensities of metabolites in the OVX group by the control group, and the OVXG group by the OVX group. FC with a value >1 indicated a relatively higher intensity present in treated animals, whereas a value <1 indicated a relatively lower intensity compared with their respective control animals. All FC values, which are in bold, are significant (p-value < 0.05). p-value calculated using post-hoc Fisher's least significant difference (LSD) test for pair-wise multiple comparison of the group means.

To assess the relationship between bone clinical parameters, serum osteocalcin (OC) (a bone turnover marker), serum C-terminal telopeptide *of type 1 collagen (CTx-1), the BMDs* of OVX sheep, and the selected metabolites, Pearson correlations were calculated. The correlation coefficient values between the metabolites and bone clinical parameters are shown in Table 5.4. Overall, plasma metabolites were more frequently negatively associated with OC, while positive associations were noted with CTx-1. Similarly, negative associations were observed with lumbar spine and femoral BMD. The associations between bone turnover biomarkers, serum OC and CTx-1, and for all the selected metabolites in sheep at month two, were not significant, with the exception of methionine. A negative correlation between methionine and serum biomarker OC (r = –0.384, p-value = 0.044) was observed. This study also did not show significant associations between BMD measurements, femur and lumbar spine, and all the selected metabolites, with the exception of glutaric acid. Negative correlations with glutaric acid and femoral (r = –0.738,

p-value = 0.015) and lumbar spine BMD (r = –0.747; *p*-value = 0.013) were observed.

Table 5.4: Correlation coefficients between metabolites selected by univariate analysis in the short-term approach. Pearson correlation between bone formation marker (OC), bone resorption marker (CTx-1), femoral BMD and lumbar spine BMD and selected metabolites at month two.

	OC		CTx-1		Femoral BMD		Lumbar spine BMD	
	n = 28		*n* = 28		*n* = 11		*n* = 11	
Metabolite	Pearson correlation	*p* -value	Pearson correlation	*p* -value	Pearson correlation	*p* -value	Pearson correlation	*p* -value
5-Methoxytryptophan	0.041	0.834	0.075	0.705	-0.112	0.758	-0.232	0.519
Methionine	**-0.384**	**0.044**	0.296	0.126	-0.151	0.676	-0.342	0.333
5-Hydroxylysine	-0.225	0.25	-0.056	0.776	0.1	0.783	0.054	0.883
Indole-3-carboxaldehyde	-0.273	0.16	0.147	0.454	-0.678	0.031	-0.233	0.517
L-Valine	0.225	0.249	0.2	0.307	-0.178	0.623	-0.359	0.308
2-Pyrrolidone-5-carboxylic acid	-0.151	0.443	0.017	0.932	-0.301	0.399	-0.288	0.42
Glutaric acid	0.25	0.2	0.227	0.246	**-0.738**	**0.015**	**-0.747**	**0.013**
D-Tryptophan	0.239	0.221	0.134	0.498	-0.202	0.576	-0.284	0.427

Bolded numbers indicate statistically significant correlation (*p*-value < 0.05)

5.3.2 Effect of OVX on the plasma metabolome of sheep: long-term approach

5.3.2.1 PCA: long-term approach

The results from the PCA did not reveal a clear separation among groups. It was difficult to observe the variance in the metabolite profiles among the four groups when analysing all treatments per individual time point (see Appendix B, Figure B.2). Thus, each group and all its time points were analysed individually to obtain global information regarding the metabolite changes.

PCA plots of the metabolite profiles obtained from the analysis of OVX sheep over five months are shown in Figure 5.4. The resulting scatter plots showed clearly that animals were clustered in the middle of the plot, suggesting there were only modest differences between the treated animals.

A modest disease progression can be noticed in the OVX sheep (Figure 5.4 B); PC1 and PC2 explained 26.8% of the variance) when compared with the control group (Figure 5.4A); PC1 and PC2 explained 26.2%). However, the glucocorticoid-treated ewes (Figure 5.4C); PC1 and PC2 explained 33.4%)

showed a different plasma metabolite profile in comparison with the OVXG2 group and OVX group. A smaller difference in OVXG2 (Figure 5.4 (D); PC1 and PC2 explained 28.3%) was observed from month three to month five when compared with OVXG. Furthermore, two outliers from month one were noted in the OVX group and one from month three in the OVXG group.

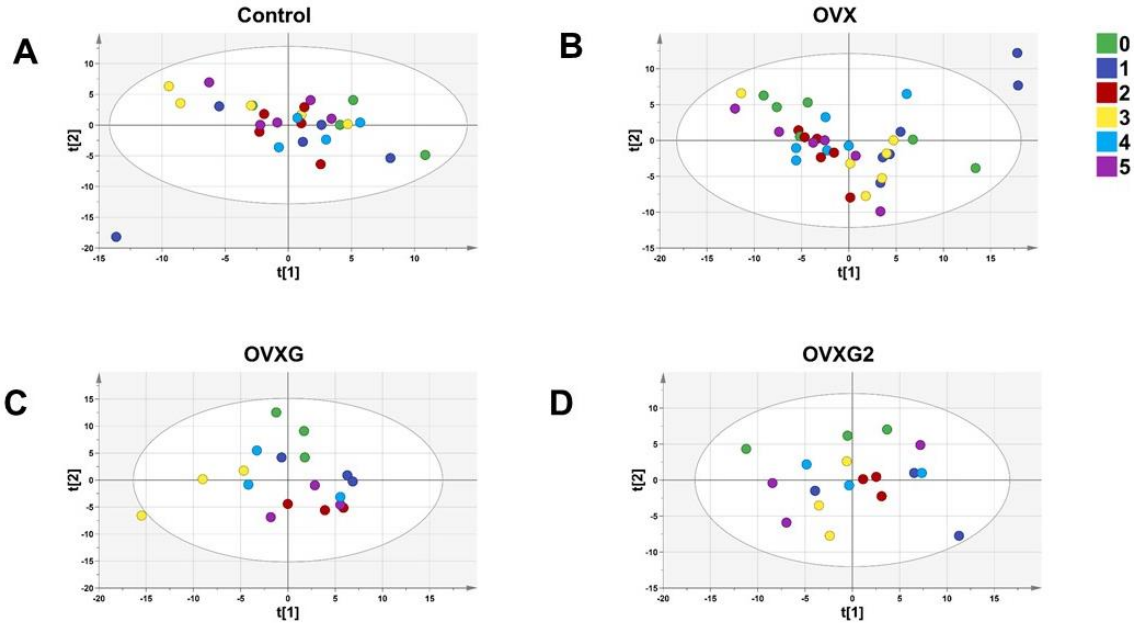

Figure 5.4: Inter-animal variation in the plasma metabolome of sheep over five months of the study period. PCA scatter plots derived from HILIC–MS spectra dataset based on normalised and autoscaled data. Each data point represents the metabolite profile of a single ewe. PCA scoring plot showing the variation of control group (A) (● baseline (month zero); ● month one; ● month two; ● month three; ● month four; and ● month five) R2 = 48.1% and Q2 = –5.1%; OVX group (B) R2 = 52.6% and Q2 = 21.4%; OVXG group (C) R2 = 43.7% and Q2 = –2.2%; and OVXG2 group (D) R2 = 28.3% and Q2 = –1.2%.

5.3.2.2 Linear mixed model: long-term approach

Overall, the metabolites selected by the linear mixed model presented a significant interaction between treatment and time (Table 5.5). At month one, the OVX group showed decreased relative intensities of all amino acids, with the exception of 5-methoxytryptophan and methionine. In contrast, OVXG and

OVXG2 groups showed increased relative intensities of all metabolites, with the exception of malic acid.

At month three, the OVX group also showed decreased relative intensities of all metabolites, with the exception of methionine. Further, all the relative intensities of the metabolites in the OVXG decreased. Similarly, the metabolite profile of OVXG2 showed a decrease in the relative intensities of all the amino acids, with the exception of methionine and phenylalanine.

At month five, OVX increased the relative intensities of 5-methoxytryptophan, methionine, hydroxylysine, phenylalanine, tryptophan and valine in the OVXG, with the exception of indole-3-carboxaldehyde and malic acid. In addition, OVXG animals showed increased relative intensities of all amino acids, with the exception of hydroxylysine. Ewes in the group that only received two doses of glucocorticoids had decreased concentrations of 5-methoxytryptophan, methionine, phenylalanine, indole-3-carboxaldehyde and valine, and increased levels of hydroxylysine, tryptophan and malic acid.

The OVX group showed a significant FC of six metabolites over time (Table 5.6). The FC of 5-methoxytryptophan was greater than 2 at all the time points, with the exception of month one when compared with control. 5-hydroxylysine, phenylalanine and tryptophan fold changes were lower than in month one. Methionine and malic acid FC values were higher than 1 only at month five. The OVXG group showed higher FC values than 1 for all the metabolites in month one. Phenylalanine and indole-3-carboxadehyde had greater FC values than 2 at month one, while the FC value was greater than 2 for 5-hydroxylysine, tryptophan and valine. Interestingly, the FC value of 5-

hydroxylysine was lower than 1 at month three. Methionine's FC value was higher than 3 only at month two.

Similarly, the OVXG2 group showed higher FC values than 1 in all the metabolites in month one. Interestingly, at month three, 5-hydroxylysine and phenylalanine remained steady at the same level, but 5-methoxytryptophan and malic acid were lower than 1. In addition, methionine's FC value was lower at month five.

Table 5.5: Effect of OVX and glucocorticoids on the metabolite profile of sheep in the long-term analysis. Relative intensities were measured in plasma samples of control group (*n* = 5), OVX group (*n* = 6), OVXG (*n* = 3) and OVXG2 (*n* = 3). Using a linear mixed model, the relative intensities of the metabolite profiles were found to significantly change over time.

				Mean									
RT				(Relative intensity, E+05)							*p* -value		
m/z	(sec)	Metabolite	Trt	0	1	2	3	4	5	SEM	Trt	Time	Int
233.803	493.615	5-Methoxytryptophan	Control	0.1596	0.4888	0.47	0.5068	0.3829	0.5287	0.1934	0.001	<0.0001	0.015
			OVX	0.6922	1.0302	1.5665	1.2696	1.0824	1.1867	0.1766			
			OVXG	0.1801	1.4326	1.7105	1.3698	0.9956	1.261	0.2497			
			OVXG2	0.3187	1.88	1.3663	0.5425	0.7875	0.5672	0.2497			
148.039	506.035	Methionine	Control	0.3362	0.9287	0.4989	0.859	1.0658	0.5777	0.2149	0.098	0.003	0.012
			OVX	0.6955	0.8981	0.3958	0.6952	0.9834	1.1463	0.1962			
			OVXG	0.2878	1.0584	1.354	0.7628	0.9625	1.671	0.2775			
			OVXG2	0.6576	1.6706	1.4673	1.1644	1.609	0.5964	0.2775			
161.903	622.743	5-Hydroxylysine	Control	0.9798	1.1285	1.0556	1.2217	1.054	1.2502	0.1177	0.335	0.374	0.007
			OVX	1.368	0.7656	1.2021	1.1741	0.9816	1.3272	0.1074			
			OVXG	1.1355	1.3303	1.3193	0.7909	1.1707	1.105	0.152			
			OVXG2	1.1276	1.5694	1.4322	1.3247	1.2472	1.2686	0.152			
164.071	623.132	L-Phenylalanine	Control	0.6805	0.7464	0.7365	0.8559	0.6208	0.7922	0.0983	0.057	0.229	0.003
			OVX	0.8212	0.4408	0.8315	0.6666	0.7328	0.892	0.0897			
			OVXG	0.8886	0.9784	0.9917	0.4641	0.799	0.8578	0.1269			
			OVXG2	0.7656	1.2565	1.0843	0.9174	0.8883	0.8842	0.1269			
144.044	635.951	Indole-3-carboxaldehyde	Control	0.29	0.4752	0.4332	0.4199	0.3145	0.2523	0.0959	0.493	<0.0001	<0.0001
			OVX	0.4873	0.2687	0.4611	0.4091	0.3995	0.3841	0.0876			
			OVXG	0.4423	0.8541	0.6486	0.2666	0.3479	0.3945	0.1238			
			OVXG2	0.5258	0.8238	0.91	0.3708	0.2901	0.1729	0.1238			
116.070	686.643	L-Valine	Control	0.6234	0.5386	0.5874	0.6117	0.5247	0.5492	0.25	0.418	0.136	0.011
			OVX	0.5314	0.3769	0.618	0.5058	0.6096	0.6322	0.2282			
			OVXG	0.5509	0.7335	0.6612	0.3747	0.4982	0.6388	0.3227			
			OVXG2	0.6011	0.7335	0.8346	0.5967	0.6438	0.5057	0.3227			
133.043	767.096	Malic acid	Control	2.0082	1.6814	1.6442	1.5266	1.7401	1.2604	0.1713	0.643	0.027	0.03
			OVX	1.761	1.5331	1.9866	1.7873	1.6098	1.9203	0.1563			
			OVXG	1.9592	1.6821	2.0199	1.8405	1.3172	1.9708	0.2211			
			OVXG2	2.0405	1.8404	1.9864	1.0289	1.6596	1.8711	0.2211			
203.138	926.230	D-Tryptophan	Control	0.7264	1.3593	0.9804	1.1351	0.8683	1.0072	0.1618	0.673	<0.0001	0.001
			OVX	0.7721	0.7741	1.0454	0.7909	0.9119	0.9933	0.1477			
			OVXG	0.6178	1.4953	1.2982	0.6536	0.7189	0.7432	0.2089			
			OVXG2	0.6025	2.0175	1.0603	0.8138	0.6444	0.792	0.2089			

Data presented are predicted means, standard error of the difference (SED) and p-values.
Sec (seconds). Trt (Treatment). Int (Interaction treatment and time).

Table 5.6: FC of the metabolite abundance between the OVX and control groups, between the OVXG and the OVX groups and between the OVXG2 and the OVXG groups from month one to month five.

Metabolite	OVX vs Control				
	FC 1 month	FC 2 months	FC 3 months	FC 4 months	FC 5 months
5-Methoxytryptophan	2.108	**3.333**	**2.505**	**2.827**	**2.245**
Methionine	0.967	0.793	0.809	0.923	**1.984**
5-Hydroxylysine	**0.678**	1.139	0.961	0.931	1.062
L-Phenylalanine	**0.591**	1.129	0.779	1.180	1.126
Indole-3-carboxaldehyde	**0.565**	1.064	0.974	1.270	1.522
L-Valine	0.700	1.052	0.827	1.162	1.151
Malic acid	0.912	1.208	1.171	0.925	**1.524**
D-Tryptophan	**0.569**	1.066	0.697	1.050	0.986

Metabolite	OVXG vs OVX				
	FC 1 month	FC 2 months	FC 3 months	FC 4 months	FC 5 months
5-Methoxytryptophan	1.391	1.092	1.079	0.920	1.063
Methionine	1.178	**3.421**	1.097	0.979	1.458
5-Hydroxylysine	**1.738**	1.097	**0.674**	1.193	0.833
L-Phenylalanine	**2.220**	1.193	0.696	1.090	0.962
Indole-3-carboxaldehyde	**3.179**	1.407	0.652	0.871	1.027
L-Valine	**1.946**	1.070	0.741	0.817	1.010
Malic acid	1.097	1.017	1.030	0.818	1.026
D-Tryptophan	**1.932**	1.242	0.826	0.788	0.748

Metabolite	OVXG2 vs OVXG				
	FC 1 month	FC 2 months	FC 3 months	FC 4 months	FC 5 months
5-Methoxytryptophan	1.312	0.799	**0.396**	0.791	0.450
Methionine	1.579	1.084	1.526	1.672	**0.357**
5-Hydroxylysine	1.180	1.086	**1.675**	1.065	1.148
L-Phenylalanine	1.284	1.093	**1.977**	1.112	1.031
Indole-3-carboxaldehyde	0.965	1.403	1.391	0.834	0.438
L-Valine	1.000	1.262	1.592	1.292	0.792
Malic acid	1.094	0.983	**0.559**	1.260	0.949
D-Tryptophan	1.349	0.817	1.245	0.896	1.066

FC was calculated by dividing the value of relative intensities of metabolites in the OVX group by the control group, the OVXG group by the OVX group and OVXG2 by OVXG. All FC values in bold are significant. FC with a value >1 indicates a relatively higher intensity present in treated ewes, whereas a value <1 indicates a relatively lower intensity compared with their respective control animals. p-value < 0.05. p-value calculated using post-hoc Fisher's least significant difference (LSD) test for pair-wise multiple comparison of the group means.

The correlation coefficient values between the metabolites and bone clinical parameters at month five are shown in Table 5.7. After five months of oestrogen deficiency and glucocorticoid treatments, plasma metabolites were positively associated with serum OC and CTx-1, with the exception of malic acid. However, more negative associations were observed with femoral BMD and lumbar spine. The associations between bone turnover biomarkers, serum OC and CTx-1, and all the identified metabolites in sheep at month five were not significant, with the exception of 5-methoxytryptophan with serum CTx-1 (r = 0.482, *p*-value = 0.05). The associations between all the metabolites and BMD measurements, femur and lumbar spine BMD, were not significant with the exception of 5-methoxytryptophan (r= –0.658, *p*-value = 0.004) and methionine (r = –0.482, *p*-value = 0.05).

Table 5.7: Correlation coefficients between metabolites selected by univariate analysis in the long-term approach. Pearson correlation between bone formation marker (OC), bone resorption marker (CTx-1), femoral BMD and lumbar spine BMD and selected metabolites at month five.

	OC		CTx-1		Femoral BMD		Lumbar spine BMD	
	n = 17		*n* = 17		*n* = 17		*n* = 17	
	Pearson		Pearson		Pearson		Pearson	
Metabolite	correlation	*p* -value	correlation	*p* -value	correlation	*p* -value	correlation	*p* -value
5-Methoxytryptophan	0.156	0.551	**0.482**	**0.05**	**-0.658**	**0.004**	-0.399	0.113
Methionine	0.019	0.943	0.412	0.101	**-0.482**	**0.05**	-0.319	0.213
5-Hydroxylysine	0.279	0.279	0.025	0.925	0.139	0.596	0.203	0.435
L-Phenylalanine	0.321	0.21	0.115	0.661	-0.283	0.272	-0.184	0.479
Indole-3-carboxaldehyde	0.25	0.333	0.364	0.151	-0.436	0.08	-0.328	0.199
L-Valine	0.253	0.327	0.181	0.488	-0.442	0.076	-0.345	0.175
Malic acid	-0.108	0.68	0.385	0.127	-0.238	0.357	-0.175	0.501
D-Tryptophan	0.366	0.149	0.089	0.735	0.112	0.67	0.079	0.763

Bolded numbers indicate statistically significant correlation (p-value < 0.05)

5.4 Discussion

The study described in this chapter applies a HILIC–MS untargeted metabolomics approach to identify changes in the metabolome of OVX sheep. This is the first longitudinal study that presents results on the plasma metabolite

profile of OVX sheep treated with glucocorticoids in an animal model of postmenopausal osteoporosis, and their metabolite profiles were compared with those of the control group. The preliminary results obtained demonstrate the metabolites' changes in response to hormonal interventions, and OVX alone or in combination with glucocorticoid treatments over time. Furthermore, in the short-term approach (two months), methionine was found to be negatively associated with bone turnover, and glutaric acid was found negatively associated with femoral and lumbar spine BMD. In the long-term approach (five months), 5-methoxytryptophan and methionine were found to be negatively associated with femoral BMD. This suggests that combining OVX and glucocorticoids affects bone remodelling leading to bone loss in ewes by regulating osteoclast differentiation and apoptosis of osteoblast bone cells involved in bone remodelling.

Initially, the results from the treated groups were examined using PCA. However, due to the relatively large number of animal groups, with small sample size and unbalanced design, the separation was difficult to visualise. Nevertheless, it could be seen that the ewes responded to the surgical or hormonal interventions, which resulted in a metabolic change over time. Subsequently, the results of both the short-term and long-term approach from the linear mixed models showed features that changed over the two- or five-month study period.

Osteoporosis was associated with early changes in the plasma metabolite profile, including amino acids and other metabolites. Overall, circulating metabolites were accumulated in plasma after OVX in sheep. On the other hand, compared to the OVX animals, OVXG2 animals could reverse the impacts of

glucocorticoids on the plasma metabolites at month four and month five. The results suggest that long administration of glucocorticoid treatment to the OVX sheep (OVXG) affects their metabolite profile. This dynamic change observed in the metabolite profile of the OVX sheep may reflect the increased bone turnover observed in oestrogen deficiency models, where an imbalance within the bone remodelling process suggests enhanced bone resorption and a reduced bone formation. In addition, due to uncoupling of the bone turnover cycle in the presence of low oestrogen, bone resorption increases at basic multicellular units of bone, and the rate of bone loss is greater than the formation of new bone (Kalervo Väänänen and Härkönen, 1996; Greendale Gail et al., 2011). On the other hand, in the glucocorticoid-induced osteoporosis model, bone resorption markers have been associated with a decreased BMD as a result of an excessive bone resorption rate and reduced osteoblast activity (Mazziotti et al., 2006).

Amino acids are not only part of the building blocks of proteins, but also are derivatives of many secondary metabolites and are involved in the process of cell signalling and signal transduction of key metabolic pathways. Amino acids enhance immunity by upregulating pro-inflammatory and downregulating anti-inflammatory cytokines (Zhang et al., 2007). Menopause is associated with the risk of developing a number of chronic diseases including cardiovascular disease, diabetes and osteoporosis, among others. Osteoporosis is accompanied by oxidative stress and inflammation, and changes of amino acid levels may indicate which key metabolic pathways may be altered in postmenopausal women (Jousse et al., 2004; Obayashi et al., 2004; Bellanti et al., 2013; Grygiel-Górniak et al., 2014). Thus, the analysis of all the detectable metabolites in serum may be a method for discovering biomarkers for early detection of bone loss in women.

Although this is the first study that reports the metabolite profile in OVX sheep, previous metabolomics analyses have shown altered metabolism in OVX rats, another common animal model for postmenopausal osteoporosis. A study using nuclear magnetic resonance (NMR) reported that six months after OVX, serum levels of alanine, asparagine, glutamine, isoleucine, leucine, valine, tryptophan, lysine, proline, serine and threonine increased, and glutamate, glycine, phenylalanine and tyrosine were decreased (Assadi-Porter et al., 2015). Another study reported increased concentrations of isoleucine, valine and leucine after OVX using gas chromatography time-of-flight mass spectrometry (GC–TOF–MS) (Ma et al., 2011). Similarly, branched-chain amino acids (valine, leucine and isoleucine), homocysteine, hydroxyproline and ketone bodies (3-hydroxybutyric acid) were elevated, while levels of lysine decreased in the OVX group compared to the sham group (Ma et al., 2013a).

The relationship between bone markers and BMD with the identified metabolites was assessed. In this study, we found negative associations between methionine and serum OC, lumbar spine and femoral BMD in OVX sheep. Furthermore, methionine was found to be associated with bone loss. A previous study on methionine reported changes in bone turnover in hyperhomocysteinemia aged rats, where OC decreased and urine N-terminal type 1 collagen, a marker of bone resorption, increased (Ozdem et al., 2007). Herrmann et al. (2005a) reported a significant correlation between hyperhomocysteinemia and urinary deoxypyridinoline crosslinks in peri- and postmenopausal women; however, no significant correlations were observed between hyperhomocysteinemia and OC. In another study, hyperhomocysteinemia levels were associated with higher bone turnover and

lower BMD (Gerdhem et al., 2009). Methionine plays key roles in cell metabolism. Methionine as one of the essential amino acids is required for cellular proliferation, protein synthesis, RNA synthesis and transamination. Further, methionine can be catabolised into homocysteine and cysteine (Brosnan and Brosnan, 2006; Tyagi et al., 2011). This suggests that methionine levels may alter bone remodelling and could possible explain the reduced BMD observed in treated ewes by upregulating osteoclast development induced by OVX and glucocorticoid treatments.

Homocysteine, a metabolite of methionine, has been reported to increase oxidative stress, inducing increased production of reactive oxygen species of inflammation, and these can elevate the risk factor for fractures (Yang et al., 2012). During oestrogen deficiency, increased levels of homocysteine may lead to increased matrix metalloproteinases, proteins that degrade the bone matrix, decreased bone blood flow and increased activity of the osteoclasts, with decreased osteoblast activity (Herrmann et al., 2005b; Vacek et al., 2013). Further, it can damage hydroxyproline, mitochondria and collagen. Higher concentrations of homocysteine downregulate lysyl-oxidase, which induces crosslinks of collagen, a key component of the bone matrix (Liu et al., 1997; Thaler et al., 2011). Nevertheless, the results of this study did not include homocysteine measurements; however, homocysteine may also be formed via methionine metabolism and may be involved in the bone breakdown in the OVX sheep. These findings suggest that the circulating levels of methionine play a role in changes in bone metabolism, which may lead to dysregulated bone remodelling and may be detrimental to bone quality through modifications of bone collagen proteins.

In this study, tryptophan levels were increased in the OVX group. Tryptophan and its metabolites impact bone formation, stimulating the proliferation and differentiation of bone marrow-derived mesenchymal stem cells (Michalowska et al., 2015). The possible mechanism of altered tryptophan in bone loss may be enhanced osteoclastogenesis. Studies indicated that tryptophan may play a role in osteoclastogenesis via the kynurenine pathway of tryptophan catabolism, as interferon *y* (IFN-*y*) is formed via the kynurenine pathway (El Refaey et al., 2015). IFN-*y* is a cytokine that is produced in the bone microenvironment by cells, and it promotes osteoclast activity. During menopause, oestrogen deficiency upregulates the pro-inflammatory cytokines, as IFN-*y* increases the bone loss in postmenopausal women (Pfeilschifter et al., 2002; Weitzmann and Pacifici, 2006). The results in this study provide evidence that OVX and glucocorticoid treatment perturbed tryptophan levels in both OVX and OVXG sheep, and further studies in animal models are needed to determine whether tryptophan metabolites could be utilised as novel biomarkers for bone loss in postmenopausal women.

Plasma concentrations of hydroxylysine were increased in the OVXG group when compared with the OVX control group. Hydroxylysine is a urinary marker of bone resorption derived from collagen crosslinks (Guerrero et al., 1996). In bone tissue, bone collagen proteins comprise about 90% of the organic matrix of the bone. Bone collagen supports properties of bone such as tissue mass, micro- and macro-architecture and material properties, which all contribute to bone strength (Viguet-Carrin et al., 2006). Bone collagen is rich in proline, hydroxyproline and glycine. Proline and lysine residues are hydroxylated to hydroxyproline and hydroxylysine, respectively, which contribute to the formation

of collagen crosslinks and to bone matrix quality (Yamauchi and Shiiba, 2008; Hu et al., 2011; Boskey, 2013). Circulating levels of hydroxylysine as biomarker have been reported in human osteoporotic bone matrix (Bailey et al., 1993). Although the hydroxylysine urinary marker was not measured here, an increase in CTx-1 level was seen in the OVX sheep. Thus, the plasma levels of hydroxylysine in OVX sheep may reflect the increased bone remodelling as a response to oestrogen deficiency.

The strengths of this study are the application of untargeted metabolite profiling using HILIC–MS analysis of plasma samples from OVX sheep to explore the dynamics of disease progression in the metabolite profile, and subsequent identification of plasma biomarkers of postmenopausal osteoporosis. The limitations of this study include the small sample size of treated groups, specifically the ewes that were treated with glucocorticoids, and due to the large variability of the data further validation will be required. In addition, blood samples were collected once a month, as the study design considered both a short- and long-term response to treatments. Larger sample size, and multiple sampling time points from the early stage of oestrogen deficiency and glucocorticoid treatment, should be considered in future studies to identify biomarkers that are unique to the early onset of osteoporosis in postmenopausal women.

5.5 Conclusions

In this chapter it was proposed to employ a HILIC–MS-based metabolomics approach in OVX sheep to improve our understanding of bone loss in women. The present study is the first to elucidate the relation between the metabolome and bone loss in OVX sheep. Circulating metabolites were altered with OVX during the five months of intervention. The results indicated that metabolite profiles were affected in the OVX and OVX-plus-glucocorticoid groups over two months. In addition, the association between potential metabolites including methionine, phenylalanine, tryptophan, valine and hydroxylysine showed a correlation with bone loss by using BMD and bone turnover markers. In summary, the findings of this study showed that the biosynthesis of phenylalanine, tyrosine and tryptophan, and the metabolism of cysteine, methionine, valine, leucine and isoleucine, are potentially the main perturbed metabolic pathways regulating bone loss in OVX sheep. These findings suggest new directions to examine the mechanisms of bone loss in OVX sheep, and indicate that these specific metabolites may have value as prognostic biomarkers for osteoporosis in humans.

Chapter 6

MS-based lipidomics approach reveals changes in lipid profiles of ovariectomised sheep

This chapter describes the impact of short-term and long-term ovariectomy (OVX) and glucocorticoid hormonal interventions in sheep by lipid profiling using ultra-performance liquid chromatography−mass spectrometry (UHPLC-MS). This study aimed to determine the dynamic changes of circulating lipids in the OVX sheep. This chapter also assessed the relationship between clinical bone parameters and lipid profiles in order to determine whether those significant features are linked to bone metabolism and bone loss.

Abstract

In this chapter, it was hypothesised that lipidomics would identify novel lipids in the plasma lipidome of ovariectomised sheep that may better explain the association between bone loss and menopause. The purposes of this study were to determine the effect of ovariectomy (OVX) and glucocorticoid treatment on the plasma lipid profile in sheep in two different approaches, a short-term (two months) and long-term (five months) approach, and assess correlations between bone clinical parameters and lipid profiles. Ultra-performance liquid chromatography−mass spectrometry untargeted lipidomics analysis of blood plasma was applied to follow the progression of disease in four hormonal intervention models related to postmenopausal osteoporosis: an OVX group, a group of OVX plus five doses of glucocorticoids, a group of OVX with only two doses of glucocorticoids, and a control group. Plasma samples were collected at baseline and once per month over five months. Bone biomarkers, serum of C-terminal telopeptide of type 1 collagen and osteocalcin were measured using immunoenzymatic assays. Bone mineral density was assessed by dual-energy x-ray absorptiometry. Dynamic variations were observed in the lipid profiles of the two evaluated approaches, the short-term and the long-term approaches. Lower relative intensities of the lipid profiles of ewes after ovariectomy and glucocorticoid treatments were detected. The short-term approach showed the change in relative intensities of five lipids, while the long-term approach revealed changes in 14 lipids over time, including cardiolipin, ceramide 1-phosphates, phosphatidylinositol, phosphatidic acid, lysophosphatidylethanolamines, phosphatidylserines and phosphatidylglycerol. Cardiolipin was negatively associated with the lumbar spine bone mineral density at two months, while

ceramide 1-phosphates was positively associated at five months. Differences observed in lipid profiles of sheep after oestrogen deficiency and glucocorticoid interventions suggest that the identified lipids can be potential clinical targets for developing new biomarkers for osteoporosis prognosis. Lipidomics analysis represents a novel technique that would be helpful in the future to detect perturbed lipids in postmenopausal women.

6.1 Introduction

Osteoporosis cases are most common in the elderly population, but postmenopausal women are the most affected as oestrogen withdrawal induces bone loss. During menopause, there are several changes such as decreased oestrogen levels, and postmenopausal women are also at increased risk of cardiovascular events. Serum lipids may be the link between cardiovascular disease and osteoporosis in postmenopausal women (Cui et al., 2005).

Lipids play an important role in skeletal metabolism and bone health. Triglycerides (TGs), total cholesterol (TCHO), low-density lipoprotein cholesterol (LDL-C) or high-density lipoprotein cholesterol (HDL-C) are the common clinical parameters to measure lipid metabolism (Tian and Yu, 2015). A role of the cholesterol biosynthetic pathway in differentiation of mesenchymal stem cells in bone marrow has been reported, where products of this pathways reduce BMD and lipid oxidation inhibits osteoblast cells (Parhami et al., 2002). Furthermore, the association between TGs and lipoproteins in bone loss has been studied; however, the information published is controversial. Adami et al. (2004) reported that lipid profiles are associated with BMD, where a positive relationship between BMD and low-density lipoprotein and total triglycerides, and a negative association between BMD and high-density lipoprotein, were found. Postmenopausal women with hypercholesterolemia, high LDL-C or HDL-C had a lower lumbar spine and femoral BMD than those women with a normal lipid profile (Orozco, 2004). Chen et al. (2018) reported higher levels of HDL and TCHO in postmenopausal osteoporosis. However, several studies have reported that there was no relationship between lipids and BMD (Tankó et al., 2003; Samelson et al., 2004; Solomon et al., 2005). Despite this, osteoporosis is a progressive and

complex disease that is associated with changes particularly in lipid metabolism, where those changes promote lipid oxidation and adipogenesis rather than osteogenesis in the bone marrow (Chen et al., 2018). However, the exact molecular mechanisms for lowering the BMD in postmenopausal women remain unclear. A better understanding of the biological mechanisms underlying postmenopausal bone loss is required.

Despite menopause being associated with a variety of pathologies such as cardiovascular abnormalities, diabetes and bone loss in women, early detection of osteoporosis is difficult (Tankó et al., 2003). While bone imaging scans are generally accepted as non-invasive methods, they cannot predict bone loss. Currently, the diagnosis of osteoporosis is carried out using dual-energy x-ray absorptiometry (DXA), the gold standard technique for measuring the BMD in postmenopausal women as well as measuring bone turnover biomarkers (Kanis, 2002; Naylor and Eastell, 2012). While DXA is highly reliable, changes in BMD can only be detected by this method over a period of years. Thus, the development of a fast and simple prognostic method is desired, where the detection of early biomarkers for osteoporosis can be used to diagnose or predict the risk of bone loss in postmenopausal women.

In this sense, metabolomics is an emerging tool for studying many diseases including cancer, diabetes, Alzheimer's, osteoarthritis disease and others (Adams et al., 2013; Trushina and Mielke, 2014; Trivedi et al., 2017). Metabolomics allows the measurement and characterisation of small molecules such as organic and amino acids, saccharides, lipids and other biomarkers in a biological system (Newgard, 2017). Lipidomics is a subset of metabolomics, which studies the full characterisation of lipid molecular species (Lagarde et al.,

2003). Lipid metabolism alterations in bone, specifically in the cellular balances between adipocytogenesis and osteoblastogenesis at the bone marrow, are controlled by many factors, including lipids. During menopause, lipid accumulation alters bone marrow cells and could be a determinant of increased bone remodelling that could affect bone mass, and this is associated with obesity and osteoporosis in postmenopausal women (Reid, 2010; Hardouin et al., 2014). In this sense, lipids and their derivatives, such as sphingosine-1-phosphate, lysophosphatidic acid and some fatty acid amides, are known to regulate many cellular process and any change can lead to bone pathologies such as osteoporosis (During et al., 2015). Further and detailed studies might be needed to uncover the underlying lipid profiles for postmenopausal osteoporosis.

In the present study, it was hypothesised that OVX alone or combining OVX with glucocorticoids would change the plasma lipid profiles in ewes and alter the bone remodelling process to lead to bone loss. The aim was to determine the effect of OVX and glucocorticoid treatment on the plasma lipid profile in ewes using UPLC–MS untargeted lipidomics analysis. Furthermore, a second aim was to assess correlations between bone clinical parameters and the lipid profile in OVX sheep.

6.2 Materials and methods

6.2.1 Animals used and experimental design

The animal model characterisation, presented in Chapter 3 of this thesis, was performed as described in Section 3.2.1. Briefly, this study consisted of 28 Merino ewes that were group pen-housed in a barn. Sheep were allocated into four groups at random intervention treatments, an OVX alone group (n = 12) or

combined with a glucocorticoid treatment, one group received five monthly doses (OVXG *n* = 3) or two monthly doses followed by no treatment (OVXG2 *n* = 3), and a control group (*n* = 10) for five months. Blood samples were collected monthly and plasma samples were stored at –80 °C prior to lipid extraction. Femoral and lumbar spine bone samples were collected from culled animals at months two or five.

6.2.2 Lipidome extraction from OVX sheep plasma samples

Lipid extraction was performed as described in Section 5.2.5.2 of this thesis. Briefly, plasma samples were collected from the OVX sheep and stored at –80 °C. Then, the samples were thawed at 4 °C, and 100 µL of plasma was collected and transferred into a microcentrifuge tube and 800 µL of cold chloroform:methanol (1:1 v/v) was added. Thereafter, the resulting solutions were homogenised for 1 min and incubated for 30 min at –20 °C. Then, 400 µL of water was added to each sample, which were then vortexed for 30 s. 200 µL of the bottom layer was transferred to a new microcentrifuge tube to evaporate to dryness under a stream of nitrogen. Finally, samples were reconstituted in 100 µL of Folch solvent mixture (chloroform:methanol 2:1 v/v) containing 16:0 d_{31}-18:1-phosphatidylethanolamine internal standard at 10 µg/mL concentration. All the samples were vortexed for 1 min, centrifuged for 10 min at 11,000 rpm at 4 °C and 100 µL was transferred to a vial containing an insert and stored at 4 °C for immediate analysis by UPLC–MS. The lipid quality control (QC) samples were prepared with 20 µL of each sample. The pooled lipid QC samples were aliquoted into multiple quality control vials and stored at –80 °C for future analysis.

6.2.3 Lipid analysis

The order of the LC-MS chromatographic runs of individual samples, QC samples and blanks was performed as describe in Section 5.2.5.3 of this thesis.

Lipid analysis was performed on a Thermo UPLC–MS system (Thermo Fisher Scientific, Waltham, MA, USA) that consisted of an Accela 1250 quaternary pump, a Thermo-PAL autosampler fitted with a 15,000 psi injection valve (CTC Analytics AG., Zwingen, Switzerland), a 2 µL injection loop and an Q-Exactive Orbitrap mass spectrometer

Chromatographic separation of lipid samples was conducted using a CSH-C18 column (100 × 2.1 mm; 1.7 µm particle size, Waters, Milford, MA, USA). The gradient elution began at a flow rate of 600 µL/min. The analysis was performed using three solvents: solvent A was a mixture of 0.1% formic acid in ACN–isopropanol (50:50 v/v), solvent B was a mixture of 0.1% formic acid in ACN–water (60:40 v/v) with 10 mM ammonium formate, and solvent C was a mixture of 0.1% formic acid in isopropanol–ACN (90:10 v/v) with 10 mM ammonium formate. The mobile phase was a mixture of solvent B and solvent C. The gradient elution programme was conducted as follows: starting with 85% solvent B (0–1 min), decreased from 70–18% (2–11 min) and held at 1% (11.50–14 min), returned to 85% (22–27 min), while solvent A was held at 100% (14.1–22 min) and allowed to equilibrate for 5 min prior to the next sample injection. Data were collected in profile data acquisition mode over a mass range of *m/z* 200–2000 at a mass resolution setting of 70,000 with a maximum trap fill time of 100 ms using the Xcalibur v2.1 software (Thermo Scientific, Hemel Hemstead, UK) provided by the manufacturer. The parameter settings for MS^2 analysis were a mass resolution of 35,000 with a maximum trap fill time of 250 ms. Lipid positive ion

mode parameters were as follows: spray voltage, 3.2 kV; capillary temperature, 275 °C; capillary voltage, −0.2 V; tube lens, 120 V. Negative ion mode parameters were as follows: spray voltage, −3.2 kV; capillary temperature, 275 °C; capillary voltage, −0.1 V; tube lens, −100 V.

Data preprocessing for the lipidomics analysis was performed as described in Section 5.2.5.3 of this thesis. Table 6.1 summarised the extraction parameters applied for this untargeted lipidomics analysis.

Table 6.1: XCMS main parameters applied for untargeted LC-MS-based lipidomics spectral processing.

Parameters	Related to	Settings
ppm	*m/z*	10
peakwidth	Retention time	5,20
Prefilter	intensity	3, 20000
Snthresh*	intensity	20
noise	intensity	10000

*signal to noise threshold

For lipid annotations, the mass spectra were searched within the plasma samples of OVX sheep using the software tool LipidSearch™. Briefly, the software settings allowed one to search through Q-Exactive MS^2 fragmentation spectra with a parent mass tolerance of 5 ppm and a product mass tolerance of 10 ppm to match fragmentation spectra against the LipidSearch™ library. The software was programmed to search for the parent ions M+H, M+NH_4 and M+Na in positive ionisation mode, and M–H, M–H+HCOO and M–H+CH_3COO in negative ionisation mode. A similar search on the parent mass alone was done using LipidBlast and lipids were identified with the matching precursor ion mass uncertainty 0.008 Da for positive mode and 0.01 Da for negative mode.

6.2.4 Bone biomarkers analysis

The bone biomarker analysis of C-terminal telopeptide of type 1 collagen and osteocalcin was performed as described in Section 3.2.4 of this thesis.

6.2.5 Bone mineral density

Lumbar spine and femoral BMD assessments have been described in Section 3.1.5 of this thesis.

6.2.6 Statistical analysis

The statistical analyses were performed as described in Section 5.2.6 of this thesis.

6.3 Results

The present study is the first to report the effects of OVX alone or combined with glucocorticoids on the plasma lipidome with follow-up measurements in OVX sheep. The lipid profiles of 28 ewes (10 samples from the control group, 12 samples from the OVX group, 3 samples from the OVXG group and 3 from the OVXG2) over five months of the study were characterised and compared. This untargeted plasma lipid profiling aimed to measure the circulating lipids of OVX sheep and OVX sheep that received either five or two monthly doses of glucocorticoids (OVXG and OVXG2, respectively). Detailed lipidomics analysis of these groups of treated sheep revealed differences. In this chapter, the relationship between lipids and clinical bone parameters was also assessed.

In Figure 6.1, the total ion current chromatograms produced by UPLC–MS of a quality control sample of OVX sheep are shown in positive mode (A) and negative mode (B), demonstrating that most of the lipids eluted from the column

in the region between 3–10 minutes where phospholipids elute. It can be observed that several lipid classes were detected in both positive and negative ionisation modes in the OVX sheep. Several compounds were detected within different lipid classes such as lysophosphatidylcholines (LPCs), lysophosphatidylethanolamines (LPEs), between 1–4 minutes, phosphatidylinositol (PI), phosphatidylcholines (PCs), phosphatidylethanolamines (PEs), phosphatidylserines (PSs), phosphatidylglycerols (PGs), sphingomyelins (SMs), ceramides (Cer). Specifically, cholesterol esters (ChEs), diacylglycerols (DGs) and triacylglycerols (TGs) were detected only in positive ionisation mode and between 11–13 minutes.

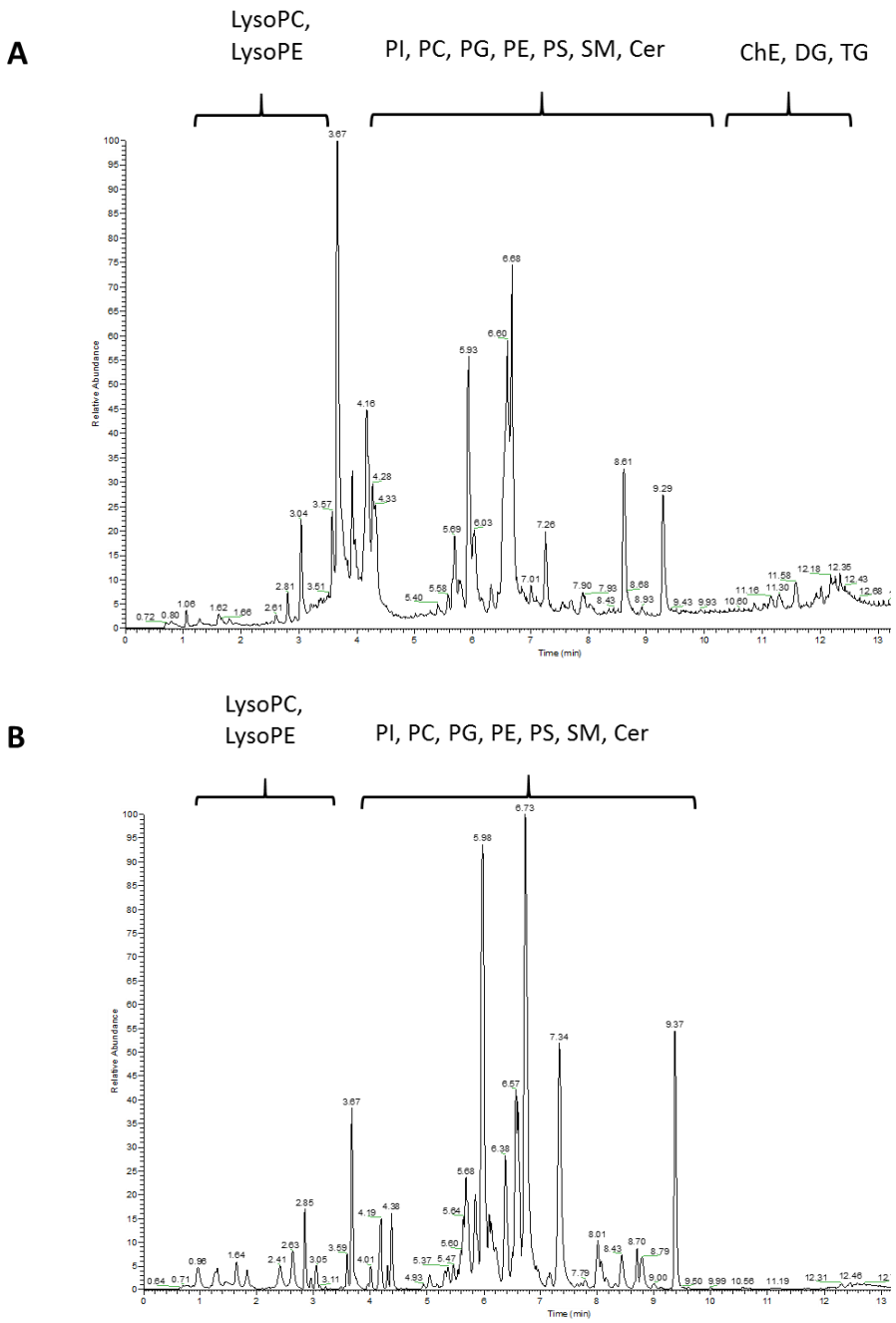

Figure 6.1: UPLC–MS total ion chromatograms of plasma lipid profiling in positive (A) and negative (B) modes for lipid identification of a quality control sample of OVX sheep. LPC (lysophosphatidylcholine), LPE (lysophosphatidylethanolamine), PI (phosphatidylinositol), PC (phosphatidylcholine), PG (phosphatidylglycerol), PE (phosphatidylethanolamine), PS (phosphatidylserine), SM (sphingomyelin), Cer (ceramide), DG (diacylglycerol), TG (triacylglycerol).

The samples were analysed in both positive and negative ion modes. A total of 2612 features (positive ionisation) were detected and after filtration and

removal of background noise and unstable compounds, the remaining 165 lipid features were fitted within the linear mixed model. Similarly, 4456 features (negative ionisation) were detected and after filtration and removal of background noise and unstable compounds, the remaining 391 lipid features were fitted within the linear mixed model.

6.3.1 Effect of OVX on the plasma lipidome of sheep: short-term approach

6.3.1.2 PCA: short-term approach

It was difficult to directly observe changes in the lipid profiles among the three groups (see Appendix C, Figure C.1). Thus, all time points for each group were analysed individually to obtain global information regarding the lipid changes.

PCA was performed to visualise grouping trends and outliers in the data. Principal component 1 (PC1) versus principal component 2 (PC2) scores plots of the plasma samples are shown in Figure 6.2. No noticeable differences can be observed in the PCA over the period of time. The distribution of all the serum samples from the control group at baseline, month one and month two are shown in Figure 6.2A, with the majority of samples located near the centre of the plot, over that period of time. At baseline, the resulting scatter plot showed that PC1 and PC2 explained 64.5% of the variance, while two outliers from month two can be observed. For the OVX group (Figure 6.2B), PC1 and PC2 explained 69.9% of the total variance. Plasma samples from OVX changed over the time points, and at month two were generally separated from the OVX samples from baseline (month zero), with only minor overlap between these two sampling times. Again, two outliers from baseline were observed. The OVXG group is shown in Figure

6.2C, with PC1 and PC2 explaining 65.1% of the variance. Consistent with the OVX group, the OVXG samples similarly changed over time (although again there was some minor overlap between baseline and month two), suggesting that the lipid profiles changed in the ewes in a dose-dependent manner as a result of the interventions when samples from all time points are analysed together.

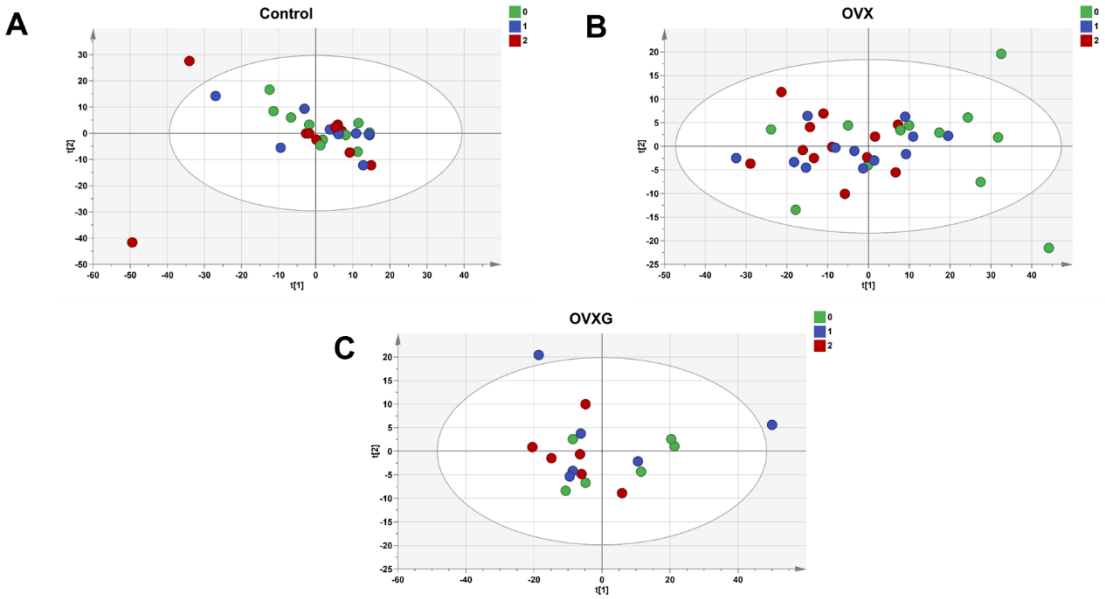

Figure 6.2: Inter-animal variation in the plasma of sheep over two months of the study period. PCA scatter plots derived from UPLC–MS spectra dataset based on normalised and autoscaled data. Each data point represents the lipid profile of a single ewe. PCA scoring plot showing the variation of control group (A) (● baseline (month zero); ● month one; ● month two) R2 = 70.9% and Q2 = 43.7%; (B) R2 = 77.7% and Q2 = 64.5%; and (C) R2 = 73.7% and Q2 = 46.4%.

6.3.2.2 Linear mixed model: short-term approach

To identify individual lipidomics changes, all detected features obtained from both positive and negative ionisation were analysed using a linear mixed model, and only those features that yielded significant results from the interaction of treatment and time were further analysed. Forty-eight features were significant from the linear mixed model; however, only five of these were subsequently identified: one phosphatidylglycerol, two cardiolipins and two phosphatidylinositol lipids. In this chapter, only those five identified lipids are described and all the

remaining unidentified features are shown in a complementary section of this chapter (see Appendix C, Table C.1).

In general, in this study, the lipid profiles of all the identified lipids at month one and month two (Table 6.2) for the OVX group decreased in relative intensity. The same trend was noticed in the OVXG group at month one, with the exception of cardiolipin (CL) (76:7). At month two, the relative intensities of PG, CL (76:7) and PI (35:5) decreased, with the exception of CL (72:5) and PI (14:0).

Table 6.2: Effect of OVX and glucocorticoids on the lipidome of sheep in the short-term approach. Relative intensities were measured in plasma samples of control group (*n* = 10), OVX group (*n* = 12) and OVXG (*n* = 6). Using linear mixed models, the relative intensities of the lipid profiles were found to significantly change over two months.

				Mean						
RT				(Relative intensity, E+05)				*p* -value		
m/z	(sec)	Feature	Trt	0	1	2	SEM	Trt	Time	Int
735.521	183.607	PG 33:0	Control	1.819	1.910	2.114	0.209	0.002	0.076	0.004
			OVX	2.672	2.145	2.059	0.191			
			OVXG	2.080	2.064	1.825	0.270			
752.511	183.615	CL 76:7	Control	3.483	3.419	3.583	0.187	0.005	0.004	0.013
			OVX	4.575	3.800	3.592	0.171			
			OVXG	3.787	3.843	2.984	0.242			
726.496	183.625	CL 72:5	Control	0.456	0.449	0.460	0.024	0.005	0.011	0.016
			OVX	0.602	0.485	0.467	0.022			
			OVXG	0.464	0.484	0.447	0.031			
785.429	183.632	PI 31:5	Control	0.509	0.497	0.536	0.038	0.011	0.011	0.028
			OVX	0.724	0.574	0.523	0.035			
			OVXG	0.565	0.569	0.453	0.049			
557.236	210.017	PI 14:0	Control	0.175	0.170	0.198	0.017	0.035	0.104	0.038
			OVX	0.256	0.209	0.186	0.016			
			OVXG	0.198	0.214	0.152	0.023			

Data presented are predicted means, standard error of the difference (SED) and p-values. Trt (Treatment). Int (Interaction treatment and time) Trt (Treatment). Int (Interaction treatment and time). PG = phosphatidylglycerol, CL = cardiolipin, PI = phosphatidylinositol.

To identify the magnitude of the individual changes of the identified lipids, the FCs and mean values in the OVX group with respect to the control group, and the OVXG group with respect to the OVX group, of the selected lipids at each time point were calculated (Table 6.3). In general, fold changes of the selected lipids changed in relative intensity of the treated groups when

compared with their control groups; however, those changes were not statistically significant. In the OVX group at month one, the relative intensity of PI species and CL (76:7) were increased by >1.1-fold when compared with the control group. However, at month two, the relative intensity of all the lipids decreased by ≤1-fold. In the OVXG group, the relative intensity of all lipids decreased by ≤1-fold when compared with the OVX group at month one and month two. Together, these results suggest that perturbed plasma lipid species might reflect the change of lipid profiles of sheep after OVX and glucocorticoid interventions.

Table 6.3: FC of the lipid abundance between the OVX and control groups and between the OVXG and the OVX groups at month one and month two.

		OVX vs Control		OVXG vs OVX	
		FC	FC	FC	FC
Lipid class	Pathways	1 month	2 months	1 month	2 months
PG 33:0	Glycerophospholipid	1.082	0.905	1.011	1.006
CL 76:7	Glycerophospholipid	1.111	1.002	1.011	0.831
CL 72:5	Glycerophospholipid	1.082	1.016	0.997	0.958
PI 31:5	Phosphatidylinositol phosphate	1.154	0.976	0.991	0.866
PI 14:0	Phosphatidylinositol phosphate	1.230	0.936	1.021	0.817

FC was calculated by dividing the value of the relative intensities of lipids in OVX group by control group, OVXG group by OVX group. FC with a value >1 indicated a relatively higher intensity present in treated animals, whereas a value <1 indicated a relatively lower intensity compared with their respective control animals. PG =phosphatidylglycerol, CL = cardiolipin, PI = phosphatidylinositol.

To assess the relationship between bone turnover markers, BMD and the lipids in OVX sheep, Pearson correlations were calculated. The correlation coefficient values between the lipids and bone clinical parameter markers are shown in Table 6.4. This study showed no statistically significant association between the relative intensity of identified lipids and the clinical bone parameters in OVX sheep, with the exception of one CL (72:5), which was negatively correlated with lumbar spine BMD. An inverse relationship was observed with PG and all clinical bone parameters. Likewise, an inverse relationship between the

identified lipids and the CTx-1 marker was observed, with the exception of CL (72:5), while an inverse relationship was observed between CL (72:5) and femoral BMD. PI species showed no relationship with serum OC biomarker. Weak positive associations with PI species and femoral and lumbar spine BMD were also observed.

Table 6.4: Correlation coefficients between lipids selected by univariate analysis in the short-term approach. Pearson correlation between bone formation marker (OC), bone resorption marker (CTx-1), femoral BMD and lumbar spine BMD and selected lipids at month two.

	OC *n* = 28		CTx-1 *n* = 28		Femoral BMD *n* = 11		Lumbar spine BMD *n* = 11	
Lipid class	Pearson correlation	*p*-value	Pearson correlation	*p*-value	Pearson correlation	*p*-value	Pearson correlation	*p*-value
PG 33:0	-0.262	0.178	-0.251	0.198	-0.159	0.641	-0.019	0.955
CL 76:7	0.177	0.369	-0.358	0.061	0.272	0.419	0.191	0.575
CL 72:5	0.317	0.1	0.24	0.219	-0.366	0.269	**-0.866**	**0.001**
PI 31:5	0.002	0.992	-0.125	0.526	0.149	0.662	0.182	0.592
PI 14:0	-0.001	0.997	-0.349	0.069	0.221	0.514	0.225	0.505

Bold numbers indicate statistically significant correlation (p-value < 0.05) PG = phosphatidylglycerol, CL = cardiolipin, PI = phosphatidylinositol.

6.3.2 Effect of OVX on the plasma lipidome of sheep: long-term approach

6.3.2.1 PCA: long-term approach

PCA analysis was also performed on the dataset for the long-term approach. The PCA did not reveal a clear separation among groups. Lipid profiles acquired with UPLC–MS were not able to distinguish between controls or treated groups, when analysing all treatments per individual time point (see Appendix C, Figure C.2). Thus, each group and all its time points were analysed individually to obtain global information regarding possible lipid changes.

PCA plots of the lipid profiles obtained from the analysis of OVX sheep over five months are shown in Figure 6.3. Examining the resulting PCA score plots, samples in the control and treated groups were mostly located near the centre of the plot, suggesting there were modest differences in the treated ewes.

Moreover, while there were no sample separations between treatment groups with time, a small disease progression can be noticed in the OVX sheep (Figure 6.3B); PC1 and PC2 explained 71.6% of the variance) when compared with the control group (Figure 6.3A); PC1 and PC2 explained 64.8%). Two outliers can be observed in the OVX group from baseline, and two from month two in the control group. Glucocorticoid-treated sheep (Figure 6.3C); PC1 and PC2 explained 67.8%) showed a different plasma lipid profile in comparison with the OVXG2 group and OVX group. Further, all samples from OVXG2 were clustered in the middle of the score plot, with the exception of two samples from month one (Figure 6.3D); PC1 and PC2 explained 65.1%).

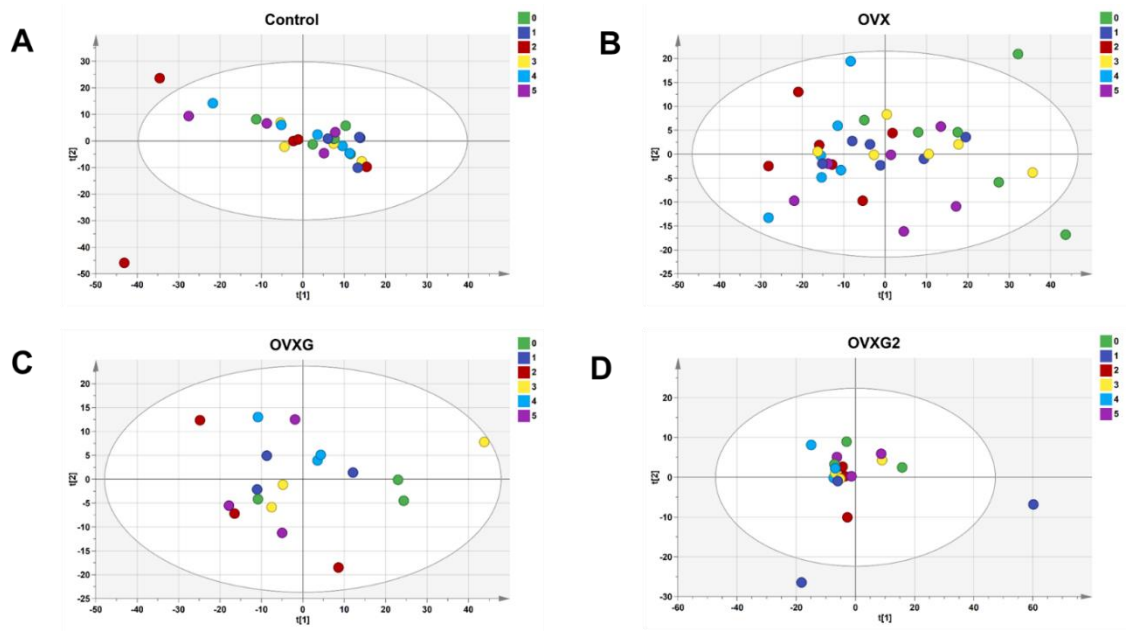

Figure 6.3: Inter-animal variation in the plasma of sheep over five months of the study period. PCA scatter plots derived from UPLC–MS spectra dataset based on normalised and autoscaled data. Each data point represents the lipid profile of a single ewe. PCA scoring plot showing the variation of control group (A) (● baseline (month zero); ● month one; ● month two; ● month three; ● month four; and ● month five) R2 = 71.5% and Q2 = 49.5%; OVX group (B) R2 = 75.9% and Q2 = 66.5%; OVXG group (C) R2 = 67.8% and Q2 = 55.2%; and OVXG2 group (D) R2 = 73.4% and Q2 = 35.4%.

6.3.2.2 Linear mixed model: long-term approach

One-hundred-and-twenty-six features were significant from the interaction between treatment and time; however, only 14 of these features were subsequently identified. The lipids identified by the linear mixed model presented a significant interaction between treatment and time (Table 6.5). At month one, the OVX group showed decreased relative intensities of all lipids, with the exception of CerP (39:1). Similarly, in the OVXG groups, all the relative intensities of the selected lipids decreased, with the exception of PG (42:0). In the OVXG2 group, however, all the selected lipids increased relative intensities, with the exception of CL (84:15). By contrast, at month three, the OVX and OVXG groups showed increased relative intensities of all the lipids. In the OVXG2 group, increased relative intensities of three CL species (76:7, 72:5, 76:8), two PI species (31:5, 14:0), PA (21:2), lysoPE and PS were observed. At month five, increased relative intensities of all the lipids in the OVX and OVXG2 groups were observed, while in the OVXG group, all the peak intensities of lipids were decreased, with the exception of PA (25:3) and lysoPE.

Table 6.5: Effect of OVX and glucocorticoids on the lipidome of sheep in the long-term analysis. Relative intensities were measured in plasma samples of control group (*n* = 5), OVX group (*n* = 6), OVXG (*n* = 3) and OVXG2 (*n* = 3). Using a linear mixed model, the relative intensities of the lipid profiles were found to significantly change over time.

				Mean (Relative intensity, E+5)							*p* -value		
mz	RT	Lipid	Trt	0	1	2	3	4	5	SEM	Trt	Time	Int
725.492	183.614	CL 72:6	Control	1.004	0.982	1.162	0.995	1.062	1.078	0.062	0.018	0.082	0.023
			OVX	1.433	1.176	1.053	1.156	1.041	1.136	0.056			
			OVXG	1.109	1.052	1.011	1.139	1.102	1.019	0.080			
			OVXG2	1.093	1.120	1.061	1.040	0.990	1.059	0.080			
752.511	183.615	CL 76:7	Control	3.506	3.338	3.894	3.496	3.628	3.730	0.252	0.088	0.023	0.016
			OVX	4.655	3.849	3.465	4.215	3.164	4.122	0.230			
			OVXG	3.932	3.656	2.849	3.978	3.647	3.085	0.326			
			OVXG2	3.642	4.030	3.119	3.252	3.430	3.613	0.326			
726.496	183.625	CL 72:5	Control	0.445	0.420	0.492	0.450	0.450	0.494	0.030	0.030	0.026	0.018
			OVX	0.633	0.500	0.446	0.533	0.426	0.506	0.027			
			OVXG	0.491	0.442	0.436	0.461	0.450	0.446	0.039			
			OVXG2	0.436	0.527	0.459	0.465	0.435	0.467	0.039			
751.518	183.651	CL 76:8	Control	0.655	0.636	0.767	0.676	0.671	0.751	0.055	0.011	0.060	0.042
			OVX	0.971	0.779	0.704	0.855	0.682	0.842	0.050			
			OVXG	0.800	0.686	0.693	0.784	0.731	0.704	0.071			
			OVXG2	0.673	0.873	0.600	0.702	0.631	0.728	0.071			
800.511	524.119	CL 84:1	Control	0.656	0.638	0.754	0.637	0.694	0.676	0.031	0.027	0.060	0.005
			OVX	0.825	0.734	0.637	0.742	0.676	0.722	0.028			
			OVXG	0.734	0.673	0.593	0.646	0.670	0.636	0.040			
			OVXG2	0.726	0.694	0.745	0.707	0.620	0.660	0.040			
686.546	524.192	CerP 39	Control	1.006	0.938	1.131	0.982	0.989	1.045	0.061	0.042	0.071	0.014
			OVX	1.301	1.135	1.026	1.187	1.005	1.138	0.055			
			OVXG	1.121	1.103	0.952	1.177	1.080	0.916	0.078			
			OVXG2	1.043	1.193	1.164	1.017	0.900	1.034	0.078			
660.543	564.314	CerP 37	Control	30.813	29.823	34.655	30.705	30.661	31.521	1.417	0.019	0.029	0.045
			OVX	37.761	34.926	32.182	35.569	30.496	34.523	1.294			
			OVXG	36.159	32.864	29.254	31.352	31.646	31.601	1.830			
			OVXG2	33.828	34.127	33.006	28.673	31.193	31.655	1.830			
785.429	183.632	PI 31:5	Control	0.486	0.456	0.573	0.469	0.531	0.544	0.051	0.022	0.022	0.016
			OVX	0.800	0.596	0.498	0.667	0.475	0.594	0.047			
			OVXG	0.607	0.508	0.425	0.623	0.526	0.455	0.066			
			OVXG2	0.522	0.630	0.482	0.513	0.466	0.535	0.066			
557.236	210.017	PI 14:0	Control	0.165	0.153	0.239	0.166	0.195	0.205	0.025	0.120	0.153	0.019
			OVX	0.281	0.219	0.174	0.252	0.158	0.233	0.023			
			OVXG	0.214	0.194	0.132	0.258	0.190	0.187	0.032			
			OVXG2	0.182	0.233	0.172	0.177	0.158	0.193	0.032			
543.316	209.543	PA 25:3	Control	0.614	0.581	0.801	0.618	0.675	0.701	0.057	0.117	0.103	0.018
			OVX	0.927	0.712	0.646	0.820	0.622	0.741	0.052			
			OVXG	0.715	0.656	0.574	0.746	0.678	0.697	0.074			
			OVXG2	0.727	0.778	0.715	0.655	0.561	0.690	0.074			
558.243	249.978	PS 20:4	Control	0.696	0.607	0.809	0.716	0.680	0.824	0.077	0.073	0.036	0.038
			OVX	1.119	0.823	0.687	0.943	0.691	0.767	0.071			
			OVXG	0.820	0.743	0.573	0.856	0.845	0.672	0.100			
			OVXG2	0.733	0.834	0.685	0.739	0.678	0.735	0.100			
464.323	214.017	lysoPE 1	Control	0.770	0.594	0.883	0.700	0.743	0.790	0.076	0.014	0.004	0.043
			OVX	1.158	0.858	0.735	0.986	0.691	0.943	0.069			
			OVXG	0.872	0.663	0.646	0.807	0.716	0.865	0.098			
			OVXG2	0.748	0.883	0.752	0.769	0.642	0.806	0.098			
558.243	249.978	PS 20:4	Control	0.696	0.607	0.809	0.716	0.680	0.824	0.077	0.073	0.036	0.038
			OVX	1.119	0.823	0.687	0.943	0.691	0.767	0.071			
			OVXG	0.820	0.743	0.573	0.856	0.845	0.672	0.100			
			OVXG2	0.733	0.834	0.685	0.739	0.678	0.735	0.100			
861.656	251.742	PG 42:0	Control	1.524	1.299	1.807	1.616	1.555	1.857	0.167	0.138	0.185	0.026
			OVX	2.458	1.802	1.516	1.974	1.560	1.656	0.153			
			OVXG	1.590	1.603	1.416	1.776	1.968	1.618	0.216			
			OVXG2	1.611	1.656	1.643	1.642	1.565	1.609	0.216			

Data presented are predicted means, standard error of the difference (SED) and p-values.
Trt (Treatment). Int (Interaction treatment and time). CL = cardiolipin, CerP = ceramide 1-phosphates, . PI = phosphatidylinositol, PA = phosphatidic acid, lysoPE = lysophosphatidylethanolamines, PS = phosphatidylserines, PG = phosphatidylglycerol.

To identify the individual changes of the identified lipids, the FCs and mean values of these lipids were calculated for the OVX group with respect to the control group, the OVXG group with respect to the OVX group, and the OVXG2 group with respect to the OVX group (Table 6.6).

The OVX group showed a significant FC of five lipids at month one, three at month two and eleven at month three (significant lipids presented with bolded FC values, *p*-value < 0.05, Table 6.5). All the lipids at month one, month three and month five (with the exception PA (21:2), PS and PG) were increased in relative intensities by >1-fold when compared with the control group. A significant increase of FC values was noticed at month one in CL (84:15), CerP species and PG; at month two in CL (84:15), PI (14:0) and PA (25:3); and at month three in CL (76:7, 72:5, 76:8, 84:15), CerP species, PI species, PA (25:3), lysoPE and PS. In contrast, only <1-fold increases of all lipids were observed at month two.

Combination treatments in the OVXG group induced an increase in relative intensities of lipids by >1-fold at month four when compared with the OVX group. A significant increase of FC values was noticed at month three in CL (84:15) and CerP (37:0); and month five in CerP (39:1). Conversely, cessation of glucocorticoids in the OVXG2 group resulted in the observation of FC values higher than 1 in all lipids in month one; month two with the exception of CL (76:8); and month five with the exception of PA (25:3), lysoPE and PG. CL (84:15) was significantly increased at month two when compared with the OVXG group. These results suggest that OVX or the combination of OVX and glucocorticoid treatments affected the lipid profiles of sheep by inducing changes in lipid metabolism.

Table 6.6: FC of the lipid abundance between the OVX and control groups, between the OVXG and the OVX groups and between the OVXG2 and the OVXG groups from month one to month five.

		OVX vs Control				
		FC	FC	FC	FC	FC
Lipid class	Pathways	1 month	2 months	3 months	4 months	5 months
CL 72:6	Glycerophospholipid	1.198	0.906	1.161	0.980	1.053
CL 76:7	Glycerophospholipid	1.153	0.890	**1.206**	0.872	1.105
CL 72:5	Glycerophospholipid	1.190	0.907	**1.185**	0.947	1.025
CL 76:8	Glycerophospholipid	1.225	0.918	**1.264**	1.017	1.121
CL 84:15	Glycerophospholipid	**1.150**	**0.845**	**1.165**	0.975	1.069
CerP 39:1	Glycosphingolipid	**1.210**	0.907	**1.208**	1.017	1.089
CerP 37:0	Glycosphingolipid	**1.171**	0.929	**1.158**	0.995	1.095
PI 31:5	Phosphatidylinositol phosphate	1.307	0.869	**1.423**	0.896	1.092
PI 14:0	Phosphatidylinositol phosphate	1.432	**0.727**	**1.525**	0.809	1.137
PA 25:3	Glycerophospholipid, phosphatidylinositol phosphate	1.225	**0.806**	**1.326**	0.922	1.057
PA 21:2	Glycerophospholipid, phosphatidylinositol phosphate	1.396	0.789	1.313	0.937	0.934
lysoPE 18:0	Glycerophospholipid	1.444	0.833	**1.410**	0.930	1.193
PS 20:4	Glycerophospholipid	1.355	0.849	**1.318**	1.017	0.931
PG 42:0	Glycerophospholipid	**1.386**	0.839	1.222	1.003	0.892

		OVXG vs OVX				
		FC	FC	FC	FC	FC
Lipid class	Pathways	1 month	2 months	3 months	4 months	5 months
CL 72:6	Glycerophospholipid	0.894	0.960	0.986	1.059	0.897
CL 76:7	Glycerophospholipid	0.950	0.822	0.944	1.153	**0.748**
CL 72:5	Glycerophospholipid	0.883	0.978	0.865	1.057	0.881
CL 76:8	Glycerophospholipid	0.881	0.985	0.916	1.071	0.837
CL 84:15	Glycerophospholipid	0.917	0.931	**0.870**	0.991	0.881
CerP 39:1	Glycosphingolipid	0.972	0.928	0.991	1.075	**0.805**
CerP 37:0	Glycosphingolipid	0.941	0.909	**0.881**	1.038	0.915
PI 31:5	Phosphatidylinositol phosphate	0.852	0.852	0.934	1.106	0.766
PI 14:0	Phosphatidylinositol phosphate	0.889	0.757	1.023	1.200	0.804
PA 25:3	Glycerophospholipid, phosphatidylinositol phosphate	0.921	0.888	0.910	1.090	0.941
PA 21:2	Glycerophospholipid, phosphatidylinositol phosphate	0.864	0.935	0.900	1.236	0.900
lysoPE 18:0	Glycerophospholipid	0.773	0.878	0.818	1.036	0.918
PS 20:4	Glycerophospholipid	0.903	0.835	0.908	1.222	0.876
PG 42:0	Glycerophospholipid	0.890	0.934	0.900	1.262	0.977

		OVXG2 vs OVXG				
		FC	FC	FC	FC	FC
Lipid class	Pathways	1 month	2 months	3 months	4 months	5 months
CL 72:6	Glycerophospholipid	1.065	1.049	0.913	0.898	1.040
CL 76:7	Glycerophospholipid	1.102	1.095	0.817	0.940	1.171
CL 72:5	Glycerophospholipid	1.192	1.053	1.009	0.967	1.048
CL 76:8	Glycerophospholipid	1.273	0.866	0.896	0.863	1.033
CL 84:15	Glycerophospholipid	1.031	**1.255**	1.095	0.925	1.038
CerP 39:1	Glycosphingolipid	1.081	1.223	0.864	0.833	1.129
CerP 37:0	Glycosphingolipid	1.038	1.128	0.915	0.986	1.002
PI 31:5	Phosphatidylinositol phosphate	1.240	1.135	0.824	0.887	1.175
PI 14:0	Phosphatidylinositol phosphate	1.196	1.304	0.687	0.834	1.027
PA 25:3	Glycerophospholipid, phosphatidylinositol phosphate	1.186	1.246	0.878	0.828	0.990
PA 21:2	Glycerophospholipid, phosphatidylinositol phosphate	1.134	1.129	0.863	0.794	1.041
lysoPE 18:0	Glycerophospholipid	1.332	1.165	0.953	0.896	0.931
PS 20:4	Glycerophospholipid	1.123	1.196	0.863	0.802	1.094
PG 42:0	Glycerophospholipid	1.033	1.160	0.925	0.795	0.995

FC was calculated by dividing the value the relative intensities of lipids in OVX group by control group, OVXG group by OVX group and OVXG2 by OVXG. FC with a value >1 indicated a relatively higher intensity present in treated animals, whereas a value <1 indicated a relatively lower intensity compared with their respective control animals. All FC values, which are in bold, are significant at p-value < 0.05 calculated using post-hoc Fisher's Least Significant Difference (LSD) test for pair-wise multiple comparison of the group means. CL = cardiolipin, Cer-P = ceramide 1-phosphates, PI = phosphatidylinositol, PA = phosphatidic acid, lysoPE = lysophosphatidylethanolamines, PS = phosphatidylserines, PG = phosphatidylglycerol.

The correlation coefficient values between the lipids and bone clinical parameters at month five are shown in Table 6.7. After five months of oestrogen deficiency and glucocorticoid treatments, the relative intensities of all the plasma lipids were more frequently negatively correlated with serum OC and CTx-1. However, more positive correlations were observed with femoral BMD and lumbar spine. The correlations between bone turnover biomarkers, serum OC and CTx-1, and for all the identified lipids in sheep at month five, were not significant, with exception of CerP (39:1), which was positively correlated with lumbar spine BMD.

Table 6.7: Correlation coefficients between lipids selected by univariate analysis in the long-term analysis. Pearson correlation between bone formation marker (OC), bone resorption marker (CTx-1), femoral BMD and lumbar spine BMD and selected lipids at month five.

	OC		CTx-1		Femoral BMD		Lumbar spine BMD	
	n =17		*n* = 17		*n* = 17		*n* = 17	
	Pearson		Pearson		Pearson		Pearson	
Lipid class	correlation	*p*-value	correlation	*p*-value	correlation	*p*-value	correlation	*p*-value
CL 72:6	-0.215	0.407	0.107	0.683	0.392	0.12	0.458	0.064
CL 76:7	-0.057	0.827	0.038	0.884	0.381	0.132	0.442	0.076
CL 72:5	-0.195	0.454	-0.076	0.771	0.452	0.068	0.397	0.115
CL 76:8	-0.086	0.744	0.062	0.813	0.09	0.731	0.253	0.327
CL 84:15	-0.199	0.445	-0.45	0.864	0.4	0.112	0.383	0.129
CerP 39:1	0.045	0.863	-0.016	0.953	0.353	0.165	**0.509**	**0.037**
CerP 37:0	-0.12	0.647	0.13	0.619	0.117	0.656	0.014	0.985
PI 31:5	-0.056	0.832	-0.074	0.779	0.285	0.268	0.362	0.154
PI 14:0	-0.132	0.612	-0.062	0.814	-0.03	0.909	0.119	0.65
PA 25:3	-0.19	0.465	-0.114	0.662	0.002	0.993	0.014	0.957
PA 21:2	-0.381	0.131	-0.24	0.354	0.333	0.192	0.376	0.137
lysoPE 18:0	-0.019	0.943	0.063	0.809	-0.186	0.476	-0.085	0.747
PS 20:4	-0.382	0.13	-0.289	0.261	0.34	0.181	0.342	0.179
PG 42:0	-0.284	0.269	-0.176	0.498	0.27	0.294	0.27	0.295

Bold numbers indicate statistically significant correlation (p-value < 0.05). CL = cardiolipin, Cer-P = ceramide 1-phosphates, PI = phosphatidylinositol, PA = phosphatidic acid, lysoPE = lysophosphatidylethanolamines, PS = phosphatidylserines, PG = phosphatidylglycerol.

6.4 Discussion

In this study, an untargeted lipidomics approach was applied for plasma samples using UPLC–MS analysis to further analyse the impact of oestrogen deficiency on the lipidome of OVX sheep. The results showed a dynamic change in the plasma lipid profiles of OVX sheep in response to the treatments, and the lipid species altered were from varying lipid classes including lysophosphatidylethanolamines (lysoPEs), phosphatidylinositols (PIs), phosphatidylcholines (PCs), phosphatidylethanolamines (PEs), phosphatidylserines (PSs), phosphatidylglycerols (PGs), and ceramides (Cer). In addition, from this study, a second purpose was to assess the correlations with bone clinical parameters. None of the associations were significant in either the short-term or the long-term approach, with the exception of CL (72:5) in the short-term approach. These results revealed differences in the lipidome in both short-term and long-term approaches, which affect circulating plasma lipids, but there were no associations with bone remodelling in OVX sheep.

It was of interest to evaluate the dynamic changes of the lipidome of OVX sheep not only after treatments were initiated but also up to five months after those interventions. In the short-term approach, OVX increased CL (76:7) and PI species at month one. In contrast, in the glucocorticoid-treated animals, a decrease in levels of all identified lipids was observed at month one, and the same effect was observed at month two. In general, this study had a small sample size for a lipidomics analysis; however, the short-term approach provided a better probability to improve the characterisation of the lipidome in OVX sheep due to it having more animals in each treatment group (control group n = 10; OVX n = 12; and OVXG n = 6).

In the long-term approach, lipid profiles changed after OVX or glucocorticoid treatments. Relative intensities of lipids were increased at months one and three, and remained relatively stable until the end of the study in the OVX group. In the OVXG treatment, the relative intensities of the all lipids decreased in the OVXG group after five months. In contrast, in the OVXG2, a dynamic lipid compositional change could be observed from month one. These relative intensities decreased steadily until the end of this study, with the exception of CL (72:6), CerP (39:1) and PI (31:5) at month five; however, these lipids showed an opposite trend compared to the one observed in the OVXG group over time. These results suggested that suppression of glucocorticoids altered changes in the lipidome of those animals in the OVXG2.

The OVX sheep model was selected because it mimics postmenopausal bone loss and it is recommended by the WHO as a large species for evaluating skeletal osteoporosis therapies (Bonjour et al., 1999). Lipids are involved in several cellular functions and physiological conditions associated with energy storage, structure, apoptosis and signalling, and these have an effect on skeletal metabolism and bone health (Gross and Han, 2011). In this study, lipid profiles were affected, where various relative intensities of lipids changed in the early stage of oestrogen withdrawal in the OVX sheep. Although lipid clinical markers such as TGs, TCHO, LDL-C or HDL-C were not measured, these findings coincide with previous results, where it was reported that perturbed levels of lipid metabolism are associated with osteoporosis (Manelli and Giustina, 2000; Mazziotti et al., 2006; van Staa, 2006; Buizert Petra et al., 2009). The mechanism underlying this altered lipid metabolism seems to be related to the main effect of oestrogen withdrawal and glucocorticoids treatment. The effects of oestrogen

loss on bone metabolism are well known, where the main effect is to induce an imbalance between bone formation and resorption phases due to apoptosis of osteoblasts and increase in osteoclastogenesis (Khosla et al., 2012). Further, it is known that excessive use of glucocorticoids can disturb lipid metabolism, induce adipogenesis and suppress osteoblastogenesis in the bone marrow (Henneicke et al., 2014). Overall, glucocorticoids increase bone fragility with increased bone loss and decreased mechanical strength. Glucocorticoids affect bone remodelling, and induce an increased osteoclast bone resorption and a reduced osteoblast formation; they also perturb calcium metabolism by inhibiting intestinal calcium absorption, which leads to a calcium deficit and an altered mineral metabolism (Fitzpatrick, 2002; Weinstein, 2010; Cooper et al., 2016). Future studies are needed to further investigate the link between lipids and bone loss, especially at the lipidome level.

This study detected some perturbed phospholipids in the OVX sheep. Phospholipids play a critical role in the bone marrow as fatty acid reservoirs, and are a major component of all cell and lipoprotein membranes. The six major phospholipid subclasses are PC, PS, PE, PI, PG and PA (Gimenez et al., 2011; Frega et al., 2012). In this study, levels of phospholipids decreased after OVX and increased at month three until the end of the study period. Although this is the first study that presents lipid profiles from OVX sheep, previous studies have reported lipidome changes in OVX rats. Zhu et al. (2010) reported decreased eicosapentaenoic acid, ergocalciferol and cholecalciferol, and increased arachidonic acid, in OVX rats. Conversely, an earlier study reported increased levels of fatty acids (arachidonic acid and octadecadienoic acid) and cholesterol after OVX compared with those levels before surgery in OVX rats (Ma et al.,

2013a; Zhang et al., 2014a). However, in this study, arachidonic acid was not detected; PCs and PIs are substrates for this fatty acid (Hayakawa et al., 1993). This implies that altered phospholipids might be involved in osteoclastogenesis promoting loss of BMD, which affects bone remodelling as a result of oestrogen depletion.

Sphingolipids are a major component of cell membranes and play a role in cell signalling. Ceramides are precursors to many other sphingolipids. In blood plasma, they are associated with lipoproteins (Zheng et al., 2006; Gault et al., 2010). The major subclass identified in this study was two species of ceramide phosphate. Our findings were similar to a previous study that reported that levels of ceramide, ceramide-1-phosphate, sphingomyelin, 1-*O*-alkenyl-lysophosphatidylethanolamine and lysophosphatidylethanolamine were elevated in the OVX rats compared to those in the sham-operated rats (Vinayavekhin et al., 2016). Ceramide has been implicated in increasing the cellular oxidative state, and this has been linked to stress or death signals. Ceramide levels have been reported to affect osteoblast apoptosis (Tepper et al., 1995; Hill and Tumber, 2010). Thus, perturbed ceramide levels may play a key role in bone loss in postmenopausal women.

Cardiolipins (CL) are phospholipids that are embedded in the inner mitochondrial membrane and are a key factor for energy production. Current evidence highlights that mitochondrial dysfunction by reactive oxygen species leads to the oxidation of mitochondrial cardiolipins, and this has been linked to atherosclerosis (Lane et al., 2015; Schlame and Greenberg, 2017). Although our results are unable to establish a direct role of CL in osteoporosis, this might be

related via bone marrow cells, where oestrogen withdrawal regulates the complex cell differentiation of osteoblasts and adipocytes (Elbaz et al., 2009).

In addition, in this study, the correlations of detected plasma lipids with traditional bone clinical parameters were measured. Bone clinical parameters are used to measure or monitor bone remodelling in postmenopausal osteoporosis. These findings showed weak associations between the lipid profiles and bone loss in OVX sheep. An earlier study reported that higher concentrations of phosphatidylcholine (docosahexaenoic acid) and arachidonic acid were positively associated with loss of femoral BMD in postmenopausal women (K et al., 2012). These long-chain fatty acids serve as precursors in the production of cytokines involved in bone remodelling, indicating the main role of this lipid in bone health (Coetzee et al., 2007). Phospholipid species identified from the lipidomics analysis could be potentially used for developing biomarkers for postmenopausal osteoporosis. However, validation of these results need to further investigated using other biological matrixes as osteoporotic bone tissues to analyse the changes of the bone microenvironment in postmenopausal conditions.

6.5 Conclusions

OVX and glucocorticoid treatments altered plasma lipid profiles in sheep over the five months of the study. Differences observed in the relative intensities of the lipid classes CL, PI, PA and PS after OVX relate to disorders in glycerophospholipid and phosphatidylinositol pathways. The measurement of the changes in circulating lipids has potential implications for identification of further risk factors associated with oestrogen withdrawal in women, and may contribute to loss of BMD. Understanding the intrinsic mechanisms of the CL, PI, P and PS classes in bone remodelling, as well as their potential connection to bone loss, is needed to provide evidence to not just predict bone loss but also to design novel drugs for the treatment of osteoporosis.

Chapter 7

Association of plasma lipids and polar metabolites with low bone mineral density in Singaporean–Chinese postmenopausal women

This chapter compares the plasma lipid and metabolite profiles of Singaporean–Chinese (SC) postmenopausal women with normal and low bone mineral density (BMD) using an untargeted LC–MS metabolomics approach. This chapter also evaluates the relationship between bone mineral density measurements, bone turnover markers and plasma lipid and metabolite profiles in order to determine whether those significant features are linked to bone loss.

This chapter is based on paper 2

Diana Cabrera[1,2*], Marlena Kruger[1,3], Frances M. Wolber[4], Nicole C. Roy[2,3,5], John J. Totman[6], Christiani Jeyakumar Henry[7], David Cameron-Smith[2,3,8] and Karl Fraser[2,3, 5]. (2018). Association of plasma lipids and polar metabolites with low bone mineral density in Singaporean-Chinese Menopausal women: a pilot study. *Intl J Environ Res Public health*. *5*(5), 1045.

[1]School of Food and Nutrition, Massey University, Tennent Drive, Palmerston North 4442, New Zealand
[2]Food Nutrition & Health Team, Food & Bio-based Products Group, AgResearch Grasslands, Palmerston North 4442, New Zealand
[3]Riddet Institute, Massey University, Palmerston North 4442, New Zealand
[4]Centre for Metabolic Health Research, Massey University, Tennent Drive, Palmerston North 4442, New Zealand
[5]High-Value Nutrition National Science Challenge, Auckland
1142, New Zealand
[6]A*Star-NUS Clinical Imaging Research Centre, Singapore 117599, Singapore
[7]A*Star-NUS Clinical Nutrition Research Centre, Singapore
[8]The Liggins Institute, The University of Auckland, Auckland 1142, New Zealand

Author contribution

Marlena Kruger, Fran Wolber, Nicole Roy, Jonh Totman, Christiani Jeyakumar, David Cameron-Smith and Karl Fraser conceived of study. Christiani Jeyakumar supervised patient recruitment. Diana Cabrera, Marlena Kruger, Frances Wolber, Nicole Roy and Karl Fraser contributed to the study execution, analysis, and interpretation of data. Diana Cabrera and Karl Fraser performed data analysis and interpretation. Diana Cabrera wrote the manuscript. All the authors reviewed and contributed to edit and approve the final version of this paper for submission.

The format has been adjusted to the general format of the thesis. Tables and figures were kept as in publication.

Abstract

The diagnosis of osteoporosis is mainly based on clinical examination and bone mineral density assessments. The present pilot study compares the lipid and metabolite profiles in blood plasma of 95 Singaporean–Chinese (SC) postmenopausal women with normal and low bone mineral density (BMD) using an untargeted LC–MS metabolomics approach. The primary finding of this study was to report the associations between lipids and femoral neck BMD in SC postmenopausal women. Twelve lipids were identified by the orthogonal partial least-squares (OPLS) model to be associated with low mineral density. There was a significant decrease in plasma concentrations of eight glycerophospholipid, glycerolipid and sphingolipid species in postmenopausal women with low BMD, but increased plasma concentrations of four glycerophospholipid species (phosphatidylserine, phosphatidylinositol, phosphatidylethanolamine and phosphatidic acid species). Further, this study found no significant differences in plasma amino acid metabolites. However, trends for lower ranges of 4-aminobutyric acid, turanose, proline, aminopropionitrile, threonine, methionine and a peptide in women with low BMD were noted. This pilot study showed associations between lipid metabolism and femoral neck BMD in SC women. Further studies should be conducted on larger populations for evaluating the bone health effect of these compounds and their usefulness to be clinical biomarkers for osteoporosis prediction in women.

7.1 Introduction

Postmenopausal women have a greater risk of bone loss and developing osteoporosis. Osteoporosis affects above 200 million people worldwide, and about nine million osteoporotic fractures—of which 1.6 million are at the hip—are registered per year (Aaseth et al., 2012). Hip fractures from Asian populations account for around 30% of the worldwide total; in Singapore, hip fracture rates have been increasing by 1.2% annually in Chinese women (Cooper et al., 2011).

In women, low oestrogen level is a risk factor for osteoporosis. Oestrogen withdrawal promotes the activation of bone remodelling at the basic multicellular units (BMUs). Bone formation decreases because there is a reduction of osteoblastic cell lifespan, and bone resorption increases as a result of an increased differentiation and lifespan of osteoclasts (Weitzmann and Pacifici, 2006). The impact of oestrogen loss in bone metabolism, including several biochemical and physiological alterations, is characterised by a high level of oxidative stress, inflammation and altered metabolism in the bone microenvironment (Manolagas, 2010; Redlich and Smolen, 2012). Previous studies demonstrated that oxidative stress, caused by mitochondrial alterations, induces reactive oxygen species (ROS) generation, and leads to osteoblast cell death by increasing the oxidised bone microenvironment (Mody et al., 2001; Maggio et al., 2003). In addition, oestrogen withdrawal upregulates bone microenvironment pro-inflammatory cytokines like interleukin-1 (IL-1), interleukin-6 (IL-6), TNF-α, granulocyte macrophage colony-stimulating factor, M-CSF and prostaglandin-E_2 (PGE_2), which regulate osteoclast differentiation and function and therefore bone loss (Jilka et al., 1992; Riggs, 2000). Osteoporosis may be present well before diagnosis; despite the current serum biochemical

analysis and radiological examination methods for screening of osteoporosis and fracture risk in postmenopausal women (Kanis, 2002), none of these methods are suitable for prediction of early bone loss in women. The elucidation of the cellular and biochemical events of bone metabolism after oestrogen withdrawal may lead to a better understanding of the molecular mechanism involved in osteoporosis and bone cell signalling pathways in women, and subsequently may allow identification of early predictors of bone loss that can be used as prognostic markers.

Metabolomics offers the potential for analysing the biochemical changes in the pathology of diseases. Metabolomics studies are conducted by using several analytical platforms; however, NMR and MS are the most widely reported techniques (Patti et al., 2012). A small number of plasma metabolomics studies have reported the metabolite concentration shifts under postmenopausal conditions in OVX animals and humans (Liu et al., 2014; Ke et al., 2015; Liu et al., 2015; Iida et al., 2016), while numerous studies on the relationship between bone loss and oestrogen deficiency have been reported in both OVX animals and humans (Long et al., 2009; Xue et al., 2011; Liu et al., 2012; Ma et al., 2013a; You et al., 2014; Lee et al., 2016; Miyamoto et al., 2017).

Because of the limited information reported on the association between the plasma metabolome and BMD in SC women, research in this area is required to allow the identification of potential metabolites that can be used to understand the causal pathways involved in postmenopausal osteoporosis. It was hypothesised that novel metabolomic markers will improve the prediction of SC postmenopausal women at increased osteoporotic risk. Therefore, this study aimed to analyse the lipid and metabolite profiles of blood plasma from SC

postmenopausal women using an LC–MS untargeted metabolomics approach. Moreover, to maximise the identification of biomarkers associated with bone loss in postmenopausal women, we also performed statistical tests on a restricted subset of the SC women with either osteoporosis (T-score < −2.5) or normal BMD (T-score > −1). It was hypothesised that lipids and metabolites of women with osteoporosis differed from the whole population. Further, correlation analyses were conducted between metabolites and femoral neck BMD in postmenopausal women.

7.2 Materials and methods

7.2.1 Study population, inclusion and exclusion criteria

All subjects were informed about the objective of the study and gave their informed consent for the participation in the present study. The study was approved by the Ethics Committee for Research Involving Human Subjects, Singapore (Approval No. 2014/01066). The study was done in accordance with the Declaration of Helsinki (2000) of the World Medical Association.

Ninety-seven SC postmenopausal women aged between 55 and 70 years were included in the study. The key inclusion criterion was women who were at least five years postmenopausal (based on a history of cessation of menstruation). Exclusion criteria included prior diagnosis with osteoporosis, diabetes mellitus or any condition that affects bone and liver function, and to not be taking any medication that will affect the study.

7.2.2 Blood collection

Blood samples were taken only once between 8 and 10 a.m. Blood was collected in ethylenediamine tetraacetic acid (EDTA) tubes (BD Vacutainer™ K3E 15%, Becton, Dickinson and Company, Plymouth, UK). Then, EDTA tubes were put on ice and centrifuged at 1500 *g* for 10 min. Plasma samples were transferred into separate 1 mL tubes for extractions for metabolomics analysis, CTx-1, parathyroid hormone (PTH) and 25-hydroxyvitamin D_3 were stored frozen at −80 °C and thawed on the day of the analysis.

7.2.3 Analysis of blood parameters

Blood samples were taken to measure plasma markers of CTx-1 as well as PTH and 25-hydroxyvitamin D_3. CTx-1 and PTH concentrations were analysed by electrochemiluminescence immunoassay using the Roche COBAS® e411 system (Roche Diagnostics, Indianapolis, IN, USA). 25-hydroxyvitamin D_3 concentration was analysed using isotope-dilution liquid chromatography–tandem mass spectrometry (IDLC–MS–MS) (Maunsell et al., 2005) by Canterbury Health Laboratories, Christchurch, New Zealand. The CTx-1 blood marker of two participants was outside of the range, and data acquired were thus excluded from further analysis. Data from 95 participants was available.

7.2.4 Bone mineral density

BMD was measured using dual x-ray absorptiometry (DXA). DXA scans of hip (femoral neck) were carried out using a Hologic QDR-Discovery A densitometer (Hologic Discovery QDR 4500A densitometer, Hologic Inc., Bedford, MA, USA). BMD was determined and women were classified into

normal or low BMD according to the WHO classification. WHO provides an operational definition of osteoporosis based on T-score, where the T-score is the number of the standard deviations below the mean peak BMD for young adults. Women with a BMD 2.5 standard deviations below are classified as osteoporotic. In this study, participants in the entire cohort were classified into two groups according to bone status: (1) low BMD = women with a T-score < −1, and (2) normal BMD = women with a T-score > −1.0. Further, a selected subset of participants were also classified into two groups: (1) osteoporosis = women with a T-score < −2.5, and (2) normal BMD: women with T-score > −0.1 (World Health Organization, 1994).

7.2.5 Metabolomics analysis

7.2.5.1 Sample preparation

The sample preparation method has been described in Chapter 5, Section 5.2.5.2.

7.2.5.2 Metabolite and lipid analyses

Metabolite analysis has been described in Chapter 5, Section 5.2.5.3. Lipid analyses has been described in Chapter 6, Section 6.2.3. Table 7.1 summarised the extraction parameters applied for the untargeted metabolomics analysis.

Table 7.1: XCMS main parameters applied for the metabolomics analysis of the LC-MS spectral processing.

Parameters	Related to	Settings for lipidomics analysis	Settings for metabolomics analysis
ppm	*m/z*	5	10
peakwidth	Retention time	5,20	20,50
Prefilter	intensity	3, 10000	3, 2000
Snthresh*	intensity	20	10
noise	intensity	3000	500

*signal to noise threshold

7.2.6 Statistical analyses

7.2.6.1 Univariate analysis

The characteristics of the study population were compared using a *t*-test. Normality of the data was tested using the Shapiro–Wilk normality test, where age, BMI, CTx-1, PTH, 25-hydroxyvitamin D_3 and BMD parameters were expressed as mean and standard deviation (SD). Linear regression was applied to model the relationship between age-BMI adjusted mean concentrations. Thus, analysis of covariance was performed to adjust for possible confounders using age and BMI. In addition, the objective was to assess whether lipids and metabolites were associated with BMD. Age-adjusted correlation coefficients were calculated for each lipid and metabolite. Age- and BMI-adjusted mean concentrations of each lipid and metabolite were calculated in both groups. To assess whether those associations were independent, pairwise correlations were evaluated between identified lipids and metabolites. The *p*-values were calculated using Benjamini–Hochberg false discovery rate (FDR), where FDR *p*-value < 0.05 was considered as statistically significant. The fold changes in lipids and metabolites between BMD groups were performed by parametric test using MetaboAnalyst 4.0 web server (Chong et al., 2018). Statistical data analysis was

performed using R (R 3.3.3, R Foundation for Statistical Computing, Vienna, Austria).

7.2.6.2 Multivariate analysis

Prior to multivariate analysis (MVA), different datasets were created: (1) an entire cohort containing all samples (n = 95), and (2) a subset (n = 30), in which only 15 women with osteoporosis and 15 women with normal BMD were included. Both the entire cohort and subset were used for modelling the correlations between BMD and metabolites in SC postmenopausal women. For MVA, each variable was mean centered and univariate scaled over all the samples and imported into SIMCA-P+ v14.1 software (Umetrics, Umea, Sweden). SIMCA was used to construct an orthogonal partial least-squares (OPLS) regression model for analyzing BMD. The supervised method analyses the linear relationship between BMD and metabolite profiles. In OPLS, the R2X, R2Y, and Q2 (cum) parameters were used for the model evaluation, representing the explanation, fitness and prediction power, respectively. R2X is the percentage of all LC–MS response variables explained by the model. R2Y is the percentage of all sample variables explained by the model. Q2 is the percentage of all sample variables predicted by the model (Liland, 2011). Only one component was extracted to predict membership probability in each group. Then, from the coefficient score plot, a normal probability plot was created and 95% of features were excluded to fit a new model. The objective was to select the most relevant variables from the interaction between the metabolites and femoral neck BMD relative to bone status (step 1, OPLS methods) and to add these variables into a new model to

display the contribution of each metabolite to the modulation of osteoporosis (step 2).

7.3. Results

This study analysed lipids and metabolites in blood plasma of SC postmenopausal women. Overall, after analysing lipids and metabolites, two datasets were created for further multivariate analysis. The correlations between those compounds and femoral neck BMD were investigated by using univariate and OPLS regression statistical analyses. The lipid profiles revealed differences in the plasma of women with normal BMD and lower BMD/osteoporosis. Metabolites exhibited no differences; however, a trend was observed in several metabolites such as a peptide, amino acids and amines.

7.3.1. Characteristics of the postmenopausal women bone status

Women with low BMD were older and had lower BMI when compared with women in the normal group. PTH concentrations were lower in the postmenopausal groups with low BMD/osteoporosis compared to normal-BMD groups (Table 7.2). Serum 25-hydroxyvitamin D_3 concentrations were adequate (equal to or >50 nmol/L) for all the groups. Bone resorption marker (CTx-1) concentrations were significantly higher in the postmenopausal group with low BMD/osteoporosis compared to normal-BMD groups.

Table 7.2: Characteristics of the SC postmenopausal women according to bone status, entire cohort (*n* = 95) and subset (*n* = 30) analyses.

	Entire Cohort (*n* = 95)			Subset (*n* = 30)		
Parameters	Normal BMD (*n* = 23)	Low BMD (*n* = 72)	*p*-value	Normal BMD (*n* = 15)	Osteoporosis (*n* = 15)	*p*-value
Age (years)	59.4 (4.19)	61.3 (4.19)	0.06	58 (3.42)	61 (3.42)	0.02
BMI (kg/m^2)	23.8 (2.61)	22.5 (2.61)	0.04	23.8 (2.25)	20.7 (2.25)	<0.001
PTH (pmol/L)	4.7 (1.35)	4.5 (1.32)	0.29	4.8 (1.59)	4.3 (1.59)	0.08
CTx-1 (µg/L)	0.44 (0.21)	0.55 (0.20)	0.02	0.41 (0.26)	0.64 (0.26)	0.04
25-hydroxyvitamin D_3 (nmol/L)	57.4 (15.24)	60.1 (14.87)	0.23	56.5 (16.84)	54.8 (16.84)	0.81
Femoral neck BMD (g/cm^2)	0.75 (0.05)	0.60 (0.05)	<0.001	0.78 (0.04)	0.51 (0.04)	<0.001

Data are presented as mean (SD). The resulting *p*-values obtained by ANOVA are given. A *p*-value < 0.05 was considered as statistically significant.

7.3.1.1 Entire cohort

Table 7.2 shows the population characteristics for the postmenopausal women. The mean ages for these groups were 59.4 and 61.3 years for the normal- and low-BMD groups, respectively. Women with low BMD had lower BMI than those with normal BMD (23.8 vs 22.5 kg/m^2, *p*-value = 0.04). There were no significant differences between the groups for PTH and 25-hydroxyvitamin D_3 concentrations. Mean PTH values were 4.7 and 4.5 pmol/L (*p*-value = 0.29), and mean 25-hydroxyvitamin D_3 concentrations were 57.4 and 60.1 nmol/L (*p*-value = 0.23) for the normal- and low-BMD groups, respectively. However, CTx-1 concentrations and femoral neck BMD were significantly different. Mean CTx-1 concentrations were 0.44 and 0.55 µg/L for the normal- versus low-BMD groups, respectively. Femoral neck BMD was 0.75 g/cm^2 and 0.60 g/cm^2 (*p*-value ≤ 0.001) for the normal- and low-BMD groups, respectively.

7.3.1.2 Subset

Women with osteoporosis were older than those with normal BMD (58 vs 61, $p = 0.02$), and had lower BMI (23.8 vs 20.7 kg/m^2, p-value = 0.008). Similarly, there were no significant differences between the groups for PTH, CTx-1 and 25-hydroxyvitamin D_3 concentrations. Mean PTH values were 4.8 and 4.3 pmol/L (p-value = 0.08) and mean 25-hydroxyvitamin D_3 concentrations were 56.1 and 54.8 nmol/L (p-value = 0.81) for the normal BMD and osteoporosis groups, respectively. Serum CTx-1 concentrations were 0.41 and 0.64 µg/L (p-value = 0.04) and femoral neck BMD values were 0.78 g/cm^2 and 0.51 g/cm^2 (p-value < 0.001) for the normal BMD and osteoporosis groups, respectively.

7.3.2. Metabolomics approach

7. 3.2.1 Lipids

7.3.2.1.1 Entire cohort

Overall, 7082 features (positive and negative ionisation) were detected by lipidomics, and after filtration and removal of noise and unstable compounds, the remaining 1662 lipid features were fitted within the OPLS model. The OPLS model 1 was fitted and the cumulative R2Y and Q2 values were 0.302 and 0.042, respectively (Table 7.3). However, the predictive ability for the model Q2 was low, which indicated that it was not a good model. Therefore, the OPLS model with 1662 features was not able to explain the association of the explanatory variables and femoral neck BMD.

Subsequently, a new model (model 2) was created by selecting those features based on the exclusion of uncorrelated lipid features on the normal

probability coefficient score plot (between 0.05% and 0.95%) from model 1, resulting in 98 lipids being selected. The new model yielded R2Y and Q2 values of 0.469 and 0.233, respectively (Table 7.3). The new OPLS model parameters for fitness and the predictive capability Q2 were better than in the previous model (step 1) and significant based on the cross-validated analysis of variance (CV-ANOVA) (*p*-value ≤ 0.001). Figure 7.1A shows the OPLS predictive model for femoral neck BMD of the lipidomic plasma extracts from normal- and low-BMD postmenopausal women. A lineal clustering of the low-BMD postmenopausal women occurred on the left-hand side of the plot, while normal-BMD subjects were clustered on the top right-hand side. The results indicated that lipids change linearly with femoral neck BMD (R2Y = 0.469). Further, positive correlation values (upper portion of the plot) indicated increased serum lipid concentrations in normal BMD versus low BMD.

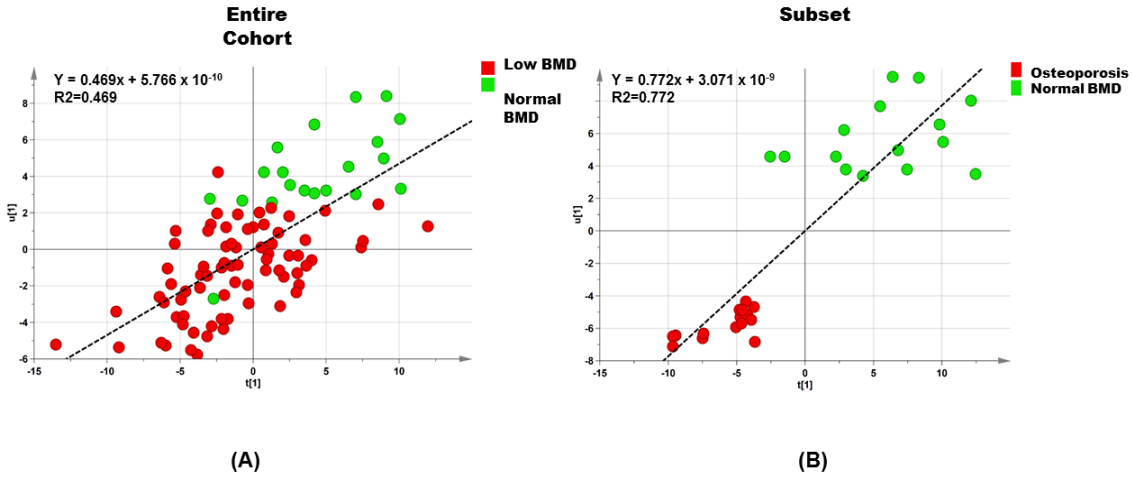

Figure 7.1: Orthogonal partial least squares (OPLS) from the lipid profiles of SC postmenopausal women. OPLS scatter plot of SC postmenopausal women with normal (green circles) and low BMD and osteoporosis (red circles) values based on orthogonally filtered partial square (OPLS) regression model 2. Graph (A): 98 features among 95 women, entire cohort. Graph (B): 149 features among 30 women, subset. t[1]/u[1] correlation plot; t1 refers to scores of the first component in independent variables; u1 refers to scores of the first component in responses.

Table 7.3: Parameters of orthogonal partial least-squares regression models based on the data from lipids separation for the entire cohort and the selected subset of SC postmenopausal women.

Dataset	Step	Component	R2X	R2Y	Q2
Entire cohort (*n* = 95)	1	1P and O1	0.395	0.302	0.042
Entire cohort (*n* = 95)	2	1P and O2	0.678	0.469	0.233
Subset (*n* = 30)	1	1P and O1	0.434	0.601	0.209
Subset (*n* = 30)	2	1P and O1	0.540	0.773	0.540

P predictive. O orthogonal in X. Component: number of significant components calculated by cross validation. R2X value is the predictive and orthogonal variation in model samples (X) explained by the model. R2Y value is the amount of variation in X which is correlated to Y (response matrix). Q2 value describes the predictive ability of the model.

Negative associations were found between femoral neck BMD and the lipids of postmenopausal women. Based on univariate analysis, the top 50 features were significant by *t*-tests. However, only five features were known lipids and these were associated with femoral neck BMD (Table 7.4; Appendix D, Table D.1, Figure D.1). The five known lipids include three phosphatidylserines (PSs), one diacylglycerol (DG) and one plasmenylphosphatidylethanolamine (plasmenyl-PE). The PS species detected comprised 36:1, 33:6 and 29:6, where a decreasing common trend was observed in the low-BMD group. A correlation matrix revealed negative correlations among the five lipids and femoral neck BMD, PS 36:1 (r = −0.027), PS 33:6 (r = −0.070), PS 29:6 (r = −0.086), DG 42:4 (r = −0.075), and plasmenyl-PE 38:4 (r = −0.01).

Table 7.4: Means and 95% confidence interval of lipids associated to the entire cohort of SC postmenopausal women (*n* = 95) with normal and low femoral neck BMD in univariate and multivariate approaches.

Lipid	Normal BMD[a] (*n* = 23)	Low BMD[a] (*n* = 72)	p-value	Log2 (FC)	Correlation[b]
PS 31:6; $[M + H]^+$	0.893 (0.427–1.871)	0.867 (0.675–1.114)	0.939	−0.455	−0.027
PS 33:6; $[M + H]^+$	0.857 (0.408–1.800)	0.876 (0.681–1.127)	0.955	−0.373	−0.070
PS 29:6; $[M + H]^+$	0.906 (0.428–1.918)	0.921 (0.714–1.188)	0.967	−0.296	−0.086
DG 42:4; $[M + NH4]^+$	0.850 (0.395–1.828)	0.947 (0.725–1.219)	0.804	−0.176	−0.075
Plasmenyl-PE 38:4; $[M + H]^+$	0.745 (0.353–1.571)	0.841 (0.653–1.083)	0.760	−0.174	−0.01

Lipids are expressed as mean and 95% confidence interval (CI). ANOVA was used to compare lipid mean concentrations. [a] Covariates: age and BMI; [b] Age-adjusted correlation coefficient. Statistical *p*-value calculated using Benjamini–Hochberg false discovery rate (FDR). A *p*-value < 0.05 was considered as statistically significant. Fold of change (FC) expressed as the relation between the lipid mean of the normal BMD group to the lipid mean of the low BMD group. $^+$ Adducts in positive ionisation. $^-$ Adducts in negative ionisation. PS (phosphatidylserine), DG (diacylglycerol), plasmenyl-PE (plasmenylphosphatidylethanolamines).

7.3.2.1.2 Subset

Similarly, an additional OPLS regression model was fitted to the subset of samples (*n* = 30) with the 1662 features to analyse the relationship of femoral neck BMD and lipids.

This OPLS model showed the relationship between the lipids and femoral neck BMD and this was described by high values of R2Y and Q2, 0.601 and 0.209, respectively (Table 7.3). After excluding 95% of the lipids, a new OPLS model (step 2) was fitted with 149 lipids. The scatter plot for this statistical analysis showed a straight line indicating a relationship between the predictive values and the observed responses (Figure 7.1B). This new model showed higher values of R2Y and Q2, 0.773 and 0.54, respectively, and was significant based on the CV-ANOVA (*p*-value ≤ 0.001), and also showed a strong linear correlation of R2Y = 0.772. Lipids that were highly associated with the normal

and osteoporosis groups through both approaches are listed in Table 7.5. Twelve known lipids were significant and included one phosphatidic acid (PA), two ceramide-1-phosphates (CerPs), four phosphatidylserine (PS) species, three diacylglycerol (DG) species, one phosphatidylethanolamine (PE), and one phosphatidylinositol (PI) (Table 7.5, Appendix D, Table D.2, Figure D.2). A correlation matrix revealed negative correlations among eight lipids and femoral neck BMD, while a positive correlation was observed with PS (20:4), PI, CerP (24:0) and PE (Table 7.5).

Table 7.5: Means and 95% confidence intervals of lipids associated to the subset of selected SC postmenopausal women (*n* = 30) with normal BMD and osteoporosis in univariate and multivariate approaches.

Lipid	Normal BMD[a] (*n* = 15)	Osteoporosis[a] (*n* = 15)	*p*-value	Log2 (FC)	Correlation[b]
PA 34:4; $[M - H]^-$	0.531 (0.321–0.878)	1.617 (0.822–3.182)	0.005	0.412	−0.403
CerP 38:1; $[M + H]^+$	1.871 (1.196–2.927)	0.605 (0.3319–1.105)	0.002	−0.637	−0.384
PS 20:4; $[M - H]^-$	0.547 (0.330–0.906)	1.585 (0.804–3.124)	0.008	0.395	0.274
DG 40:0; $[M + NH4]^+$	1.545 (0.907–2.630)	0.425 (0.207–0.870)	0.002	0.729	−0.270
PS 33:6; $[M + H]^+$	1.435 (0.908–2.267)	0.504 (0.277–0.933)	0.004	−0.560	−0.363
PS 31:6; $[M + H]^+$	1.423 (0.886–2.286)	0.506 (0.267–0.958)	0.006	−0.656	−0.377
PS 32:6; $[M + H]^+$	1.414 (0.885–2.259)	0.515 (0.274–0.967)	0.007	−0.573	−0.359
PI 14:0; $[M - H]^-$	0.608 (0.357–1.036)	1.572 (0.767–3.220)	0.022	0.327	0.165
DG 42:4; $[M + NH4]^+$	1.510 (0.976–2.336)	0.574 (0.319–1.033)	0.005	−0.327	−0.374
CerP 24:0; $[M - H]^-$	1.254 (0.728–2.160)	0.418 (0.201–0.869)	0.010	−0.265	0.008
DG 47:5; $[M + NH4]^+$	1.670 (0.920–3.032)	0.854 (0.382–1.905)	0.135	−0.351	−0.014
PE 42:1; $[M - H]^-$	0.592 (0.346–1.013)	1.246 (0.605–2.568)	0.069	0.585	0.034

Lipids are expressed as mean and 95% confidence interval (CI). ANOVA was used to compare lipid mean concentrations. [a] Covariates: age and BMI; [b] Age-adjusted correlation coefficient; Statistical *p*-value calculated using Benjamini–Hochberg false discovery rate (FDR). *p*-value < 0.05 was considered as statistically significant. Fold of change (FC) expressed as the relation between the lipid mean of the normal BMD group to the lipid mean of the osteoporosis group. $^+$ Adducts in positive ionisation. $^-$ Adducts in negative ionisation. PS (phosphatidylserine), PA (phosphatidic acid), DG (diacylglycerol), PE (phosphatidylethanolamine), CerP (ceramide-1-phosphate), PE (phosphatidylethanolamine), and PI (phosphatidylinositol).

7.3.2.2 Metabolites

7.3.2.2.1 Entire cohort

Five hundred and seventy-four features (positive ionisation) were detected by metabolomics. After filtration and removal of unwanted background and unstable compounds, the remaining 127 metabolites were fitted in an OPLS regression model. However, cumulative R2Y and Q2 values were 0.223 and −0.371, respectively (Table 7.6), and the predictive ability for the model Q2 was very low, which indicated that it was not a suitable model.

Features scoring between 0.05% and 0.95% on the normal probability coefficient score plot were taken out to fit a new model (step 2), which had only 12 features. Values of cumulative R2Y and Q2 values for this OPLS model were 0.205 and 0.035, respectively (Figure 7.2A). Both step 1 and step 2 for metabolites showed little prediction for the two OPLS regression models. Therefore, the OPLS model with 127 features was not able to explain the association of the explanatory variables and femoral neck BMD. However, this analysis provided evidence for the association between four metabolites and femoral neck BMD (Table 7.7, Appendix D, Table D.3, Figure D.3), 4-aminobutyric acid (r = −0.013), threonine (r = −0.172), a tripeptide formed by asparagine–glycine–cystine (Asn–Gly–Cys) (r = −0.059), and turanose (r = −0.039).

Table 7.6: Parameters of orthogonal partial least squares regression models based on the data from metabolites separation for the entire cohort and the selected subset of SC postmenopausal women.

Dataset	Step	Component	R2X	R2Y	Q2
Entire cohort (*n* = 95)	1	1P and O1	0.483	0.223	−0.371
Entire cohort (*n* = 95)	2	1P and O1	0.512	0.205	0.035
Subset (*n* = 30)	1	1P and O1	0.437	0.749	−0.399
Subset (*n* = 30)	2	1P and O1	0.514	0.526	0.247

P predictive. O orthogonal in X. Component: number of significant components calculated by cross-validation. R2X value is the predictive and orthogonal variation in model samples (X) explained by the model. R2Y value is the amount of variation in X which is correlated to Y (response matrix). Q2 value describes the predictive ability of the model.

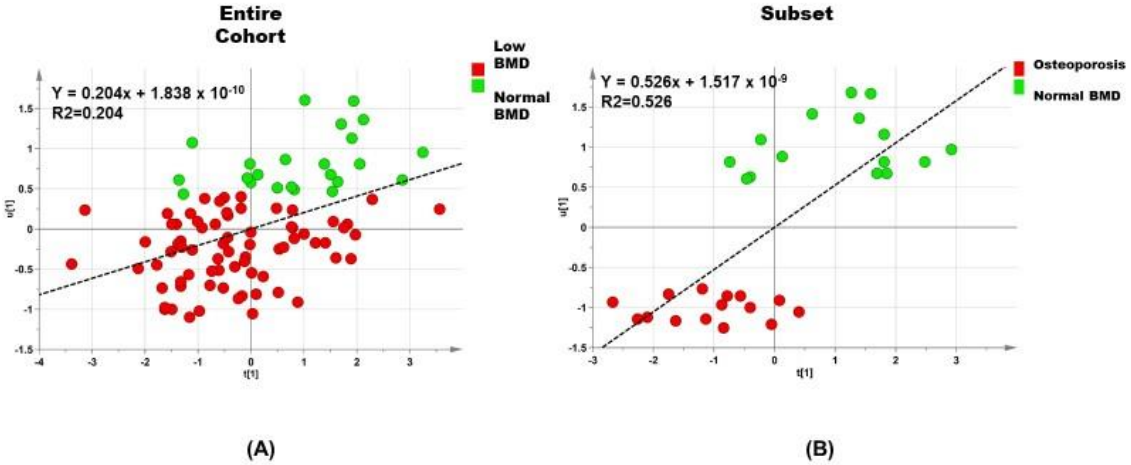

Figure 7.2: Orthogonal partial least squares (OPLS) from the metabolite profiles of SC postmenopausal women. OPLS scatter plot showing relationship between metabolites and femoral neck BMD in SC postmenopausal women with normal (green circles) and low BMD and osteoporosis (red circles) values based on orthogonally filtered partial square (OPLS) regression model 2 with 12 metabolites among 95 women, entire cohort (A) and 30 women, subset (B). t[1]/u[1] correlation plot; t1 refers to scores of the first component in independent variables; u1 refers to scores of the first component in responses.

Table 7.7: Means and 95% confidence intervals of metabolites associated to the entire cohort of SC postmenopausal women (*n* = 95) with normal and low femoral neck BMD in univariate and multivariate approaches.

Metabolite	Normal BMD[a] (*n* = 23)	Low BMD[a] (*n* = 72)	*p*-value	Log2 (FC)	Correlation[b]
4-Aminobutyric acid	1.400 (0.909–2.155)	0.874 (0.679–1.125)	0.062	−0.185	−0.013
Threonine	1.315 (0.806–2.011)	0.843 (0.658–1.081)	0.073	−0.159	−0.172
Asn–Gly–Cys	0.794 (0.512–1.230)	1.014 (0.512–1.230)	0.337	0.058	0.059
Turanose	1.319 (0.858–2.028)	0.845 (0.657–1.087)	0.076	−0.174	−0.039

Metabolites are expressed as mean and 95% confidence interval (CI). ANOVA was used to compare metabolites mean concentrations. [a] Covariates: age and BMI; [b] Age-adjusted correlation coefficient. Statistical *p*-value calculated using Benjamini–Hochberg false discovery rate (FDR). *p*-value < 0.05 was considered as statistically significant. FC expressed as the relation between the metabolite mean of the normal BMD group to the metabolite mean of the low BMD group.

7.3.2.2.2 Subset

In addition, the OPLS regression (step 1) was fitted to the subset of samples (*n* = 30) with the 127 metabolites to analyse the relationship of femoral neck BMD and metabolites, but this model did not show prediction (Q2 = −0.399) (Figure 7.2B). After filtering using coefficient selection (as described above), the OPLS model 2 showed a higher cross-validation value, Q2 = 0.247, when compared with the model from step 1 (Table 7.6, Appendix D, Table D.4, Figure D.4). The correlation matrix revealed negative correlations among metabolites and femoral neck BMD, proline (r = −0.295), aminopropionitrile (r = −0.315), threonine (r = −0.170), and Asn−Gly−Cys (r = −0.038); while positive correlation was observed with methionine (r = −0.494) (Table 7.8).

Table 7.8: Means and 95% confidence intervals of metabolites associated to a subset of selected SC postmenopausal women (n = 30) with normal BMD and osteoporosis in univariate and multivariate approaches.

Metabolite	Normal BMD[a] (*n* = 15)	Osteoporosis[a] (*n* = 15)	*p*-value	Log2 (FC)	Correlation[b]
Proline	1.581 (0.928–2.692)	0.786 (0.384–1.609)	0.084	−0.234	−0.295
Aminopropionitrile	0.729 (0.418–1.272)	1.848 (0.875–3.905)	0.03	−0.270	−0.315
Threonine	1.561 (0.911–2.674)	0.765 (0.371–1.579)	0.081	−0.219	−0.170
Methionine	1.534 (0.894–2.632)	0.758 (0.366–1.567)	0.085	0.141	0.494
Asn-Gly-Cys	1.428 (0.782–2.607)	0.593 (0.264–1.334)	0.056	0.142	−0.038

Metabolites are expressed as mean and 95% confidence interval (CI). ANOVA was used to compare metabolites mean concentrations. [a] Covariates: age and BMI; [b] Age-adjusted correlation. Statistical *p*-value calculated using Benjamini–Hochberg false discovery rate (FDR). A *p*-value < 0.05 was considered as statistically significant. FC expressed as the relation between the metabolite mean of the normal BMD group to the metabolite mean of the osteoporosis group.

7.4. Discussion

The potential of metabolomics was explored for the discovery of molecules associated with BMD loss in SC postmenopausal women. It is well established that bone loss is linked to age and low levels of oestrogen in women in both Caucasian and Asian populations. After menopause, there are several molecular changes affecting bone metabolism, where those alterations result in an increased bone resorption and a declined BMD (Manolagas and Parfitt, 2010; Nakashima et al., 2011). Thus, the identification of novel potential biomarkers may be useful for understanding the connections of the lipids and metabolites associated with osteoporosis and their capacity to predict bone loss in SC postmenopausal women.

In order to optimise the prediction of biomarkers for bone loss, a second dataset (subset) was created to analyse the relationship between the plasma metabolome of SC women with severe osteoporosis (T-score < −2.5) and normal BMD (T-score > −1). Therefore, in this study, the results from univariate and multivariate analyses were presented using two different datasets: the entire work set and a subset of samples. This statistical filtering using OPLS regression modelling facilitated the removal of uncorrelated lipid features and allowed several lipids to be detected as predictors of postmenopausal osteoporosis in women.

7.4.1 Lipids

In this study, changes of the lipid profiles, and the relationship of those lipids with femoral neck BMD, were compared in SC postmenopausal women. Glycerophospholipid species PS (20:4/29:6/31:6/32:6/33:6), PE (42:1), PA (34:4) and PI (14:0) were found to be different between normal and low femoral BMD groups.

Lipid metabolism disorders have been linked to pathological conditions including obesity, metabolic syndrome, cardiovascular diseases and bone loss, where cells and signalling pathways may be affected (Cui et al., 2005). Adipocytes and osteoblasts are derived from the mesenchymal stem cells (MSC) and the balance of osteoblast versus adipocyte requires interactions between extracellular signalling stimuli. Changes in one any of those factors enhances bone fat deposition and promote bone loss (Almeida and O'Brien, 2013). Oestrogen plays a key role in the cell fate of MSCs to differentiate into either osteoblasts or adipocytes; oestrogen also regulates inflammation (Zhao et al.; Muruganandan et al., 2009). Further, peroxisome proliferator-activated receptor (PPARy) transcription factor is essential for adipogenesis. Thus, altered lipid metabolism causes oxidative stress and increased expression of PPARy, which reduces osteoblast numbers in the skeleton, and oestrogen contributes to the regulation of this PPARy signalling pathway (Dieudonne et al., 2000; Almeida et al., 2009).

Oestrogen deficiency induces bone loss and changes in lipid profiles, BMD and cytokines; however, little information exists on the application of plasma lipidomics for studying postmenopausal osteoporosis. *In vivo* and *in vitro* studies

have reported that lipid metabolism disorders promote bone loss by inhibiting osteoblast differentiation and promoting adipogenic differentiation through MSC stimuli. Phosphatidylinositol (PI) metabolism is essential for signalling by RANK, a local regulator of osteoclastogenesis and bone resorption (Takeshita et al., 2002; Wada et al., 2006). This study showed elevated concentrations of PI species (14:0) in SC women with low BMD/osteoporosis compared with the normal-BMD group, suggesting that PI species may lead to chronic inflammatory processes and this might induce bone loss in postmenopausal osteoporosis. Circulating levels of several lipid classes also have been associated with physiological processes including the regulation of inflammation. In an *in vitro* study, lipid metabolism of PE, PS and lysoPC changed during MSC activation due to pro-inflammatory stimuli with TNF-α and IFN-γ (Campos et al., 2016). This suggests that changes in lipid profiles promote production of cytokines and differentiation of osteoclasts and may be attributed to oestrogen withdrawal.

Diacylglycerols (DGs) are cellular mediators released from membrane lipids that play a key role in the regulation of inflammation and disease (Kilpinen et al., 2013). The results in this study showed a decrease in the concentrations of glycerolipid species identified as DG (40:0/42:4) in the osteoporosis group compared to the normal BMD postmenopausal group. While it is not clear whether DG levels are associated with bone mass, there is evidence suggesting a relationship between circulating DG profiles and oestrogen loss. A previous study reported plasma DG (33:2) decreased with ageing (Jové et al., 2016). Additionally, an animal study reported that serum monoacylglycerol and triacylglycerol concentrations decreased in OVX rats as a model of oestrogen deficiency (Vinayavekhin et al., 2016), suggesting that lipid profiles and

oestrogen loss upregulate bone pro-inflammatory cytokines, which control osteoclast differentiation and promote bone loss.

However, information on the association between plasma lipids and femoral neck BMD in postmenopausal women is limited. Previous studies in postmenopausal women have reported conflicting associations between triacylglycerol and hip BMD (Makovey et al.; Cui et al., 2005; Brownbill and Ilich, 2006). The findings in this study showed a positive association between DG species and hip femoral neck BMD. This result indicates that lipid profile changes may be involved in MSCs' functional, anti-inflammatory activities and cytokine production as a result of oestrogen withdrawal, which enhances MSC signalling and inhibits osteoblast differentiation (Pacifici et al., 1991; Zheng et al., 1997; Zhou et al., 2001). However, further studies are needed to clarify the links between plasma lipid concentrations and femoral neck bone loss in postmenopausal women.

Sphingolipids also play a structural role in cellular membranes, and act as bioactive signalling molecules. Ceramide is one of the simple sphingolipids and is involved in the control of many cellular processes including proliferation, differentiation and apoptosis (Gómez-Muñoz, 2004; Arana et al., 2010). It has been shown that phosphorylated ceramide (CerP) stimulates cell survival and proliferation in bone marrow-derived macrophages through molecules such as NF-κB, RANK and its ligand RANKL (Gómez-Muñoz et al., 2004; Gangoiti et al., 2008). However, in our study, two sphingolipid species, CerP (24:0/38:1), were significantly reduced in the low BMD postmenopausal group compared with the normal-BMD group. These results contradict a previous animal study of oestrogen loss, where CerP concentrations were upregulated in OVX rats

(Vinayavekhin et al., 2016). Further, in a human study, Lee et al. (2012) found that higher sphingosine-1-phosphate (S1P) concentrations were associated with low BMD in postmenopausal women. This suggests that the increased levels of CerP promote differentiation of bone marrow-derived macrophages with biological effects on bone metabolism, and could be attributed to oestrogen deficiency.

Taken together, these findings suggest that altered lipid metabolism could be a regulator of osteoclast differentiation and bone loss in SC postmenopausal women. Further studies are required to investigate the potential role of these lipids as biomarkers for early diagnosis of bone loss in SC postmenopausal women.

7.4.2 Metabolites

This approach enabled the identification of amino acids, amines and other polar metabolites. Our study found no significant associations between polar metabolites and femoral neck BMD in SC postmenopausal groups based on OPLS analysis. However, proline, threonine and aminopropionitrile concentrations were found to be lower in SC postmenopausal women with low BMD and osteoporosis based on univariate analysis.

Amino acids play a key role in bone health and are involved in bone remodelling. During osteoporosis, alterations in amino acids may affect bone mass, suggesting that lower levels of circulating amino acids are associated with low BMD. Previous metabolomics studies in postmenopausal women have reported that tryptophan, lysine, homoserine and 3-hydroxy-L-proline

concentrations decreased in the osteoporosis group compared with pre/postmenopausal women with normal BMD using GC–MS (Qi et al., 2016). Miyamoto et al. (2017) reported that serum concentrations of a dipeptide formed with glycine and glycine (Gly–Gly) and cysteine were lower and hydroxyproline concentrations were higher in low-BMD postmenopausal women using capillary electrophoresis/mass spectrometry (CE–MS). You et al. (2014) found higher glutamine concentrations and lower lactate and acetone concentrations associated with low BMD in Taiwanese women using NMR spectroscopy.

Amino acids modulate bone marrow stem cell (BMSC) function, signalling, proliferation and differentiation. Arginine is the precursor for the synthesis of many molecules including urea, nitric oxide, proline and glutamate (Morris, 2006). Disorders in arginine metabolism are suggested to cause decalcification, disturbance in calcium absorption and osteomalcia. Growth hormone and insulin-like growth factor-I, both bone-forming growth factors, are stimulated by arginine, and a disorder in these factors causes an increase in inflammatory cytokines and osteoporosis (Chevalley et al., 1998). Proline and its metabolite hydroxyproline are the major amino acid components in collagen, and serum hydroxyproline can be used as a bone collagen degradation marker (Ma et al., 2013a; Wood et al., 2014). Homocysteine is a metabolite in methionine metabolism, and at high levels interferes with collagen crosslinking, suggesting that increased homocysteine levels can lead to increased fracture risk in ageing (van Meurs et al., 2004). Further, aminopropionitrile has been reported in *in vitro* studies as a collagen crosslinking inhibitor, and with homocysteine, caused a decreased bone strength (Turecek et al., 2008). The mechanistic implications of altered metabolites and their association with bone remodelling and the link to

BMD are not clear, but both BMSC differentiation and collagen formation are critical factors that influence BMD, suggesting that perturbations of amino acids under postmenopausal osteoporosis may partly contribute to bone loss in elderly women. Information on the association between metabolites and SC postmenopausal women is scarce and needs to be corroborated with further work. As it was not possible to test for a possible relationship between metabolites and femoral neck BMD due to the small study groups and the high variability among participants, these findings need to be kept in perspective.

The limitations of our study include the small number of participants and higher variability among them such as genetic, age, environment, diet and lifestyle factors, and body composition. This was addressed when two different datasets were analysed, the entire cohort and subset, and the subset study showed that two compounds for the polar metabolites and three for the lipids were similar to those already detected in the entire cohort. Supporting these findings is the fact that the same compounds were associated with BMD in both dataset analyses for the pathology of osteoporosis. Overall, future studies on larger populations are needed to confirm these findings and enable more reliable results for assessing the association between the metabolome and femoral neck BMD for prognosis of osteoporosis in SC postmenopausal women.

7.5. Conclusions

This pilot study suggested that plasma lipids and metabolites differed between women of normal versus low BMD, and these are involved in several metabolic pathways such as sphingolipid metabolism, phospholipid metabolism and fatty acid *β*-oxidation. Moreover, this study demonstrated that lipidomic and metabolic profiling are promising tools for finding novel biomarkers for bone loss in SC women. Further, prospective studies on larger populations are needed to corroborate these findings and elucidate their key roles in osteoporosis development and progression in SC postmenopausal women. Thus, understanding the cellular responses to molecular changes of bone metabolism, and how these are associated with bone loss in postmenopausal women, may offer the potential of discovering new biomarkers for prognosis of bone loss in elderly women.

Chapter 8

Thesis discussion

Osteoporosis is a bone disorder characterised by low mass and micro-architectural deterioration of bone tissue, which lead to bone fragility and an increase in fracture risk. Many studies have investigated the role of biomarkers of bone turnover, which are currently blood-based biomarkers, in postmenopausal osteoporosis. Further studies are needed to consolidate their use for prediction of bone loss.

From the research conducted (Chapter 2) on various animal models used in published studies for the study of postmenopausal osteoporosis, it is clear that the OVX sheep model is useful to understand the mechanisms that contribute to bone loss. However, there has been controversy about the optimal period of time for achieving bone loss in this model. More recent studies have proposed metabolomics to identify novel biomarkers for an earlier diagnosis of a particular disease, and to develop new treatments or nutritional strategies for the treatment of bone loss. Most of the metabolomics analyses of osteoporosis, which are based on serum or plasma, have been conducted in OVX rats. However, profiling of all the detectable metabolites present in blood needs to be conducted on animal models that have similar anatomy, cell biology and physiological changes to those seen in humans in order to translate the findings to clinical practice in humans (Turner, 2001).

The purpose of this thesis's research was to optimise a sheep model for postmenopausal osteoporosis, and identify novel biomarkers to improve our understanding of postmenopausal bone loss. Additionally, the research included a study cohort of SC postmenopausal women, where the aim was to describe the

association between the plasma metabolome and lipidome according to BMD status, as well as to identify novel blood biomarkers for osteoporosis.

In this sheep model, ovariectomy in combination with monthly injections of glucocorticoids successfully resulted in decreased BMD and increased bone remodelling over five months. Metabolomics analyses showed differences between the plasma metabolome and lipidome of OVX and OVX combined with glucocorticoid treatments in ewes. Additionally, the findings from the OVX sheep revealed lipids and metabolites associated with BMD and bone biomarkers, including alterations in multiple amino acids, metabolites, fatty acid *β*-oxidation and lipid metabolism, as well as altered metabolic pathways that could provide new insights into postmenopausal osteoporosis.

This PhD thesis reports the improvement and characterisation of a large animal model of postmenopausal osteoporosis, the OVX sheep. The results of this PhD thesis contribute to the published knowledge of using OVX sheep in combination with glucocorticoids to generate a faster onset of bone loss. Today, there is growing interest to test new therapies against bone loss, and the use of animal models has the advantage of allowing more-invasive methods than those used in humans to assess bone loss in order to predict what occurs in humans. In this sense, the OVX sheep model can be used to generate bone samples for compositional assessment, as well as provide serial blood samples for measurement of known bone markers to monitor responses to osteoporosis therapies for identification of new biomarkers.

This PhD thesis also reports the metabolic changes in the OVX sheep model in response to oestrogen deficiency, providing novel information about the specific alterations in lipids and metabolites associated with bone loss in

postmenopausal osteoporosis. These findings are in agreement with the results from the human study, where perturbations of methionine and ceramide 1-phosphates were also observed in SC postmenopausal women with low BMD. The results from the metabolomics analyses support the proposed application of LC–MS-based metabolomics as a diagnostic approach to identify lipids and metabolites associated with bone loss in postmenopausal women. Future studies are required to explain how the metabolites and lipids are involved in the development of postmenopausal osteoporosis.

8.1 Thesis discussion

8.1.1 Effect of OVX combined with glucocorticoids on bone remodelling and BMD

This study investigated which measurement outcomes are the most suitable to optimise and characterise a sheep model for postmenopausal osteoporosis using OVX alone or OVX combined with glucocorticoids. According to the results obtained in Chapter 3, the OVX ewes that received five months of glucocorticoid treatment showed a lower BMD as well as variation of the bone turnover markers OC and CTx-1, when compared with the OVX group. Strong negative correlations were found between lumbar spine and OC at two months, and femoral BMD and CTx-1 at five months.

The findings in Chapter 3 are similar to previous studies reported in postmenopausal women, where changes of biomarkers of bone turnover during menopause are correlated with bone loss (Garnero et al., 1996). It is established that combining OVX and glucocorticoids accelerates bone loss in a short time, by inducing bone resorption and suppressing bone formation (Mazziotti et al., 2006). Glucocorticoids promote osteoclastogenesis, and thus

after glucocorticoid exposure there is an increase in bone resorption. Inhibition of osteoblastogenesis and promotion of apoptosis of osteoblasts and osteocytes have been reported as effects of glucocorticoid exposure (Canalis, 2003; Mazziotti et al., 2006; Manolagas, 2009). Glucocorticoids also inhibit osteoblast synthesis of type 1 collagen, a major component of bone tissue. The synthesis of collagen is the scaffold for mineralisation, so suppression of collagen synthesis results in reduced bone mass and therefore increased bone loss and higher risk of fracture (Seeman and Delmas, 2006).

In this study, increased concentrations of bone biomarkers were observed during the first two months in OVX sheep but decreased thereafter, and were regulated by oestrogen deficiency and glucocorticoids. Previous studies have been conducted using an OVX sheep model for osteoporosis, but there has been controversy about the optimal period of time for inducing bone loss in OVX ewes (Chavassieux et al., 2001; Lill et al., 2002c; Sigrist et al., 2007; Ding et al., 2010). Here, the OVX combined with glucocorticoids provides a better model for postmenopausal osteoporosis due to the results showing higher bone turnover rate and reduced BMD, suggesting the generation of bone loss in a short time (five months). Validation of these findings in an additional study with a larger sample size per treatment group is required to confirm whether the OVX sheep model could provide information of prediction of bone loss, and diagnosis and test of new dietary interventions or drug treatments for postmenopausal osteoporosis.

In addition, there are variations within skeletal sites which need to be assessed to understand the details of bone loss in osteoporosis. In Chapter 4, the aims were: 1) to investigate the direct changes after OVX and glucocorticoid

treatment on left tibias of ewes; 2) to evaluate correlations between proximal and distal metaphyseal bone parameters of the left tibias; and 3) to determine the bone mechanical properties using the three-point bending test. The bone samples were taken from the ewe model described in Chapter 3. There were no differences in the longitudinal measurements of the distal tibial metaphysis in the OVX model; however, the findings showed that vBMD of the distal tibial metaphysis decreased over time. The effects of OVX plus glucocorticoids on the proximal tibial metaphysis showed decreased vBMD, bone area and BMC, trabecular vBMD, trabecular area, and trabecular BMC; periosteal and endosteal circumference and cortical thickness also decreased at five months. When metaphyseal sites were examined, bone parameters in both distal and proximal sites correlated well.

There were no differences in maximum load, stiffness and energy among the four groups determined from the three-point bending test in the mid-diaphysis of the tibia after sacrifice. However, mechanical properties of bone such as maximum load, stiffness, and energy to failure decreased over time. Combining OVX with glucocorticoids decreased trabecular and cortical strength parameters in the tibia of ewes over five months. When glucocorticoid treatment was discontinued after two months, a recovery process was noticed in the ewes that received only two doses, where bone mechanical properties increased at five months.

Bone provides mechanical and protective functions against fracture, and these functions are compromised as a result of long-term oestrogen depletion plus glucocorticoid treatment. The major predictors of bone strength are material composition and architecture, where bone mass, geometric distribution and

mechanical properties are functions of bone strength. Previous studies in ewes treated with prednisolone have shown reductions in trabecular bone volume and trabecular thickness (Lill et al., 2002c; Arens et al., 2007). Bone consists of a mineral phase formed by crystals of hydroxyapatite and an organic part, mainly formed by type 1 collagen (Seeman and Delmas, 2006). Modifications in bone mineral tissue affect both mechanical and protective functions. This might be explained because glucocorticoids affect the metabolism and function of osteocytes, where the elastic modulus surrounding osteocyte lacunae is altered, and as a result there is a reduction of mineralization in the bone matrix (Lane, 2006). Future studies are required to investigate whether the same amount of bone loss occurs in other anatomical areas of OVX sheep.

8.1.2 Application of MS-based metabolomics approach in OVX sheep as a model of osteoporosis

To gain insight into the mechanisms behind bone loss in the OVX sheep model, plasma metabolites were evaluated using HILIC–MS-based metabolomics analysis (Chapter 5) and related to bone turnover markers and BDM. The relative intensities of 5-methoxytryptophan, valine, methionine, tryptophan, glutaric acid, 2-pyrrolidone-5-carboxylic acid, indole-3-carboxaldehyde, 5-hydroxylysine and malic acid showed dynamic changes over time. In the short-term approach (two months), a negative correlation between methionine and OC was observed. Glutaric acid was negatively associated with femoral and lumbar spine BMD. In the long-term approach (five months), 5-methoxytryptophan was negatively associated with CTx-1 marker and femoral BMD. Methionine was also negatively associated with femoral BMD.

Postmenopausal osteoporosis is accompanied by oxidative stress and inflammation, which can affect the bone microenvironment, specifically the bone marrow, and alter the bone remodelling process. Previous metabolomics analyses have shown altered metabolite profiles after OVX in rats. Branched-chain amino acids (valine, leucine and isoleucine), homocysteine, hydroxyproline, ketone bodies, asparagine, glutamine, tryptophan, lysine, proline, serine and threonine circulating levels varied in OVX rats (Ma et al., 2011; Ma et al., 2013b; Assadi-Porter et al., 2015). Amino acids play a role in bone health and modulate bone marrow stem cells' functions, signalling and proliferation. Thus, altered amino acid metabolism due to oestrogen withdrawal may lead to disturbances in bone remodelling, not only suppressing bone formation cells but also increasing the production of pro-inflammatory cytokines and ROS generation in the bone marrow.

In addition, a UPLC–MS metabolomics analysis was used to measure the plasma lipid profile of the OVX sheep in two different approaches (Chapter 6). Correlations between bone clinical parameters and the lipid profile were assessed in OVX sheep. The relative intensities of 14 lipids changed over five months, including cardiolipin (CL), ceramide-1-phosphates (CerPs), phosphatidylinositol, phosphatidic acid, lysophosphatidylethanolamines, phosphatidylserines and phosphatidylglycerol. Pearson correlations analysis showed that cardiolipin was negatively associated with the lumbar spine at two months, and ceramide-1-phosphate was associated positively with lumbar spine at five months. Lipids play an important role in skeletal metabolism and bone health, and plasma lipids may be the link between oestrogen deficiency and bone loss in postmenopausal women (Rosen and Bouxsein, 2006). Previous studies

have reported lipidome changes in OVX rats (Zhu et al., 2010; Ma et al., 2013b; Zhang et al., 2014a), where the main findings suggested that perturbed phospholipid metabolism might be involved in a pro-inflammatory process, which affects bone formation and bone remodelling as a result of oestrogen depletion. Perturbations in specific metabolic pathways such as glycolysis, the TCA cycle, glutamine metabolism and fatty acid metabolism due to oestrogen deficiency have been reported as metabolic pathways that might impact on bone remodelling (Lee et al., 2017). Further studies are required to optimise the sheep as an experimental model and validate the results presented in Chapters 5 and 6 to obtain a more controlled study of bone loss in response to oestrogen deficiency and glucocorticoids.

The main limitation of this study was that the OVX sheep model was based on a small sample size, with four treatment groups. This experimental design was underpowered when determining the statistical significance for the longitudinal assessment of the distal metaphysis of the tibia. However, bone remodelling, lumbar spine and femoral BMD, and plasma lipidome and metabolome could be assessed over five months. The minimum number necessary of animals per group can be estimated from the results of Chapter 3 and Chapter 4, whether it is accepted 5% of alpha error (meaning $p < 0.05$) and 20% of beta error (meaning 80% of statistical power) (Kadam and Bhalerao, 2010). Thus, the required sample size per group (n) to see a difference is 27 animals per group for OC, 31 for CTx-1 markers and 8 animals for distal tibia. However, for biomarker discovery studies, estimating the sample size per group for high dimensional can be calculated using the average power and the significance levels using false discovery rate (Xia et al., 2015). The sample size was estimated with the results

from Chapter 5 and Chapter 6, and 200 samples per group will be needed to guide a next study design. Therefore, the number of animals per group required to achieve a reasonable statistical power and detect clearer differences among treated groups would vary depending of the variable measured. However, the findings from the OVX sheep model provided specific information in the context of clinical study for postmenopausal osteoporosis. The strengths of this study are: 1) the improvement of an OVX sheep model, where significant bone loss was generated over five months; 2) the assessment of bone metabolism and mass during and after the cessation of glucocorticoids combined with OVX in sheep; and 3) this study is the first to report plasma lipids and metabolites in OVX sheep, and their associations with bone loss.

8.1.3 Association of plasma lipids and metabolites with low BMD in SC postmenopausal women

This study aimed to analyse the plasma lipid and metabolite profiles from SC postmenopausal women using an LC–MS metabolomics analysis. Further, correlation analyses were established between plasma metabolites and femoral neck BMD in postmenopausal women. Plasma concentrations of glycerophospholipid, glycerolipid and sphingolipid species in postmenopausal women with low BMD were decreased, while plasma concentrations of glycerophospholipid species phosphatidylserine, phosphatidylinositol, phosphatidylethanolamine and phosphatidic acid were increased. Trends for lower levels of 4-aminobutyric acid, turanose, proline, aminopropionitrile, threonine, methionine and the peptide asparagine–glycine–cystine in women with low BMD were found. Osteoporosis is associated with increased marrow fat

content and lower BMD (Yeung et al., 2005). Therefore, accumulation of plasma lipids might be associated with increased marrow fat and decreased BDM. However, histomorphometric analyses would be required to evaluate whether the accumulation of bone marrow affects BDM (Verma et al., 2002; Zhou et al., 2008; Sheu and Cauley, 2011). Further, information on the association between metabolites and SC postmenopausal women remains limited and needs to be corroborated with future work.

The limitations of this study include the small number of participants and higher variability among them such as environment, diet, lifestyle and body composition. However, this was addressed when two different datasets were analysed, and both the entire cohort and subset findings were consistent, as the subset study showed similar compounds to those already detected in the entire cohort.

In addition, the metabolomics analyses were performed separately on the plasma of OVX sheep and the SC postmenopausal women. In the OVX sheep, metabolite and lipid alterations associated with bone loss included methionine, glutaric acid, tryptophan, 5-methoxytryptophan, CL and CerP (Chapters 5 and 6), and these correlated with OC, CTx-1, femoral BMD and lumbar spine BMD. In the SC women, proline, threonine, methionine, 4-aminobutyric acid, aminopropionitrile, phosphatidic acid, diacylglycerol, CerP and phosphatidylinositol correlated well with low femoral neck BMD (Chapter 7). From these findings, it was found that only methionine and CerP were the common compounds altered in both the OVX sheep and SC women studies (Table 8.1). Methionine level increased in OVX sheep vs control group at month two and month five but decreased in the SC women with osteoporosis compared with

those in the normal BMD group. The observations from the OVX sheep agreed with previous studies that have reported higher levels of homocysteine, a metabolite of methionine, altered bone turnover markers and lower BMD (Herrmann et al., 2005a; Ozdem et al., 2007; Gerdhem et al., 2009). CerP showed lower relative abundance in OVX sheep and SC women with bone loss when compared with healthy groups. Those compounds, which are known to be involved in bone remodelling, could be considered to be of clinical relevance in postmenopausal bone loss. Further work is needed to validate these metabolomics findings, and clarify the functional mechanisms of methionine, CerP in relation to bone mineral density in postmenopausal osteoporosis.

The small sample size of the studies described in this thesis might have limited the statistical power and the results should be interpreted with caution. Despite the limited sample size, the present metabolomics analysis indicates that the OVX sheep is an ideal model for prediction of human bone loss, demonstrating alterations in both species in the plasma lipid and metabolite profiles, as well as the association between those compounds and bone mineral density.

Table 8.1: List of the altered metabolites in OVX sheep and in SC women with low BMD.

Metabolite	Altered in OVX sheep	Altered in SC women with low BMD	Potential biomarker
Methionine	↑	↓	√
Glutaric acid	↓		
Tryptophan	↓		
5-Methoxytryptophan	↓		
Proline		↓	
Threonine		↓	
4-Aminobutyric acid		↓	
Asn–Gly–Cys		↓	
Aminopropionitrile		↑	
Phosphatidic acid		↑	
Ceramide-1-phosphate	↓	↓	√
Phosphatidylserine		↓	
Diacylglycerol		↓	
Phosphatidylinositol		↑	
Cardiolipin	↓		

↑ indicates an up-regulated increase in metabolite level, whereas ↓ indicates a down-regulated in metabolite level.√ indicates potential biomarker.

8.2 Thesis conclusions

Validation of the OVX sheep model was achieved and showed to be suitable as a model for postmenopausal osteoporosis by combining OVX and glucocorticoids over five months. These treatments resulted in a reduction of bone formation and increased bone resorption. These results suggest that, after considering the differences of sample sizes in the experimental groups, glucocorticoid treatment affected the bone remodelling process more than oestrogen deficiency over five months.

This research applied LC–MS-based metabolomics to investigate the differences in lipids between OVX alone and OVX with glucocorticoid treatments in sheep. OVX alone and OVX with glucocorticoid treatments altered plasma lipid

profiles in sheep over five months, which could indicate oxidative stress and inflammation in the bone marrow.

Variation in the relative intensities of CL, PI, PA and PS species after OVX may relate to dysfunctional glycerophospholipid and phosphatidylinositol pathways, and may increase marrow fat accumulation as well as bone loss in postmenopausal osteoporosis. Understanding the roles of the CL, PI, PA and PS species in bone remodelling, as well as their potential connection to bone loss, is needed to provide evidence to not just predict bone loss but also to design novel drugs for the treatment of osteoporosis.

This OVX sheep model provides opportunities to enhance our understanding of bone diseases, to test new drugs, and to develop dietary interventions for the prevention of bone loss in postmenopausal women.

In the human study, the findings suggest that plasma lipids and amino acids differed between women of normal versus low BMD. There was a decrease in plasma relative intensities of eight glycerophospholipid, glycerolipid and sphingolipid species in postmenopausal women with low BMD, but increased plasma relative intensities of four glycerophospholipid species (phosphatidylserine, phosphatidylinositol, phosphatidylethanolamine and phosphatidic acid). Further, this study found no significant differences in plasma amino acid metabolites.

The findings from the lipid profiles identified lipids that are involved in sphingolipid metabolism, phospholipid metabolism and fatty acid *β*-oxidation. Lipid metabolism and fatty acid metabolism pathways, especially those with a key role in energy metabolism, were found to be associated with bone loss in SC women. This group of potential biomarkers are correlated with clinical bone

parameters and could be used for early detection, clinical diagnosis and monitoring of postmenopausal osteoporosis induced by oestrogen deficiency. As with the currently known bone markers, some of the metabolic changes revealed in this research may be predictive of future fracture, but to prove this relationship, longer-term studies are required.

Further validations of methionine and CerP over a larger population may aid in the development of a rapid and reliable method for the early diagnosis of bone loss, and the monitoring and improvement of treatments in postmenopausal women.

8.3 Future directions

During the progression of this study, several areas of future research were identified. The results of this study contribute to the identification of predictive biomarkers of bone metabolic diseases such as osteoporosis. However, for the experimental design of ewe models for postmenopausal osteoporosis, three treatment groups would be best suited: group 1, OVX and low calcium and vitamin D diet; group 2, OVX combined with glucocorticoids and low calcium and vitamin D diet; and group 3, control group normal calcium and vitamin D diet. This would help to evaluate that the effects of different interventions are not only based on hormonal interventions, but also allow assessment of different diets and how these would affect the metabolome and lipidome in the OVX sheep model. Alternatively, using OVX with or without glucocorticoids on grass-fed animals in an outdoor flock might alleviate the time-induced bone loss observed in the current study and attributed to the indoor housing and resultant reduction in physical activity. Further studies, including molecular and histomorphometry

evaluations, are needed to further characterise the OVX sheep model. Additionally, assessments of clinical parameters, such as oestrogen, glucose, inflammatory cytokines, cholesterol and triglycerides, ideally would aid the identification of the intrinsic mechanisms that regulate the expression of osteoblast and osteoclast phenotypes during post-menopause.

Furthermore, the current study design allowed for repeated blood sampling (monthly) of ewes, to evaluate the assumptions that oestrogen regulates bone remodelling and to understand disease progression over time. For this, the plasma lipid and metabolite profiles of treated and nontreated ewes were compared at baseline and once-monthly after initiated treatments over five months. However, changes in bone metabolism status occur quickly. To ensure that those changes can be monitored, the ideal approach should be to collect blood samples every two weeks where possible to investigate the onset of the disease, as bone loss and increased fracture risk occur before symptoms are apparent. Such an approach necessitates the use of the sheep (or other large animal) model, as frequent collection of large volumes of blood from rodents cannot be done.

Validation of the identified metabolites and lipids will allow more reliable assessment of bone loss in postmenopausal women. This validation can be done by analytical validation, where external standards can be used to corroborate whether the identified feature co-elutes at the correct retention time from the chromatographic column and that the fragment ions of the potential biomarker match those of the actual compound. This also offers an opportunity to subsequently quantify their concentrations by utilising the responses of the compound and the internal standards added to the samples. Further validation of

the metabolites and lipid alterations should be analysed on larger and independent populations to reduce the effect of higher variability among them.

In this study, measurements of bone biomarkers and bone mass were the parameters used to evaluate the association of the plasma metabolome and lipidome with bone loss. Metabolites present in blood may reflect the changes in other tissues, but the analysis of other biological matrixes such as bone tissues in LC-MS based metabolomics and lipidomics studies would allow direct measurement of the molecular changes of the bone microenvironment in postmenopausal osteoporosis.

Follow-up studies are also recommended to analyse changes in the metabolite and lipid profiles relative to BMD of pre and postmenopausal women and could be useful to predict early bone loss. In addition, follow-up studies to predict bone mass changes as well as to investigate the effects of genetics, age, environment, diet, lifestyle and body composition on osteoporosis development are needed.

In this context, dietary intake has been proven to affect bone loss in post-menopause, and therefore, studies using dietary interventions could detect bone health markers as a response to nutritional intake. The validation of the novel biomarkers in a human nutritional intervention study, in which the metabolites could improve bone metabolic health, would be valuable to understand the effect of nutritional interventions on the bone mass of postmenopausal women.

References

Aaseth, J., Boivin, G., and Andersen, O. (2012) Osteoporosis and trace elements – An overview. *J. Trace. Elem. Med. Bio.* **26**: 149-152.

Adami, S., Braga, V., Zamboni, M., Gatti, D., Rossini, M., Bakri, J., and Battaglia, E. (2004) Relationship between lipids and bone mass in 2 cohorts of healthy women and men. *Calcif. Tissue Int.* **74**: 136-142.

Adams, S.B., Setton, L.A., and Nettles, D.L. (2013) The role of metabolomics in osteoarthritis research. *J. Am. Acad. Orthop. Surg.* **21**: 63-64.

Allen, M.J. (2003) Biochemical markers of bone metabolism in animals: uses and limitations. *Vet. Clin. Path.* **32**: 101-113.

Allwood, J.W., and Goodacre, R. (2010) An introduction to liquid chromatography–mass spectrometry instrumentation applied in plant metabolomic analyses. *Phytochem. Anal.* **21**: 33-47.

Almeida, M., and O'Brien, C.A. (2013) Basic biology of skeletal aging: role of stress response pathways. *J. Gerontol. A.* **68**: 1197-1208.

Almeida, M., Ambrogini, E., Han, L., Manolagas, S.C., and Jilka, R.L. (2009) Increased lipid oxidation causes oxidative stress, increased peroxisome proliferator-activated receptor-γ expression, and diminished pro-osteogenic Wnt signaling in the skeleton. *J. Biol. Chem.* **284**: 27438-27448.

Álvarez-Sánchez, B., Priego-Capote, F., and Luque de Castro, M.D. (2010a) Metabolomics analysis I. Selection of biological samples and practical aspects preceding sample preparation. *Trac-Trend. Anal. Chem.* **29**: 111-119.

Álvarez-Sánchez, B., Priego-Capote, F., and Castro, M.D.L.d. (2010b) Metabolomics analysis II. Preparation of biological samples prior to detection. *Trac-Trend. Anal. Chem.* **29**: 120-127.

Amstrup, A.K., Jakobsen, N.F.B., Moser, E., Sikjaer, T., Mosekilde, L., and Rejnmark, L. (2016) Association between bone indices assessed by DXA, HR-pQCT and QCT scans in post-menopausal women. *J. Bone Miner. Metab.* **34**: 638-645.

Andreasen, C.M., Ding, M., Overgaard, S., Bollen, P., and Andersen, T.L. (2015) A reversal phase arrest uncoupling the bone formation and resorption contributes to the bone loss in glucocorticoid treated ovariectomised aged sheep. *Bone* **75**: 32-39.

Anton, G., Wilson, R., Yu, Z.-h., Prehn, C., Zukunft, S., Adamski, J., Heier, M., Meisinger, C., Römisch-Margl, W., and Wang-Sattler, R. (2015) Pre-analytical sample quality: metabolite ratios as an intrinsic marker for prolonged room temperature exposure of serum samples. *PLoS One* **10**: e0121495.

Arana, L., Gangoiti, P., Ouro, A., Trueba, M., and Gómez-Muñoz, A. (2010) Ceramide and ceramide 1-phosphate in health and disease. *Lipids. Health. Dis.* **9**: 15.

Arens, D., Sigrist, I., Alini, M., Schawalder, P., Schneider, E., and Egermann, M. (2007) Seasonal changes in bone metabolism in sheep. *Vet. J.* **174**: 585-591.

Assadi-Porter, F., Selen, E., and Shen, C. (2015) NMR-based metabolomics analysis in muscle and serum of middle-aged ovariectomized rats supplemented with 6-month green tea polyphenols. *FASEB. J.* **29**: 745.742.

Assfalg, M., Bertini, I., Colangiuli, D., Luchinat, C., Schäfer, H., Schütz, B., and Spraul, M. (2008) Evidence of different metabolic phenotypes in humans. *Proc. Natl. Acad. Sci.* **105**: 1420.

Augat, P., Schorlemmer, S., Gohl, C., Iwabu, S., Ignatius, A., and Claes, L. (2003) Glucocorticoid-treated sheep as a model for osteopenic trabecular bone in biomaterials research. *J. Biomed. Mater. Res. A.* **66A**: 457-462.

Auro, K., Joensuu, A., Fischer, K., Kettunen, J., Salo, P., Mattsson, H., Niironen, M., Kaprio, J., Eriksson, J.G., Lehtimäki, T., Raitakari, O., Jula, A., Tiitinen, A., Jauhiainen, M., Soininen, P., Kangas, A.J., Kähönen, M., Havulinna, A.S., Ala-Korpela, M., Salomaa, V., Metspalu, A., and Perola, M. (2014) A metabolic view on menopause and ageing. *Nat. Commun.* **5**: 4708.

Bai, X.-c., Lu, D., Bai, J., Zheng, H., Ke, Z.-y., Li, X.-m., and Luo, S.-q. (2004) Oxidative stress inhibits osteoblastic differentiation of bone cells by ERK and NF-κB. *Biochem. Biophys. Res. Commun.* **314**: 197-207.

Bailey, A.J., Wotton, S.F., Sims, T.J., and Thompson, P.W. (1993) Biochemical changes in the collagen of human osteoporotic bone matrix. *Connect. Tissue Res.* **29**: 119-132.

Bain, G., Müller, T., Wang, X., and Papkoff, J. (2003) Activated β-catenin induces osteoblast differentiation of C3H10T1/2 cells and participates in BMP2 mediated signal transduction. *Biochem. Biophys. Res. Commun.* **301**: 84-91.

Bar-Shavit, Z. (2007) The osteoclast: A multinucleated, hematopoietic-origin, bone-resorbing osteoimmune cell. *J. Cell. Biochem.* **102**: 1130-1139.

Barrère, F., van Blitterswijk, C.A., and de Groot, K. (2006) Bone regeneration: Molecular and cellular interactions with calcium phosphate ceramics. *Int. J. Nanomed.* **1**: 317-332.

Beck, T.J., Oreskovic, T.L., Stone, K.L., Ruff, C.B., Ensrud, K., Nevitt, M.C., Genant, H.K., and Cummings, S.R. (2001) Structural adaptation to changing skeletal load in the progression toward hip fragility: the study of osteoporotic fractures. *J. Bone Miner. Res.* **16**: 1108-1119.

Beger, R.D., Dunn, W., Schmidt, M.A., Gross, S.S., Kirwan, J.A., Cascante, M., Brennan, L., Wishart, D.S., Oresic, M., Hankemeier, T., Broadhurst, D.I., Lane, A.N., Suhre, K., Kastenmüller, G., Sumner, S.J., Thiele, I., Fiehn, O., and Kaddurah-Daouk, R. (2016) Metabolomics enables precision medicine: "A white paper, community perspective". *Metabolomics* **12**: 149.

Begley, P., Francis-McIntyre, S., Dunn, W.B., Broadhurst, D.I., Halsall, A., Tseng, A., Knowles, J., Goodacre, R., and Kell, D.B. (2009) Development and performance of a gas chromatography−time-of-flight mass spectrometry analysis for large-scale nontargeted metabolomic studies of human serum. *Anal. Chem.* **81**: 7038-7046.

Bellanti, F., Matteo, M., Rollo, T., De Rosario, F., Greco, P., Vendemiale, G., and Serviddio, G. (2013) Sex hormones modulate circulating antioxidant enzymes: Impact of estrogen therapy. *Redox. Biol.* **1**: 340-346.

Bellido, T., Saini, V., and Pajevic, P.D. (2013) Effects of PTH on osteocyte function. *Bone* **54**: 250-257.

Beresford, J.N., Gallagher, J.A., Poser, J.W., and Russell, R.G.G. (1984) Production of osteocalcin by human bone cells in vitro. Effects of 1,25(OH)2D3, 24,25(OH)2D3, parathyroid hormone, and glucocorticoids. *Metab. Bone. Dis. Relat.* **5**: 229-234.

Blake, G.M., and Fogelman, I. (2001) Bone densitometry and the diagnosis of osteoporosis. In *Semin. Nucl. Med.*: Elsevier, pp. 69-81.

Bonewald, L.F. (2007) Osteocytes as dynamic multifunctional cells. *Ann. N. Y. Acad. Sci.* **1116**: 281-290.

Bonewald, L.F., and Johnson, M.L. (2008) Osteocytes, mechanosensing and Wnt signaling. *Bone* **42**: 606-615.

Bonjour, j.-p., Kohrt, W., Levasseur, R., Warren, M., Whiting, S., and Kraenzlin, M. (2014) *Biochemical markers for assessment of calcium economy and bone metabolism: Application in clinical trials from pharmaceutical agents to nutritional products*. Nutrition Research Reviews.

Bonjour, J.P., Ammann, P., and Rizzoli, R. (1999) Importance of preclinical studies in the development of drugs for treatment of osteoporosis: a review related to the 1998 WHO Guidelines. *Osteoporosis Int.* **9**: 379-393.

Bonnick, S.L., and Shulman, L. (2006) Monitoring osteoporosis therapy: bone mineral density, bone turnover markers, or both? *Am. J. Med.* **119**: S25-S31.

Boskey, A.L. (2013) Bone composition: relationship to bone fragility and antiosteoporotic drug effects. *BoneKey Rep.* **2**.

Bouillon, R., Van Cromphaut, S., and Carmeliet, G. (2003) Intestinal calcium absorption: molecular vitamin D mediated mechanisms. *J. Cell. Biochem.* **88**: 332-339.

Boumah, C.E., Lee, M., Selvamurugan, N., Shimizu, E., and Partridge, N.C. (2009) Runx2 recruits p300 to mediate parathyroid hormone's effects on histone acetylation and transcriptional activation of the matrix metalloproteinase-13 gene. *Mol. Endocrinol.* **23**: 1255-1263.

Boyce, B.F., and Xing, L. (2006) Osteoclasts, no longer osteoblast slaves. *Nat. Med.* **12**: 1356-1358.

Bozzini, C., Picasso, E.O., Champin, G.M., Alippi, R.M., and Bozzini, C.E. (2012) Biomechanical properties of the mid-shaft femur in middle-aged hypophysectomized rats as assessed by bending test. *Endocrine* **42**: 411-418.

Brandi, M.L. (2009) Microarchitecture, the key to bone quality. *Rheumatology* **48**: iv3-iv8.

Briot, K., and Roux, C. (2015) Glucocorticoid-induced osteoporosis. *RMD Open* **1**: e000014.

Broadhurst, D., Goodacre, R., Reinke, S.N., Kuligowski, J., Wilson, I.D., Lewis, M.R., and Dunn, W.B. (2018) Guidelines and considerations for the use of system suitability and quality control samples in mass spectrometry assays applied in untargeted clinical metabolomic studies. *Metabolomics* **14**: 72.

Brodsky, B., and Persikov, A.V. (2005) Molecular Structure of the Collagen Triple Helix. In *Advances in Protein Chemistry*: Academic Press, pp. 301-339.

Brosnan, J.T., and Brosnan, M.E. (2006) The sulfur-containing amino acids: an overview. *J. Nutr.* **136**: 1636S-1640S.

Brownbill, R.A., and Ilich, J.Z. (2006) Lipid profile and bone paradox: higher serum lipids are associated with higher bone mineral density in postmenopausal women. *J. Womens Health* **15**: 261-270.

Bruce, S.J., Tavazzi, I., Parisod, V., Rezzi, S., Kochhar, S., and Guy, P.A. (2009) Investigation of human blood plasma sample preparation for performing metabolomics using ultrahigh performance Liquid Chromatography/Mass Spectrometry. *Anal. Chem.* **81**: 3285-3296.

Buizert Petra, J., van Schoor Natasja, M., Lips, P., Deeg Dorly, J.H., and Eekhoff Elisabeth, M. (2009) Lipid levels: a link between cardiovascular disease and osteoporosis? *J. Bone Miner. Res.* **24**: 1103-1109.

Büscher, J.M., Czernik, D., Ewald, J.C., Sauer, U., and Zamboni, N. (2009) Cross-Platform Comparison of Methods for Quantitative Metabolomics of Primary Metabolism. *Anal. Chem.* **81**: 2135-2143.

Calvi, L., Sims, N., Hunzelman, J., Knight, M., Giovannetti, A., Saxton, J., Kronenberg, H., Baron, R., and Schipani, E. (2001) Activated parathyroid hormone/parathyroid hormone–related protein receptor in osteoblastic cells differentially affects cortical and trabecular bone. *J. Clin. Invest.* **107**: 277-286.

Campos, A.M., Maciel, E., Moreira, A.S.P., Sousa, B., Melo, T., Domingues, P., Curado, L., Antunes, B., Domingues, M.R.M., and Santos, F. (2016) Lipidomics of mesenchymal stromal cells: understanding the adaptation of phospholipid profile in response to pro-inflammatory cytokines. *J. Cell. Physiol.* **231**: 1024-1032.

Canalis, E. (2003) Mechanisms of glucocorticoid-induced osteoporosis. *Curr. Opin. Rheumatol.* **15**: 454-457.

Canalis, E., Mazziotti, G., Giustina, A., and Bilezikian, J. (2007) Glucocorticoid-induced osteoporosis: pathophysiology and therapy. *Osteoporosis Int.* **18**: 1319-1328.

Capulli, M., Paone, R., and Rucci, N. (2014) Osteoblast and osteocyte: Games without frontiers. *Arch. Biochem. Biophys.* **561**: 3-12.

Carbonare, L.D., Arlot, M.E., Chavassieux, P.M., Roux, J.P., Portero, N.R., and Meunier, P.J. (2001) Comparison of Trabecular Bone Microarchitecture and Remodeling in Glucocorticoid-Induced and Postmenopausal Osteoporosis. *J. Bone Miner. Res.* **16**: 97-103.

Cashman, K.D. (2007) Diet, nutrition, and bone health. *J. Nutr.* **137**: 2507S-2512S.

Chan, D.C. (2006) Mitochondria: dynamic organelles in disease, aging, and development. *Cell* **125**: 1241-1252.

Charatcharoenwitthaya, N., Khosla, S., Atkinson, E.J., McCready, L.K., and Riggs, B.L. (2007) Effect of blockade of TNF-α and interleukin-1 action on bone resorption in early postmenopausal women. *J. Bone Miner. Res.* **22**: 724-729.

Chavassieux, P., Pastoureau, P., Chapuy, M., Delmas, P., and Meunier, P. (1993) Glucocorticoid-induced inhibition of osteoblastic bone formation in ewes: a biochemical and histomorphometric study. *Osteoporosis Int.* **3**: 97-102.

Chavassieux, P., Buffet, A., Vergnaud, P., Garnero, P., and Meunier, P.J. (1997a) Short-term effects of corticosteroids on trabecular bone remodeling in old ewes. *Bone* **20**: 451-455.

Chavassieux, P., Buffet, A., Vergnaud, P., Garnero, P., and Meunier, P. (1997b) Short-term effects of corticosteroids on trabecular bone remodeling in old ewes. *Bone* **20**: 451-455.

Chavassieux, P., Garnero, P., Duboeuf, F., Vergnaud, P., Brunner-Ferber, F., Delmas, P.D., and Meunier, P.J. (2001) Effects of a new selective estrogen receptor modulator (MDL 103,323) on cancellous and cortical bone in ovariectomized ewes: a biochemical, histomorphometric, and densitometric study. *J. Bone Miner. Res.* **16**: 89-96.

Chen, J.-Q., Brown, T.R., and Russo, J. (2009) Regulation of energy metabolism pathways by estrogens and estrogenic chemicals and potential implications in obesity associated with increased exposure to endocrine disruptors. *BBA-Mol. Cell. Res.* **1793**: 1128-1143.

Chen, P., Satterwhite, J.H., Licata, A.A., Lewiecki, E.M., Sipos, A.A., Misurski, D.M., and Wagman, R.B. (2005) Early changes in biochemical markers of bone formation predict BMD response to teriparatide in postmenopausal women with osteoporosis. *J. Bone Miner. Res.* **20**: 962-970.

Chen, S.-Y., Yu, H.-T., Kao, J.-P., Yang, C.-C., Chiang, S.-S., Mishchuk, D.O., Mau, J.-L., and Slupsky, C.M. (2014) An NMR metabolomic study on the effect of alendronate in ovariectomized mice. *PloS one* **9**: e106559.

Chen, S.-Y., Yu, H.-T., Kao, J.-P., Yang, C.-C., Chiang, S.-S., Mishchuk, D.O., Mau, J.-L., and Slupsky, C.M. (2015) Consumption of vitamin D2 enhanced mushrooms is associated with improved bone health. *J. Nutr. Biochem.* **26**: 696-703.

Chen, S., Hoene, M., Li, J., Li, Y., Zhao, X., Häring, H.-U., Schleicher, E.D., Weigert, C., Xu, G., and Lehmann, R. (2013) Simultaneous extraction of metabolome and lipidome with methyl tert-butyl ether from a single small tissue sample for ultra-high performance liquid chromatography/mass spectrometry. *J. Chromatogr.* **1298**: 9-16.

Chen, Y., Wang, W., Yang, L., Chen, W., and Zhang, H. (2018) Association between lipid profiles and osteoporosis in postmenopausal women: a meta-analysis. *Eur. Rev. Med. Pharmacol. Sci.* **22**: 1-9.

Chevalley, T., Rizzoli, R., Manen, D., Caverzasio, J., and Bonjour, J.P. (1998) Arginine increases insulin-like growth factor-I production and collagen synthesis in osteoblast-like cells. *Bone* **23**: 103-109.

Chong, J., Soufan, O., Li, C., Caraus, I., Li, S., Bourque, G., Wishart, D.S., and Xia, J. (2018) MetaboAnalyst 4.0: towards more transparent and integrative metabolomics analysis. *Nucleic Acids Res.*: W486-W494.

Christenson, R.H. (1997) Biochemical markers of bone metabolism: an overview. *Clin. Biochem.* **30**: 573-593.

Clarke, B. (2008) Normal bone anatomy and physiology. *Clin. J. Am. Soc. Nephrol.* **3**: S131-S139.

Coetzee, M., Haag, M., Joubert, A.M., and Kruger, M.C. (2007) Effects of arachidonic acid, docosahexaenoic acid and prostaglandin E2 on cell proliferation and morphology of MG-63 and MC3T3-E1 osteoblast-like cells. *Prostag. Leukotr. Ess.* **76**: 35-45.

Cohen Jr, M.M. (2006) The new bone biology: Pathologic, molecular, and clinical correlates. *Am. J. Med. Genet. A* **140A**: 2646-2706.

Compston, J. (2010) Management of glucocorticoid-induced osteoporosis. *Nat. Rev. Rheumatol.* **6**: 82-88.

Cooper, C., Cole, Z.A., Holroyd, C.R., Earl, S.C., Harvey, N.C., Dennison, E.M., Melton, L.J., Cummings, S.R., and Kanis, J.A. (2011) Secular trends in the incidence of hip and other osteoporotic fractures. *Osteoporosis Int.* **22**: 1277.

Cooper, M.S., Seibel, M.J., and Zhou, H. (2016) Glucocorticoids, bone and energy metabolism. *Bone* **82**: 64-68.

Cosman, F., de Beur, S.J., LeBoff, M.S., Lewiecki, E.M., Tanner, B., Randall, S., and Lindsay, R. (2014) Clinician's guide to prevention and treatment of osteoporosis. *Osteoporosis Int.* **25**: 2359-2381.

Crews, B., Wikoff, W.R., Patti, G.J., Woo, H.-K., Kalisiak, E., Heideker, J., and Siuzdak, G. (2009) Variability analysis of human plasma and cerebral spinal fluid reveals statistical significance of changes in mass spectrometry-based metabolomics data. *Anal. Chem.* **81**: 8538-8544.

Crockett, J.C., Mellis, D.J., Scott, D.I., and Helfrich, M.H. (2011) New knowledge on critical osteoclast formation and activation pathways from study of rare genetic

diseases of osteoclasts: focus on the RANK/RANKL axis. *Osteoporosis Int.* **22**: 1-20.

Cubbon, S., Antonio, C., Wilson, J., and Thomas-Oates, J. (2010) Metabolomic applications of hilic–lc–ms. *Mass. Spectrom. Rev.* **29**: 671-684.

Cui, L.H., Shin, M.H., Chung, E.K., Lee, Y.H., Kweon, S.S., Park, K.S., and Choi, J.S. (2005) Association between bone mineral densities and serum lipid profiles of pre- and post-menopausal rural women in South Korea. *Osteoporosis Int.* **16**: 1975-1981.

Currey, J.D. (2003) Role of collagen and other organics in the mechanical properties of bone. *Osteoporosis Int.* **14**: S29-S36.

Damilakis, J., Maris, T.G., and Karantanas, A.H. (2007) An update on the assessment of osteoporosis using radiologic techniques. *Eur. Radiol.* **17**: 1591-1602.

Delany, A.M., Durant, D., and Canalis, E. (2001) Glucocorticoid suppression of IGF I transcription in osteoblasts. *Mol. Endocrinol.* **15**: 1781-1789.

Delmas, P.D., Eastell, R., Garnero, P., Seibel, M., and Stepan, J. (2000) The use of biochemical markers of bone turnover in osteoporosis. *Osteoporosis Int.* **11**: S2-S17.

den Boer, F.C., Patka, P., Bakker, F.C., Wippermann, B.W., van Lingen, A., Vink, G.Q.M., Boshuizen, K., and Haarman, H.J.T.M. (1999) New segmental long bone defect model in sheep: quantitative analysis of healing with dual energy x-ray absorptiometry. *J. Orth. Res.* **17**: 654-660.

Dias, I.R., Viegas, C.A., Azevedo, J.T., Costa, E., Lourenço, P., Rodrigues, A., and Cabrita, A. (2008) Assessment of bone formation markers under controlled environmental conditions and their correlations with serum minerals in the adult sheep as a model for orthopaedic research. *Lab. Anim.* **42**: 465-472.

Dias, I.R., Camassa, J.A., Bordelo, J.A., Babo, P.S., Viegas, C.A., Dourado, N., Reis, R.L., and Gomes, M.E. (2018) Preclinical and translational studies in small ruminants (sheep and goat) as models for osteoporosis research. *Curr. Osteoporos. Rep.* **16**: 182-197.

Dieudonne, M.N., Pecquery, R., Leneveu, M.C., and Giudicelli, Y. (2000) Opposite effects of androgens and estrogens on adipogenesis in rat preadipocytes: evidence for sex and site-related specificities and possible involvement of insulin-like growth factor 1 receptor and peroxisome proliferator activated receptor gamma2. *Endocrinology* **141**: 649-656.

Ding, M., Danielsen, C.C., and Overgaard, S. (2012) The effects of glucocorticoid on microarchitecture, collagen, mineral and mechanical properties of sheep femur cortical bone. *J. Tissue. Eng. Regen. Med.* **6**: 443-450.

Ding, M., Cheng, L., Bollen, P., Schwarz, P., and Overgaard, S. (2010) Glucocorticoid induced osteopenia in cancellous bone of sheep: validation of large animal model for spine fusion and biomaterial research. *Spine* **35**: 363-370.

Dixon, R.A., Gang, D.R., Charlton, A.J., Fiehn, O., Kuiper, H.A., Reynolds, T.L., Tjeerdema, R.S., Jeffery, E.H., German, J.B., and Ridley, W.P. (2006) Applications of metabolomics in agriculture. *J. Agric. Food Chem.* **54**: 8984-8994.

Drake, M.T., Clarke, B.L., and Lewiecki, E.M. (2015) The pathophysiology and treatment of osteoporosis. *Clin.Ther.* **37**: 1837-1850.

Dunn, W.B., Wilson, I.D., Nicholls, A.W., and Broadhurst, D. (2012) The importance of experimental design and QC samples in large-scale and MS-driven untargeted metabolomic studies of humans. *Bioanalysis* **4**: 2249-2264.

Dunn, W.B., Broadhurst, D.I., Atherton, H.J., Goodacre, R., and Griffin, J.L. (2011a) Systems level studies of mammalian metabolomes: the roles of mass spectrometry and nuclear magnetic resonance spectroscopy. *Chem. Soc. Rev.* **40**: 387-426.

Dunn, W.B., Broadhurst, D., Begley, P., Zelena, E., Francis-McIntyre, S., Anderson, N., Brown, M., Knowles, J.D., Halsall, A., Haselden, J.N., Nicholls, A.W., Wilson, I.D., Kell, D.B., Goodacre, R., and The Human Serum Metabolome, C. (2011b) Procedures for large-scale metabolic profiling of serum and plasma using gas chromatography and liquid chromatography coupled to mass spectrometry. *Nature Protocols* **6**: 1060.

During, A., Penel, G., and Hardouin, P. (2015) Understanding the local actions of lipids in bone physiology. *Prog. Lipid. Res.* **59**: 126-146.

Eastell, R., and Hannon, R.A. (2008) Biomarkers of bone health and osteoporosis risk. *Proc. Nutr. Soc.* **67**: 157-162.

Eastell, R., Robins, S.P., Colwell, T., Assiri, A.M.A., Riggs, B.L., and Russell, R.G.G. (1993) Evaluation of bone turnover in type I osteoporosis using biochemical markers specific for both bone formation and bone resorption. *Osteoporosis Int.* **3**: 255-260.

Egermann, M., Goldhahn, J., and Schneider, E. (2005) Animal models for fracture treatment in osteoporosis. *Osteoporosis Int.* **16**: S129-S138.

Egermann, M., Goldhahn, J., Holz, R., Schneider, E., and Lill, C. (2008) A sheep model for fracture treatment in osteoporosis: benefits of the model versus animal welfare. *Lab. Anim.* **42**: 453-464.

Egermann, M., Gerhardt, C., Barth, A., Maestroni, G.J., Schneider, E., and Alini, M. (2011) Pinealectomy affects bone mineral density and structure-an experimental study in sheep. *BMC Musculoskel. Disord.* **12**: 271.

El Refaey, M., Watkins, C.P., Kennedy, E.J., Chang, A., Zhong, Q., Ding, K.-H., Shi, X.-m., Xu, J., Bollag, W.B., and Hill, W.D. (2015) Oxidation of the aromatic amino acids tryptophan and tyrosine disrupts their anabolic effects on bone marrow mesenchymal stem cells. *Mol. Cell. Endocrinol.* **410**: 87-96.

Elbaz, A., Rivas, D., and Duque, G. (2009) Effect of estrogens on bone marrow adipogenesis and Sirt1 in aging C57BL/6J mice. *Biogerontology* **10**: 747.

Engelke, K., Adams, J.E., Armbrecht, G., Augat, P., Bogado, C.E., Bouxsein, M.L., Felsenberg, D., Ito, M., Prevrhal, S., Hans, D.B., and Lewiecki, E.M. (2008) Clinical use of quantitative computed tomography and peripheral quantitative computed tomography in the management of osteoporosis in adults: The 2007 ISCD official positions. *J. Clin. Densitometry* **11**: 123-162.

Eschler, A., Röpenack, P., Herlyn, P.K., Roesner, J., Pille, K., Büsing, K., Vollmar, B., Mittlmeier, T., and Gradl, G. (2015) The standardized creation of a lumbar spine vertebral compression fracture in a sheep osteoporosis model induced by ovariectomy, corticosteroid therapy and calcium/phosphorus/vitamin D-deficient diet. *Injury* **46**: S17-S23.

Feng, X., and McDonald, J.M. (2011) Disorders of Bone Remodeling. *Annual review of pathology* **6**: 121-145.

Firth, E.C. (2006) The response of bone, articular cartilage and tendon to exercise in the horse. *J. Anat.* **208**: 513-526.

Fitzpatrick, L.A. (2002) Secondary causes of osteoporosis. *Mayo Clin. Proc.* **77**: 453-468.

Flynn, A. (2003) The role of dietary calcium in bone health. *Proc. Nutr. Soc.* **62**: 851-858.

Fratzl, P., Gupta, H.S., Paschalis, E.P., and Roschger, P. (2004) Structure and mechanical quality of the collagen-mineral nano-composite in bone. *J. Mater. Chem.* **14**: 2115-2123.

Frega, N.G., Pacetti, D., and Boselli, E. (2012) Characterization of phospholipid molecular species by means of HPLC-tandem mass spectrometry. In *Tandem Mass Spectrometry-Applications and Principles*: InTech.

Gallant, M.A., Brown, D.M., Organ, J.M., Allen, M.R., and Burr, D.B. (2013) Reference-point indentation correlates with bone toughness assessed using whole-bone traditional mechanical testing. *Bone* **53**: 301-305.

Gamsjaeger, S., Brozek, W., Recker, R., Klaushofer, K., and Paschalis, E.P. (2013) Transmenopausal changes in trabecular bone quality. *J. Bone Miner. Res.* **29**: 608-617.

Gangoiti, P., Granado, M.H., Wang, S.W., Kong, J.Y., Steinbrecher, U.P., and Gómez-Muñoz, A. (2008) Ceramide 1-phosphate stimulates macrophage proliferation through activation of the PI3-kinase/PKB, JNK and ERK1/2 pathways. *Cell. Signal.* **20**: 726-736.

Garnero, P., Sornay-Rendu, E., Chapuy, M.C., and Delmas, P.D. (1996) Increased bone turnover in late postmenopausal women is a major determinant of osteoporosis. *J. Bone Miner. Res.* **11**: 337-349.

Garnero, P., Sornay-Rendu, E., Claustrat, B., and Delmas, P.D. (2000) Biochemical markers of bone turnover, endogenous hormones and the risk of fractures in postmenopausal women: the OFELY study. *J. Bone Miner. Res.* **15**: 1526-1536.

Garnero, P., Ferreras, M., Karsdal, M.A., Nicamhlaoibh, R., Risteli, J., Borel, O., Qvist, P., Delmas, P.D., Foged, N.T., and Delaissé, J.M. (2003) The type I collagen fragments ICTP and CTX reveal distinct enzymatic pathways of bone collagen degradation. *J. Bone Miner. Res.* **18**: 859-867.

Garrett, I.R., Boyce, B.F., Oreffo, R.O., Bonewald, L., Poser, J., and Mundy, G.R. (1990) Oxygen-derived free radicals stimulate osteoclastic bone resorption in rodent bone in vitro and in vivo. *J. Clin. Invest.* **85**: 632-639.

Gault, C.R., Obeid, L.M., and Hannun, Y.A. (2010) An overview of sphingolipid metabolism: from synthesis to breakdown. *Adv. Exp. Med. Biol.* **688**: 1-23.

Gaur, T., Lengner, C.J., Hovhannisyan, H., Bhat, R.A., Bodine, P.V.N., Komm, B.S., Javed, A., van Wijnen, A.J., Stein, J.L., Stein, G.S., and Lian, J.B. (2005) Canonical WNT signaling promotes osteogenesis by directly stimulating Runx2 gene expression. *J. Biol. Chem.* **280**: 33132-33140.

Gerdhem, P., Ivaska Kaisa, K., Isaksson, A., Pettersson, K., Väänänen, H.K., Obrant Karl, J., and Åkesson, K. (2009) Associations between homocysteine, bone turnover, BMD, mortality, and fracture risk in elderly women. *J. Bone Miner. Res.* **22**: 127-134.

German, J.B., Hammock, B.D., and Watkins, S.M. (2005) Metabolomics: building on a century of biochemistry to guide human health. *Metabolomics* **1**: 3-9.

Giacomoni, F., Le Corguillé, G., Monsoor, M., Landi, M., Pericard, P., Pétéra, M., Duperier, C., Tremblay-Franco, M., Martin, J.-F., Jacob, D., Goulitquer, S., Thévenot, E.A., and Caron, C. (2015) Workflow4Metabolomics: a collaborative research infrastructure for computational metabolomics. *Bioinformatics* **31**: 1493-1495.

Gika, H.G., and Theodoridis, G. (2011) Sample preparation prior to the LC–MS-based metabolomics/metabonomics of blood-derived samples. *Bioanalysis* **3**: 1647-1661.

Gika, H.G., Theodoridis, G.A., Plumb, R.S., and Wilson, I.D. (2014) Current practice of liquid chromatography–mass spectrometry in metabolomics and metabonomics. *J. Pharm. Biomed. Anal.* **87**: 12-25.

Gimenez, M.S., Oliveros, L.B., and Gomez, N.N. (2011) Nutritional deficiencies and phospholipid metabolism. *Int. J. Mol. Sci.* **12**: 2408-2433.

Glass, D.A., Bialek, P., Ahn, J.D., Starbuck, M., Patel, M.S., Clevers, H., Taketo, M.M., Long, F., McMahon, A.P., Lang, R.A., and Karsenty, G. (2005) Canonical Wnt Signaling in differentiated osteoblasts controls osteoclast differentiation. *Dev. Cell* **8**: 751-764.

Glendenning, P., Chubb, S.A.P., and Vasikaran, S. (2018) Clinical utility of bone turnover markers in the management of common metabolic bone diseases in adults. *Clin. Chim. Acta* **481**: 161-170.

Goldhahn, J., Jenet, A., Schneider, E., and Christoph, A.L. (2005) Slow rebound of cancellous bone after mainly steroid-induced osteoporosis in ovariectomized sheep. *J. Orthop. Trauma* **19**: 23-28.

Goltzman, D. (1999) Interactions of PTH and PTHrP with the PTH/PTHrP Receptor and with Downstream Signaling Pathways: Exceptions That Provide the Rules. *J. Bone Miner. Res.* **14**: 173-177.

Gomes, P.S., and Fernandes, M.H. (2011) Rodent models in bone-related research: the relevance of calvarial defects in the assessment of bone regeneration strategies. *Lab. Anim.* **45**: 14-24.

Gómez-Muñoz, A. (2004) Ceramide-1-phosphate: a novel regulator of cell activation. *FEBS Lett.* **562**: 5-10.

Gómez-Muñoz, A., Kong, J.Y., Salh, B., and Steinbrecher, U.P. (2004) Ceramide-1-phosphate blocks apoptosis through inhibition of acid sphingomyelinase in macrophages. *J. Lipid Res.* **45**: 99-105.

Goodacre, R., Vaidyanathan, S., Dunn, W.B., Harrigan, G.G., and Kell, D.B. (2004) Metabolomics by numbers: acquiring and understanding global metabolite data. *Trends Biotechnol.* **22**: 245-252.

Greendale Gail, A., Sowers, M., Han, W., Huang, M.H., Finkelstein Joel, S., Crandall Carolyn, J., Lee Jennifer, S., and Karlamangla Arun, S. (2011) Bone mineral density loss in relation to the final menstrual period in a multiethnic cohort: results from the study of Women's Health Across the Nation (SWAN). *J. Bone Miner. Res.* **27**: 111-118.

Gross, Richard W., and Han, X. (2011) Lipidomics at the Interface of Structure and Function in Systems Biology. *Chem. Biol.* **18**: 284-291.

Grygiel-Górniak, B., Marcinkowska, J., Szczepanik, A., and Przysławski, J. (2014) Nutritional habits and oxidative stress in postmenopausal age. *Pol Arch Med Wewn* **124**: 298-305.

Guerrero, R., Martin, M.D., Diego, E.D., Disla, T., Rapado, A., and De la Piedra, C. (1996) New biochemical markers of bone resorption derived from collagen breakdown in the study of postmenopausal osteoporosis. *Osteoporosis Int.* **6**: 297-302.

Hadjidakis, D.J., and Androulakis, I.I. (2006) Bone remodeling. *Ann. N. Y. Acad. Sci.* **1092**: 385-396.

Halket, J.M., Waterman, D., Przyborowska, A.M., Patel, R.K.P., Fraser, P.D., and Bramley, P.M. (2005) Chemical derivatization and mass spectral libraries in metabolic profiling by GC/MS and LC/MS/MS. *J. Exp. Bot.* **56**: 219-243.

Halleen, J.M., Alatalo, S.L., Janckila, A.J., Woitge, H.W., Seibel, M.J., and Väänänen, H.K. (2001) Serum tartrate-resistant acid phosphatase 5b is a specific and sensitive marker of bone resorption. *Clin. Chem.* **47**: 597.

Hanaa, H., and Hamza, A.H. (2009) Potential role of arginine, glutamine and taurine in ameliorating osteoporotic biomarkers in ovariectomized rats. *Rep. Opin* **1**: 24-35.

Harada, S.-i., and Rodan, G.A. (2003) Control of osteoblast function and regulation of bone mass. *Nature* **423**: 349.

Hardouin, P., Pansini, V., and Cortet, B. (2014) Bone marrow fat. *Joint Bone Spine* **81**: 313-319.

Harvey, N., Dennison, E., and Cooper, C. (2010) Osteoporosis: impact on health and economics. *Nat. Rev. Rheumatol.* **6**: 99.

Hayakawa, M., Ishida, N., Takeuchi, K., Shibamoto, S., Hori, T., Oku, N., Ito, F., and Tsujimoto, M. (1993) Arachidonic acid-selective cytosolic phospholipase A2 is crucial in the cytotoxic action of tumor necrosis factor. *J. Biol. Chem.* **268**: 11290-11295.

Heaney, R.P. (2002) The importance of calcium intake for lifelong skeletal health. *Calcif. Tissue Int.* **70**: 70-73.

Henneicke, H., Gasparini, S.J., Brennan-Speranza, T.C., Zhou, H., and Seibel, M.J. (2014) Glucocorticoids and bone: local effects and systemic implications. *Trends Endocrinol. Metab.* **25**: 197-211.

Henriksen, K., Neutzsky-Wulff, A.V., Bonewald, L.F., and Karsdal, M.A. (2009) Local communication on and within bone controls bone remodeling. *Bone* **44**: 1026-1033.

Herrmann, M., Kraenzlin, M., Pape, G., Sand-Hill, M., and Herrmann, W. (2005a) Relation between homocysteine and biochemical bone turnover markers and bone mineral density in peri-and post-menopausal women. *Clin. Chem. Lab. Med.* **43**: 1118-1123.

Herrmann, M., Widmann, T., Colaianni, G., Colucci, S., Zallone, A., and Herrmann, W. (2005b) Increased osteoclast activity in the presence of increased homocysteine concentrations. *Clin. Chem.* **51**: 2348.

Hill, P., and Tumber, A. (2010) Ceramide-induced cell death/survival in murine osteoblasts. *J. Endocrinol.* **206**: 225-233.

Hill, T.P., Später, D., Taketo, M.M., Birchmeier, W., and Hartmann, C. (2005) Canonical Wnt/β-catenin signaling prevents osteoblasts from differentiating into chondrocytes. *Dev. Cell* **8**: 727-738.

Hlaing, T.T., and Compston, J.E. (2014) Biochemical markers of bone turnover – uses and limitations. *Ann. Clin. Biochem.* **51**: 189-202.

Hofbauer, L.C., Kuhne, C.A., and Viereck, V. (2004) The OPG/RANKL/RANK system in metabolic bone diseases. *J. Musculoskelet. Neuronal. Interact.* **4**: 268.

Hofbauer, L.C., Gori, F., Riggs, B.L., Lacey, D.L., Dunstan, C.R., Spelsberg, T.C., and Khosla, S. (1999) Stimulation of osteoprotegerin ligand and inhibition of osteoprotegerin production by glucocorticoids in human osteoblastic lineage cells: potential paracrine mechanisms of glucocorticoid-induced osteoporosis 1. *Endocrinology* **140**: 4382-4389.

Holick, M.F. (2004) Sunlight and vitamin D for bone health and prevention of autoimmune diseases, cancers, and cardiovascular disease. *Am. J. Clin. Nutr.* **80**: 1678S-1688S.

Holland, J.C., Brennan, O., Kennedy, O.D., Rackard, S.M., O'Brien, F.J., and Lee, T.C. (2011) Subchondral trabecular structural changes in the proximal tibia in an ovine model of increased bone turnover. *J. Anat.* **218**: 619-624.

Holroyd, C., Cooper, C., and Dennison, E. (2008) Epidemiology of osteoporosis. *Best Pract. Res. Clin. Endocrin. Metab.* **22**: 671-685.

Hornby, S., Ford, S., Mase, C., and Evans, G. (1995) Skeletal changes in the ovariectomised ewe and subsequent response to treatment with 17β oestradiol. *Bone* **17**: S389-S394.

Hu, L.-L., Niu, S., Huang, T., Wang, K., Shi, X.-H., and Cai, Y.-D. (2011) Prediction and analysis of protein hydroxyproline and hydroxylysine. *PloS one* **5**: e15917.

Iida, M., Harada, S., Kurihara, A., Fukai, K., Kuwabara, K., Sugiyama, D., Takeuchi, A., Okamura, T., Akiyama, M., Nishiwaki, Y., Suzuki, A., Hirayama, A., Sugimoto, M., Soga, T., Tomita, M., Banno, K., Aoki, D., and Takebayashi, T. (2016) Profiling of plasma metabolites in postmenopausal women with metabolic syndrome. *Menopause* **23**: 749-758.

Ikonen, E. (2008) Cellular cholesterol trafficking and compartmentalization. *Nat. Rev. Mol. Cell Biol.* **9**: 125.

Indahl, U.G., Martens, H., and Næs, T. (2007) From dummy regression to prior probabilities in PLS-DA. *J. Chemometrics* **21**: 529-536.

Ingólfsson, H.I., Melo, M.N., van Eerden, F.J., Arnarez, C., Lopez, C.A., Wassenaar, T.A., Periole, X., de Vries, A.H., Tieleman, D.P., and Marrink, S.J. (2014) Lipid organization of the plasma membrane. *J. Am. Chem. Soc.* **136**: 14554-14559.

Isogai, Y., Akatsu, T., Ishizuya, T., Yamaguchi, A., Hori, M., Takahashi, N., and Suda, T. (1996) Parathyroid hormone regulates osteoblast differentiation positively or negatively depending on the differentiation stages. *J. Bone Miner. Res.* **11**: 1384-1393.

Jia, D., O'brien, C., Stewart, S., Manolagas, S., and Weinstein, R. (2006) Glucocorticoids act directly on osteoclasts to increase their life span and reduce bone density. *Endocrinology* **147**: 5592-5599.

Jilka, R.L., Hangoc, G., Girasole, G., Passeri, G., Williams, D.C., Abrams, J.S., Boyce, B., Broxmeyer, H., and Manolagas, S.C. (1992) Increased osteoclast development after estrogen loss: mediation by interleukin-6. *Science* **257**: 88.

Johnell, O., and Kanis, J. (2006) An estimate of the worldwide prevalence and disability associated with osteoporotic fractures. *Osteoporosis Int.* **17**: 1726-1733.

Johnson, R., Gilbert, J., Cooper, R., Parsell, D., Stewart, B., Dai, X., Nick, T., Streckfus, C., Butler, R., and Boring, J. (2002) Effect of estrogen deficiency on skeletal and alveolar bone density in sheep. *J. Periodontol.* **73**: 383-391.

Jousse, C., Averous, J., Bruhat, A., Carraro, V., Mordier, S., and Fafournoux, P. (2004) Amino acids as regulators of gene expression: molecular mechanisms. *Biochem. Biophys. Res. Commun.* **313**: 447-452.

Jové, M., Maté, I., Naudí, A., Mota-Martorell, N., Portero-Otín, M., De la Fuente, M., and Pamplona, R. (2016) Human aging Is a metabolome-related matter of gender. *J. Gerontol. A.* **71**: 578-585.

K, F.E., P, K.D., Ronenn, R., J, S.E., Adrienne, C.L., and L, T.K. (2012) Plasma phosphatidylcholine concentrations of polyunsaturated fatty acids are differentially associated with hip bone mineral density and hip fracture in older adults: The framingham osteoporosis study. *J. Bone Miner. Res.* **27**: 1222-1230.

Kadam, P., and Bhalerao, S. (2010) Sample size calculation. *International journal of Ayurveda research* **1**: 55.

Kalervo Väänänen, H., and Härkönen, P.L. (1996) Estrogen and bone metabolism. *Maturitas* **23**: S65-S69.

Kanis, J., and Group, W.H.O.S. (2007) WHO technical report. *University of Sheffield, UK* **66**.

Kanis, J.A. (2002) Diagnosis of osteoporosis and assessment of fracture risk. *The Lancet* **359**: 1929-1936.

Kanis, J.A., Melton, L.r., Christiansen, C., Johnston, C.C., and Khaltaev, N. (1994) The diagnosis of osteoporosis. *J Bone Miner Res* **9**: 1137-1141.

Kanis, J.A., Delmas, P., Burckhardt, P., Cooper, C., and Torgerson, D.o. (1997) Guidelines for diagnosis and management of osteoporosis. *Osteoporosis Int.* **7**: 390-406.

Kanis, J.A., McCloskey, E.V., Johansson, H., Oden, A., Melton, L.J., III, and Khaltaev, N. (2008) A reference standard for the description of osteoporosis. *Bone* **42**: 467-475.

Kapinas, K., and Delany, A.M. (2011) MicroRNA biogenesis and regulation of bone remodeling. *Arthrit. Res. Ther.* **13**: 220.

Karimifar, M., Pasha, M.A.P., Salari, A., Zamani, A., Salesi, M., and Motaghi, P. (2012) Evaluation of bone loss in diabetic postmenopausal women. *J. Res. Med. Sci.* **17**: 1033-1038.

Katajamaa, M., and Orešič, M. (2005) Processing methods for differential analysis of LC/MS profile data. *BMC Bioinformatics* **6**: 179.

Ke, C., Hou, Y., Zhang, H., Yang, K., Wang, J., Guo, B., Zhang, F., Li, H., Zhou, X., Li, Y., and Li, K. (2015) Plasma metabolic profiles in women are menopause dependent. *PloS one* **10**: e0141743.

Kennedy, O.D., Brennan, O., Rackard, S.M., Staines, A., O'Brien, F.J., Taylor, D., and Lee, T.C. (2009) Effects of ovariectomy on bone turnover, porosity, and biomechanical properties in ovine compact bone 12 months postsurgery. *J. Orth. Res.* **27**: 303-309.

Khosla, S. (2001) Minireview: The opg/rankl/rank system. *Endocrinology* **142**: 5050-5055.

Khosla, S., Melton, L.J., and Riggs, B.L. (2011) The unitary model for estrogen deficiency and the pathogenesis of osteoporosis: is a revision needed? *J. Bone Miner. Res.* **26**: 441-451.

Khosla, S., Oursler, M.J., and Monroe, D.G. (2012) Estrogen and the skeleton. *Trends Endocrinol. Metab.* **23**: 576-581.

Kiełbowicz, Z., Piątek, A., Bieżyński, J., Skrzypczak, P., Kuropka, P., Kuryszko, J., Nikodem, A., Kafarski, P., and Pezowicz, C. (2015) The experimental osteoporosis in sheep – clinical approach. *Polish Journal of Veterinary Sciences* **18**: 645-654.

Kilpinen, L., Tigistu-Sahle, F., Oja, S., Greco, D., Parmar, A., Saavalainen, P., Nikkilä, J., Korhonen, M., Lehenkari, P., Käkelä, R., and Laitinen, S. (2013) Aging bone marrow mesenchymal stromal cells have altered membrane glycerophospholipid composition and functionality. *J. Lipid Res.* **54**: 622-635.

Kim, C.H., Takai, E., Zhou, H., Von Stechow, D., Müller, R., Dempster, D.W., and Guo, X.E. (2003) Trabecular bone response to mechanical and parathyroid hormone stimulation: the role of mechanical microenvironment. *J. Bone Miner. Res.* **18**: 2116-2125.

Klein-Nulend, J., van Oers, R.F., Bakker, A.D., and Bacabac, R.G. (2015) Bone cell mechanosensitivity, estrogen deficiency, and osteoporosis. *J Biomech* **48**: 855-865.

Komori, T. (2015) Animal models for osteoporosis. *Eur. J. Pharmacol.* **759**: 287-294.

Krum, S.A., Miranda-Carboni, G.A., Hauschka, P.V., Carroll, J.S., Lane, T.F., Freedman, L.P., and Brown, M. (2008) Estrogen protects bone by inducing Fas ligand in osteoblasts to regulate osteoclast survival. *EMBO J.* **27**: 535-545.

Kuhl, C., Tautenhahn, R., Bottcher, C., Larson, T.R., and Neumann, S. (2011) CAMERA: an integrated strategy for compound spectra extraction and annotation of liquid chromatography/mass spectrometry data sets. *Anal. Chem.* **84**: 283-289.

Kular, J., Tickner, J., Chim, S.M., and Xu, J. (2012) An overview of the regulation of bone remodelling at the cellular level. *Clin. Biochem.* **45**: 863-873.

Kuo, T.-R., and Chen, C.-H. (2017) Bone biomarker for the clinical assessment of osteoporosis: recent developments and future perspectives. *Biomark. Res.* **5**: 18.

Lagarde, M., Géloën, A., Record, M., Vance, D., and Spener, F. (2003) Lipidomics is emerging. *BBA-Mol. Cell. Biol. L.* **1634**: 61.

Lane, N.E. (2006) Epidemiology, etiology, and diagnosis of osteoporosis. *American journal of obstetrics and gynecology* **194**: S3-S11.

Lane, N.E., Yao, W., Balooch, M., Nalla, R.K., Balooch, G., Habelitz, S., Kinney, J.H., and Bonewald, L.F. (2006) Glucocorticoid-treated mice have localized changes in trabecular bone material properties and osteocyte lacunar size that are not observed in placebo-treated or estrogen-deficient mice. *J. Bone Miner. Res.* **21**: 466-476.

Lane, R.K., Hilsabeck, T., and Rea, S.L. (2015) The role of mitochondrial dysfunction in age-related diseases. *BBA-Bioenerg.* **1847**: 1387-1400.

Langlois, M.R., Delanghe, J.R., Kaufman, J.M., De Buyzere, M.L., Hoecke, M.J., and Leroux-Roels, G.G. (1994) Posttranslational heterogeneity of bone alkaline phosphatase in metabolic bone disease. In *Clin. Chem. Lab. Med.*, p. 675.

Larive, C.K., Barding, G.A., and Dinges, M.M. (2015) NMR spectroscopy for metabolomics and metabolic profiling. *Anal. Chem.* **87**: 133-146.

Lean, J.M., Jagger, C.J., Kirstein, B., Fuller, K., and Chambers, T.J. (2005) Hydrogen peroxide Is essential for estrogen-deficiency bone loss and osteoclast formation. *Endocrinology* **146**: 728-735.

Lee, M.Y., Kim, H.Y., Singh, D., Yeo, S.H., Baek, S.Y., Park, Y.K., and Lee, C.H. (2016) Metabolite profiling reveals the effect of dietary Rubus coreanus vinegar on ovariectomy-induced osteoporosis in a rat model. *Molecules* **21**: 149.

Lee, N.K., Choi, Y.G., Baik, J.Y., Han, S.Y., Jeong, D.-w., Bae, Y.S., Kim, N., and Lee, S.Y. (2005) A crucial role for reactive oxygen species in RANKL-induced osteoclast differentiation. *Blood* **106**: 852.

Lee, S.H., Lee, S.-Y., Lee, Y.-S., Kim, B.-J., Lim, K.-H., Cho, E.-H., Kim, S.-W., Koh, J.-M., and Kim, G.S. (2012) Higher circulating Sphingosine 1-Phosphate

levels are associated with lower bone mineral density and higher bone resorption marker in humans. *J. Clin. Endocrinol. Metab.* **97**: E1421-E1428.

Lee, W.-C., Guntur, A.R., Long, F., and Rosen, C.J. (2017) Energy metabolism of the osteoblast: implications for osteoporosis. *Endocr. Rev.* **38**: 255-266.

Lelovas, P.P., Xanthos, T.T., Thoma, S.E., Lyritis, G.P., and Dontas, I.A. (2008) The laboratory rat as an animal model for osteoporosis research. *Comp. Med.* **58**: 424-430.

Les, C., Vance, J., Christopherson, G., Turner, A., Divine, G., and Fyhrie, D. (2005) Long-term ovariectomy decreases ovine compact bone viscoelasticity. *J. Orth. Res.* **23**: 869-876.

Lesclous, P., Guez, D., Llorens, A., and Saffar, J. (2001) Time-course of mast cell accumulation in rat bone marrow after ovariectomy. *Calcif. Tissue Int.* **68**: 297-303.

Lesclous, P., Schramm, F., Gallina, S., Baroukh, B., Guez, D., and Saffar, J.L. (2006) Histamine mediates osteoclastic resorption only during the acute phase of bone loss in ovariectomized rats. *Exp. Physiol.* **91**: 561-570.

Li, M., Shen, Y., Qi, H., and Wronski, T. (1996) Comparative study of skeletal response to estrogen depletion at red and yellow marrow sites in rats. *Anat. Rec.* **245**: 472-480.

Li, X., Zhang, Y., Kang, H., Liu, W., Liu, P., Zhang, J., Harris, S.E., and Wu, D. (2005) Sclerostin binds to LRP5/6 and antagonizes canonical Wnt signaling. *J. Biol. Chem.* **280**: 19883-19887.

Liebschner, M.A. (2004) Biomechanical considerations of animal models used in tissue engineering of bone. *Biomaterials* **25**: 1697-1714.

Liland, K.H. (2011) Multivariate methods in metabolomics – from pre-processing to dimension reduction and statistical analysis. *Trac-Trend. Anal. Chem.* **30**: 827-841.

Lill, C., Fluegel, A., and Schneider, E. (2002a) Effect of ovariectomy, malnutrition and glucocorticoid application on bone properties in sheep: a pilot study. *Osteoporosis Int.* **13**: 480-486.

Lill, C.A., Fluegel, A.K., and Schneider, E. (2002b) Effect of ovariectomy, malnutrition and glucocorticoid application on bone properties in sheep: a pilot study. *Osteoporosis Int.* **13**: 480-486.

Lill, C.A., Gerlach, U.V., Eckhardt, C., Goldhahn, J., and Schneider, E. (2002c) Bone changes due to glucocorticoid application in an ovariectomized animal model for fracture treatment in osteoporosis. *Osteoporosis Int.* **13**: 407-414.

Lindon, J.C., Holmes, E., and Nicholson, J.K. (2004) Metabonomics and its role in drug development and disease diagnosis. *Expert. Rev. Mol. Diagn.*

Liu, G., Nellaiappan, K., and Kagan, H.M. (1997) Irreversible inhibition of lysyl oxidase by homocysteine thiolactone and its selenium and oxygen analogues. Implications for homocystinuria. *J. Biol. Chem.* **272**: 32370-32377.

Liu, X., Zhang, S., Lu, X., Zheng, S., Li, F., and Xiong, Z. (2012) Metabonomic study on the anti-osteoporosis effect of Rhizoma Drynariae and its action mechanism using ultra-performance liquid chromatography–tandem mass spectrometry. *J. Ethnopharmacol.* **139**: 311-317.

Liu, Y., Huang, R., Xiao, B., Yang, J., and Dong, J. (2014) 1H NMR metabolic profiling analysis offers evaluation of Nilestriol treatment in ovariectomised rats. *Mol. Cell. Endocrinol.* **387**: 19-34.

Liu, Y., Xiao, B., Yang, J., Guo, C., Shen, S., Tang, Z., Dong, J., and Huang, R. (2015) 1H-NMR and HPLC–MS/MS-based global/targeted metabolomic evaluation of Hypericum perforatum L. intervention for menopause. *J. Funct. Foods.* **17**: 722-741.

Long, W.F., Li, L., Chen, H.Q., Tang, Y., He, X.L., and Jing, R.Z. (2009) 1H-NMR-based metabonomics analysis of plasma from osteoporotic rats induced by ovariectomy. *Sichuan Da Xue Xue Bao Yi Xue Ban* **40**: 843-847.

Lu, W., Clasquin, M.F., Melamud, E., Amador-Noguez, D., Caudy, A.A., and Rabinowitz, J.D. (2010) Metabolomic Analysis via Reversed-Phase Ion-Pairing Liquid Chromatography Coupled to a Stand Alone Orbitrap Mass Spectrometer. *Anal. Chem.* **82**: 3212-3221.

Łukaszkiewicz, J., Karczmarewicz, E., Płudowski, P., Jaworski, M., Czerwiński, E., Lewiński, A., Marcinowska-Suchowierska, E., Milewicz, A., Spaczyński, M., and Lorenc, R.S. (2008) Feasibility of simultaneous measurement of bone formation and bone resorption markers to assess bone turnover rate in postmenopausal women: an EPOLOS study. *Med. Sci. Monit.* **14**: PH65-PH70.

Ma, B., Liu, J., Zhang, Q., Ying, H., Sun, J., Wu, D., Wang, Y., Li, J., and Liu, Y. (2013a) Metabolomic profiles delineate signature metabolic shifts during estrogen deficiency-induced bone loss in rat by GC-TOF/MS. *PloS one* **8**: e54965.

Ma, B., Zhang, Q., Wang, G., Jiye, A., Wu, D., Liu, Y., Cao, B., Liu, L., Hu, Y., and Wang, Y. (2011) GC-TOF/MS-based metabolomic profiling of estrogen deficiency-induced obesity in ovariectomized rats. *Acta. Pharmacol. Sin.* **32**: 270.

Ma, B., Li, X., Zhang, Q., Wu, D., Wang, G., Jiye, A., Sun, J., Li, J., Liu, Y., and Wang, Y. (2013b) Metabonomic profiling in studying anti-osteoporosis effects of strontium fructose 1, 6-diphosphate on estrogen deficiency-induced osteoporosis in rats by GC/TOF-MS. *Eur. J. Pharmacol.* **718**: 524-532.

Ma, Y., Ke, H.Z., and Jee, W.S. (1994) Prostaglaridin E2 adds bone to a cancellous bone site with a closed growth plate and low bone turnover in ovariectomized rats. *Bone* **15**: 137-146.

Ma, Y.L., Cain, R.L., Halladay, D.L., Yang, X., Zeng, Q., Miles, R.R., Chandrasekhar, S., Martin, T.J., and Onyia, J.E. (2001) Catabolic effects of continuous human PTH (1–38) in vivo is associated with sustained stimulation of RANKL and inhibition of osteoprotegerin and gene-associated bone formation. *Endocrinology* **142**: 4047-4054.

MacLeay, J.M., Olson, J.D., and Turner, A.S. (2004) Effect of dietary-induced metabolic acidosis and ovariectomy on bone mineral density and markers of bone turnover. *J. Bone Miner. Metab.* **22**: 561-568.

Maeda, K., Kobayashi, Y., Udagawa, N., Uehara, S., Ishihara, A., Mizoguchi, T., Kikuchi, Y., Takada, I., Kato, S., Kani, S., Nishita, M., Marumo, K., Martin, T.J., Minami, Y., and Takahashi, N. (2012) Wnt5a-Ror2 signaling between osteoblast-lineage cells and osteoclast precursors enhances osteoclastogenesis. *Nat. Med.* **18**: 405.

Maggio, D., Barabani, M., Pierandrei, M., Polidori, M.C., Catani, M., Mecocci, P., Senin, U., Pacifici, R., and Cherubini, A. (2003) Marked decrease in plasma antioxidants in aged osteoporotic women: results of a cross-sectional study. *J. Clin. Endocrinol. Metab.* **88**: 1523-1527.

Makovey, J., Chen, J.S., Hayward, C., Williams, F.M.K., and Sambrook, P.N. Association between serum cholesterol and bone mineral density. *Bone* **44**: 208-213.

Manelli, F., and Giustina, A. (2000) Glucocorticoid-induced osteoporosis. *Trends Endocrinol. Metab.* **11**: 79-85.

Manolagas, S.C. (2000) Birth and death of bone cells: basic regulatory mechanisms and implications for the pathogenesis and treatment of osteoporosis*. *Endocr. Rev.* **21**: 115-137.

Manolagas, S.C. (2009) Corticosteroids and Fractures: A Close Encounter of the Third Cell Kind. *J. Bone Miner. Res.* **15**: 1001-1005.

Manolagas, S.C. (2010) From estrogen-centric to aging and oxidative stress: a revised perspective of the pathogenesis of osteoporosis. *Endocr. Rev.* **31**: 266-300.

Manolagas, S.C., and Parfitt, A.M. (2010) What old means to bone. *Trends Endocrinol. Metab.* **21**: 369-374.

Marks, S.C., and Popoff, S.N. (1988) Bone cell biology: the regulation of development, structure, and function in the skeleton. *Am. J. Anat.* **183**: 1-44.

Martin, T.J., and Ng, K.W. (1994) Mechanisms by which cells of the osteoblast lineage control osteoclast formation and activity. *J. Cell. Biochem.* **56**: 357-366.

Martin, T.J., and Sims, N.A. (2005) Osteoclast-derived activity in the coupling of bone formation to resorption. *Trends Mol. Med.* **11**: 76-81.

Matsuo, K., and Irie, N. (2008) Osteoclast–osteoblast communication. *Arch. Biochem. Biophys.* **473**: 201-209.

Maunsell, Z., Wright, D.J., and Rainbow, S.J. (2005) Routine isotope-dilution liquid chromatography–tandem mass spectrometry assay for simultaneous measurement of the 25-hydroxy metabolites of vitamins D2 and D3. *Clin. Chem.* **51**: 1683-1690.

Mazziotti, G., Angeli, A., Bilezikian, J.P., Canalis, E., and Giustina, A. (2006) Glucocorticoid-induced osteoporosis: an update. *Trends Endocrinol. Metab.* **17**: 144-149.

McGovern, J.A., Griffin, M., and Hutmacher, D.W. (2018) Animal models for bone tissue engineering and modelling disease. *Dis. Model. Mech.* **11**.

McNiven, E.M.S., German, J.B., and Slupsky, C.M. (2011) Analytical metabolomics: nutritional opportunities for personalized health. *J. Nutr. Biochem.* **22**: 995-1002.

Melkko, J., Niemi, S., Risteli, L., and Risteli, J. (1990) Radioimmunoassay of the carboxyterminal propeptide of human type I procollagen. *Clin. Chem.* **36**: 1328.

Michalowska, M., Znorko, B., Kaminski, T., Oksztulska-Kolanek, E., and Pawlak, D. (2015) New insights into tryptophan and its metabolites in the regulation of bone metabolism. *J Physiol Pharmacol* **66**: 779-791.

Miller, S.C., Bowman, B.M., and Jee, W.S.S. (1995) Available animal models of osteopenia — Small and large. *Bone* **17**: S117-S123.

Mishur, R.J., and Rea, S.L. (2012) Applications of mass spectrometry to metabolomics and metabonomics: detection of biomarkers of aging and of age-related diseases. *Mass. Spectrom. Rev.* **31**: 70-95.

Miyamoto, T., Hirayama, A., Sato, Y., Koboyashi, T., Katsuyama, E., Kanagawa, H., Fujie, A., Morita, M., Watanabe, R., Tando, T., Miyamoto, K., Tsuji, T., Funayama, A., Soga, T., Tomita, M., Nakamura, M., and Matsumoto, M. (2018) Metabolomics-based profiles predictive of low bone mass in menopausal women. *Bone Reports* **9**: 11-18.

Miyamoto, T., Hirayama, A., Sato, Y., Koboyashi, T., Katsuyama, E., Kanagawa, H., Miyamoto, H., Mori, T., Yoshida, S., Fujie, A., Morita, M., Watanabe, R., Tando, T., Miyamoto, K., Tsuji, T., Funayama, A., Nakamura, M., Matsumoto, M., Soga, T., Tomita, M., and Toyama, Y. (2017) A serum metabolomics-based profile in low bone mineral density postmenopausal women. *Bone* **95**: 1-4.

Mody, N., Parhami, F., Sarafian, T.A., and Demer, L.L. (2001) Oxidative stress modulates osteoblastic differentiation of vascular and bone cells. *Free Radical Biol. Med.* **31**: 509-519.

Moreira, L.D.F., de Oliveira, M.L., Lirani-Galvão, A.P., Marin-Mio, R.V., dos Santos, R.N., and Lazaretti-Castro, M. (2014) Physical exercise and osteoporosis: effects of different types of exercises on bone and physical function of postmenopausal women. *Arq. Bras. Endocrinol. Metab.* **58**: 514-522.

Morris, J.S.M. (2006) Arginine: beyond protein1–4. *Am. J. Clin. Nutr.* **83**: 508S-512S.

Muruganandan, S., and Sinal, C.J. (2014) The impact of bone marrow adipocytes on osteoblast and osteoclast differentiation. *IUBMB Life* **66**: 147-155.

Muruganandan, S., Roman, A.A., and Sinal, C.J. (2009) Adipocyte differentiation of bone marrow-derived mesenchymal stem cells: Cross talk with the osteoblastogenic program. *Cell. Mol. Life Sci.* **66**: 236-253.

Nakamura, T., Imai, Y., Matsumoto, T., Sato, S., Takeuchi, K., Igarashi, K., Harada, Y., Azuma, Y., Krust, A., Yamamoto, Y., Nishina, H., Takeda, S., Takayanagi, H., Metzger, D., Kanno, J., Takaoka, K., Martin, T.J., Chambon, P., and Kato, S. (2007) Estrogen prevents bone loss via estrogen receptor α and induction of Fas ligand in osteoclasts. *Cell* **130**: 811-823.

Nakashima, T., Hayashi, M., Fukunaga, T., Kurata, K., Oh-hora, M., Feng, J.Q., Bonewald, L.F., Kodama, T., Wutz, A., Wagner, E.F., Penninger, J.M., and Takayanagi, H. (2011) Evidence for osteocyte regulation of bone homeostasis through RANKL expression. *Nat. Med.* **17**: 1231.

Naylor, K., and Eastell, R. (2012) Bone turnover markers: use in osteoporosis. *Nat. Rev. Rheumatol.* **8**: 379.

Neu, C., Manz, F., Rauch, F., Merkel, A., and Schoenau, E. (2001) Bone densities and bone size at the distal radius in healthy children and adolescents: a study using peripheral quantitative computed tomography. *Bone* **28**: 227-232.

Newgard, C.B. (2017) Metabolomics and metabolic diseases: where do we stand? *Cell. Metab.* **25**: 43-56.

Newman, E., Turner, A., and Wark, J. (1995) The potential of sheep for the study of osteopenia: current status and comparison with other animal models. *Bone* **16**: S277-S284.

Newton, B., Cooper, R., Gilbert, J., Johnson, R., and Zardiackas, L. (2004a) The ovariectomized sheep as a model for human bone loss. *J. Comp. Pathol.* **130**: 323-326.

Newton, B.I., Cooper, R.C., Gilbert, J.A., Johnson, R.B., and Zardiackas, L.D. (2004b) The ovariectomized sheep as a model for human bone loss. *J. Comp. Pathol.* **130**: 323-326.

O'brien, C.A., Jia, D., Plotkin, L.I., Bellido, T., Powers, C.C., Stewart, S.A., Manolagas, S.C., and Weinstein, R.S. (2004) Glucocorticoids act directly on osteoblasts and osteocytes to induce their apoptosis and reduce bone formation and strength. *Endocrinology* **145**: 1835-1841.

Obayashi, M., Shimomura, Y., Nakai, N., Jeoung, N.H., Nagasaki, M., Murakami, T., Sato, Y., and Harris, R.A. (2004) Estrogen controls branched-chain amino acid catabolism in female rats. *J. Nutr.* **134**: 2628-2633.

Oheim, R., Schinke, T., Amling, M., and Pogoda, P. (2016) Can we induce osteoporosis in animals comparable to the human situation? *Injury* **47**: S3-S9.

Oliver, S.G., Winson, M.K., Kell, D.B., and Baganz, F. (1998) Systematic functional analysis of the yeast genome. *Trends Biotechnol.* **16**: 373-378.

Orimo, H., Hayashi, Y., Fukunaga, M., Sone, T., Fujiwara, S., Shiraki, M., Kushida, K., Miyamoto, S., Soen, S., Nishimura, J., Oh-hashi, Y., Hosoi, T., Gorai, I., Tanaka, H., Igai, T., and Kishimoto, H. (2001) Diagnostic criteria for primary osteoporosis: year 2000 revision. *J. Bone Miner. Metab.* **19**: 331-337.

Orozco, P. (2004) Atherogenic lipid profile and elevated lipoprotein (a) are associated with lower bone mineral density in early postmenopausal overweight women. *Eur. J. Epidemiol.* **19**: 1105-1112.

Ozdem, S., Samanci, N., Taşatargil, A., Yildiz, A., Sadan, G., Donmez, L., and Herrmann, M. (2007) Experimental hyperhomocysteinemia disturbs bone metabolism in rats. *Scand. J. Clin. Lab. Invest.* **67**: 748-756.

Paccou, J., Hardouin, P., Cotten, A., Penel, G., and Cortet, B. (2015) The role of bone marrow fat in skeletal health: usefulness and perspectives for clinicians. *J. Clin. Endocrinol. Metab.* **100**: 3613-3621.

Pacifici, R., Brown, C., Puscheck, E., Friedrich, E., Slatopolsky, E., Maggio, D., McCracken, R., and Avioli, L.V. (1991) Effect of surgical menopause and estrogen replacement on cytokine release from human blood mononuclear cells. *Proc. Natl. Acad. Sci.* **88**: 5134.

Parhami, F., Mody, N., Gharavi, N., Ballard, A.J., Tintut, Y., and Demer, L.L. (2002) Role of the cholesterol biosynthetic pathway in osteoblastic differentiation of marrow stromal cells. *J. Bone Miner. Res.* **17**: 1997-2003.

Patti, G.J., Yanes, O., and Siuzdak, G. (2012) Metabolomics: the apogee of the omics trilogy. *Nat. Rev. Mol. Cell Biol.* **13**: 263.

Peacock, M. (2010) Calcium metabolism in health and disease. *Clin. J. Am. Soc. Nephrol.* **5**: S23-S30.

Pearce, A., Richards, R., Milz, S., Schneider, E., and Pearce, S. (2007) Animal models for implant biomaterial research in bone: a review. *Eur Cell Mater* **13**: 1-10.

Perez de Souza, L., Tohge, T., Naake, T., and Fernie, A.R. (2017) From chromatogram to analyte to metabolite. How to pick horses for courses from the massive web resources for mass spectral plant metabolomics. *GigaScience* **6**.

Pfeilschifter, J., Köditz, R., Pfohl, M., and Schatz, H. (2002) Changes in proinflammatory cytokine activity after enopause. *Endocr. Rev.* **23**: 90-119.

Pinheiro, J., Bates, D., DebRoy, S., and Sarkar, D. (2015) R Development Core Team.(2014). nlme: Linear and nonlinear mixed effects models. In: R package version 3.1-117.

Poole, K.E.S., and Reeve, J. (2005) Parathyroid hormone — a bone anabolic and catabolic agent. *Curr. Opin. Pharm.* **5**: 612-617.

Prentice, A. (2001) The relative contribution of diet and genotype to bone development. *Proc. Nutr. Soc.* **60**: 45-52.

Proff, P., and Römer, P. (2009) The molecular mechanism behind bone remodelling: a review. *Clin. Oral. Invest.* **13**: 355-362.

Qi, H., Bao, J., An, G., Ouyang, G., Zhang, P., Wang, C., Ying, H., Ouyang, P., Ma, B., and Zhang, Q. (2016) Association between the metabolome and bone mineral density in pre- and post-menopausal Chinese women using GC-MS. *Mol. BioSyst.* **12**: 2265-2275.

Qin, L., Raggatt, L.J., and Partridge, N.C. (2004) Parathyroid hormone: a double-edged sword for bone metabolism. *Trends Endocrinol. Metab.* **15**: 60-65.

Raggatt, L.J., and Partridge, N.C. (2010) Cellular and molecular mechanisms of bone remodeling. *J. Biol. Chem.* **285**: 25103-25108.

Raisz, L.G. (2005) Pathogenesis of osteoporosis: concepts, conflicts, and prospects. *J. Clin. Invest.* **115**: 3318-3325.

Redlich, K., and Smolen, J.S. (2012) Inflammatory bone loss: pathogenesis and therapeutic intervention. *Nat. Rev. Drug. Discov.* **11**: 234.

Reginster, J.-Y., and Burlet, N. (2006) Osteoporosis: A still increasing prevalence. *Bone* **38**: 4-9.

Reginster, J.-Y., Henrotin, Y., Christiansen, C., Gamwell-Henriksen, E., Bruyère, O., Collette, J., and Christgau, S. (2001) Bone resorption in post-menopausal women with normal and low BMD assessed with biochemical markers specific for telopeptide derived degradation products of collagen type I. *Calcif. Tissue Int.* **69**: 130-137.

Reichert, J.C., Saifzadeh, S., Wullschleger, M.E., Epari, D.R., Schütz, M.A., Duda, G.N., Schell, H., van Griensven, M., Redl, H., and Hutmacher, D.W. (2009) The challenge of establishing preclinical models for segmental bone defect research. *Biomaterials* **30**: 2149-2163.

Reid, D.G., Shanahan, C.M., Duer, M.J., Arroyo, L.G., Schoppet, M., Brooks, R.A., and Murray, R.C. (2012) Lipids in biocalcification: contrasts and similarities between intimal and medial vascular calcification and bone by NMR. *J. Lipid Res.* **53**: 1569-1575.

Reid, I.R. (2010) Fat and bone. *Arch. Biochem. Biophys.* **503**: 20-27.

Reinwald, S., and Burr, D. (2008) Review of nonprimate, large animal models for osteoporosis research. *J. Bone Miner. Res.* **23**: 1353-1368.

Riggs, B.L. (2000) The mechanisms of estrogen regulation of bone resorption. *J. Clin. Invest.* **106**: 1203.

Riggs, B.L., Khosla, S., and Melton, L.J. (1998) A unitary model for involutional osteoporosis: estrogen deficiency causes both type I and type II osteoporosis in

postmenopausal women and contributes to bone loss in aging men. *J. Bone Miner. Res.* **13**: 763-773.

Riggs, B.L., Khosla, S., and Melton III, L.J. (2002) Sex steroids and the construction and conservation of the adult skeleton. *Endocr. Rev.* **23**: 279-302.

Ringnér, M. (2008) What is principal component analysis? *Nat. Biotechnol.* **26**: 303.

Risteli, L., and Risteli, J. (1993) Biochemical markers of bone metabolism. *Ann. Med.* **25**: 385-393.

Robling, A.G., Castillo, A.B., and Turner, C.H. (2006) Biomechanical and molecular regulation of bone remodeling. *Annu. Rev. Biomed. Eng.* **8**: 455-498.

Rodan, G.A., and Martin, T.J. (2000) Therapeutic approaches to bone diseases. *Science* **289**: 1508-1514.

Roghani, T., Torkaman, G., Movasseghe, S., Hedayati, M., Goosheh, B., and Bayat, N. (2013) Effects of short-term aerobic exercise with and without external loading on bone metabolism and balance in postmenopausal women with osteoporosis. *Rheumatol. Int.* **33**: 291-298.

Rosen, C.J., and Bouxsein, M.L. (2006) Mechanisms of Disease: is osteoporosis the obesity of bone? *Nat. Clin. Pract. Rheumatol.* **2**: 35.

Rosen, H.N., Moses, A.C., Garber, J., Iloputaife, I.D., Ross, D.S., Lee, S.L., and Greenspan, S.L. (2000) Serum CTX: a new marker of bone resorption that shows treatment effect more often than other markers because of low coefficient of variability and large changes with bisphosphonate therapy. *Calcif. Tissue Int.* **66**: 100-103.

Rosenberg, N., Rosenberg, O., and Soudry, M. (2012) Osteoblasts in bone physiology—Mini Review. *Rambam. Maimonides. Med. J.* **3**.

Ross, F.P., and Teitelbaum, S.L. (2005) αvβ3 and macrophage colony-stimulating factor: partners in osteoclast biology. *Immunol. Rev.* **208**: 88-105.

Rothney, M.P., Brychta, R.J., Schaefer, E.V., Chen, K.Y., and Skarulis, M.C. (2009) Body composition measured by dual-energy x-ray absorptiometry half-body scans in obese adults. *Obesity* **17**: 1281-1286.

Rüegsegger, P., Elsasser, U., Anliker, M., Gnehm, H., Kind, H., and Prader, A. (1976) Quantification of bone mineralization using computed tomography. *Radiology* **121**: 93-97.

Saika, M., Inoue, D., Kido, S., and Matsumoto, T. (2001) 17β-estradiol stimulates expression of osteoprotegerin by a mouse stromal lell line, ST-2, via estrogen receptor-α 1. *Endocrinology* **142**: 2205-2212.

Samelson, E.J., Cupples, L.A., Hannan, M.T., Wilson, P.W.F., Williams, S.A., Vaccarino, V., Zhang, Y., and Kiel, D.P. (2004) Long-term effects of serum cholesterol on bone mineral density in women and men: the Framingham Osteoporosis Study. *Bone* **34**: 557-561.

Scalbert, A., Brennan, L., Fiehn, O., Hankemeier, T., Kristal, B.S., van Ommen, B., Pujos-Guillot, E., Verheij, E., Wishart, D., and Wopereis, S. (2009) Mass-spectrometry-based metabolomics: limitations and recommendations for future progress with particular focus on nutrition research. *Metabolomics* **5**: 435.

Schlame, M., and Greenberg, M.L. (2017) Biosynthesis, remodeling and turnover of mitochondrial cardiolipin. *BBA-Mol. Cell. Biol. L.* **1862**: 3-7.

Schorlemmer, S., Ignatius, A., Claes, L., and Augat, P. (2005) Inhibition of cortical and cancellous bone formation in glucocorticoid-treated OVX sheep. *Bone* **37**: 491-496.

Schorlemmer, S., Gohl, C., Iwabu, S., Ignatius, A., Claes, L., and Augat, P. (2003) Glucocorticoid treatment of ovariectomized sheep affects mineral density, structure, and mechanical properties of cancellous bone. *J. Bone Miner. Res.* **18**: 2010.

Seeman, E., and Delmas, P.D. (2006) Bone quality—the material and structural basis of bone strength and fragility. *New Engl. J. Med.* **354**: 2250-2261.

Seibel, M.J. (2005) Biochemical markers of bone turnover part I: biochemistry and variability. *Clin. Biochem. Rev.* **26**: 97.

Seibel, M.J. (2006) Biochemical markers of bone turnover part II: clinical applications in the management of osteoporosis. *Clin. Biochem. Rev.* **27**: 123-138.

Seifert-Klauss, V., Mueller, J.E., Luppa, P., Probst, R., Wilker, J., Höß, C., Treumann, T., Kastner, C., and Ulm, K. (2002) Bone metabolism during the perimenopausal transition: a prospective study. *Maturitas* **41**: 23-33.

Selvamurugan, N., Pulumati, M.R., Tyson, D.R., and Partridge, N.C. (2000) Parathyroid hormone regulation of the rat collagenase-3 promoter by protein kinase A-dependent transactivation of core binding factor α1. *J. Biol. Chem.* **275**: 5037-5042.

Sheu, Y., and Cauley, J.A. (2011) The Role of Bone Marrow and Visceral Fat on Bone Metabolism. *Curr. Osteoporos. Rep.* **9**: 67-75.

Sigrist, I.M., Gerhardt, C., Alini, M., Schneider, E., and Egermann, M. (2007) The long-term effects of ovariectomy on bone metabolism in sheep. *J. Bone Miner. Metab.* **25**: 28-35.

Silva, B.C., and Bilezikian, J.P. (2015) Parathyroid hormone: anabolic and catabolic actions on the skeleton. *Curr. Opin. Pharm.* **22**: 41-50.

Smith, C.A., Want, E.J., O'Maille, G., Abagyan, R., and Siuzdak, G. (2006) XCMS: processing mass spectrometry data for metabolite profiling using nonlinear peak alignment, matching, and identification. *Anal. Chem.* **78**: 779-787.

Snyman, L. (2014) Menopause-related osteoporosis. *S. Afr. Fam. Pract,* **56**: 174-177.

Solomon, D.H., Avorn, J., Canning, C.F., and Wang, P.S. (2005) Lipid levels and bone mineral density. *Am. J. Med.* **118**.

Sousa, S., Teixeira, D., Santos, C., Delerue-Matos, C., Calhau, C., and Domingues, V.F. (2018) The relationship of plasma fatty acid profile and metabolic biomarkers among postmenopausal obese and overweight women. *Obes. Med.* **10**: 8-15.

Stevens, M.M. (2008) Biomaterials for bone tissue engineering. *Mater. Today* **11**: 18-25.

Streicher, C., Heyny, A., Andrukhova, O., Haigl, B., Slavic, S., Schüler, C., Kollmann, K., Kantner, I., Sexl, V., Kleiter, M., Hofbauer, L.C., Kostenuik, P.J., and Erben, R.G. (2017) Estrogen regulates bone turnover by targeting RANKL expression in bone lining cells. *Sci. Rep.* **7**: 6460.

Styczynski, M.P., Moxley, J.F., Tong, L.V., Walther, J.L., Jensen, K.L., and Stephanopoulos, G.N. (2007) Systematic identification of conserved metabolites in GC/MS data for metabolomics and biomarker discovery. *Anal. Chem.* **79**: 966-973.

Sugimoto, M., Kawakami, M., Robert, M., Soga, T., and Tomita, M. (2012) Bioinformatics tools for mass spectroscopy-based metabolomic data processing and analysis. *Curr. Bioinform.* **7**: 96-108.

Swaminathan, R. (2001) Biochemical markers of bone turnover. *Clin. Chim. Acta* **313**: 95-105.

Sysi-Aho, M., Katajamaa, M., Yetukuri, L., and Orešič, M. (2007) Normalization method for metabolomics data using optimal selection of multiple internal standards. *BMC Bioinformatics* **8**: 93.

Szabo, K.A., Webber, C.E., Gordon, C., Adachi, J.D., Tozer, R., and Papaioannou, A. (2011) Reproducibility of peripheral quantitative computed tomography measurements at the radius and tibia in healthy pre- and postmenopausal women. *Can. Assoc. Radiol. J.* **62**: 183-189.

Szulc, P. (2012) The role of bone turnover markers in monitoring treatment in postmenopausal osteoporosis. *Clin. Biochem.* **45**: 907-919.

Takeshita, S., Namba, N., Zhao, J.J., Jiang, Y., Genant, H.K., Silva, M.J., Brodt, M.D., Helgason, C.D., Kalesnikoff, J., Rauh, M.J., Humphries, R.K., Krystal, G., Teitelbaum, S.L., and Ross, F.P. (2002) SHIP-deficient mice are severely osteoporotic due to increased numbers of hyper-resorptive osteoclasts. *Nat. Med.* **8**: 943.

Takuma, A., Kaneda, T., Sato, T., Ninomiya, S., Kumegawa, M., and Hakeda, Y. (2003) Dexamethasone enhances osteoclast formation synergistically with transforming growth factor-β by stimulating the priming of osteoclast progenitors for differentiation into osteoclasts. *J. Biol. Chem.* **278**: 44667-44674.

Tankó, L.B., Bagger, Y.Z., Nielsen, S.B., and Christiansen, C. (2003) Does serum cholesterol contribute to vertebral bone loss in postmenopausal women? *Bone* **32**: 8-14.

Teitelbaum, S.L. (2000) Bone resorption by osteoclasts. *Science* **289**: 1504-1508.

Teitelbaum, S.L., and Ross, F.P. (2003) Genetic regulation of osteoclast development and function. *Nat. Rev. Genet.* **4**: 638-649.

Tepper, C.G., Jayadev, S., Liu, B., Bielawska, A., Wolff, R., Yonehara, S., Hannun, Y.A., and Seldin, M.F. (1995) Role for ceramide as an endogenous mediator of Fas-induced cytotoxicity. *Proc. Natl. Acad. Sci.* **92**: 8443.

Teti, A. (2013) Mechanisms of osteoclast-dependent bone formation. *BoneKEy Rep* **2**.

Thaler, R., Agsten, M., Spitzer, S., Paschalis, E.P., Karlic, H., Klaushofer, K., and Varga, F. (2011) Homocysteine suppresses the expression of the collagen cross-linker lysyl oxidase involving IL-6, Fli1, and epigenetic DNA methylation. *J. Biol. Chem.* **286**: 5578-5588.

Theodoridis, G., Gika, H.G., and Wilson, I.D. (2008) LC-MS-based methodology for global metabolite profiling in metabonomics/metabolomics. *Trac-Trend. Anal. Chem.* **27**: 251-260.

Theodoridis, G.A., Gika, H.G., Want, E.J., and Wilson, I.D. (2012) Liquid chromatography–mass spectrometry based global metabolite profiling: A review. *Anal. Chim. Acta* **711**: 7-16.

Thompson, D.D., Simmons, H.A., Pirie, C.M., and Ke, H.Z. (1995) FDA guidelines and animal models for osteoporosis. *Bone* **17**: S125-S133.

Tian, L.I., and Yu, X. (2015) Lipid metabolism disorders and bone dysfunction-interrelated and mutually regulated (Review). *Mol. Med. Rep.* **12**: 783-794.

Tintut, Y., and Demer, L.L. (2014) Effects of bioactive lipids and lipoproteins on bone. *Trends Endocrinol. Metab.* **25**: 53-59.

Tranquilli Leali, P., Doria, C., Zachos, A., Ruggiu, A., Milia, F., and Barca, F. (2009) Bone fragility: current reviews and clinical features. *Clinical cases in mineral and bone metabolism : the official journal of the Italian Society of Osteoporosis, Mineral Metabolism, and Skeletal Diseases* **6**: 109-113.

Triba, M.N., Le Moyec, L., Amathieu, R., Goossens, C., Bouchemal, N., Nahon, P., Rutledge, D.N., and Savarin, P. (2015) PLS/OPLS models in metabolomics: the impact of permutation of dataset rows on the K-fold cross-validation quality parameters. *Mol. BioSyst.* **11**: 13-19.

Trivedi, D.K., Hollywood, K.A., and Goodacre, R. (2017) Metabolomics for the masses: The future of metabolomics in a personalized world. *New. Horiz. Transl. Med.* **3**: 294-305.

Trushina, E., and Mielke, M.M. (2014) Recent advances in the application of metabolomics to Alzheimer's disease. *Biochim. Biophys. Acta.* **1842**: 1232-1239.

Trygg, J., and Wold, S. (2002) Orthogonal projections to latent structures (O-PLS). *J. Chemometrics* **16**: 119-128.

Tsartsalis, A.N., Dokos, C., Kaiafa, G.D., Tsartsalis, D.N., Kattamis, A., Hatzitolios, A.I., and Savopoulos, C.G. (2012) Statins, bone formation and osteoporosis: hope or hype. *Hormones (Athens)* **11**: 126-139.

Turecek, C., Fratzl-Zelman, N., Rumpler, M., Buchinger, B., Spitzer, S., Zoehrer, R., Durchschlag, E., Klaushofer, K., Paschalis, E.P., and Varga, F. (2008) Collagen cross-linking influences osteoblastic differentiation. *Calcif. Tissue Int.* **82**: 392-400.

Turner, A., Alvis, M., Myers, W., Stevens, M., and Lundy, M. (1995) Changes in bone mineral density and bone-specific alkaline phosphatase in ovariectomized ewes. *Bone* **17**: S395-S402.

Turner, A.S. (2001) Animal models of osteoporosis—necessity and limitations. *Eur Cell Mater* **1**: 13.

Turner, C.H. (2002) Biomechanics of Bone: Determinants of Skeletal Fragility and Bone Quality. *Osteoporosis Int.* **13**: 97-104.

Turner, C.H. (2006) Bone strength: current concepts. *Ann. N. Y. Acad. Sci.* **1068**: 429-446.

Tyagi, N., Kandel, M., Munjal, C., Qipshidze, N., Vacek, J.C., Pushpakumar, S.B., Metreveli, N., and Tyagi, S.C. (2011) Homocysteine mediated decrease in bone blood flow and remodeling: role of folic acid. *J. Orth. Res.* **29**: 1511-1516.

Vaananen, H., Zhao, H., Mulari, M., and Halleen, J.M. (2000) The cell biology of osteoclast function. *J. Cell Sci.* **113**: 377-381.

Väänänen, H.K., Liu, Y.-k., Lehenkari, P., and Uemara, T. (1998) How do osteoclasts resorb bone? *Mat. Sci. Eng. C-Mater.* **6**: 205-209.

Vacek, T.P., Kalani, A., Voor, M.J., Tyagi, S.C., and Tyagi, N. (2013) The role of homocysteine in bone remodeling. *Clin. Chem. Lab. Med.* **51**: 579-590.

van den Berg, R.A., Hoefsloot, H.C.J., Westerhuis, J.A., Smilde, A.K., and van der Werf, M.J. (2006) Centering, scaling, and transformations: improving the biological information content of metabolomics data. *BMC Genomics* **7**: 142.

van Meurs, J.B.J., Dhonukshe-Rutten, R.A.M., Pluijm, S.M.F., van der Klift, M., de Jonge, R., Lindemans, J., de Groot, L.C.P.G.M., Hofman, A., Witteman, J.C.M., van Leeuwen, J.P.T.M., Breteler, M.M.B., Lips, P., Pols, H.A.P., and Uitterlinden, A.G. (2004) Homocysteine levels and the risk of osteoporotic fracture. *New Engl. J. Med.* **350**: 2033-2041.

Van Staa, T., Leufkens, H., and Cooper, C. (2002) The epidemiology of corticosteroid-induced osteoporosis: a meta-analysis. *Osteoporosis Int.* **13**: 777-787.

Van Staa, T., Leufkens, H., Abenhaim, L., Zhang, B., and Cooper, C. (2005) Use of oral corticosteroids and risk of fractures. *J. Bone Miner. Res.* **20**: 1486-1493.

van Staa, T.P. (2006) The pathogenesis, epidemiology and management of glucocorticoid-induced osteoporosis. *Calcif. Tissue Int.* **79**: 129-137.

Varanasi, S.S., Francis, R.M., Berger, C.E.M., Papiha, S.S., and Datta, H.K. (1999) Mitochondrial DNA deletion associated oxidative stress and severe male osteoporosis. *Osteoporosis Int.* **10**: 143-149.

Vasikaran, S., Eastell, R., Bruyère, O., Foldes, A., Garnero, P., Griesmacher, A., McClung, M., Morris, H., Silverman, S., and Trenti, T. (2011a) Markers of bone turnover for the prediction of fracture risk and monitoring of osteoporosis treatment: a need for international reference standards. *Osteoporosis Int.* **22**: 391-420.

Vasikaran, S., Eastell, R., Bruyère, O., Foldes, A.J., Garnero, P., Griesmacher, A., McClung, M., Morris, H.A., Silverman, S., Trenti, T., Wahl, D.A., Cooper, C., and Kanis, J.A. (2011b) Markers of bone turnover for the prediction of fracture risk and monitoring of osteoporosis treatment: a need for international reference standards. *Osteoporosis Int.* **22**: 391-420.

Veigel, E., Moore, R., Zarrinkalam, M., Schulze, D., Sauerbier, S., Schmelzeisen, R., and Voss, P. (2011) Osteopenia in the maxillofacial area: a study in sheep. *Osteoporosis Int.* **22**: 1115-1121.

Verma, S., Rajaratnam, J.H., Denton, J., Hoyland, J.A., and Byers, R.J. (2002) Adipocytic proportion of bone marrow is inversely related to bone formation in osteoporosis. *J. Clin. Pathol.* **55**: 693-698.

Viguet-Carrin, S., Garnero, P., and Delmas, P.D. (2006) The role of collagen in bone strength. *Osteoporosis Int.* **17**: 319-336.

Vinaixa, M., Samino, S., Saez, I., Duran, J., Guinovart, J.J., and Yanes, O. (2012) A guideline to univariate statistical analysis for LC-MS-based untargeted metabolomics-derived data. *Metabolites* **2**: 775-795.

Vinaixa, M., Schymanski, E.L., Neumann, S., Navarro, M., Salek, R.M., and Yanes, O. (2016) Mass spectral databases for LC/MS- and GC/MS-based metabolomics: State of the field and future prospects. *TrAC Trends in Analytical Chemistry* **78**: 23-35.

Vinayavekhin, N., Sueajai, J., Chaihad, N., Panrak, R., Chokchaisiri, R., Sangvanich, P., Suksamrarn, A., and Piyachaturawat, P. (2016) Serum lipidomics analysis of ovariectomized rats under Curcuma comosa treatment. *J. Ethnopharmacol.* **192**: 273-282.

Vuckovic, D. (2012) Current trends and challenges in sample preparation for global metabolomics using liquid chromatography–mass spectrometry. *Anal. Bioanal. Chem.* **403**: 1523-1548.

Wada, T., Nakashima, T., Hiroshi, N., and Penninger, J.M. (2006) RANKL–RANK signaling in osteoclastogenesis and bone disease. *Trends Mol. Med.* **12**: 17-25.

Wang, Q., Ferreira, D.L.S., Nelson, S.M., Sattar, N., Ala-Korpela, M., and Lawlor, D.A. (2018) Metabolic characterization of menopause: cross-sectional and longitudinal evidence. *BMC Medicine* **16**: 17.

Wein, M.N., and Kronenberg, H.M. (2018) Regulation of Bone Remodeling by Parathyroid Hormone. *Cold. Spring. Harb. Perspect. Med.* **8**.

Weinstein, R.S. (2010) Glucocorticoids, osteocytes, and skeletal fragility: The role of bone vascularity. *Bone* **46**: 564-570.

Weitzmann, M.N., and Pacifici, R. (2006) Estrogen deficiency and bone loss: an inflammatory tale. *J. Clin. Invest.* **116**: 1186-1194.

Wheater, G., Elshahaly, M., Tuck, S.P., Datta, H.K., and van Laar, J.M. (2013) The clinical utility of bone marker measurements in osteoporosis. *J. Transl. Med.* **11**: 201.

Wheelock, Å.M., and Wheelock, C.E. (2013) Trials and tribulations of 'omics data analysis: assessing quality of SIMCA-based multivariate models using examples from pulmonary medicine. *Mol. BioSyst.* **9**: 2589-2596.

Whitfield, P.D., German, A.J., and Noble, P.-J.M. (2004) Metabolomics: an emerging post-genomic tool for nutrition. *Br. J. Nutr.* **92**: 549-555.

Wijenayaka, A.R., Kogawa, M., Lim, H.P., Bonewald, L.F., Findlay, D.M., and Atkins, G.J. (2011) Sclerostin stimulates osteocyte support of osteoclast activity by a RANKL-dependent pathway. *PloS one* **6**: e25900.

Wilke, H.-J., Kettler, A., and Claes, L.E. (1997) Are sheep spines a valid biomechanical model for human spines? *Spine* **22**: 2365-2374.

Wilkens, M.R., Liesegang, A., Richter, J., Fraser, D.R., Breves, G., and Schröder, B. (2014) Differences in peripartal plasma parameters related to calcium homeostasis of dairy sheep and goats in comparison with cows. *J. Dairy Res.* **81**: 325.

Wishart, D.S., Jewison, T., Guo, A.C., Wilson, M., Knox, C., Liu, Y., Djoumbou, Y., Mandal, R., Aziat, F., Dong, E., Bouatra, S., Sinelnikov, I., Arndt, D., Xia, J., Liu, P., Yallou, F., Bjorndahl, T., Perez-Pineiro, R., Eisner, R., Allen, F., Neveu, V., Greiner, R., and Scalbert, A. (2013) HMDB 3.0—The Human Metabolome Database in 2013. *Nucleic Acids Res.* **41**: D801-D807.

Wolfender, J.-L., Marti, G., Thomas, A., and Bertrand, S. (2015) Current approaches and challenges for the metabolite profiling of complex natural extracts. *J. Chromatogr.* **1382**: 136-164.

Wood, S.L., Westbrook, J.A., and Brown, J.E. (2014) Omic-profiling in breast cancer metastasis to bone: implications for mechanisms, biomarkers and treatment. *Cancer. Treat. Rev.* **40**: 139-152.

World Health Organization (1994) Assessment of fracture risk and its application to screening for postmenopausal osteoporosis: report of a WHO study group [meeting held in Rome from 22 to 25 June 1992].

Wu, Z.-x., Lei, W., Hu, Y.-y., Wang, H.-q., Wan, S.-y., Ma, Z.-s., Sang, H.-x., Fu, S.-c., and Han, Y.-s. (2008) Effect of ovariectomy on BMD, micro-architecture and biomechanics of cortical and cancellous bones in a sheep model. *Med. Eng. Phys.* **30**: 1112-1118.

Xia, J., and Wishart, D.S. (2002) Metabolomic data processing, analysis, and interpretation using MetaboAnalyst. In *Curr. Protoc. Bioinformatics*: John Wiley & Sons, Inc.

Xia, J., Sinelnikov, I.V., Han, B., and Wishart, D.S. (2015) MetaboAnalyst 3.0—making metabolomics more meaningful. *Nucleic Acids Res.* **43**: W251-W257.

Xiao, J.F., Zhou, B., and Ressom, H.W. (2012) Metabolite identification and quantitation in LC-MS/MS-based metabolomics. *TrAC Trends in Analytical Chemistry* **32**: 1-14.

Xu, J., Begley, P., Church, S.J., Patassini, S., Hollywood, K.A., Jüllig, M., Curtis, M.A., Waldvogel, H.J., Faull, R.L.M., Unwin, R.D., and Cooper, G.J.S. (2016) Graded perturbations of metabolism in multiple regions of human brain in Alzheimer's disease: snapshot of a pervasive metabolic disorder. *Biochim. Biophys. Acta.* **1862**: 1084-1092.

Xue, L., Wang, Y., Liu, L., Zhao, L., Han, T., Zhang, Q., and Qin, L. (2011) A 1HNMR-sased metabonomics study of postmenopausal osteoporosis and intervention effects of Er-Xian decoction in ovariectomized rats. *Int. J. Mol. Sci.* **12**.

Yamashita, T., Takahashi, N., and Udagawa, N. (2012) New roles of osteoblasts involved in osteoclast differentiation. *World J. Orthop.* **3**: 175-181.

Yamatani, H., Takahashi, K., Yoshida, T., Soga, T., and Kurachi, H. (2014) Differences in the fatty acid metabolism of visceral adipose tissue in postmenopausal women. *Menopause* **21**: 170-176.

Yamauchi, M., and Shiiba, M. (2008) Lysine Hydroxylation and Cross-linking of Collagen. In *Post-translational modifications of proteins: tools for functional proteomics*. Kannicht, C. (ed). Totowa, NJ: Humana Press, pp. 95-108.

Yang, J., Hu, X., Zhang, Q., Cao, H., Wang, J., and Liu, B. (2012) Homocysteine level and risk of fracture: a meta-analysis and systematic review. *Bone* **51**: 376-382.

Yeung, D.K.W., Griffith, J.F., Antonio, G.E., Lee, F.K.H., Woo, J., and Leung, P.C. (2005) Osteoporosis is associated with increased marrow fat content and decreased marrow fat unsaturation: A proton MR spectroscopy study. *J. Magn. Reson. Imaging* **22**: 279-285.

Yin, P., Lehmann, R., and Xu, G. (2015) Effects of pre-analytical processes on blood samples used in metabolomics studies. *Anal. Bioanal. Chem.* **407**: 4879-4892.

Yin, P., Peter, A., Franken, H., Zhao, X., Neukamm, S.S., Rosenbaum, L., Lucio, M., Zell, A., Häring, H.-U., Xu, G., and Lehmann, R. (2013) Preanalytical aspects and sample quality assessment in metabolomics studies of human blood. *Clin. Chem.*: clinchem.2012.199257.

Yoon, K.-H., Cho, D.-C., Yu, S.-H., Kim, K.-T., Jeon, Y., and Sung, J.-K. (2012) The change of bone metabolism in ovariectomized rats: analyses of microCT scan and biochemical markers of bone turnover. *J. Korean. Neurosurg. Soc.* **51**: 323-327.

You, Y.-S., Lin, C.-Y., Liang, H.-J., Lee, S.-H., Tsai, K.-S., Chiou, J.-M., Chen, Y.-C., Tsao, C.-K., and Chen, J.-H. (2014) Association between the metabolome and low bone mineral density in Taiwanese women determined by 1H NMR spectroscopy. *J. Bone Miner. Res.* **29**: 212-222.

Young, M.F. (2003) Bone matrix proteins: their function, regulation, and relationship to osteoporosis. *Osteoporosis Int.* **14**: 35-42.

Zarrinkalam, M.-R., Schultz, C.G., Parkinson, I.H., and Moore, R.J. (2012) Osteoporotic characteristics persist in the spine of ovariectomized sheep after withdrawal of corticosteroid administration. *J. Osteoporosis* **2012**: 6.

Zarrinkalam, M., Beard, H., Schultz, C., and Moore, R. (2009a) Validation of the sheep as a large animal model for the study of vertebral osteoporosis. *Eur. Spine. J.* **18**: 244-253.

Zarrinkalam, M.R., Beard, H., Schultz, C.G., and Moore, R.J. (2009b) Validation of the sheep as a large animal model for the study of vertebral osteoporosis. *Eur. Spine. J.* **18**: 244-253.

Zernicke, R., MacKay, C., and Lorincz, C. (2006) Mechanisms of bone remodeling during weight-bearing exercise. *Appl. Physiol. Nutr. Metab.* **31**: 655-660.

Zhang, A., Sun, H., Wang, P., Han, Y., and Wang, X. (2012) Modern analytical techniques in metabolomics analysis. *Analyst* **137**: 293.

Zhang, L., Wang, Y., Xu, Y., Lei, H., Zhao, Y., Li, H., Lin, X., Chen, G., and Tang, H. (2014a) Metabonomic analysis reveals efficient ameliorating effects of acupoint stimulations on the menopause-caused alterations in mammalian metabolism. *Sci. Rep.* **4**: 3641.

Zhang, W., Feng, F., Wang, W.Z., Li, M.B., Ji, G., and Guan, C. (2007) The effects of BCAA-enriched amino acid solution on immune function and protein metabolism in postoperative patients with rectal cancer. *J. Parenter. Enteral. Nutr.* **2**.

Zhang, Y., Li, Y., Gao, Q., Shao, B., Xiao, J., Zhou, H., Niu, Q., Shen, M., Liu, B., and Hu, K. (2014b) The variation of cancellous bones at lumbar vertebra, femoral neck, mandibular angle and rib in ovariectomized sheep. *Arch. Oral. Biol.* **59**: 663-669.

Zhao, H., Li, X., Zhang, D., Chen, H., Chao, Y., Wu, K., Dong, X., and Su, J. (2018a) Integrative Bone Metabolomics—Lipidomics Strategy for Pathological Mechanism of Postmenopausal Osteoporosis Mouse Model. *Sci. Rep.* **8**: 16456.

Zhao, J.-W., Gao, Z.-L., Wang, Y., Mei, H., and Li, Y.-L. Differentiation of human mesenchymal stem cells: the potential mechanism for estrogen-induced preferential osteoblast versus adipocyte differentiation. *Am. J. Med. Sci.* **341**: 460-468.

Zhao, Q., Shen, H., Su, K.-J., Zhang, J.-G., Tian, Q., Zhao, L.-J., Qiu, C., Zhang, Q., Garrett, T.J., and Liu, J. (2018b) Metabolomic profiles associated with bone mineral density in US Caucasian women. *Nutrition & metabolism* **15**: 57.

Zheng, S.X., Vrindts, Y., Lopez, M., De Groote, D., Zangerle, P.F., Collette, J., Franchimont, N., Geenen, V., Albert, A., and Reginster, J.Y. (1997) Increase in cytokine production (IL-1β, IL-6, TNF-α but not IFN-γ, GM-CSF or LIF) by stimulated whole blood cells in postmenopausal osteoporosis. *Maturitas* **26**: 63-71.

Zheng, W., Kollmeyer, J., Symolon, H., Momin, A., Munter, E., Wang, E., Kelly, S., Allegood, J.C., Liu, Y., Peng, Q., Ramaraju, H., Sullards, M.C., Cabot, M., and Merrill, A.H. (2006) Ceramides and other bioactive sphingolipid backbones in health and disease: lipidomic analysis, metabolism and roles in membrane structure, dynamics, signaling and autophagy. *BBA-Biomembranes* **1758**: 1864-1884.

Zhou, B., Xiao, J.F., Tuli, L., and Ressom, H.W. (2012) LC-MS-based metabolomics. *Mol. BioSyst.* **8**: 470-481.

Zhou, S., Zilberman, Y., Wassermann, K., Bain, S.D., Sadovsky, Y., and Gazit, D. (2001) Estrogen modulates estrogen receptor α and β expression, osteogenic

activity, and apoptosis in mesenchymal stem cells (MSCs) of osteoporotic mice. *J. Cell. Biochem.* **81**: 144-155.

Zhou, S., Greenberger, J.S., Epperly, M.W., Goff, J.P., Adler, C., LeBoff, M.S., and Glowacki, J. (2008) Age-Related Intrinsic Changes in Human Bone Marrow-Derived Mesenchymal Stem Cells and Their Differentiation to Osteoblasts. *Aging cell* **7**: 335-343.

Zhu, W., Chen, T., Ding, S., Yang, G., Xu, Z., Xu, K., Zhang, S., Ma, T., and Zhang, J. (2016) Metabolomic study of the bone trabecula of osteonecrosis femoral head patients based on UPLC–MS/MS. *Metabolomics* **12**: 1-14.

Zhu, X., Liu, X., He, P., Cao, B., Lv, Y., Zhang, W., and Ni, X. (2010) Metabolomics in serum of ovariectomised rats and those exposed to 17β-oestradiol and genistein. *Gynecol. Endocrinol.* **26**: 760-767.

Zou, W., She, J., and Tolstikov, V.V. (2013) A comprehensive workflow of mass spectrometry-based untargeted metabolomics in cancer metabolic biomarker discovery using human plasma and urine. *Metabolites* **3**: 787-819.

Zubarev, R.A., and Makarov, A. (2013) Orbitrap Mass Spectrometry. *Anal. Chem.* **85**: 5288-5296.

Appendix A. Statement of contributions

MASSEY UNIVERSITY
GRADUATE RESEARCH SCHOOL

STATEMENT OF CONTRIBUTION
TO DOCTORAL THESIS CONTAINING PUBLICATIONS

(To appear at the end of each thesis chapter/section/appendix submitted as an article/paper or collected as an appendix at the end of the thesis)

We, the candidate and the candidate's Principal Supervisor, certify that all co-authors have consented to their work being included in the thesis and they have accepted the candidate's contribution as indicated below in the Statement of Originality.

Name of Candidate: Diana Leticia Cabrera-Amaro

Name/Title of Principal Supervisor: Marlena Kruger

Name of Published Research Output and full reference:

Cabrera, D., Kruger, M., Wolber, F. M., Roy, N. C., Totman, J. J., Henry, C. J., Cameron-Smith D. and Fraser, K. 2018. Association of Plasma Lipids and Polar Metabolites with Low Bone Mineral Density in Singaporean-Chinese Menopausal Women: A Pilot Study.Int. J. Environ. Res. Public Health. https://doi.org/10.3390/ijerph15051045

In which Chapter is the Published Work: Chapter 7

Please indicate either:

- The percentage of the Published Work that was contributed by the candidate: 90

  and / or
- Describe the contribution that the candidate has made to the Published Work:

  Chemical analysis, stats, writing

Candidate's Signature — 5/9/18 Date

MCKruger

Principal Supervisor's signature — 5/9/18 Date

GRS Version 3– 16 September 2011

MASSEY UNIVERSITY
GRADUATE RESEARCH SCHOOL

STATEMENT OF CONTRIBUTION
DOCTORATE WITH PUBLICATIONS/MANUSCRIPTS

We, the candidate and the candidate's Primary Supervisor, certify that all co-authors have consented to their work being included in the thesis and they have accepted the candidate's contribution as indicated below in the *Statement of Originality*.

Name of candidate:	Diana Leticia Cabrera-Amaro
Name/title of Primary Supervisor:	Marlena Kruger
Name of Research Output and full reference:	
Cabrera et al. 2018/Glucocorticoids affect bone mineral density and bone remodelling in OVX sheep: A pilot Bone Reports, 9, 173-180	
In which Chapter is the Manuscript /Published work:	
Please indicate:	
• The percentage of the manuscript/Published Work that was contributed by the candidate:	90
and	
• Describe the contribution that the candidate has made to the Manuscript/Published Work:	
Performed the majority of the experiments. Contributed materials/analysis. Drafted the manuscript. All authors read and approved the final manuscript.	
For manuscripts intended for publication please indicate target journal:	
Candidate's Signature:	Diana Cabrera Digitally signed by Diana Cabrera DN: cn=Diana Cabrera, o, ou, email=Diana.cabrera@agresearch.co.nz, c=NZ Date: 2019.03.03 17:28:28 +13'00'
Date:	2/03/2019
Primary Supervisor's Signature:	Marlena Kruger Digitally signed by Marlena Kruger Date: 2019.03.03 14:10:56 +13'00'
Date:	3/3/19

(This form should appear at the end of each thesis chapter/section/appendix submitted as a manuscript/ publication or collected as an appendix at the end of the thesis)

Appendix B. Effect of OVX on the plasma metabolome of sheep

PCA: short-term approach

PCA was used to analyse the plasma metabolite profiles of all treatments groups per individual time point. No noticeable differences can be observed in the PCA over two months. At baseline, the resulting scatter plot of PC1 and PC2, which explains 28.1% of the variance, showed that over time samples were clustered in the middle of the plot. One outlier from the control group and one from the OVX group were observed. Moreover, at month one a smaller difference was noticed between the OVXG group and the OVX group as shown by separation (Figure B.1B), as well as between the OVX group and control group, where PC1 and PC2 explained 35.3% of the variance. Two outliers were observed in the OVX group and one in the control group. However, at month two (Figure B.1C), the largest difference can be noticed between the OVXG group compared with OVX group, where the resulting scatter plot of PC1 and PC2 explained 30.1% of the variance. One outlier was observed in the control group. These results show that the samples have different metabolite profiles over time. The fact that bone metabolism is increased after oestrogen withdrawal suggests that rapid changes observed in the metabolome are in response to the surgical or hormonal interventions.

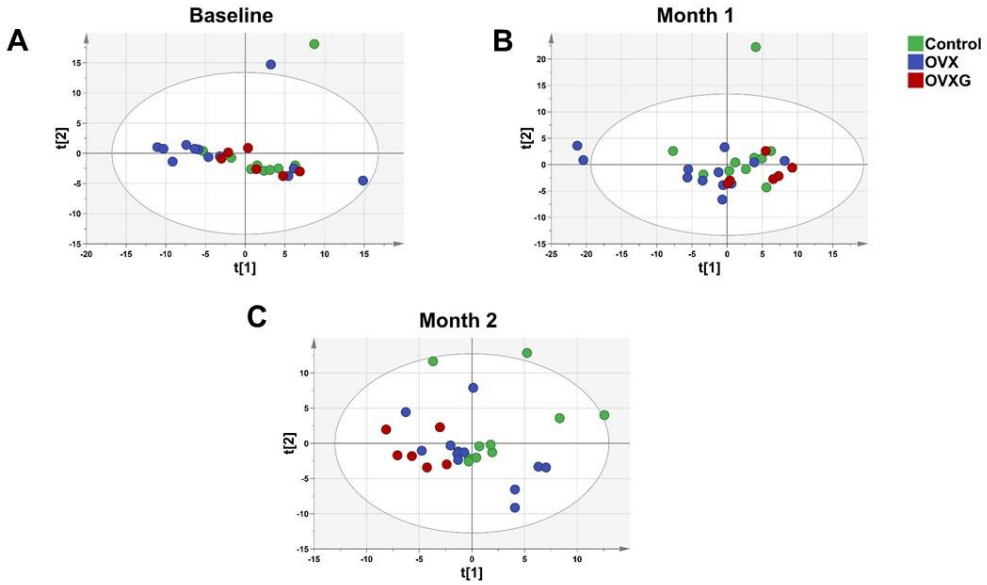

Figure B.1: Inter-animal variation in the plasma metabolome of sheep over two months of the study period. PCA scatter plots derived from HILIC-MS spectra dataset based on normalised and autoscaled data. Each data point represents the metabolite profile of a single ewe. PCA scoring plot showing the variation of control group (●), OVX group (●) and OVXG (●) at baseline measurement (**A**) 28.1% R2 = 54.2% and Q2 = -5.5%, month one (**B**) 35.3%, R2 = 53.8% and Q2= 16%, month two (**C**) 30.1%, R2 = 30% and Q2 = 1.8%

Linear mixed model: short-term approach

In this study, multiple circulating compounds were identified (annotated and unknown). Among the 26 features that showed significance based on the interaction, treatment, 18 remaining unidentified (unknown) and are presented in Table B.1. Changes on the plasma metabolome of the OVX sheep were observed, and from the statistical analysis those appeared as key features but remained unidentified.

Table B.1: List of unknown features based on the interaction, treatment and time of the metabolite profiles of ewes in the short-term approach.

				Mean						
RT				(Relative intensity, E+05)				*p* -value		
m/z	(sec)	Feature	Trt	0	1	2	SEM	Trt	Time	Int
126.903	493.065	Unknown	Control	4.201	7.376	6.306	1.265	<0.05	<0.05	<0.05
			OVX	7.757	15.257	16.797	1.103			
			OVXG	4.776	20.796	17.399	1.560			
166.087	593.293	Unknown	Control	1.667	2.454	2.589	1.455	0.423	0.001	0.006
			OVX	2.316	1.981	2.877	1.224			
			OVXG	2.249	2.825	2.517	1.432			
132.102	594.714	Unknown	Control	1.117	0.694	0.896	1.117	0.176	0.070	0.033
			OVX	1.097	0.885	0.964	1.097			
			OVXG	0.930	1.205	1.027	0.930			
70.066	653.194	Unknown	Control	6.856	6.341	7.334	0.594	0.040	0.107	0.041
			OVX	7.384	7.436	9.296	0.514			
			OVXG	8.961	7.311	6.748	0.727			
263.996	622.424	Unknown	Control	0.431	0.363	0.380	0.055	0.041	0.217	0.050
			OVX	0.577	0.385	0.447	0.047			
			OVXG	0.439	0.591	0.556	0.067			
147.044	623.194	Unknown	Control	0.373	0.970	0.448	0.094	0.003	0.395	0.001
			OVX	0.467	0.875	0.526	0.081			
			OVXG	0.473	1.364	1.411	0.115			
359.148	624.229	Unknown	Control	0.367	0.412	0.417	0.043	0.007	0.061	0.036
			OVX	0.379	0.277	0.414	0.037			
			OVXG	0.383	0.543	0.566	0.052			
114.029	656.025	Unknown	Control	5.875	8.047	7.622	5.875	0.287	0.001	0.005
			OVX	7.857	6.315	9.771	7.857			
			OVXG	6.536	8.550	9.324	6.536			
98.006	656.046	Unknown	Control	0.298	0.416	0.397	0.038	0.762	0.000	0.016
			OVX	0.367	0.326	0.489	0.033			
			OVXG	0.289	0.445	0.461	0.046			
116.049	657.474	Unknown	Control	1.667	2.454	2.589	0.202	0.423	0.001	0.006
			OVX	2.316	1.981	2.877	0.175			
			OVXG	2.249	2.825	2.517	0.248			
142.065	657.288	Unknown	Control	0.368	0.533	0.566	0.050	0.932	0.067	0.001
			OVX	0.525	0.416	0.581	0.043			
			OVXG	0.487	0.610	0.445	0.061			
146.081	670.701	Unknown	Control	0.975	1.017	0.776	0.102	0.026	0.094	0.044
			OVX	1.107	0.792	1.081	0.089			
			OVXG	1.365	1.198	1.033	0.125			
254.733	730.747	Unknown	Control	0.907	0.666	0.486	0.085	0.524	<0.05	0.021
			OVX	0.718	0.650	0.462	0.074			
			OVXG	1.147	0.573	0.313	0.105			
124.006	797.024	Unknown	Control	19.820	26.279	14.276	2.220	0.001	< 0.05	0.021
			OVX	15.716	19.419	10.694	1.923			
			OVXG	15.567	34.766	20.146	2.720			
127.050	817.752	Unknown	Control	2.762	3.433	3.510	0.237	0.973	0.002	0.036
			OVX	3.297	2.709	3.841	0.205			
			OVXG	3.060	3.140	3.497	0.290			
83.060	851.458	Unknown	Control	0.099	0.179	0.133	0.022	0.086	0.067	0.009
			OVX	0.188	0.151	0.140	0.019			
			OVXG	0.174	0.238	0.183	0.027			
62.963	893.059	Unknown	Control	0.939	0.926	1.014	0.077	0.338	0.009	0.002
			OVX	1.168	0.698	0.880	0.066			
			OVXG	0.923	1.023	1.119	0.094			
453.924	915.178	Unknown	Control	0.174	0.186	0.189	0.021	0.345	0.172	0.008
			OVX	0.241	0.138	0.191	0.019			
			OVXG	0.172	0.223	0.241	0.026			

Effect of OVX on the metabolite profile in OVX sheep: long-term approach

PCA: long-term approach

To further investigate the dynamic changes on the plasma metabolome of OVX sheep, the metabolite profiles of all treatments groups per individual time point were analysed. The results from the PCA did not reveal a clear separation among groups when analysing the metabolite profiles per individual time point. PCA of the metabolite profiles obtained from the analysis of OVX sheep over five months are shown in Figure B.2. The resulting scatter plots showed clearly that animals were clustered in the middle of the plot, suggesting there were only modest differences between the treated animals. A modest difference can be noticed in the OVX group when compared with the control group at month three (Figure B.2D). However, the glucocorticoid-treated ewes OVXG showed a larger difference at month two (Figure B.2C), PC1 and PC2 explained 38.1% of the variance) and month three (Figure B.2D), PC1 and PC2 explained 36.6% of the variance) in comparison with the OVXG2 group and OVX group.

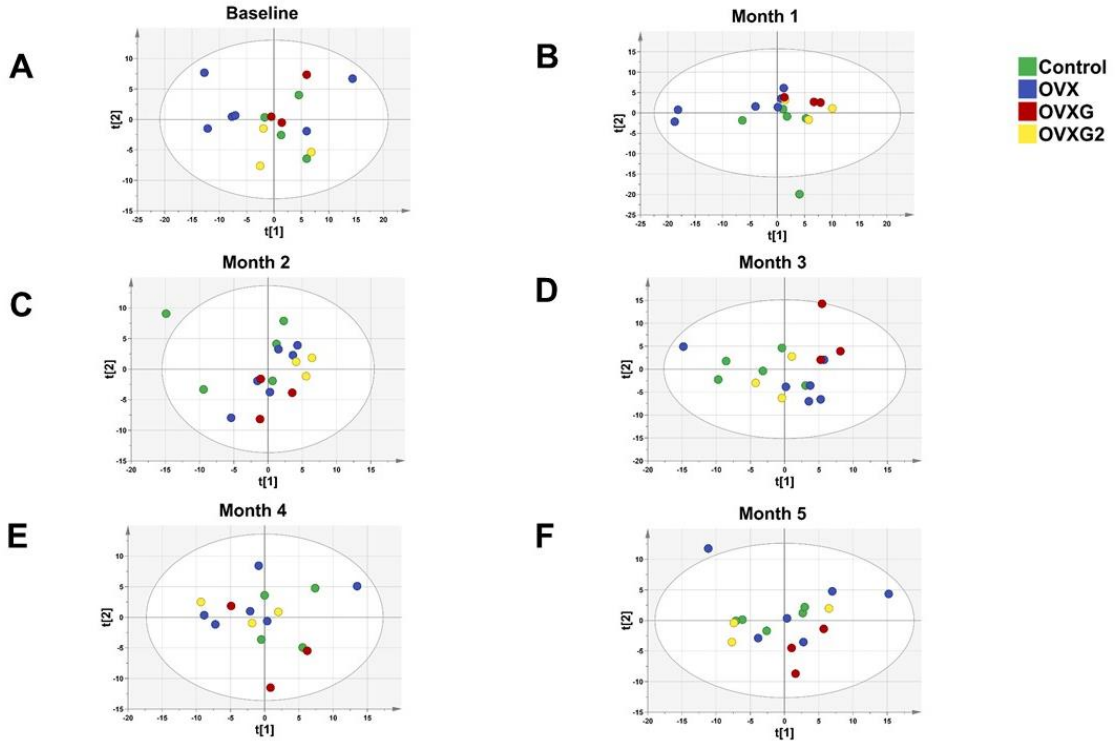

Figure B.2: Inter-animal variation in the plasma metabolome of sheep over five months of the study period. PCA scatter plots derived from HILIC-MS spectra dataset based on normalised and autoscaled data. Each data point represents the metabolite profile of a single ewe. PCA scoring plot showing the variation of control group (●), OVX group (●), OVXG (●) and OVXG2 (●) at baseline measurement (**A**) 39.2% R2 = 49.3% and Q2 = -1.3%, month one (**B**) 49.6%, R2=49.6% and Q2 = 19.2%, month two (**C**) 28.1%, R2 = 48.5% and Q2 = -13.8%, month three (**D**) 44.7%, R2 = 35.6% and Q2 = 0.9%, month four (**E**) 31.4%, R2 = 42.9% and Q2 = -0.08% and month (**F**) 34.1%, R2 = 43.3% and Q2 = -0.5%

Linear mixed model: long-term approach

The metabolites selected by linear mixed model presented a significant interaction between treatment and time; however, 22 remaining unidentified (unknown) and are presented in Table B.2. Dynamic changes on the plasma metabolome of the OVX sheep were noticed, and from the statistical analysis those appeared as key compounds but remained unidentified. This study intended to cover most of the metabolome for the identification and generation of potential diagnostic markers for postmenopausal osteoporosis. Future studies are needed to validate these findings and identify the source adducts or fragment ions.

Table B.2: List of unknown features based on the interaction, treatment and time of the metabolite profiles of ewes in the long-term approach.

				Mean									
m/z	RT			(Relative intensity, E+05)							*p* -value		
	(sec)	Feature	Trt	0	1	2	3	4	5	SEM	Trt	Time	Int
126.903	493.065	Unknown	Control	3.519	6.812	6.257	6.638	6.098	7.815	1.860	0.001	< 0.0001	< 0.0001
			OVX	8.286	14.130	18.537	16.025	13.093	15.041	1.698			
			OVXG	4.471	17.867	17.498	16.371	15.006	18.236	2.401			
			OVXG2	5.080	23.725	17.300	8.747	11.033	7.994	2.401			
148.039	506.035	Unknown	Control	0.336	0.929	0.499	0.859	1.066	0.578	0.929	0.098	0.003	0.013
			OVX	0.696	0.898	0.396	0.695	0.983	1.146	0.898			
			OVXG	0.288	1.058	1.354	0.763	0.962	1.671	1.058			
			OVXG2	0.658	1.671	1.467	1.164	1.609	0.596	1.671			
267.072	588.664	Unknown	Control	2.414	1.753	2.955	3.117	2.330	3.162	0.545	0.347	< 0.0001	0.049
			OVX	4.447	1.661	2.869	2.522	2.973	3.537	0.497			
			OVXG	6.136	1.918	2.351	2.364	1.658	3.078	0.703			
			OVXG2	4.513	3.661	3.893	2.595	2.824	3.738	0.703			
253.966	622.590	Unknown	Control	1.814	2.013	1.894	2.260	2.011	2.302	0.413	0.439	0.182	0.001
			OVX	2.622	1.546	2.236	2.042	1.803	2.637	0.377			
			OVXG	2.275	2.442	2.513	1.430	2.162	1.638	0.533			
			OVXG2	2.118	2.949	2.608	2.000	2.303	2.416	0.533			
117.914	623.014	Unknown	Control	0.321	0.338	0.310	0.396	0.314	0.414	0.035	0.107	0.296	0.002
			OVX	0.351	0.277	0.390	0.351	0.320	0.427	0.032			
			OVXG	0.405	0.376	0.389	0.286	0.384	0.285	0.045			
			OVXG2	0.323	0.520	0.466	0.451	0.399	0.400	0.045			
147.044	623.194	Unknown	Control	0.912	0.993	0.829	1.134	0.892	1.054	0.136	0.113	0.477	0.001
			OVX	1.083	0.565	1.131	0.944	0.979	1.180	0.124			
			OVXG	1.190	1.306	1.343	0.580	1.065	1.025	0.176			
			OVXG2	1.019	1.654	1.461	1.209	1.195	1.187	0.176			
359.148	624.229	Unknown	Control	0.349	0.426	0.412	0.487	0.302	0.420	0.054	0.139	0.081	0.003
			OVX	0.386	0.178	0.448	0.364	0.402	0.435	0.049			
			OVXG	0.346	0.486	0.571	0.262	0.424	0.438	0.070			
			OVXG2	0.419	0.599	0.561	0.386	0.488	0.424	0.070			
144.044	635.951	Unknown	Control	0.290	0.475	0.433	0.420	0.315	0.252	0.096	0.494	< 0.0001	< 0.0001
			OVX	0.487	0.269	0.461	0.409	0.399	0.384	0.088			
			OVXG	0.442	0.854	0.649	0.267	0.348	0.394	0.124			
			OVXG2	0.526	0.824	0.910	0.371	0.290	0.173	0.124			

142.065	657.288	Unknown	Control	0.275	0.560	0.568	0.609	0.496	0.505	0.065	0.588	0.202	0.007
			OVX	0.445	0.327	0.568	0.464	0.454	0.507	0.060			
			OVXG	0.403	0.575	0.467	0.403	0.477	0.473	0.084			
			OVXG2	0.571	0.645	0.423	0.478	0.567	0.590	0.084			
453.924	915.178	Unknown	Control	0.193	0.174	0.220	0.214	0.141	0.184	0.029	0.753	0.042	0.027
			OVX	0.218	0.106	0.231	0.180	0.230	0.252	0.027			
			OVXG	0.138	0.171	0.293	0.168	0.196	0.276	0.038			
			OVXG2	0.206	0.274	0.189	0.180	0.195	0.206	0.038			
146.081	670.701	Unknown	Control	0.857	0.839	0.706	0.861	0.769	0.965	0.162	0.058	0.259	0.035
			OVX	0.912	0.657	1.175	1.072	0.998	1.227	0.148			
			OVXG	1.344	1.044	1.004	0.559	0.814	1.007	0.209			
			OVXG2	1.385	1.352	1.061	0.964	0.937	0.997	0.209			
116.070	686.643	Unknown	Control	0.623	0.539	0.587	0.612	0.525	0.549	0.067	0.418	0.137	0.011
			OVX	0.531	0.377	0.618	0.506	0.610	0.632	0.061			
			OVXG	0.551	0.733	0.661	0.375	0.498	0.639	0.086			
			OVXG2	0.601	0.733	0.835	0.597	0.644	0.506	0.086			
			OVXG2	1.385	1.352	1.061	0.964	0.937	0.997	0.209			
180.065	717.126	Unknown	Control	1.043	1.067	1.267	1.542	1.137	1.257	0.196	0.107	0.043	0.029
			OVX	1.360	0.671	1.434	1.325	1.529	1.522	0.179			
			OVXG	0.881	1.151	1.681	0.856	1.432	1.609	0.253			
			OVXG2	0.951	2.074	1.839	1.605	1.615	1.368	0.253			
248.739	730.524	Unknown	Control	3.215	1.964	1.799	1.312	1.023	0.969	0.259	0.620	< 0.0001	0.017
			OVX	1.903	1.939	1.542	1.211	1.068	1.269	0.237			
			OVXG	3.173	1.841	1.023	0.878	1.005	0.989	0.335			
			OVXG2	3.733	1.780	0.901	0.933	0.926	1.062	0.335			
107.064	766.480	Unknown	Control	2.070	1.783	1.840	1.476	1.721	1.650	0.162	0.599	0.331	0.048
			OVX	1.796	1.478	2.028	1.705	1.795	1.747	0.148			
			OVXG	1.955	2.160	1.983	1.825	1.367	1.681	0.210			
			OVXG2	2.151	1.824	1.417	2.079	2.052	1.917	0.210			

493.064	788.802	Unknown	Control	0.133	0.119	0.105	0.136	0.078	0.062	0.018	0.872	0.042	0.007
			OVX	0.111	0.122	0.125	0.074	0.130	0.121	0.017			
			OVXG	0.075	0.163	0.118	0.100	0.104	0.124	0.024			
			OVXG2	0.156	0.155	0.114	0.080	0.122	0.095	0.024			
766.043	793.674	Unknown	Control	20.467	22.350	17.229	8.492	10.708	11.111	0.022	0.599	0.000	0.018
			OVX	14.046	17.517	11.231	7.508	14.332	12.465	0.020			
			OVXG	14.019	37.016	19.419	12.799	24.222	17.607	0.029			
			OVXG2	17.116	32.516	20.873	13.142	18.187	10.143	0.029			
124.006	797.024	Unknown	Control	0.609	0.752	0.749	0.859	0.593	0.849	2.476	0.009	< 0.0001	0.007
			OVX	0.627	0.483	0.821	0.700	0.797	0.894	2.260			
			OVXG	0.537	0.558	0.721	0.480	0.695	0.723	3.196			
			OVXG2	0.735	0.704	0.707	0.860	0.847	0.911	3.196			
109.039	817.678	Unknown	Control	0.609	0.752	0.749	0.859	0.593	0.849	0.064	0.027	< 0.0001	0.037
			OVX	0.627	0.483	0.821	0.700	0.797	0.894	0.058			
			OVXG	0.537	0.558	0.721	0.480	0.695	0.723	0.083			
			OVXG2	0.735	0.704	0.707	0.860	0.847	0.911	0.083			
168.982	835.422	Unknown	Control	0.786	0.876	0.659	0.622	0.680	0.656	0.113	0.304	0.871	0.010
			OVX	0.477	0.722	0.703	0.687	0.725	0.718	0.103			
			OVXG	0.641	1.043	0.654	0.592	0.478	0.594	0.146			
			OVXG2	0.887	0.293	0.976	1.127	0.673	0.892	0.146			
453.924	915.178	Unknown	Control	0.193	0.174	0.220	0.214	0.141	0.184	0.029	0.753	0.042	0.027
			OVX	0.218	0.106	0.231	0.180	0.230	0.252	0.027			
			OVXG	0.138	0.171	0.293	0.168	0.196	0.276	0.038			
			OVXG2	0.206	0.274	0.189	0.180	0.195	0.206	0.038			
203.081	658.384	Unknown	Control	1.071	1.595	1.513	1.245	1.223	1.358	0.162	0.143	0.106	0.028
			OVX	1.146	0.754	1.463	1.270	1.340	1.190	0.148			
			OVXG	1.098	1.609	1.548	1.030	1.245	1.059	0.209			
			OVXG2	1.635	1.675	1.508	1.211	1.720	1.634	0.209			

Appendix C. Effect of OVX on the plasma lipidome of sheep

PCA: short-term approach

The plasma lipid profiles of all treatments groups per individual time point were analysed using PCA. No noticeable differences can be observed in the PCA over two months. At baseline, the resulting scatter plot showed that samples were clustered in the middle of the plot (Figure C.1A, PC1 and PC2, explained 72.8% of the variance). Two outliers were observed from the OVX group. At month one, a smaller difference between OVX and control was observed (Figure C.1B, PC1 and PC2, explained 68.6% of the variance), where two outliers from the OVXG group were noticed. However, at two months the scatter plots did not reveal differences among the treatment groups (Figure C.1C, PC1 and PC2, explained 64.7% of the variance).

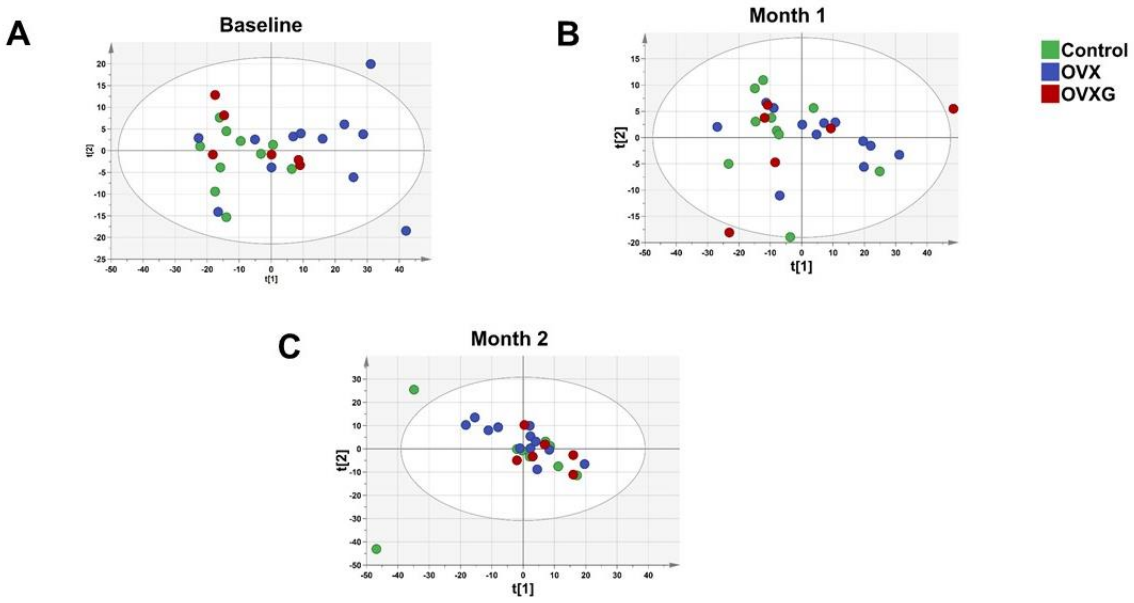

Figure C.1: Inter-animal variation in the plasma lipidome of sheep over two months of the study period. PCA scatter plots derived from UHPLC-MS spectra dataset based on normalised and autoscaled data. Each data point represents the lipid profile of a single ewe. PCA scoring plot showing the variation of control group (●), OVX group (●) and OVXG (●) at baseline measurement (**A**) 71.8% R2 = 72.6% and Q2 = 64.9%, month one (**B**) 68.6%, R2 = 74.9% and Q2 = 60.4%, month two (**C**) 64.7%, R2 = 72.7% and Q2 = 49.9%

Linear mixed model: short-term approach

In this study, multiple circulating compounds were identified (annotated and unknown). Among the 48 features that showed significance based on the interaction, treatment and time, 43 remaining unidentified (unknown) and are presented in Table C.1.

Table C.1: List of unknown features based on the interaction, treatment and time of the lipid profile of ewes in the short-term approach.

				Mean						
RT				(Relative intensity, E+05)				*p* -value		
m/z	(sec)	Feature	Trt	0	1	2	SEM	Trt	Time	Int
301.166	101.547	Unknown	Control	1.189	1.197	1.332	0.098	0.004	0.051	0.009
			OVX	1.880	1.398	1.318	0.098			
			OVXG	1.281	1.398	1.171	0.098			
347.172	101.676	Unknown	Control	4.116	4.115	4.537	0.339	0.003	0.029	0.011
			OVX	6.508	4.889	4.500	0.339			
			OVXG	4.512	4.788	3.962	0.339			
599.360	104.805	Unknown	Control	0.987	1.010	1.107	0.093	0.019	0.026	0.012
			OVX	1.590	1.107	1.039	0.093			
			OVXG	1.059	1.063	0.933	0.093			
473.284	183.588	Unknown	Control	1.460	1.457	1.526	0.078	0.003	0.003	0.003
			OVX	2.058	1.641	1.500	0.078			
			OVXG	1.589	1.662	1.376	0.078			
413.246	183.599	Unknown	Control	0.776	0.821	0.885	0.059	0.005	0.034	0.002
			OVX	1.231	0.924	0.851	0.059			
			OVXG	0.867	0.942	0.781	0.059			
666.537	183.605	Unknown	Control	8.502	8.294	9.521	0.518	0.047	0.047	0.005
			OVX	11.736	9.582	8.475	0.518			
			OVXG	9.360	9.573	8.838	0.518			
736.525	183.608	Unknown	Control	1.443	1.491	1.554	0.073	0.045	0.008	0.001
			OVX	1.980	1.560	1.427	0.073			
			OVXG	1.554	1.568	1.472	0.073			
803.510	183.612	Unknown	Control	0.923	1.013	1.070	0.058	0.034	0.185	0.007
			OVX	1.303	1.077	1.031	0.058			
			OVXG	1.086	1.136	0.922	0.058			
477.344	209.901	Unknown	Control	5.891	5.862	6.370	0.337	0.012	0.016	0.006
			OVX	8.218	6.603	5.973	0.337			
			OVXG	6.358	6.419	5.864	0.337			
404.309	221.664	Unknown	Control	71.500	70.778	76.639	4.135	0.052	0.059	0.041
			OVX	93.896	79.302	72.789	4.135			
			OVXG	78.722	80.643	69.454	4.135			
441.277	221.673	Unknown	Control	4.829	4.901	5.111	0.222	0.019	0.036	0.018
			OVX	6.228	5.280	5.031	0.222			
			OVXG	5.255	5.433	4.645	0.222			

407.293	241.746	Unknown	Control	0.481	0.466	0.515	0.031	0.041	0.066	0.031
			OVX	0.650	0.528	0.481	0.031			
			OVXG	0.490	0.515	0.465	0.031			
569.114	251.228	Unknown	Control	1.808	1.754	1.934	0.138	0.012	0.025	0.037
			OVX	2.570	2.038	1.852	0.138			
			OVXG	1.898	1.962	1.465	0.138			
721.928	252.497	Unknown	Control	1.020	1.000	1.148	0.058	0.015	0.456	0.048
			OVX	1.328	1.162	1.124	0.058			
			OVXG	1.081	1.163	1.015	0.058			
448.442	252.565	Unknown	Control	1.519	1.472	1.593	0.084	0.017	0.043	0.050
			OVX	1.995	1.687	1.557	0.084			
			OVXG	1.637	1.686	1.477	0.084			
454.385	252.671	Unknown	Control	3.065	3.038	3.275	0.151	0.006	0.085	0.037
			OVX	3.996	3.444	3.283	0.151			
			OVXG	3.357	3.471	2.994	0.151			
446.353	252.783	Unknown	Control	2.742	2.714	2.909	0.130	0.020	0.073	0.032
			OVX	3.491	2.992	2.884	0.130			
			OVXG	2.990	3.116	2.647	0.130			
444.356	252.784	Unknown	Control	4.597	4.566	4.882	0.215	0.010	0.054	0.041
			OVX	5.890	5.115	4.817	0.215			
			OVXG	5.010	5.044	4.430	0.215			
431.337	263.058	Unknown	Control	2.063	1.971	2.169	0.122	0.067	0.018	0.034
			OVX	2.731	2.175	2.032	0.122			
			OVXG	2.190	2.168	2.003	0.122			
564.345	273.277	Unknown	Control	2.795	2.810	2.957	0.134	0.003	0.027	0.028
			OVX	3.736	3.160	3.004	0.134			
			OVXG	3.135	3.119	2.770	0.134			
698.436	287.913	Unknown	Control	0.906	0.908	0.942	0.059	0.014	0.028	0.037
			OVX	1.218	0.965	0.944	0.059			
			OVXG	0.926	0.973	0.719	0.059			
459.370	308.910	Unknown	Control	1.804	1.779	2.007	0.099	0.042	0.071	0.013
			OVX	2.382	2.038	1.827	0.099			
			OVXG	1.986	1.961	1.797	0.099			
460.373	308.921	Unknown	Control	0.457	0.450	0.482	0.026	0.023	0.013	0.014
			OVX	0.618	0.511	0.449	0.026			
			OVXG	0.489	0.496	0.444	0.026			
487.400	358.665	Unknown	Control	1.202	1.112	1.226	0.064	0.420	0.013	0.031
			OVX	1.454	1.227	1.068	0.064			
			OVXG	1.216	1.255	1.108	0.064			
474.403	388.188	Unknown	Control	4.694	4.661	4.864	0.186	0.014	0.052	0.041
			OVX	5.788	5.122	4.825	0.186			
			OVXG	4.984	5.205	4.620	0.186			
473.400	388.236	Unknown	Control	14.156	13.953	14.552	0.537	0.009	0.018	0.024
			OVX	17.569	15.330	14.441	0.537			
			OVXG	15.136	15.622	13.944	0.537			
520.409	388.282	Unknown	Control	3.724	3.707	3.911	0.145	0.006	0.126	0.017
			OVX	4.644	4.109	3.863	0.145			
			OVXG	3.788	4.069	3.752	0.145			
748.720	403.700	Unknown	Control	49.719	47.990	54.849	2.778	0.042	0.082	0.007
			OVX	64.615	50.371	52.710	2.778			
			OVXG	48.697	54.006	44.549	2.778			
777.762	448.533	Unknown	Control	0.615	0.611	0.617	0.020	0.039	0.037	0.041
			OVX	0.725	0.630	0.616	0.020			
			OVXG	0.653	0.680	0.646	0.020			
738.371	480.261	Unknown	Control	0.639	0.621	0.724	0.033	0.006	< 0.0001	0.028
			OVX	0.807	0.665	0.746	0.033			
			OVXG	0.744	0.513	0.600	0.033			
1270.904	480.311	Unknown	Control	0.339	0.321	0.380	0.015	0.247	< 0.0001	0.003
			OVX	0.361	0.328	0.363	0.015			
			OVXG	0.386	0.238	0.334	0.015			

603.476	480.371	Unknown	Control	2.468	2.443	2.738	0.108	0.004	0.014	0.039
			OVX	3.035	2.625	2.671	0.108			
			OVXG	2.746	2.172	2.278	0.108			
675.667	517.916	Unknown	Control	2.784	2.955	3.096	0.112	0.175	0.359	0.038
			OVX	3.336	3.100	2.922	0.112			
			OVXG	3.166	2.970	2.774	0.112			
759.761	598.998	Unknown	Control	3.191	3.316	3.486	0.103	0.250	0.602	0.038
			OVX	3.698	3.428	3.326	0.103			
			OVXG	3.450	3.490	3.263	0.103			
656.636	643.039	Unknown	Control	5.546	5.868	6.061	0.179	0.019	0.508	0.028
			OVX	6.714	6.163	6.007	0.179			
			OVXG	6.199	6.190	5.858	0.179			
661.688	748.059	Unknown	Control	62.976	57.301	61.303	2.377	0.653	< 0.0001	0.030
			OVX	70.931	57.483	53.215	2.377			
			OVXG	68.696	54.673	52.120	2.377			
689.719	755.548	Unknown	Control	66.210	62.860	69.761	2.104	0.513	0.003	0.008
			OVX	73.157	65.679	60.308	2.104			
			OVXG	69.649	61.873	60.682	2.104			
1365.857	394.415	Unknown	Control	0.321	0.339	0.379	0.023	0.730	0.366	0.035
			OVX	0.400	0.348	0.340	0.023			
			OVXG	0.404	0.374	0.309	0.023			
1385.971	394.562	Unknown	Control	0.809	0.799	0.810	0.042	0.038	0.019	0.041
			OVX	1.029	0.838	0.821	0.042			
			OVXG	0.831	0.889	0.725	0.042			
1344.933	394.803	Unknown	Control	76.625	76.536	76.360	3.471	0.023	0.017	0.039
			OVX	96.270	80.389	78.735	3.471			
			OVXG	79.118	84.237	71.146	3.471			
1342.926	394.862	Unknown	Control	177.912	177.928	177.483	8.168	0.028	0.017	0.037
			OVX	223.999	186.159	183.731	8.168			
			OVXG	184.501	195.778	165.176	8.168			
1343.930	394.862	Unknown	Control	163.231	163.704	163.149	7.689	0.032	0.022	0.038
			OVX	205.803	171.151	168.513	7.689			
			OVXG	169.094	181.029	151.400	7.689			
1346.938	394.919	Unknown	Control	6.363	6.354	6.304	0.311	0.051	0.022	0.043
			OVX	8.006	6.577	6.558	0.311			
			OVXG	6.637	7.112	5.934	0.311			

Effect of OVX on the plasma lipidome of sheep: long-term approach

PCA: long-term approach

The resulting scatter plots did not show a clear separation among groups when analysing the lipid profiles per individual time point. PCA of the lipid profiles obtained from the analysis of OVX sheep over five months are shown in Figure C.2. A modest difference can be noticed in the OVXG sheep (Figure C.2D, PC1 and PC2 explained 74.4% of the variance) when compared with OVXG2. At month five, the scatter plots showed a smaller separation between the OVX group (Figure C.2F, PC1 and PC2 explained 74.4% of the variance) when compared with the control

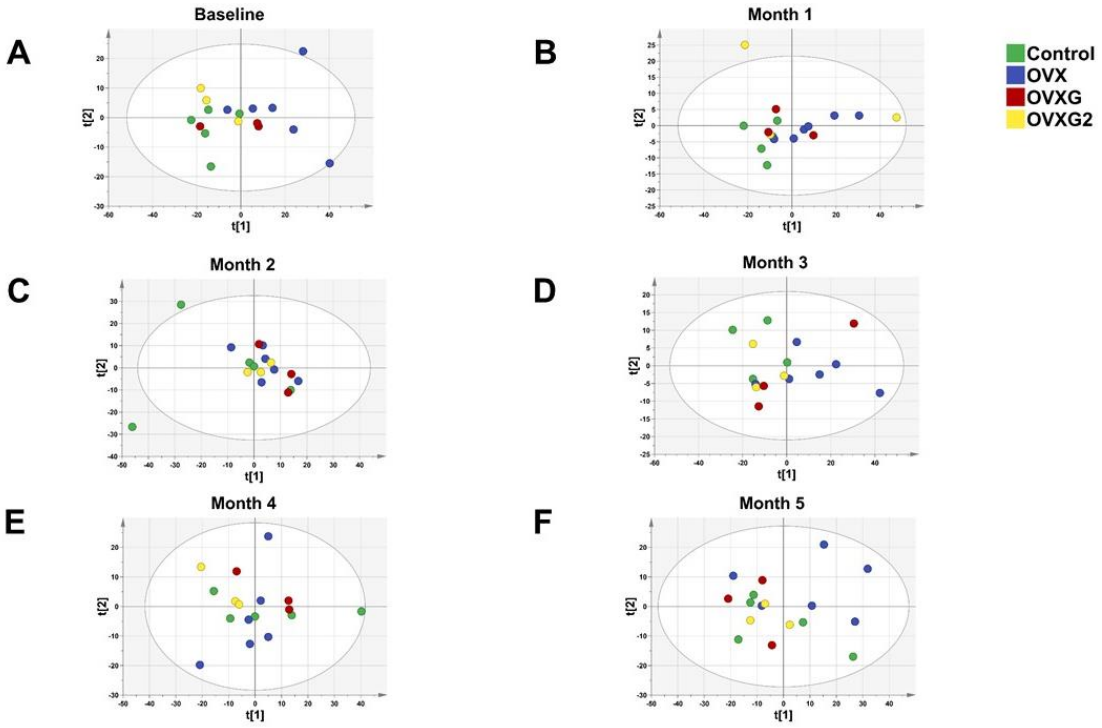

Figure C.2: Inter-animal variation in the plasma lipidome of sheep over five months of the study period. PCA scatter plots derived from UHPLC-MS spectra dataset based on normalised and autoscaled data. Each data point represents the lipid profile of a single ewe. PCA scoring plot showing the variation of control group (●), OVX group (●), OVXG (●) and OVXG2 (●) at baseline measurement (**A**) 76.9% R2 = 76.8% and Q2 = 52.9%, month one (**B**) 73.4%, R2 = 49.6% and Q2= 19.2%, month two (**C**) 70.1%, R2 = 82.5% and Q2 = 51.1%, month three (**D**) 74.4%, R2 = 74.5% and Q2 = 61.2%, month four (**E**) 59.3%, R2 = 59.3% and Q2 = 35.5% and month (**F**) 69.9%, R2 = 69.9% and Q2 = 56.1%

Linear mixed model: long-term approach

The metabolites selected by linear mixed model presented a significant interaction between treatment and time; however, 112 remaining unidentified (unknown) and are presented in Table C.2.

Table C.2: List of unknown features based on the interaction, treatment and time of the lipid profile of ewes in the long-term approach.

				Mean									
m/z	RT			(Relative intensity, E+05)							*p* -value		
	(sec)	Feature	Trt	0	1	2	3	4	5	SEM	Trt	Time	Int
393.054	48.306	Unknown	Control	1.756	1.872	2.302	1.802	1.885	1.979	0.164	0.014	0.003	0.001
			OVX	2.872	2.177	1.889	2.414	1.720	2.162	0.134			
			OVXG	2.213	1.876	1.790	2.278	1.877	1.704	0.190			
			OVXG2	1.948	2.252	1.860	1.889	1.695	1.877	0.190			
347.172	101.676	Unknown	Control	3.991	3.622	4.878	4.204	4.407	4.935	0.563	0.056	0.036	0.005
			OVX	7.297	5.074	3.907	5.904	4.123	4.507	0.460			
			OVXG	4.750	4.416	3.567	5.302	5.044	3.961	0.650			
			OVXG2	4.273	5.160	4.358	4.425	4.088	4.263	0.650			
640.149	125.909	Unknown	Control	0.547	0.457	0.616	0.517	0.576	0.643	0.065	0.037	0.035	0.015
			OVX	0.936	0.635	0.507	0.736	0.550	0.608	0.059			
			OVXG	0.611	0.547	0.468	0.637	0.653	0.549	0.084			
			OVXG2	0.518	0.660	0.473	0.560	0.524	0.555	0.084			
763.204	171.958	Unknown	Control	4.998	4.693	5.872	5.547	5.489	5.934	0.474	0.089	0.043	0.022
			OVX	7.428	5.896	4.947	6.286	4.774	5.529	0.387			
			OVXG	5.656	4.848	4.860	5.547	5.344	4.823	0.547			
			OVXG2	5.085	5.504	4.724	5.358	4.739	5.672	0.547			
701.428	178.166	Unknown	Control	14.861	12.352	15.012	16.049	15.794	18.281	1.726	0.116	0.028	0.027
			OVX	24.694	17.230	13.411	18.691	14.550	14.827	1.576			
			OVXG	15.732	14.849	13.938	15.000	17.049	14.168	2.228			
			OVXG2	14.272	16.479	12.537	15.371	14.067	15.769	2.228			
692.403	178.192	Unknown	Control	8.586	7.088	8.716	8.880	8.974	10.562	1.121	0.111	0.037	0.039
			OVX	14.053	9.888	7.848	10.795	8.224	8.884	0.915			
			OVXG	8.899	8.402	7.918	8.696	9.699	8.228	1.294			
			OVXG2	8.180	9.603	7.117	8.797	8.070	9.256	1.294			
673.375	179.623	Unknown	Control	0.327	0.311	0.422	0.317	0.379	0.397	0.038	0.160	0.236	0.017
			OVX	0.523	0.389	0.324	0.440	0.321	0.382	0.034			
			OVXG	0.378	0.332	0.285	0.388	0.376	0.357	0.049			
			OVXG2	0.337	0.430	0.294	0.351	0.323	0.347	0.049			

473.284	183.588	Unknown	Control	1.440	1.369	1.676	1.383	1.493	1.531	0.123	0.016	0.004	0.002
			OVX	2.184	1.663	1.424	1.870	1.360	1.695	0.100			
			OVXG	1.681	1.498	1.341	1.734	1.481	1.398	0.142			
			OVXG2	1.498	1.825	1.410	1.499	1.377	1.503	0.142			
413.246	183.599	Unknown	Control	0.746	0.773	0.988	0.761	0.860	0.843	0.081	0.029	0.064	0.003
			OVX	1.305	0.949	0.804	1.076	0.763	0.934	0.074			
			OVXG	0.938	0.823	0.762	0.997	0.853	0.771	0.104			
			OVXG2	0.797	1.061	0.799	0.841	0.742	0.813	0.104			
666.537	183.605	Unknown	Control	8.134	8.056	10.679	8.240	9.029	9.311	0.716	0.172	0.252	0.006
			OVX	12.236	9.714	7.879	10.440	8.408	10.103	0.654			
			OVXG	9.866	8.826	8.444	10.276	9.086	8.665	0.925			
			OVXG2	8.854	10.321	9.232	8.883	8.275	8.254	0.925			
667.534	183.607	Unknown	Control	35.479	34.395	46.632	33.353	39.300	40.819	3.557	0.395	0.078	0.002
			OVX	56.479	41.626	33.401	42.542	32.827	44.271	3.247			
			OVXG	42.030	38.136	32.569	43.633	39.281	37.385	4.593			
			OVXG2	37.903	41.656	39.905	38.475	36.104	36.383	4.593			
736.525	183.608	Unknown	Control	35.479	34.395	46.632	33.353	39.300	40.819	3.557	0.395	0.078	0.002
			OVX	56.479	41.626	33.401	42.542	32.827	44.271	3.247			
			OVXG	42.030	38.136	32.569	43.633	39.281	37.385	4.593			
			OVXG2	37.903	41.656	39.905	38.475	36.104	36.383	4.593			
669.540	183.610	Unknown	Control	3.748	3.580	4.264	3.597	3.956	4.205	0.338	0.028	0.087	0.027
			OVX	5.697	4.328	3.791	4.842	3.650	4.554	0.309			
			OVXG	3.971	3.660	3.366	4.499	4.088	3.716	0.437			
			OVXG2	3.898	4.607	4.063	4.007	3.514	3.951	0.437			
734.524	183.610	Unknown	Control	0.704	0.682	0.831	0.710	0.770	0.788	0.055	0.098	0.037	0.010
			OVX	1.041	0.775	0.702	0.865	0.703	0.816	0.050			
			OVXG	0.815	0.741	0.617	0.847	0.736	0.726	0.070			
			OVXG2	0.749	0.813	0.780	0.770	0.675	0.669	0.070			
365.246	183.610	Unknown	Control	27.759	26.539	35.022	26.807	29.645	31.341	2.539	0.024	0.020	0.003
			OVX	44.526	33.455	27.838	37.716	26.721	34.067	2.317			
			OVXG	33.418	29.464	26.622	33.894	30.060	27.096	3.277			
			OVXG2	29.646	34.525	28.494	29.565	26.595	29.400	3.277			

753.515	183.612	Unknown	Control	1.432	1.393	1.619	1.442	1.519	1.465	0.091	0.081	0.108	0.041
			OVX	1.869	1.609	1.399	1.772	1.391	1.686	0.083			
			OVXG	1.614	1.516	1.407	1.624	1.490	1.445	0.118			
			OVXG2	1.499	1.718	1.522	1.537	1.445	1.452	0.118			
375.275	183.618	Unknown	Control	11.981	11.215	15.739	11.584	12.565	13.464	1.284	0.060	0.044	0.005
			OVX	19.985	14.227	11.919	16.357	11.761	14.101	1.172			
			OVXG	13.995	12.670	11.750	15.576	13.074	11.483	1.658			
			OVXG2	12.628	15.049	13.162	12.743	11.188	12.380	1.658			
788.433	183.646	Unknown	Control	0.218	0.183	0.251	0.174	0.211	0.230	0.024	0.017	0.014	0.020
			OVX	0.344	0.243	0.200	0.283	0.204	0.243	0.022			
			OVXG	0.237	0.192	0.172	0.232	0.203	0.176	0.031			
			OVXG2	0.227	0.281	0.204	0.224	0.180	0.216	0.031			
477.344	209.901	Unknown	Control	5.852	5.355	7.060	5.774	6.087	6.476	0.555	0.070	0.051	0.007
			OVX	8.855	6.760	5.533	7.417	5.817	6.503	0.453			
			OVXG	6.737	5.940	5.572	6.801	6.487	5.719	0.640			
			OVXG2	5.980	6.897	6.156	6.034	5.563	5.830	0.640			
478.347	209.908	Unknown	Control	1.519	1.404	1.866	1.457	1.579	1.726	0.166	0.090	0.075	0.038
			OVX	2.337	1.765	1.444	1.934	1.504	1.721	0.136			
			OVXG	1.758	1.564	1.452	1.841	1.613	1.491	0.192			
			OVXG2	1.556	1.649	1.548	1.595	1.411	1.587	0.192			
447.333	213.997	Unknown	Control	5.621	4.959	6.991	5.509	6.143	6.124	0.572	0.087	0.095	0.019
			OVX	8.429	6.462	5.457	7.502	5.229	6.936	0.522			
			OVXG	6.468	5.562	5.029	6.784	5.950	6.078	0.738			
			OVXG2	5.700	7.060	5.471	5.666	5.327	5.961	0.738			
448.336	214.001	Unknown	Control	5.621	4.959	6.991	5.509	6.143	6.124	0.572	0.087	0.095	0.019
			OVX	8.429	6.462	5.457	7.502	5.229	6.936	0.522			
			OVXG	6.468	5.562	5.029	6.784	5.950	6.078	0.738			
			OVXG2	5.700	7.060	5.471	5.666	5.327	5.961	0.738			
437.304	214.021	Unknown	Control	5.194	4.331	6.289	4.982	5.801	5.727	0.551	0.078	0.078	0.034
			OVX	7.771	5.819	4.945	6.905	4.876	6.639	0.503			
			OVXG	5.882	4.972	4.566	5.964	5.463	6.062	0.711			
			OVXG2	5.200	6.266	5.045	5.219	5.060	5.417	0.711			

792.586	221.633	Unknown	Control	11.726	10.835	13.083	11.250	11.989	11.786	0.549	0.133	0.117	0.013
			OVX	14.066	12.382	11.210	13.113	11.282	12.676	0.501			
			OVXG	12.910	11.560	11.093	12.563	11.522	11.566	0.709			
			OVXG2	11.649	13.083	11.742	11.380	11.487	11.085	0.709			
779.580	221.664	Unknown	Control	4.044	4.187	4.892	4.148	4.409	4.467	0.252	0.359	0.275	0.009
			OVX	5.459	4.787	4.164	4.771	4.141	4.565	0.230			
			OVXG	4.926	4.133	3.965	4.759	4.337	4.250	0.326			
			OVXG2	4.189	4.695	4.710	4.474	4.236	4.329	0.326			
404.309	221.664	Unknown	Control	70.142	66.871	85.500	67.215	73.353	75.976	6.645	0.082	0.045	0.009
			OVX	102.490	81.825	68.638	89.415	66.879	83.019	5.426			
			OVXG	83.255	71.617	66.458	85.745	74.676	68.075	7.673			
			OVXG2	74.189	89.668	72.449	71.868	64.760	73.878	7.673			
502.223	221.667	Unknown	Control	9.470	9.300	11.669	9.386	10.012	10.371	0.861	0.078	0.033	0.013
			OVX	14.298	11.435	9.836	12.515	9.189	11.111	0.786			
			OVXG	11.870	10.107	9.765	12.097	10.313	9.028	1.111			
			OVXG2	10.255	12.728	9.836	9.912	8.579	10.528	1.111			
403.306	221.672	Unknown	Control	285.696	272.442	352.203	276.164	294.542	307.960	22.911	0.082	0.050	0.007
			OVX	411.923	329.323	280.845	357.967	275.814	332.016	20.915			
			OVXG	331.762	292.404	276.130	343.566	300.957	269.735	29.578			
			OVXG2	301.835	362.476	298.482	291.658	265.403	288.697	29.578			
441.277	221.673	Unknown	Control	4.728	4.674	5.531	4.607	4.806	4.845	0.315	0.026	0.020	0.010
			OVX	6.551	5.352	4.831	5.929	4.714	5.274	0.288			
			OVXG	5.467	4.911	4.470	5.455	5.059	4.377	0.407			
			OVXG2	5.043	5.955	4.820	4.775	4.404	4.819	0.407			
407.293	241.746	Unknown	Control	0.480	0.431	0.580	0.449	0.474	0.513	0.044	0.091	0.087	0.018
			OVX	0.714	0.535	0.444	0.583	0.443	0.550	0.041			
			OVXG	0.526	0.473	0.428	0.504	0.507	0.494	0.057			
			OVXG2	0.455	0.557	0.501	0.457	0.440	0.474	0.057			
1060.510	241.887	Unknown	Control	4.530	4.651	5.596	5.613	5.080	6.393	0.510	0.190	0.547	0.015
			OVX	7.245	5.790	4.969	5.788	4.989	4.883	0.466			
			OVXG	5.406	4.704	5.173	5.640	5.416	3.891	0.659			
			OVXG2	4.496	5.442	4.409	4.833	4.485	5.917	0.659			

819.409	249.809	Unknown	Control	4.530	4.651	5.596	5.613	5.080	6.393	0.510	0.190	0.547	0.015
			OVX	7.245	5.790	4.969	5.788	4.989	4.883	0.466			
			OVXG	5.406	4.704	5.173	5.640	5.416	3.891	0.659			
			OVXG2	4.496	5.442	4.409	4.833	4.485	5.917	0.659			
818.406	249.822	Unknown	Control	2.652	2.178	2.987	2.943	2.792	3.256	0.344	0.286	0.145	0.021
			OVX	4.165	3.064	2.426	3.415	2.664	2.673	0.314			
			OVXG	3.010	2.546	1.953	3.143	3.665	2.016	0.445			
			OVXG2	2.572	3.108	2.711	2.460	2.353	2.973	0.445			
639.245	250.058	Unknown	Control	0.132	0.109	0.148	0.159	0.144	0.157	0.016	0.031	0.006	0.020
			OVX	0.227	0.170	0.124	0.185	0.132	0.155	0.014			
			OVXG	0.155	0.150	0.114	0.186	0.169	0.127	0.020			
			OVXG2	0.140	0.143	0.127	0.139	0.121	0.138	0.020			
578.141	250.419	Unknown	Control	1.781	1.434	2.063	1.595	1.823	2.057	0.216	0.161	0.142	0.043
			OVX	2.758	2.091	1.696	2.361	1.692	1.812	0.197			
			OVXG	2.045	1.826	1.459	2.212	2.115	1.588	0.279			
			OVXG2	1.754	2.057	1.710	1.822	1.759	1.847	0.279			
506.243	251.023	Unknown	Control	1.781	1.434	2.063	1.595	1.823	2.057	0.216	0.161	0.142	0.043
			OVX	2.758	2.091	1.696	2.361	1.692	1.812	0.197			
			OVXG	2.045	1.826	1.459	2.212	2.115	1.588	0.279			
			OVXG2	1.754	2.057	1.710	1.822	1.759	1.847	0.279			
479.224	251.122	Unknown	Control	17.033	14.760	19.691	17.411	17.467	19.598	1.866	0.101	0.045	0.031
			OVX	27.322	20.058	16.131	22.325	16.678	18.063	1.703			
			OVXG	19.596	17.549	14.503	20.296	20.627	16.288	2.409			
			OVXG2	17.439	19.629	16.472	17.361	16.194	17.616	2.409			
569.114	251.228	Unknown	Control	1.774	1.556	2.138	1.827	1.852	2.041	0.212	0.106	0.057	0.026
			OVX	2.833	2.110	1.669	2.435	1.666	1.903	0.194			
			OVXG	2.117	1.829	1.421	2.130	2.182	1.640	0.274			
			OVXG2	1.679	2.094	1.509	1.808	1.685	1.843	0.274			
853.625	251.513	Unknown	Control	3.403	2.951	3.698	3.893	3.701	4.077	0.428	0.387	0.153	0.047
			OVX	5.384	3.977	3.209	4.441	3.104	3.258	0.391			
			OVXG	3.900	3.432	3.418	3.918	4.427	3.233	0.552			
			OVXG2	3.189	4.105	3.160	3.345	3.153	3.582	0.552			

854.628	251.513	Unknown	Control	1.683	1.380	1.975	1.708	1.726	1.997	0.198	0.121	0.144	0.032
			OVX	2.685	2.007	1.668	2.272	1.634	1.888	0.181			
			OVXG	1.845	1.856	1.433	2.073	2.264	1.764	0.255			
			OVXG2	1.830	1.979	1.783	1.826	1.630	1.822	0.255			
444.249	251.550	Unknown	Control	42.201	35.656	50.628	42.839	43.262	49.151	5.071	0.130	0.078	0.026
			OVX	70.318	49.896	39.270	55.000	41.536	44.827	4.629			
			OVXG	48.064	43.298	36.776	50.030	52.202	40.944	6.546			
			OVXG2	42.755	48.595	42.192	43.231	40.346	42.430	6.546			
359.153	251.554	Unknown	Control	5.252	4.408	6.367	5.381	5.485	6.088	0.644	0.104	0.062	0.020
			OVX	8.923	6.264	4.838	6.994	5.197	5.637	0.588			
			OVXG	6.103	5.391	4.648	6.223	6.371	5.085	0.832			
			OVXG2	5.268	6.226	5.185	5.333	4.947	5.286	0.832			
490.255	251.555	Unknown	Control	6.731	5.764	7.983	6.707	6.988	7.696	0.799	0.103	0.046	0.025
			OVX	11.278	8.014	6.244	8.874	6.575	7.244	0.730			
			OVXG	7.979	6.991	5.810	7.944	8.139	6.550	1.032			
			OVXG2	6.896	7.965	6.660	6.869	6.364	6.782	1.032			
443.248	251.556	Unknown	Control	113.328	97.091	136.148	115.358	116.801	131.616	13.340	0.132	0.083	0.027
			OVX	187.088	133.448	105.980	148.464	111.951	120.497	12.178			
			OVXG	129.386	116.553	99.853	134.418	139.059	110.784	17.222			
			OVXG2	114.923	132.085	114.175	116.190	107.918	113.821	17.222			
427.215	251.563	Unknown	Control	4.977	4.228	5.944	5.059	5.182	5.794	0.618	0.147	0.082	0.034
			OVX	8.285	5.834	4.526	6.482	4.909	5.333	0.565			
			OVXG	5.811	5.085	4.329	6.077	6.063	4.771	0.798			
			OVXG2	4.853	5.865	4.866	5.045	4.646	4.943	0.798			
1148.365	252.397	Unknown	Control	0.754	0.751	0.858	0.757	0.787	0.807	0.037	0.278	0.340	0.037
			OVX	0.921	0.835	0.756	0.815	0.720	0.849	0.034			
			OVXG	0.767	0.763	0.792	0.819	0.769	0.779	0.048			
			OVXG2	0.750	0.837	0.812	0.788	0.741	0.713	0.048			
1069.420	252.413	Unknown	Control	0.705	0.723	0.864	0.717	0.761	0.785	0.045	0.179	0.188	0.028
			OVX	0.912	0.847	0.719	0.819	0.715	0.836	0.041			
			OVXG	0.818	0.756	0.748	0.810	0.730	0.704	0.058			
			OVXG2	0.762	0.865	0.784	0.769	0.660	0.681	0.058			

1147.361	252.436	Unknown	Control	1.534	1.503	1.695	1.458	1.635	1.499	0.068	0.114	0.032	0.024
			OVX	1.835	1.690	1.495	1.634	1.486	1.656	0.062			
			OVXG	1.729	1.519	1.588	1.579	1.327	1.492	0.088			
			OVXG2	1.573	1.580	1.625	1.501	1.495	1.496	0.088			
806.891	252.449	Unknown	Control	1.193	1.158	1.352	1.168	1.259	1.211	0.068	0.033	0.085	0.034
			OVX	1.573	1.379	1.223	1.373	1.196	1.350	0.062			
			OVXG	1.372	1.223	1.264	1.347	1.154	1.207	0.088			
			OVXG2	1.199	1.410	1.289	1.275	1.142	1.237	0.088			
782.898	252.449	Unknown	Control	1.471	1.476	1.782	1.427	1.596	1.602	0.108	0.051	0.097	0.012
			OVX	2.142	1.733	1.510	1.812	1.471	1.741	0.099			
			OVXG	1.811	1.544	1.570	1.652	1.591	1.545	0.140			
			OVXG2	1.554	1.734	1.661	1.601	1.492	1.372	0.140			
727.945	252.462	Unknown	Control	2.686	2.666	3.226	2.731	2.963	2.960	0.186	0.045	0.102	0.010
			OVX	3.807	3.125	2.714	3.365	2.713	3.225	0.170			
			OVXG	3.116	2.825	2.816	3.046	2.816	2.649	0.240			
			OVXG2	2.919	3.292	2.848	2.841	2.565	2.776	0.240			
805.887	252.507	Unknown	Control	3.027	2.890	3.453	3.021	3.202	3.011	0.161	0.172	0.043	0.046
			OVX	3.790	3.384	3.067	3.489	2.980	3.050	0.147			
			OVXG	3.389	3.159	3.201	3.015	3.044	2.968	0.208			
			OVXG2	3.113	3.555	3.123	3.081	2.881	2.921	0.208			
863.919	252.510	Unknown	Control	0.599	0.595	0.777	0.636	0.667	0.694	0.047	0.043	0.068	0.008
			OVX	0.880	0.711	0.679	0.798	0.583	0.758	0.043			
			OVXG	0.731	0.665	0.602	0.724	0.627	0.619	0.061			
			OVXG2	0.655	0.739	0.710	0.589	0.611	0.680	0.061			
387.475	252.510	Unknown	Control	0.599	0.595	0.777	0.636	0.667	0.694	0.047	0.043	0.068	0.008
			OVX	0.880	0.711	0.679	0.798	0.583	0.758	0.043			
			OVXG	0.731	0.665	0.602	0.724	0.627	0.619	0.061			
			OVXG2	0.655	0.739	0.710	0.589	0.611	0.680	0.061			
522.446	252.513	Unknown	Control	1.206	1.146	1.416	1.152	1.263	1.317	0.093	0.015	0.072	0.017
			OVX	1.742	1.402	1.210	1.513	1.177	1.411	0.085			
			OVXG	1.318	1.243	1.115	1.320	1.265	1.112	0.120			
			OVXG2	1.238	1.427	1.186	1.210	1.092	1.232	0.120			

356.458	252.520	Unknown	Control	0.496	0.481	0.640	0.493	0.545	0.566	0.046	0.040	0.050	0.013
			OVX	0.770	0.623	0.540	0.647	0.489	0.607	0.042			
			OVXG	0.646	0.537	0.500	0.587	0.531	0.516	0.060			
			OVXG2	0.545	0.670	0.515	0.528	0.458	0.500	0.060			
386.471	252.521	Unknown	Control	0.496	0.481	0.640	0.493	0.545	0.566	0.046	0.040	0.050	0.013
			OVX	0.770	0.623	0.540	0.647	0.489	0.607	0.042			
			OVXG	0.646	0.537	0.500	0.587	0.531	0.516	0.060			
			OVXG2	0.545	0.670	0.515	0.528	0.458	0.500	0.060			
354.460	252.537	Unknown	Control	1.610	1.595	2.023	1.565	1.757	1.738	0.143	0.039	0.057	0.010
			OVX	2.443	1.965	1.656	2.120	1.556	1.990	0.131			
			OVXG	1.993	1.698	1.677	1.900	1.755	1.560	0.185			
			OVXG2	1.733	2.095	1.670	1.703	1.468	1.699	0.185			
464.414	252.564	Unknown	Control	5.897	5.723	7.193	5.850	6.293	6.441	0.469	0.032	0.053	0.012
			OVX	8.693	7.085	6.169	7.571	5.738	7.062	0.428			
			OVXG	6.971	6.284	5.950	7.026	6.361	5.734	0.606			
			OVXG2	6.398	7.528	6.027	6.142	5.621	6.181	0.606			
448.442	252.565	Unknown	Control	1.464	1.349	1.727	1.414	1.536	1.565	0.115	0.015	0.033	0.009
			OVX	2.171	1.732	1.502	1.882	1.419	1.747	0.105			
			OVXG	1.726	1.527	1.480	1.701	1.541	1.409	0.149			
			OVXG2	1.548	1.845	1.474	1.501	1.399	1.518	0.149			
454.459	252.610	Unknown	Control	2.876	2.714	3.445	2.813	3.002	3.112	0.228	0.016	0.032	0.012
			OVX	4.202	3.440	2.940	3.708	2.786	3.394	0.208			
			OVXG	3.358	2.973	2.795	3.241	3.007	2.675	0.295			
			OVXG2	3.029	3.588	2.855	2.912	2.592	2.986	0.295			
624.738	252.610	Unknown	Control	0.665	0.606	0.732	0.621	0.712	0.683	0.045	0.019	0.541	0.045
			OVX	0.807	0.735	0.665	0.775	0.665	0.787	0.041			
			OVXG	0.733	0.676	0.678	0.643	0.653	0.611	0.058			
			OVXG2	0.638	0.827	0.600	0.611	0.569	0.622	0.058			
365.492	252.612	Unknown	Control	1.032	0.971	1.360	0.986	1.070	1.105	0.104	0.054	0.035	0.010
			OVX	1.620	1.241	1.034	1.346	0.962	1.282	0.095			
			OVXG	1.265	1.074	1.020	1.175	1.073	0.963	0.135			
			OVXG2	1.109	1.350	1.108	1.065	0.943	1.027	0.135			

532.401	252.632	Unknown	Control	2.747	2.632	3.239	2.713	2.908	2.957	0.224	0.065	0.061	0.023
			OVX	3.911	3.226	2.685	3.503	2.643	3.247	0.204			
			OVXG	3.231	2.861	2.747	3.176	2.923	2.656	0.289			
			OVXG2	2.911	3.486	2.623	2.814	2.604	2.823	0.289			
454.385	252.671	Unknown	Control	2.973	2.868	3.552	2.962	3.148	3.230	0.217	0.013	0.055	0.018
			OVX	4.280	3.563	3.197	3.811	2.951	3.580	0.198			
			OVXG	3.465	3.197	2.973	3.516	3.123	2.861	0.281			
			OVXG2	3.248	3.746	3.014	3.115	2.918	3.169	0.281			
872.870	252.697	Unknown	Control	0.700	0.702	0.862	0.712	0.723	0.771	0.056	0.038	0.309	0.017
			OVX	0.990	0.835	0.749	0.866	0.706	0.892	0.051			
			OVXG	0.834	0.778	0.713	0.830	0.762	0.586	0.072			
			OVXG2	0.726	0.899	0.777	0.720	0.745	0.738	0.072			
462.419	252.707	Unknown	Control	0.700	0.702	0.862	0.712	0.723	0.771	0.056	0.038	0.309	0.017
			OVX	0.990	0.835	0.749	0.866	0.706	0.892	0.051			
			OVXG	0.834	0.778	0.713	0.830	0.762	0.586	0.072			
			OVXG2	0.726	0.899	0.777	0.720	0.745	0.738	0.072			
385.465	252.714	Unknown	Control	0.695	0.667	0.846	0.669	0.738	0.741	0.055	0.008	0.047	0.010
			OVX	1.024	0.832	0.732	0.902	0.700	0.841	0.050			
			OVXG	0.844	0.729	0.690	0.790	0.714	0.652	0.071			
			OVXG2	0.714	0.881	0.700	0.714	0.622	0.721	0.071			
363.483	252.734	Unknown	Control	1.215	1.171	1.564	1.204	1.307	1.336	0.120	0.040	0.061	0.009
			OVX	1.935	1.515	1.231	1.586	1.191	1.548	0.109			
			OVXG	1.508	1.293	1.277	1.410	1.321	1.209	0.155			
			OVXG2	1.319	1.649	1.318	1.269	1.123	1.237	0.155			
463.408	252.756	Unknown	Control	1.390	1.334	1.682	1.348	1.476	1.514	0.114	0.022	0.095	0.033
			OVX	2.005	1.700	1.424	1.798	1.370	1.693	0.104			
			OVXG	1.645	1.480	1.387	1.600	1.472	1.403	0.147			
			OVXG2	1.482	1.712	1.421	1.443	1.313	1.419	0.147			
446.353	252.783	Unknown	Control	2.671	2.564	3.119	2.658	2.841	2.880	0.178	0.019	0.050	0.010
			OVX	3.685	3.084	2.824	3.343	2.625	3.135	0.163			
			OVXG	3.126	2.809	2.655	2.986	2.777	2.542	0.230			
			OVXG2	2.855	3.423	2.639	2.717	2.506	2.740	0.230			

421.309	262.580	Unknown	Control	7.003	6.071	8.082	6.955	7.082	7.808	0.641	0.016	0.024	0.043
			OVX	10.304	7.994	6.426	8.894	6.990	8.575	0.585			
			OVXG	8.587	6.368	6.535	8.004	6.763	6.997	0.827			
			OVXG2	6.508	7.708	6.977	6.549	6.279	6.775	0.827			
431.337	263.058	Unknown	Control	2.036	1.782	2.496	1.910	2.042	2.141	0.193	0.027	0.014	0.007
			OVX	3.044	2.299	1.948	2.560	1.873	2.407	0.158			
			OVXG	2.308	2.053	1.914	2.279	2.063	1.912	0.223			
			OVXG2	2.072	2.283	2.092	2.013	1.819	1.992	0.223			
1006.634	264.130	Unknown	Control	0.476	0.393	0.517	0.522	0.479	0.471	0.034	0.400	0.006	0.026
			OVX	0.627	0.482	0.417	0.500	0.423	0.438	0.031			
			OVXG	0.478	0.473	0.428	0.474	0.459	0.375	0.044			
			OVXG2	0.443	0.432	0.451	0.456	0.463	0.420	0.044			
698.436	287.913	Unknown	Control	0.868	0.820	1.058	0.981	0.988	0.981	0.091	0.172	0.099	0.008
			OVX	1.361	1.022	0.869	1.111	0.854	0.932	0.083			
			OVXG	0.952	0.853	0.724	1.058	1.094	0.874	0.117			
			OVXG2	0.900	1.094	0.713	0.842	0.822	0.956	0.117			
697.434	287.940	Unknown	Control	2.086	1.947	2.519	2.287	2.314	2.477	0.185	0.128	0.198	0.012
			OVX	3.165	2.538	2.104	2.679	2.122	2.285	0.169			
			OVXG	2.399	2.200	2.018	2.354	2.510	2.270	0.239			
			OVXG2	2.186	2.589	2.032	2.198	2.131	2.175	0.239			
714.424	287.945	Unknown	Control	0.357	0.305	0.397	0.388	0.388	0.396	0.030	0.171	0.080	0.023
			OVX	0.519	0.386	0.338	0.422	0.355	0.371	0.027			
			OVXG	0.378	0.351	0.317	0.341	0.396	0.384	0.038			
			OVXG2	0.351	0.406	0.342	0.371	0.343	0.362	0.038			
1343.662	305.375	Unknown	Control	0.495	0.393	0.459	0.486	0.482	0.581	0.044	0.488	0.304	0.006
			OVX	0.593	0.500	0.458	0.453	0.447	0.375	0.040			
			OVXG	0.460	0.386	0.447	0.512	0.490	0.334	0.057			
			OVXG2	0.416	0.452	0.390	0.436	0.363	0.572	0.057			
1336.683	305.781	Unknown	Control	1.690	1.413	1.752	1.516	1.695	2.078	0.188	0.632	0.245	0.005
			OVX	2.299	1.802	1.537	1.726	1.542	1.386	0.172			
			OVXG	1.701	1.486	1.842	1.943	1.501	1.333	0.243			
			OVXG2	1.321	1.592	1.158	1.629	1.301	2.093	0.243			

459.370	308.910	Unknown	Control	1.759	1.650	2.252	1.764	1.883	1.841	0.141	0.056	0.077	0.006
			OVX	2.616	2.094	1.724	2.178	1.798	2.038	0.128			
			OVXG	2.092	1.840	1.748	2.080	1.891	1.726	0.181			
			OVXG2	1.880	2.082	1.845	1.867	1.746	1.771	0.181			
460.373	308.921	Unknown	Control	0.456	0.410	0.525	0.436	0.463	0.485	0.037	0.095	0.013	0.006
			OVX	0.681	0.528	0.422	0.545	0.425	0.492	0.034			
			OVXG	0.521	0.456	0.437	0.527	0.486	0.429	0.048			
			OVXG2	0.457	0.537	0.450	0.483	0.431	0.451	0.048			
726.468	329.701	Unknown	Control	7.054	6.543	8.122	7.433	7.734	7.328	0.505	0.251	0.231	0.043
			OVX	9.685	7.809	6.940	8.370	7.183	7.448	0.461			
			OVXG	7.887	7.212	6.730	7.754	8.158	7.554	0.652			
			OVXG2	7.143	8.108	6.947	7.096	7.284	7.441	0.652			
1373.753	334.826	Unknown	Control	0.488	0.423	0.490	0.645	0.585	0.633	0.053	0.387	0.101	0.004
			OVX	0.635	0.499	0.439	0.489	0.505	0.395	0.049			
			OVXG	0.419	0.429	0.473	0.516	0.570	0.419	0.069			
			OVXG2	0.490	0.395	0.440	0.508	0.366	0.664	0.069			
1229.752	334.836	Unknown	Control	7.514	6.738	7.264	8.017	7.870	8.720	0.777	0.759	0.578	0.031
			OVX	8.455	7.722	7.160	7.567	7.153	5.541	0.710			
			OVXG	6.339	6.427	6.614	8.470	8.669	6.257	1.004			
			OVXG2	7.237	6.706	6.040	7.389	5.390	9.446	1.004			
1255.772	334.890	Unknown	Control	5.663	5.506	6.155	6.702	5.892	7.362	0.599	0.691	0.532	0.026
			OVX	6.819	6.041	5.686	5.963	6.286	4.774	0.546			
			OVXG	3.636	5.583	5.119	6.556	6.646	5.827	0.773			
			OVXG2	5.943	5.138	5.393	5.976	5.527	7.299	0.773			
487.400	358.665	Unknown	Control	1.204	1.040	1.401	1.025	1.108	1.248	0.105	0.806	0.048	0.027
			OVX	1.599	1.259	0.965	1.327	1.007	1.211	0.096			
			OVXG	1.232	1.186	1.066	1.329	1.201	1.073	0.136			
			OVXG2	1.200	1.324	1.149	1.182	1.089	1.171	0.136			
474.403	388.188	Unknown	Control	4.607	4.457	5.283	4.518	4.729	4.757	0.266	0.020	0.045	0.014
			OVX	6.110	5.247	4.717	5.546	4.581	5.205	0.243			
			OVXG	5.309	4.880	4.591	5.415	4.768	4.415	0.344			
			OVXG2	4.660	5.530	4.649	4.682	4.397	4.641	0.344			
520.409	388.282	Unknown	Control	3.679	3.500	4.147	3.660	3.779	3.808	0.215	0.025	0.176	0.039
			OVX	4.856	4.186	3.725	4.432	3.609	4.123	0.197			
			OVXG	3.752	3.932	3.592	4.026	3.820	3.647	0.278			
			OVXG2	3.825	4.206	3.912	3.746	3.635	3.828	0.278			

748.720	403.700	Unknown	Control	44.136	45.701	60.513	47.490	40.579	53.153	4.110	0.002	0.105	0.001
			OVX	66.991	53.829	53.609	57.016	49.066	54.930	3.751			
			OVXG	39.241	50.416	34.798	56.008	49.049	27.226	5.305			
			OVXG2	58.153	57.596	54.300	50.387	43.122	53.193	5.305			
581.526	416.170	Unknown	Control	40.752	40.118	46.305	41.760	44.470	42.890	1.987	0.051	0.834	0.022
			OVX	51.986	46.418	43.172	48.570	43.075	46.472	1.814			
			OVXG	46.470	44.453	44.407	45.663	45.193	43.492	2.565			
			OVXG2	41.342	49.486	46.761	43.607	43.804	42.491	2.565			
582.529	416.221	Unknown	Control	15.604	15.363	17.526	15.866	16.916	16.413	0.804	0.026	0.835	0.019
			OVX	19.911	17.639	16.443	18.717	16.369	18.433	0.734			
			OVXG	17.744	17.047	16.827	17.751	17.421	16.414	1.038			
			OVXG2	15.593	19.627	17.459	16.406	16.212	16.373	1.038			
301.166	435.228	Unknown	Control	1.879	1.794	2.345	1.948	1.982	2.200	0.203	0.198	0.269	0.031
			OVX	2.906	2.370	1.816	2.483	1.982	2.086	0.185			
			OVXG	2.282	2.164	1.697	2.337	2.409	1.869	0.262			
			OVXG2	1.957	2.419	2.081	2.062	1.985	1.914	0.262			
611.564	465.028	Unknown	Control	2.606	2.592	3.006	2.703	2.728	2.805	0.154	0.030	0.456	0.016
			OVX	3.460	3.037	2.786	3.114	2.694	2.978	0.141			
			OVXG	2.972	2.811	2.664	2.967	2.787	2.613	0.199			
			OVXG2	2.373	3.282	2.819	2.690	2.617	2.802	0.199			
609.559	465.031	Unknown	Control	30.679	29.182	34.309	30.631	31.732	31.720	1.569	0.024	0.139	0.027
			OVX	39.445	34.496	31.558	35.928	30.930	34.014	1.432			
			OVXG	34.329	32.352	31.072	33.681	31.733	30.213	2.025			
			OVXG2	31.233	36.671	32.192	31.048	30.005	31.663	2.025			
610.561	465.035	Unknown	Control	12.368	12.102	13.920	12.504	12.868	12.795	0.633	0.025	0.101	0.014
			OVX	16.146	13.946	12.872	14.614	12.505	13.714	0.578			
			OVXG	14.097	13.098	12.549	13.855	12.834	11.950	0.818			
			OVXG2	12.546	15.075	13.007	12.507	12.489	12.813	0.818			
1270.904	480.311	Unknown	Control	0.328	0.312	0.398	0.383	0.379	0.397	0.022	0.082	< 0.0001	0.011
			OVX	0.366	0.337	0.357	0.413	0.347	0.383	0.020			
			OVXG	0.352	0.257	0.274	0.381	0.309	0.319	0.029			
			OVXG2	0.420	0.220	0.394	0.361	0.358	0.353	0.029			

614.509	480.487	Unknown	Control	0.465	0.443	0.544	0.446	0.490	0.504	0.033	0.038	0.058	0.012
			OVX	0.653	0.539	0.454	0.570	0.474	0.545	0.030			
			OVXG	0.542	0.473	0.442	0.527	0.506	0.442	0.042			
			OVXG2	0.500	0.538	0.519	0.530	0.420	0.492	0.042			
758.427	480.646	Unknown	Control	0.576	0.553	0.677	0.601	0.642	0.599	0.031	0.235	0.241	0.045
			OVX	0.703	0.646	0.596	0.657	0.574	0.675	0.029			
			OVXG	0.682	0.583	0.628	0.662	0.607	0.625	0.040			
			OVXG2	0.610	0.635	0.628	0.594	0.536	0.584	0.040			
613.505	480.656	Unknown	Control	1.277	1.227	1.517	1.275	1.343	1.378	0.089	0.076	0.101	0.015
			OVX	1.743	1.461	1.258	1.542	1.268	1.423	0.081			
			OVXG	1.499	1.245	1.290	1.482	1.390	1.066	0.115			
			OVXG2	1.296	1.415	1.269	1.337	1.257	1.299	0.115			
657.513	480.830	Unknown	Control	0.497	0.485	0.577	0.451	0.523	0.523	0.036	0.062	0.323	0.034
			OVX	0.681	0.578	0.494	0.595	0.484	0.574	0.033			
			OVXG	0.587	0.576	0.525	0.583	0.564	0.488	0.047			
			OVXG2	0.503	0.537	0.560	0.499	0.504	0.521	0.047			
638.593	510.821	Unknown	Control	3.148	3.034	3.365	3.134	3.250	3.180	0.138	0.076	0.046	0.045
			OVX	3.997	3.462	3.230	3.288	3.167	3.459	0.126			
			OVXG	3.578	3.354	3.447	3.383	3.272	3.239	0.178			
			OVXG2	3.215	3.561	3.438	3.220	3.175	3.261	0.178			
637.589	510.834	Unknown	Control	7.098	7.065	8.125	7.222	7.448	7.486	0.376	0.018	0.114	0.021
			OVX	9.506	8.074	7.591	8.493	7.341	8.132	0.343			
			OVXG	8.367	7.860	7.712	8.181	7.697	7.258	0.485			
			OVXG2	7.543	8.746	7.153	7.449	7.177	7.776	0.485			
639.596	510.964	Unknown	Control	7.098	7.065	8.125	7.222	7.448	7.486	0.376	0.018	0.114	0.021
			OVX	9.506	8.074	7.591	8.493	7.341	8.132	0.343			
			OVXG	8.367	7.860	7.712	8.181	7.697	7.258	0.485			
			OVXG2	7.543	8.746	7.153	7.449	7.177	7.776	0.485			
654.580	511.106	Unknown	Control	2.297	2.224	2.495	2.260	2.323	2.400	0.116	0.010	0.097	0.032
			OVX	2.914	2.490	2.373	2.634	2.251	2.505	0.106			
			OVXG	2.582	2.260	2.182	2.465	2.284	2.287	0.150			
			OVXG2	2.173	2.484	2.218	1.966	2.256	2.401	0.150			

685.542	524.206	Unknown	Control	2.452	2.233	2.721	2.310	2.548	2.316	0.118	0.043	0.029	0.004
			OVX	3.071	2.720	2.397	2.768	2.373	2.656	0.108			
			OVXG	2.814	2.631	2.467	2.684	2.537	2.440	0.153			
			OVXG2	2.520	2.856	2.653	2.444	2.420	2.385	0.153			
714.598	541.327	Unknown	Control	0.676	0.597	0.877	0.665	0.808	0.732	0.064	0.079	0.528	0.006
			OVX	0.990	0.782	0.702	0.883	0.679	0.859	0.058			
			OVXG	0.808	0.709	0.750	0.833	0.776	0.786	0.083			
			OVXG2	0.714	0.911	0.689	0.618	0.657	0.720	0.083			
527.446	564.287	Unknown	Control	5.401	5.206	5.841	5.239	5.585	5.440	0.258	0.026	0.057	0.024
			OVX	6.638	5.959	5.305	6.139	5.216	6.100	0.236			
			OVXG	6.147	5.677	5.234	5.877	5.404	5.582	0.333			
			OVXG2	5.591	5.779	5.633	4.668	5.341	5.396	0.333			
759.761	598.998	Unknown	Control	3.123	3.247	3.773	3.126	3.382	3.224	0.162	0.184	0.546	0.041
			OVX	3.898	3.425	3.280	3.641	3.330	3.595	0.148			
			OVXG	3.574	3.383	3.223	3.296	3.179	3.204	0.209			
			OVXG2	3.327	3.597	3.304	3.233	3.238	3.077	0.209			
832.494	602.039	Unknown	Control	0.399	0.373	0.451	0.369	0.392	0.401	0.022	0.150	0.050	0.047
			OVX	0.480	0.448	0.386	0.434	0.357	0.442	0.020			
			OVXG	0.444	0.406	0.424	0.417	0.414	0.376	0.028			
			OVXG2	0.401	0.413	0.401	0.413	0.371	0.382	0.028			
656.636	643.039	Unknown	Control	5.337	5.618	6.353	5.785	5.970	5.660	0.252	0.017	0.389	0.015
			OVX	7.002	6.307	5.831	6.572	5.711	6.281	0.230			
			OVXG	6.421	5.975	5.774	5.482	5.733	5.702	0.325			
			OVXG2	5.978	6.405	5.943	5.806	5.854	5.767	0.325			
1326.901	394.961	Unknown	Control	3.676	3.793	3.951	3.506	3.821	3.974	0.237	0.016	0.022	0.046
			OVX	5.093	4.272	3.827	4.550	3.734	4.229	0.217			
			OVXG	4.214	4.003	3.374	4.400	3.986	3.678	0.307			
			OVXG2	3.986	4.484	3.910	3.938	3.463	3.749	0.307			
1385.971	394.562	Unknown	Control	0.770	0.793	0.821	0.748	0.783	0.793	0.055	0.081	0.004	0.025
			OVX	1.116	0.868	0.766	0.902	0.733	0.834	0.050			
			OVXG	0.884	0.844	0.703	0.938	0.768	0.749	0.071			
			OVXG2	0.778	0.933	0.747	0.789	0.771	0.800	0.071			

Appendix D. Chapter 7 Supplementary information

Lipids

Entire cohort

Table D.1: Significant lipids associated to postmenopausal women with normal and low femoral neck BMD in univariate and multivariate approaches.

m/z	RT (sec)	Compound
710.396	167.767	PS 31:6; [M+H]+
738.427	167.765	PS 33:6; [M+H]+
682.365	167.371	PS 29:6; [M+H]+
718.634	218.244	DG 42:4; [M+NH4]+
752.567	397.265	plasmenyl-PE 38:4; [M+H]+

Box plot analysis was performed to analise the overall levels of those 5 plasma lipids between groups (Figure D.1).

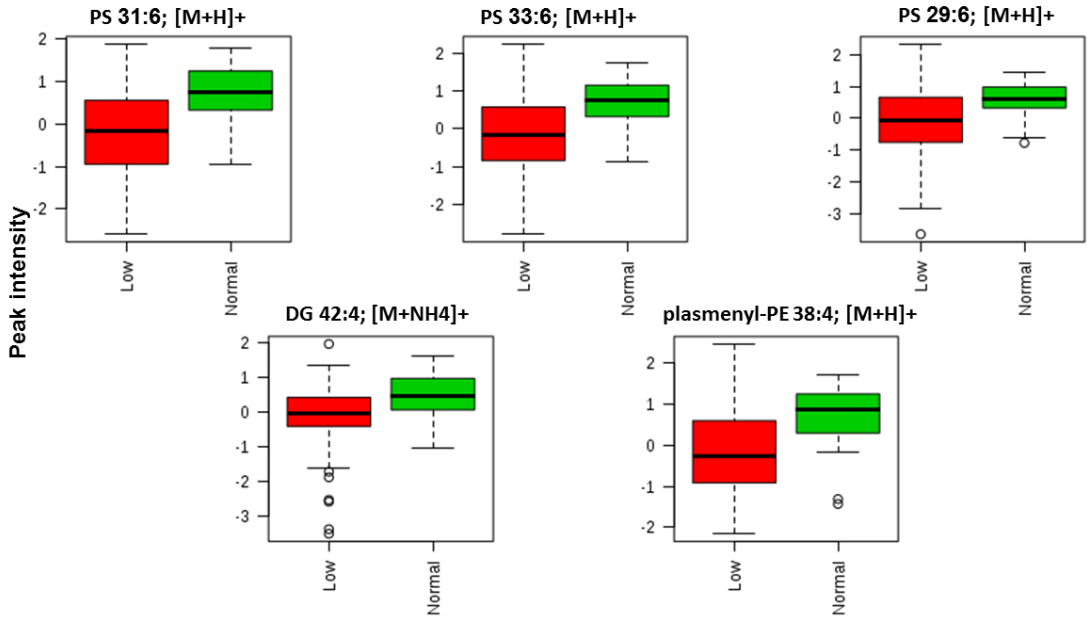

Figure D.1: Boxplots showing normalised peak intensities from original LC-MS data of lipids between postmenopausal women with low and normal BMD. PS (phosphatidylserine), DG (diacylglycerol), plasmeyl-PE (plasmenylphosphatidylethanolamines).

Subset

Table D.2: Significant lipids associated to a subset of selected postmenopausal women with normal (n =15) and low femoral neck BMD (n =15) in univariate and multivariate approaches.

m/z	RT (sec)	Compound
667.424	207.010	PA 34:4; [M-H]-
674.546	344.08	CerP 38:1; [M+H]+
558.245	248.659	PS 20:4; [M-H]-
698.663	248.467	DG 40:0; [M+NH4]+
738.427	167.765	PS 33:6; [M+H]+
710.396	167.767	PS 31:6; [M+H]+
724.411	167.417	PS 32:6; [M+H]+
557.242	248.783	PI 14:0; [M-H]-
718.634	218.244	DG 42:4; [M+NH4]+
478.320	251.065	CerP 24:0; [M-H]-
786.701	571.528	DG 47:5; [M+NH4]+
828.653	464.336	PE 42:1; [M-H]-

Normal and low femoral neck BMD showed a similar range of lipid levels (Figure 3). However, PA, PS, PI and PE compounds showed a higher level in the low group compared with the normal BMD group.

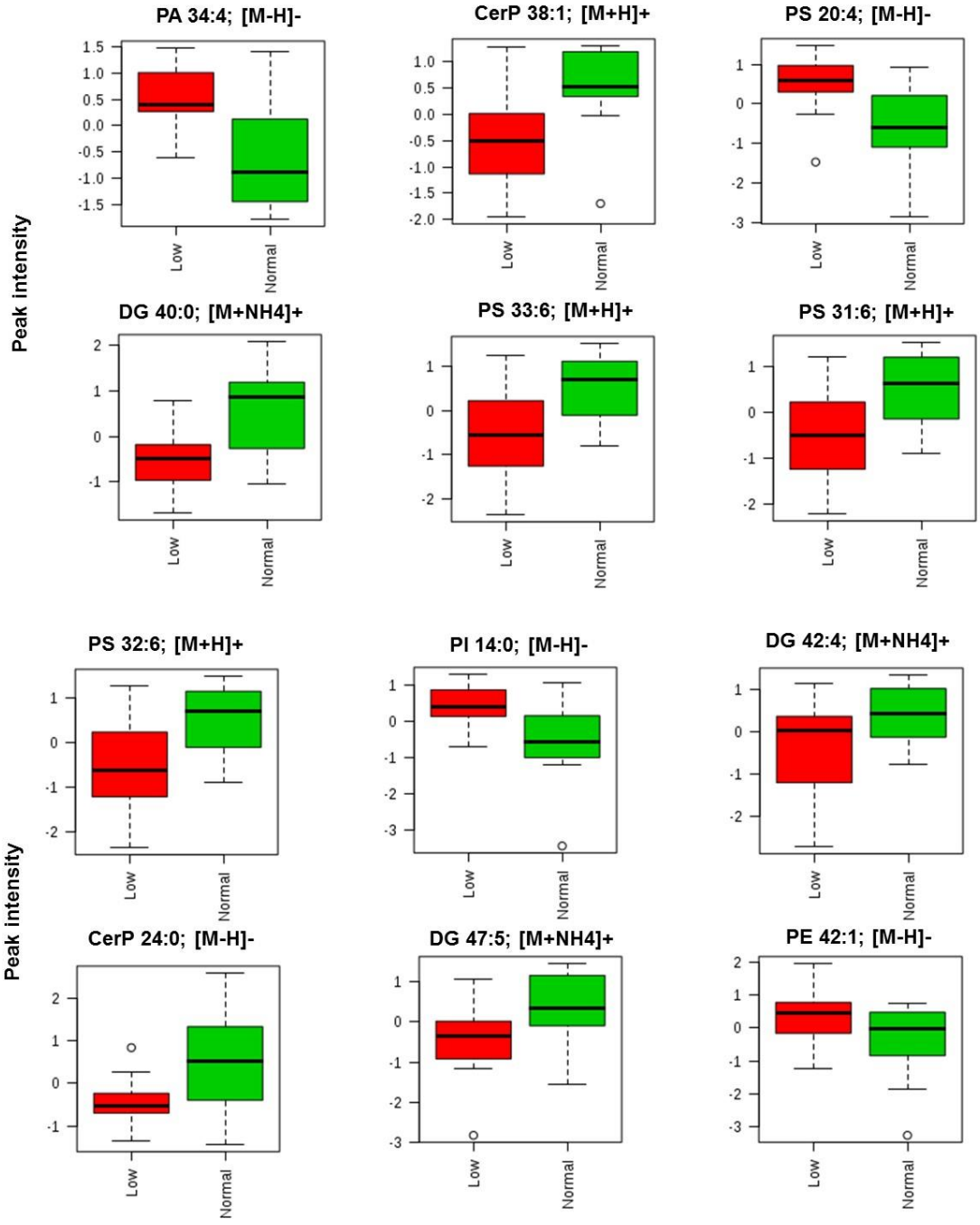

Figure D.2: Boxplots showing normalised peak intensities from original LC-MS data of lipids between postmenopausal women with low and normal BMD. PS (phosphatidylserine), PA (phosphatidic acid), DG (diacylglycerol), plasmenyl-PE (phosphatidylethanolamine), Cer-P (ceramide-1-phosphate), PE (phosphatidylethanolamine) and PI (phosphatidylinositol).

Metabolites

Entire cohort

Table D.3: Significant polar metabolites associated to postmenopausal women with normal and low femoral neck BMD in univariate and multivariate approaches.

m/z	RT (sec)	Compound
104.070	628.58	4-Aminobutyric acid
200.031	936.972	Threonine
293.091	888.961	Asn-Gly-Cys
381.026	886.248	Turanose

Normal and low femoral neck BMD showed a similar range of 4 aminobutyric acid, threonine, Asn- Gly-Cys and turanose concentratios (Figure 5

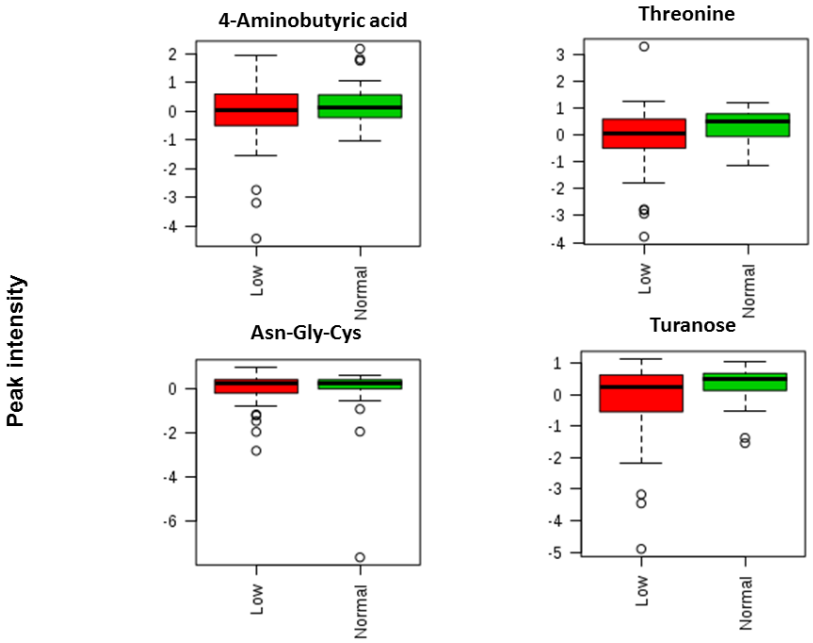

Figure D.3: Boxplots showing normalised peak intensities from original LC-MS data of polar metabolites between postmenopausal women with low and normal BMD.

Subset

Table D.4: Significant polar metabolites associated to a subset of selected postmenopausal women with normal (n =15) and low femoral neck BMD (n =15) in univariate and multivariate approaches.

m/z	RT (sec)	Compound
116.070	731.838	Proline
71.060	642.821	Aminopropionitrile
200.031	936.972	Threonine
150.058	654.108	Methionine
293.091	888.961	Asn-Gly-Cys

Results from boxplots of the plasma polar metabolomic analysis showed lower range of proline, aminopropionitrile and threonine in the low BMD group (Figure D.4).

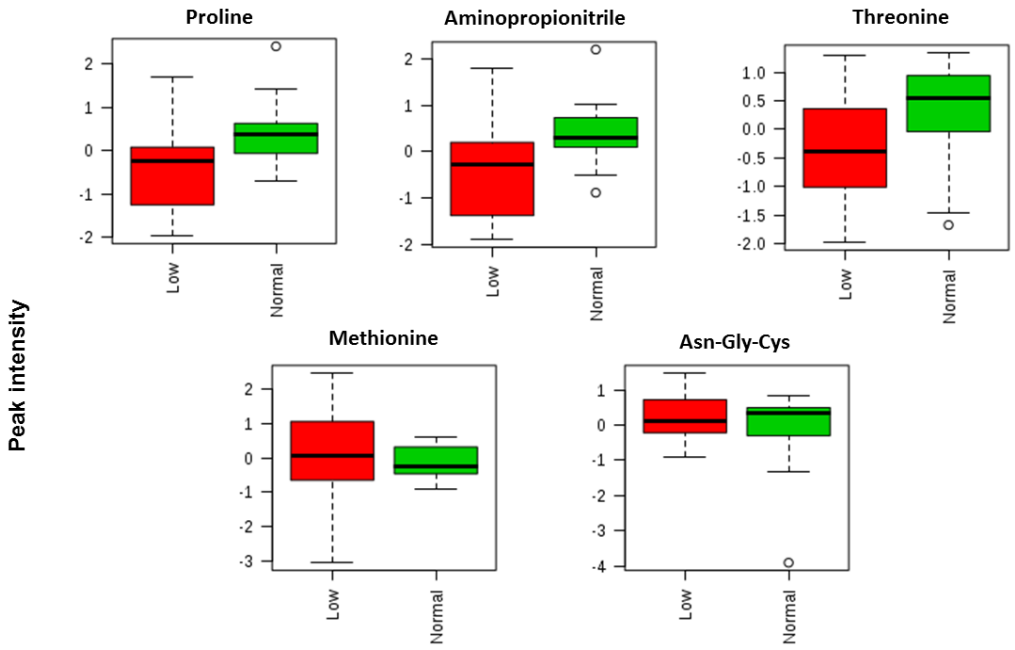

Figure D.4: Boxplots showing normalised peak intensities from original LC-MS data of polar metabolites between postmenopausal women with low and normal BMD.